

PERFORMANCE ENHANCEMENT OF UNDERLAY COGNITIVE  
RADIO NETWORKS THROUGH PRECISE LOCALIZATION,  
OPTIMUM RESOURCE SELECTION AND TRANSMISSION  
POWER OPTIMIZATION

Thesis Submitted by

**SABYASACHI CHATTERJEE**

**DOCTOR OF PHILOSOPHY (Engineering)**

Department of Computer Science and Engineering

Faculty Council of Engineering & Technology

Jadavpur University

Kolkata-700032, India

2019



JADAVPUR UNIVERSITY  
KOLKATA-700032, INDIA

INDEX NO.13/14/E

1. TITLE OF THE THESIS:

**PERFORMANCE ENHANCEMENT OF UNDERLAY COGNITIVE RADIO NETWORKS THROUGH PRECISE LOCALIZATION, OPTIMUM RESOURCE SELECTION AND TRANSMISSION POWER OPTIMIZATION**

2. NAME, DESIGNATION & INSTITUTION OF THE SUPERVISORS:

i. **DR. PRABIR BANERJEE**

PROFESSOR,  
DEPARTMENT OF ELECTRONICS AND COMMUNICATION  
ENGINEERING,  
HERITAGE INSTITUTE OF TECHNOLOGY,  
KOLKATA-700107, INDIA

ii. **DR. MITA NASIPURI**

PROFESSOR,  
DEPARTMENT OF COMPUTER SCIENCE AND ENGINEERING,  
JADAVPUR UNIVERSITY,  
KOLKATA-700032, INDIA

3. LIST OF PUBLICATIONS:

a. JOURNAL:

- i. **Chatterjee, S.**, Banerjee, P., & Nasipuri, M. (2017, September). Optimized Flexible Power Selection for Opportunistic Underlay Cognitive Radio Networks. *Wireless Personal Communications*, 96(1), 1193-1213. Impact Factor: 1.200 (SCI)
- ii. **Chatterjee, S.**, Banerjee, P., & Nasipuri, M. (2018, August). A New Protocol for Concurrently Allocating Licensed Spectrum to Underlay Cognitive Users. *Digital Communications and Networks*, 4(3), 200-208. Journal Impact: 0.531 (SCIE)



- iii. **Chatterjee, S.,** Banerjee, P., & Nasipuri, M. Enhancing Localization Accuracy of Mobile Primary Users by Internal Noise Mitigation. Telecommunication Systems (Under Review).
- iv. **Chatterjee, S.,** Banerjee, P., & Nasipuri, M. A Study on Machine Learning Based Cognitive Radio Network. International Journal of Distributed Sensor Network (Under Review).

b. CONFERENCE:

- i. **Chatterjee, S.,** & Banerjee, P. (2014, January). Hill-Climbing Approach for Optimizing Receiver Bandwidth. IEEE International Conference in Electronics, Communication and Instrumentation, 1-4.
- ii. **Chatterjee, S.,** Banerjee, P., & Nasipuri, M. (2015, January). Enhancing Accuracy of Localization for Primary Users in Cognitive Radio Networks. IEEE International Conference on Computational Intelligence & Networks, 74-79.
- iii. **Chatterjee, S.,** & Banerjee, P. (2015, July). Non Cooperative Primary Users-Localization in Cognitive Radio Networks. IEEE 2nd International Conference in Recent Trends in Information Systems, 68-75.

4. LIST OF PATENTS: NONE

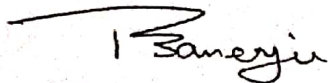
5. LIST OF PRESENTATIONS IN INTERNATIONAL/NATIONAL CONFERENCE:

- i. “Hill-Climbing Approach for Optimizing Receiver Bandwidth”. IEEE International Conference on Electronics, Communication and Instrumentation, 1-4.
- ii. “Enhancing Accuracy of Localization for Primary Users in Cognitive Radio Networks”. IEEE International Conference on Computational Intelligence & Networks, 74-79.
- iii. “Non Cooperative Primary Users-Localization in Cognitive Radio Networks”. IEEE 2nd International Conference in Recent Trends in Information Systems, 68-75.



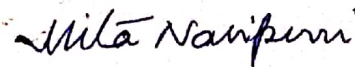
## Certificate from the Supervisors

*This is to certify that the thesis entitled "Performance Enhancement of Underlay Cognitive Radio Networks through Precise Localization, Optimum Resource Selection and Transmission Power Optimization" submitted by Shri Sabyasachi Chatterjee, who got his name registered on 16<sup>th</sup> July 2014 for the award of Ph.D.(Engg.) degree of Jadavpur University is absolutely based upon his own work under the supervision of Dr. Prabir Banerjee and Dr. Mita Nasipuri and that neither his thesis nor any part of the thesis has been submitted for any degree/diploma or any other academic award anywhere before.*



1.....  
(Dr. Prabir Banerjee)

Signature of the Supervisor  
and date with Office Seal



2.....  
(Dr. Mita Nasipuri)

Signature of the Supervisor  
and date with Office Seal

HOD  
Dept. of Electronics &  
Communication Engineering  
Heritage Institute of Technology

MITA NASIPURI  
Professor  
Computer Science & Engg. Dept.  
Jadavpur University  
Kolkata - 700 032





*Dedicated to my  
Family & Guides*



## **Acknowledgements**

It gives me a great pleasure in acknowledging my debt to all those who helped me to achieve my objective. Firstly, I would like to express my earnest gratitude and respect to my supervisors, Dr. Prabir Banerjee, Professor and Head of the Department of Electronics and Communication Engineering of Heritage Institute of Technology and Dr. Mita Naipuri, Professor, Department of Computer Science and Engineering, Jadavpur University, for their guidance, constant support and monitoring throughout the course of this work. I will always be grateful for the immense trouble they took to correct and improve my work.


I am grateful to Dr. Ram Sarkar, Department of Computer Science and Engineering, Jadavpur University and Dr. Susovan Mandal, Department of Electronics and Communication Engineering of Heritage Institute of Technology for their valuable suggestions during preparation of my thesis.

I am also thankful to other faculty members of Department of Electronics and Communication Engineering, Heritage Institute of Technology for their support during my course of work.

Thanks are due to the authorities of Heritage Institute of Technology for allowing me to work in the Design laboratory of ECE Department.

I would also like to thank Prof. Siladitya Sen, Department of Electronics and Communication Engineering, Heritage Institute of Technology and Dr. Dip Prakash Samajdar, Department of Electronics and Communication Engineering, IITDM, Jabalpur for their friendly support and encouragement during my research work.

Finally, I owe immense debt to my respected parents, my wife and my younger sister. I must acknowledge the unrelenting support and encouragement received from my father over all these years of work. I am sure that his confidence on my ability provided me strength to complete my thesis work.



KOLKATA

DATE: 27/11/2019

SABYASACHI CHATTERJEE



---

# CONTENTS

---

CONTENTS.....	VII-X
LIST OF FIGURES.....	XI-XII
LIST OF TABLES.....	XIII
NOMENCLATURES.....	XIV-XVII

## CHAPTER ONE

1. INTRODUCTION.....	1-19
1.1 COGNITIVE RADIO.....	03
1.1.1 Evolution of Cognitive Radio.....	03
1.1.2 Dynamic Spectrum Access (DSA).....	04
1.1.3 IEEE Standards of Cognitive Radio Technology.....	05
1.1.4 Cognitive Radio Network (CRN) Architecture.....	07
1.1.5 Cognitive Radio Network (CRN) Paradigms.....	08
1.2 CHALLENGES in UNDERLAY CRN.....	09
1.3 MOTIVATION.....	14
1.4 SCOPE OF THE WORK.....	15
1.5 ORGANIZATION OF THE THESIS.....	18

## CHAPTER TWO

2. LITERATURE REVIEW.....	21-39
2.1 INTRODUCTION.....	21
2.2 LOCALIZATION.....	24
2.2.1 Range Based Localization.....	25
2.2.2 RSSI Based Localization.....	26
2.2.3 Non Cooperative and Cooperative Schemes.....	27
2.2.4 Centroid Localization Algorithm.....	27

2.3	MAC PROTOCOL DESIGN.....	28
2.3.1	Design Requirement of Cognitive MAC Protocol.....	29
2.3.2	Classification of MAC Protocol.....	30
2.3.3	Learning Based Intelligent MAC Protocol.....	35
2.4	TRANSMIT POWER CONTROL IN UNDERLAY NETWORKS.....	37
2.5	DISCUSSION.....	39

## **CHAPTER THREE**

<b>3.</b>	<b>LOCALIZATION IN UNDERLAY COGNITIVE RADIO NETWORK.....</b>	<b>41-77</b>
3.1	INTRODUCTION.....	41
3.2	LOCALIZATION PROCESS.....	44
3.2.1	Importance of RSSI in Localization Process.....	44
3.2.2	Hypotheses on the PU Signaling Information.....	45
3.2.3	System Threshold Selection.....	47
3.3	LOCALIZATION OF A FIXED PRIMARY USER.....	51
3.3.1	Weighted Centroid Localization (WCL) Scheme.....	52
3.3.2	Power Law Model with a Correction Factor.....	53
3.3.3	Network Scenario.....	57
3.4	LOCATION ESTIMATION OF A MOBILE PU.....	59
3.4.1	Optimization of the Number of Collaborative Users.....	59
3.4.2	Localization of a Mobile PU.....	61
3.4.3	Internal Noise Mitigation.....	64
3.4.3.1	Modified Cognitive Radio Receiver.....	64
3.4.3.2	Operational Analysis.....	67
3.4.4	Computation of Location Coordinates.....	70
3.5	DISCUSSION.....	76

## **CHAPTER FOUR**

### **4. CHANNEL SELECTION SCHEME FOR UNDERLAY**

<b>COMMUNICATION.....</b>	<b>79-93</b>
4.1 INTRODUCTION.....	79
4.2 SELECTION PARAMETERS.....	81
4.2.1 Resource Selection Hypothesis.....	82
4.2.2 Interference Temperature Model.....	84
4.3 OPTIMUM CHANNEL SELECTION SCHEME.....	86
4.3.1 Maximizing Channel BW using Hill Climbing Method.....	86
4.3.2 Experimental Setup.....	89
4.3.3 Emulated Results of Channel Selection Scheme.....	92
4.4 DISCUSSION.....	93

## **CHAPTER FIVE**

<b>5. UNDERLAY COGNITIVE MAC PROTOCOL.....</b>	<b>95-128</b>
5.1 INTRODUCTION.....	95
5.2 OPPORTUNISTIC UNDERLAY NETWORK.....	97
5.2.1 Channel Model.....	98
5.2.2 Basic Communication Protocols.....	100
5.3 RECEIVER-INITIATED MAC (RI MAC) PROTOCOL.....	103
5.3.1 Timing Sequence of Data Transmission Scheme.....	103
5.3.2 System Throughput and Efficiency.....	106
5.3.3 System Performance Analysis .....	107
5.3.4 A Comparative Study.....	110
5.4 TRANSMITTER-INITIATED (TI) MAC PROTOCOL.....	113
5.4.1 Optimum Transmit Power Adaptation.....	113
5.4.2 Scheme of Data Transmission.....	114

5.4.3 Comparative Analysis of Proposed MAC Protocols.....	117
5.5 FLEXIBLE TRANSMIT POWER SELECTION.....	119
5.5.1 Optimum Power Selection.....	119
5.5.2 Power Control Unit.....	121
5.5.3 Performance Analysis with Flexible Transmit Power.....	124
5.6 DISCUSSION.....	128

**CHAPTER SIX**

<b>6. CONCLUSIONS AND FUTURE WORK.....</b>	<b>129-134</b>
6.1 SUMMARY OF RESULTS.....	130
6.2 FUTURE SCOPE.....	134

<b>BIBLIOGRAPHY.....</b>	<b>135-153</b>
--------------------------	----------------

**APPENDIX.....**

Appendix A.....	A1-A6
Appendix B.....	B1-B10
Appendix C.....	C1-C10



---

# LIST OF FIGURES

---

1.1	Evolution of Radio Technology	03
2.1	Classification of CR MAC Protocols	30
3.1	Relation between Miss Detection and False Detection Probabilities	48
3.2	Relation between Successful Detection and False Detection Probabilities	48
3.3	Variation of Successful Detection Probability with SNR	51
3.4	Effects of Path Loss Exponent on RSSI with Distance	55
3.5	Network Scenario	57
3.6	Variation of Detection Error with Number of CRUs	60
3.7	Network Model	61
3.8	True and Estimated Location of a Mobile PU	62
3.9	Distance Measurement at different CRUs with respect to a PU Movement to within the Network	62
3.10	SNR Measurement at different CRUs with respect to a PU Movement within to the Network	63
3.11	Operational Block of a Modified Cognitive Radio Receiver	65
3.12	Proposed Experimental Block	66
3.13	Hardware Setup	67
3.14	Operation Sequence and Filter Design Code	68
3.15	Plot of Output SNR Vs Input Noise Level for Different Filter Types	69
3.16	CRU1 as a Detector Node	73
3.17	Error in Location Estimation by CRU1	73
3.18	CRU2 as a Detector Node	73
3.19	Error in Location Estimation by CRU2	73
3.20	CRU3 as a Detector Node	73
3.21	Error in Location Estimation by CRU3	73
3.22	CRU4 as a Detector Node	74
3.23	Error in Location Estimation by CRU4	74
3.24	Estimated Mean Location Coordinates of Each Observation	75
3.25	Error in Collaborative Location Estimation	75
4.1	Underlay Cognitive Communication	83

4.2	Hill-Climbing Optimization Algorithm	87
4.3	BW Selection as per Principle of Hill Climbing Algorithm	88
4.4	Operational Flow Diagram of the Channel Selection Scheme	89
4.5	Schematic Block of Channel Selection Scheme	90
4.6	Experimental Setup of Channel Selection Scheme	91
4.7	Laboratory Setup of Experiment	92
5.1	Underlay Channel Model	98
5.2	Data Transmission Scheme under MACA Protocol	101
5.3	Data Transmission Scheme under MACA-BI Protocol	101
5.4	Command Control Frame Structure	102
5.5	Carrier-to-Receive (CTR) Frame Structure	103
5.6	Operational Flow Diagram of the Proposed Protocol	104
5.7	Scheme of Data Transfer under Hypothesis $H_{sd}$	105
5.8	Scheme of Data Transfer under Hypothesis $H_{fd}$	105
5.9	Data Transmission Scheme using RI MAC Protocol	106
5.10	Variation of Overhead Time with the Number of Attempts	108
5.11	Throughput Performance with the Number of Attempts	109
5.12	System Efficiency with Time	109
5.13	System Overhead Time during Data Transmission	111
5.14	Overall System Efficiency	112
5.15	Data Transfer Scheme for SUs under Hypothesis $H_{fp-sf}$	115
5.16	Structure of Command Control Frame	116
5.17	Step-up Transmit Power (SUTP) Frame Structure	116
5.18	Data Transmission Scheme for SUs under Hypothesis $H_{fp-sm}$	117
5.19	Overhead-Time Variation with the Number of Attempts	118
5.20	Throughput Performance Variation with the Number of Attempts	118
5.21	System Efficiency Variation with the Period of Observations	119
5.22	Power Control Hardware Module	122
5.23	Transmit Power Increment till the Maximum Interfering Limit	124
5.24	Outage Probability of PUs with the Flexible Transmit Power	125
5.25	Channel Capacity of SUs	126
5.26	Secondary Error Probability variation with SNR (dB) Levels	126
5.27	Primary Error Probability Variation for Interference Limits	127

---

# LIST OF TABLES

---

1.1	Standards of Cognitive Radio Technology	07
1.2	Network Establishment Strategy of Different Cognitive Architectures	08
2.1	Comparative Evaluation of MAC Protocols	33
2.2	Comparative Study on MAC Protocols Based on Characteristics Features	34
3.1	Network Modelling Factors	56
3.2	RSSI (mV) Measurement at the anchor CRUs	57
3.3	Absolute Location Coordinates of a Fixed PU	58
3.4	True Location Coordinates of a Mobile PU	61
3.5	Performance Analysis of Different Filter Types at Variable Noise Levels	69
3.6	SNR (dB) Improvement at Each of the Collaborative CRUs	70
3.7	RSSI at Each of the Collaborative CRUs without and with Filtering	71
3.8	Estimated Mean Location Coordinates	74
4.1	Programmable Output Divider Function	92
4.2	Emulated Results of Hardware Module	93
5.1	Channel Frequency for Multiple Retransmission Attempts	108
5.2	Simulation Parameters	111
5.3	Flexible Power Steps	121
5.4	SNR Corresponding to Binary Code	121
5.5	Variable Biasing Voltage to Control Transmit Power	123
5.6	Transmit Power Variation Corresponding to the SNR at the Receiver End	123
5.7	Simulation Parameters	125



---

# NOMENCLATURES

---

- **Abbreviations and Acronyms**

ACK	Acknowledgment
AI	Artificial Intelligence
AWGN	Adaptive White Gaussian Noise
BER	Bit Error Rate
BS	Base Station
BPS	Bits per Second
BW	Bandwidth
CFI	Channel Frequency Information
CI	Channel Information
CL	Collaborative Localization
CQI	Channel Quality Information
CR	Cognitive Radio
CRN	Cognitive Radio Network
CRU	Cognitive Radio User
CSI	Channel State Information
CT	Cognitive Terminal
CTR	Carrier to Receive
CTS	Clear to Send
dB	Decibel
dBm	Decibel-Milliwatts
DSA	Dynamic Spectrum Access
DSP	Digital Signal Processing
FCC	Federal Communication Commission
FIR	Finite Impulse Response

FPGA	Field Programmable Gate Array
FSA	Fixed Spectrum Access
GPS	Global Positioning System
ISM	Industrial Scientific and Medical
LOS	Line of Sight
MAC	Medium Access Control
NLOS	Non Line of Sight
OSA	Opportunistic Spectrum Access
OSI	Open System Interconnection
PLE	Path Loss Exponent
PLL	Phase Lock Loop
PPS	Packets per Second
PU	Primary User
QoS	Quality of Service
RA	Receiver Address
RCS	Request to Carrier Switch
RF	Radio Frequency
RI MAC	Receiver Initiated Medium Access Control
RSS	Received Signal Strength
RSSI	Received Signal Strength Indicator
RTR	Request to Receive
RTS	Request to Send
SCSI	Switched Carrier Strength Information
SDR	Software Defined Radio
SI	Secondary Interference
SIFS	Shortest Inter Frame Space
SNR	Signal to Noise Ratio
SU	Secondary User
SUTP	Step Up Transmission Power
SS	Spectrum Sharing
TA	Transmitter Address

TI MAC	Transmitter Initiated Medium Access Control
THD	Total Harmonic Distortion
TVWS	TV White Space
WCL	Weighted Centroid Localization
WLAN	Wireless Local Area Network
WRAN	Wireless Regional Area Network

- **Notations**

$\lambda_{s/m}$	Predefined System Threshold
$\sigma_G$	Zero Mean Gaussian Random Variable with Standard Deviation
$\tau_{comp}$	Computational Time
$\eta$	Transmission Efficiency
$B$	Number of Narrow Bands
$c$	Group of Collaborative Cognitive Radio Users
$D_{SI}$	Decision Statistics
$F_{XTAL}$	Frequency of the Crystal
$F_{out}$	PLL Output
$i$	Number of Retransmission Attempts
$m$	Number of Mobile Primary User
$n$	Path Loss Exponent
$N$	Number of Discrete Samples
$P_{s\_flx}$	Flexible Transmission Power Level
$P_{pk}$	Peak Transmission Power Level
$P_{sd}$	Probability of Successful Detection

$P_{md}$	Probability of Miss Detection
$P_{fd}$	Probability of False Detection
$P_e$	Total Error Probability
$P_{in}$	Internal Noise
$P_{ln}$	Link Noise
$P_p$	Primary Transmission Power
$P_r$	Received Signal Power
$P_{ref}$	Reference Power
$P_s$	Secondary Transmission Power
$r_p$	Primary Transmission Rate
$R_x$	Receiver
$T_x$	Transmitter
$T_p$	Propagation Delay Time
$T_t$	Channel Processing Time
$Th_s$	System Throughput



# CHAPTER I

---

## INTRODUCTION

---

1.1	<b>COGNITIVE RADIO</b> .....	03
1.2	<b>CHALLENGES IN UNDERLAY CRNS</b> .....	09
1.3	<b>MOTIVATION</b> .....	14
1.4	<b>SCOPE OF THE THESIS</b> .....	15
1.5	<b>ORGANIZATION OF THE THESIS</b> .....	18

Wireless communication technology has become one of the most important cornerstones for modern day civilization. It provides methods of transmitting information from one point to other, without using any physical connection like wires, cables or any other electrical conductors. The ability to communicate on the move has increased the popularity of wireless communication systems remarkably. In the early 20th century, the era of wireless communication began. Since then the wireless communication technology has significantly developed over years. Today, it encompasses every walk of human life. Devices such as

garage door openers, TV remote controllers, cellular phones, personal digital assistants (PDAs), satellite TV receivers, and GPS mapping etc. are all developed based on wireless communication technology. Now, the entire cellular wireless service subscribers have surpassed the number of wired telephone service subscribers. Furthermore, wireless local area networks (WLANs) and satellites are used widely for voice as well as data-oriented applications and entertainment services. Therefore, to support different wireless applications and services in a non-interfering fashion, the fixed spectrum access (FSA) policy [1] has traditionally been adopted by spectrum regulators. However, the fixed spectrum allocation scheme may not be able to support the rapidly increasing demand for more radio frequency (RF) spectrum.

The RF spectrum or electromagnetic spectrum is the natural and limited resource for all the wireless communication systems. Efficient utilization of the RF spectrum has become the focal point of research over the last several decades in the wireless domain. The fixed spectrum allocated systems are allowed to operate at a high transmit power without causing interference within the geographical and frequency boundaries of each authorized system. As a result, wide coverage area has been achieved with a good quality of service (QoS). However, recent analyses of the actual spectrum utilization patterns have revealed that a large portion of allocated licensed spectrum experiences underutilization or partial utilization [2] [3]. According to the Federal Communication Commission (FCC) in the USA and the Office of Communications (Ofcom) in the UK, the utilization of the frequency spectrum varies temporally and geographically between 15% and 85% [4] of the existing spectrum allocations. On the other hand, the research outcome of International Telecommunication Union- Radio communication Sector (ITU-R) [5] has predicted a demand for another 1280 MHz-1720 MHz by 2020, to accommodate the growing number of wireless technology subscribers and application. Therefore, it is necessary to develop a new communication technology which can utilize the allocated underutilized spectrum more efficiently [6]. Hence the concept of cognitive radio (CR) was proposed in 1999 [7] [8] by J. Mitola III *et.al.* at KTH (the Royal Institute of Technology in Stockholm).

## 1.1 COGNITIVE RADIO

Cognitive radios (CRs) have emerged as the most efficient solution to utilize underutilized or unutilized RF spectrum by dynamic spectrum access (DSA) [9] mechanism. The cognitive radio users (CRUs) or secondary users (SUs) are allowed to use the underutilized or unutilized frequency spectrum dynamically and intelligently [9] without interfering with the licensed users or primary users (PUs). It is possible only when the SUs learn about the occupancy of the RF spectrum in real time [10]. After learning about the radio environment, it needs to make appropriate decisions regarding the opportune moment for accessing the frequency spectrum. Therefore, it is a radio system which can sense the operational electromagnetic environment to self-adjust the radio operating parameters dynamically or automatically for performance improvement [8].

### 1.1.1 Evolution of Cognitive Radio

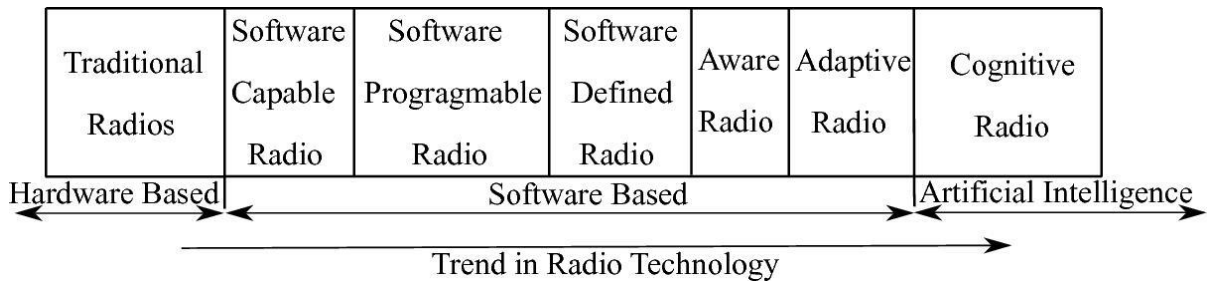


**Figure 1.1: Evolution of Radio Technology [11] [12]**

The evolution of the radio technology is shown in Fig.1.1. Over the last few decades, the design and implementation of wireless devices have undergone a substantial transition from pure hardware-based radios to a combination of hardware and software based radios. The concept of software defined radio (SDR) was introduced by Mitola in 1993 [11]. The front end receiver of the SDR contains a software-controlled local oscillator and IF stages. The quantized and coded baseband signal is demodulated by software driven reconfigurable device of the front end radio receiver. Due to this software driven reconfigurability features, it is called a software-defined radio (SDR). The model-based reasoning was integrated into the SDR in 1999 by Joseph Mitola III *et.al.* [7] [10] to develop a flexible spectrum access

CR. The word 'Cognitive' has been deduced from the word 'cognition' which means the ability to process information, learn about the environment and make decisions about its operating behavior to achieve predefined objectives [1] [8]. In [1], the term CR refers to a sophisticated system that can mimic the human brain. Ability to measure, sense, learn and be aware of the QoS parameters which are related to the radio channel are the essential features of the CR application. Joseph Mitola III *et.al.* [7], the pioneer of CR technology, introduced the concept of cognition cycle, which consists of radio performance analysis, channel state estimation, and prediction. In a cognitive radio network (CRN), the SUs can share the licensed frequency spectrum as long as it does not cross the interference tolerance limit of the PUs. This spectrum sharing concept gives advantages in terms of more than one wireless systems operating on the same frequency band and easy access of the licensed spectrum by the service providers. The opportunistic RF spectrum utilization technique in the CRNs is known as dynamic spectrum access (DSA) [1] [13].

### 1.1.2 Dynamic Spectrum Access (DSA)

DSA [14-16] supports opportunistic spectrum sharing mechanism. It is a real-time spectrum sharing management system which works on the time-varying radio environment. The variation of the radio environment depends on the change of user location, addition or removal of PUs, availability of channels and interference constraints [17] [18].

DSA has been classified as command & control, dynamic exclusive use, spectrum common and hierarchical access [17]. In [19], similar classification of DSA has been done by M. Buddhikot in a slightly different way. The command & control are one of the oldest models for spectrum access with complete spectrum usage rights given to a single user. The dynamic exclusive use model, adds flexibility to the fundamental structure of spectrum policy which, in turn, improves the spectrum utilization. There are two approaches to dynamic exclusive use model. First one is spectrum property rights [20], where the license holder can trade spectrum and choose technology based on market trends. Second is the dynamic allocation [21], where channel frequency allocation is varied at a faster rate to improve spectrum efficiency by exploiting the spatial and temporal traffic statistics of different services. In spectrum common model, every user has equal rights to use the

available spectrum. This is also called as open spectrum model. In the ISM (industrial, scientific and medical) band, Wi-Fi application is an example of the common model. In the hierarchical access model, SUs can access the primary resources by restricting the interference level of the PUs within a specific limit. Spectrum underlay and overlay approaches [17] [22] belong to this model. A new dynamic resource allocation method, based on hybrid sharing mode of overlay and underlay (Dy-HySOU) is proposed in [23] to obtain extra spectrum resources for SUs without interfering with the PUs. Oh *et.al.* [24] has introduced a hybrid CR system to control the operation mode transition between overlay and underlay and maximize the performance efficiency of the SUs.

The DSA operation [25] is based on spectrum awareness, cognitive processing, and finally spectrum access. Spectrum awareness enables acquisition of knowledge about the RF environment. The knowledge can be obtained by using either any active or any passive method. Conventionally, the spectrum awareness has been classified into three categories [16]: black spaces, gray spaces, and white spaces. Black spaces and grey spaces of the radio spectrum are occupied by the PUs with high power interference and low power interference respectively. Whereas, white spaces of the radio spectrum are free from the interference of PUs. The second task of DSA operation is cognitive processing which covers intelligent decision-making functions. These decision-making functions include several sub-tasks like efficient sensing, collection of knowledge about the radio environment, and access policies. The third task, i.e. efficient spectrum access policy of DSA operation provides ways to exploit the RF spectrum opportunistically for efficient reuse. Presently, the DSA is supported by a number of wireless standards, such as P1900.4 [26], 802.11y [27], 802.16h [28], and 802.22 [29]. The activities of DSA standards are reviewed in [30] which highlight further issues for future standardization.

### **1.1.3 IEEE Standards of Cognitive Radio Technology**

Many regulatory and standardization groups around the world have started incorporating cognitive features [10] to generate more interest in CR technology. The IEEE 802.22 wireless regional area network (WRAN) was started as a working model in 2004 and became a full IEEE standard by 2009. It is the first IEEE standard which implements CR

functionalities at the Physical (PHY) and the Medium Access Control (MAC) layers [31]. One of the most distinctive features of the IEEE 802.22 standard is centralized spectrum sensing requirement [32]. The centralized approach defines standardized air interference for opportunistic use of available TV spectrum. On the other hand, the extension of IEEE 802.11 specification results in a new standard IEEE 802.11k which also includes several cognitive features [33] of a centralized network. In this IEEE standard, the network access point (AP) collects channel information from each secondary unit to perform channel quality measurement. Therefore, to improve traffic distribution within the network, the channel quality information is used.

The dynamic spectrum access networks (DySPAN) Standards Committee was declared as the IEEE P1900 standards committee in 2005 by the IEEE communication society and the IEEE compatibility society. It was under the IEEE communication society, till December 2010. The main objective [34] of this committee was to work on dynamic spectrum access-based systems and networks for improving the spectrum utilization efficiency, radio transmission interference and information sharing capability amongst different wireless technologies. Another standardization initiative related to CR technology is IEEE 802.19 [35]. It focuses on the coexistence of wireless applications with the TV white space (TVWS). Furthermore, underdeveloped IEEE 802.11af standard also aims to modify IEEE 802.11 PHY/MAC standard for TVWS [36]. On the other hand, the European Telecommunication Standard Institute (ETSI) has formed a Technical Committee on Reconfigurable Radio Systems (RRS) [37] to regulate CR technology by software defined radio technology framework. The ETSI-RRS committee consists of four working groups namely WG-1 for System Aspects, WG-2 for Reconfigurable Radio Equipment Architecture, WG-3 for Cognitive Management and Control and WG-4 for RRS for Public Safety. Table 1.1 shows the system parameters for different IEEE standards.

**Table 1.1: Standards of Cognitive Radio Technology [38] [39]**

<b>Parameters</b>	<b>IEEE 802.22</b>	<b>IEEE 802.11af</b>	<b>IEEE 802.19</b>
Frequency Range	54-862 MHz	54-790 MHz	54-852 MHz
Bandwidth	6MHz,7MHz,8MHz	6MHz,7MHz,8MHz	6MHz,7MHz,8MHz
Modulation	QPSK,16QAM, 64QAM	BPSK,QPSK,QAM	–
Transmit Power	4W	100mW	–
Multiple Access	OFDMA	OFDM	DSSS,OFDM

#### 1.1.4 Cognitive Radio Network (CRN) Architecture

Proper network architecture is an essential component for ensuring the optimum system performance. SOAR (State, Operator and Result) [40] was one of the first architectures of cognitive science and artificial intelligence (AI) communities. The philosophy of SOAR has been based on eleven hypotheses. The main components of SOAR architecture are problem spaces, long-term, short-term, and preference memories. In the year 2001, cog-Aff architecture scheme was developed [41]. This architecture is presented in the form of a grid, considering reactive mechanisms, deliberative reasoning, meta-management and processing cycles. On the other hand, Anderson's Theory of Cognitive Architecture (ACT-R) [42] consists of different processing modules namely, sensory information, beliefs, goals, actions, and declarative knowledge. The CR technology was introduced by Mitola and Maguire in 1999 [8] based on observe, orient, decide and act (OODA) loop [43] which was proposed by Boyd in 1987.

The CRN, also known as secondary network, has been classified into three categories, namely, infrastructure-based or centralized network, ad-hoc type or decentralized network, and mesh network [38]. The infrastructure-based CRN is a network-centric architecture where the key components are cognitive terminals (CTs) and a base station (BS). On the other hand, in the ad-hoc type network, each radio node needs to do self-reconfiguration based on the local observation. The cognitive mesh architecture is the combination of infrastructure based and ad-hoc architectures [44] [45]. A single CR user of distributed architecture cannot predict the behavior of the entire network only by the local observation. Therefore, the infrastructure based centralized architectures are essential for efficient network operation. The advantages of the centralized architecture of CRNs include low

transmit power, high energy efficiency, low interference and better network coverage [46] [47]. However, extra relay traffic and end to end latency time of an infrastructure based centralized network architecture reduce overall system throughput and efficiency. Table 1.2 addresses implementation strategy of different CRN architectures.

**Table 1.2: Network Establishment Strategies of Different Cognitive Architectures**

Resource Access Strategy	Method	Contribution	Network Architecture
Partial Observable Markov Decision Process (POMDP) [48]	Decentralized Cognitive MAC	It ensures synchronous hopping in the spectrum between the transmitter and the receiver in the presence of collisions and spectrum sensing errors.	Decentralized
Secure Centralized Spectrum Sensing (SCSS) [49]	Novel Fusion Scheme based on Spatial Correlation Technique	It produces correct and efficient sensing result even during the presence of high density attackers within a geographical area.	Centralized
Classical Narrowband Spectrum Sensing Technique [50]	Distributed Algorithm	It proposes fixed handoff delay. The SUs can make the choice of either to stay on present channel spectrum with low availability or handoff to a spectrum with higher availability.	Decentralized
Partial Observable Markov Decision Process (POMDP) [51]	Maximum Likelihood	The overhead time is reduced resulting in increasing the network throughput.	Decentralized
Sequence based Spectrum Allocation Algorithm [52]	Graph Theory	It reduces the overhead time and has better fairness compared with other existing collaborative algorithm.	Centralized
Distributed Process for Information Exchange Across the Coupled Secondary Transmitter [53]	Alternating Direction Method of Multipliers (ADMM)	It considers the downlink balancing problem to minimize PU interference probability.	Decentralized

### 1.1.5 Cognitive Radio Network (CRN) Paradigms

The RF spectrum access by the CR users depends on the network characteristics and regulatory constraints. Hence, three spectrum access paradigms [17] [22] [54] namely, interweave, overlay, and underlay had been considered for efficient CRN operation. The different levels of cognition and modes of operation have been used to differentiate among these paradigms. Therefore, in the interweave paradigm or sensing based spectrum sharing [54], the SUs are allowed to select appropriate channel frequency after sensing the status of



the channel. This approach has allowed the SUs to use frequencies within the unused TV spectrum band [55]. On the other hand, the opportunistic spectrum access (OSA) approach, also known as spectrum overlay [17] paradigm, allows SUs to operate on the licensed spectrum opportunistically when the primary transmission is detected to be idle. The fundamental requirement for overlay mode of communication [17] is the prior knowledge about the codebook, message sequence, and modulation scheme of the PU transmission. The spectrum underlay paradigm or spectrum sharing (SS) allows the SUs to access licensed spectrum even when the owner (PU) of that licensed spectrum is active. The fundamental criterion of underlay mode of communication is that the resultant interference at the PU receiver must be less than the predefined tolerance limit [22] [56]. An advantage of the underlay approach over the interweave paradigm is its capability to operate in densely populated urban areas where the probability of available white spaces or spectrum holes is less. Moreover, the interweave approach requires robust spectrum sensing algorithms to detect the PU activities in order to minimize the miss-detection and false-detection probability. The robust spectrum sensing scheme is not required by the underlay communication system since users, under this approach, operate on the licensed spectrum along with the active PUs. Also the complexity of implementing underlay paradigm is less compared to the overlay approach. The implementation of the overlay paradigm is challenging because of the required knowledge of the primary messages at the secondary transmitter and the need of decoding them, as well as the encoding and decoding complexity associated with SU transmissions in the system. Further, sharing private information of a PU with the SUs raises security issues for the primary system in the overlay paradigm.

However, even with all the advantages that are offered by the underlay CRNs, successful large-scale deployment requires realistic solutions to different associated problems. Hence in the next section, some of the critical challenges associated with the successful network operation of an underlay CRN are discussed.

## 1.2 CHALLENGES IN UNDERLAY CRN

There are many implementation challenges involved in the design of reliable and consistent underlay CRN. These key challenges are related to the spectrum sensing and detection

operation, PU localization, hardware design, optimization of transmission power level for SUs, and development of the network security etc. Some of those challenges are discussed below:

- **Noise Uncertainty**

The prior knowledge of the noise power level is essential to estimate signal to noise ratio (SNR) at any radio receiver. However, it is very challenging to measure the exact noise power level at the radio receiver. Therefore, in many detection methods, the receiver noise power is assumed to be known a priori, in order to derive the test statistics and the system threshold. However, the noise power level may change over time, thus yielding the so-called noise uncertainty problem [57]. The noise uncertainty degrades the performance of spectrum sensing and detection. It has been seen that the primary transmitted signal cannot be detected over an extended sensing period when the received signal strength is lower than a specific SNR value [58]. The noise uncertainties have been classified as receiver device noise uncertainty or internal noise and environment noise uncertainty or external noise. The internal noise is caused by the nonlinearity and time-varying thermal noise of a receiver device [59] [60]. The external noise is caused by simultaneous transmission from other devices on the same channel or on nearby channels, either intentionally or unintentionally.

The energy detector based spectrum sensing under Middleton Class A noise, with parameter uncertainties, has been considered in [61]. In [62], cooperative spectrum sensing with adaptive thresholds has been proposed to improve the detection performance under noise uncertainty. This adaptive threshold has been selected to obtain an optimum balance between the probability of false alarm ( $P_{fa}$ ) and the probability of successful detection ( $P_{sd}$ ). However, in adaptive white Gaussian noise (AWGN) scenario, the threshold selection is dependent on the noise variance [63]. On the other hand, an eigenvalue-based spectrum sensing technique with double threshold concept has been proposed to minimize the problem of noise uncertainty and low SNR detection [64]. The noise uncertainty can also be handled by a multi-antenna based spectrum sensing method using the generalized likelihood ratio test (GLRT) paradigm [65]. However, the noise properties change frequently due to the variability and uncertainty of communication environment. Hence, the methods, which

consider only the static statistical properties of noise, are unable to solve the problem of dynamic noise environment. Therefore, to overcome the challenge caused by non-stationary noise, a novel Bayesian solution [66] has been proposed to recover the dynamic noise variance and detect the occupancy of the primary frequency band. However, none of the mentioned work has considered the internal noise effects. Therefore, minimization of internal noise effects is an important aspect of efficient underlay CRN design.

- **Hardware Constraints**

A CR system may need to monitor a wide frequency range to obtain the most reliable channel frequency for transmission. Therefore, to sense such wideband frequencies, ultra wideband RF frontend and very fast signal processing devices with high sampling rates are required. Practically, it is very challenging to design such devices. However, the high-speed processing units or field-programmable gate arrays (FPGAs) can be used to achieve a high sampling rate [1]. Another potential challenge arises during detection process due to the presence of multipath fading and shadowing. When the signal-to-noise ratio (SNR) of the received primary signal is remarkably low, then the detection process becomes very challenging. Therefore, to overcome the weak signal detection challenge, the receiver sensitivity must be very high. The requirement of high sensitivity increases enormously the design complexity and the associated hardware cost of CR receivers. Therefore, cost-effective, simple, and efficient hardware design is one of the most significant challenging areas in CR technology.

- **Hidden Terminal Interference Problem**

The hidden terminal interference with the transmission of the SUs is one of the well-known challenges of CRNs. Hidden terminal interference is also known as blind node collision occurs when two nodes in the network are not able to see each other and communicate with a shared visible node. In an underlay CRN, the primary transmitter has been considered as a hidden terminal since secondary and primary users in an underlay network operates on the same licensed channel concurrently. Therefore, during cognitive communication, any primary transmitter, which remains hidden from a secondary transmitter but very close to a

corresponding secondary receiver, can interfere with the secondary transmission. The hidden terminal interference leads to corruption of received data and results in unsuccessful data transmission. In [67] cloud computing-based solution has been proposed to overcome the hidden terminal problem in the CRN. However, this method has not considered the sudden appearance of hidden PUs during cognitive communication.

- **Security Issues of CRNs**

CRNs make use of an open communications medium which can be easily accessed by malicious users. Therefore, security becomes an essential factor to ensure the desired level of network performance. Security attacks may be aimed at deteriorating the CR functionalities by providing wrong information about the radio environment. For example, an attacker has altered the sensing medium of CR users. Hence, the affected users take wrong decisions about the availability or the quality of a given channel. The wrong decision leads to incorrect management of the spectrum. This class of CRN-specific security issue is known as spectrum sensing data falsification (SSDF) [68]. An infrastructure-based CRN has also been affected by the SSDF-type attack. On the other hand, the primary user emulation (PUE) attack is carried out by a malicious user which emulates as a PU to obtain the available channel resource without sharing with other SUs. The behavior of PUE attack has been investigated in [69]. An efficient combat strategy against PUE attacks has been developed in [70]. However, the other types of security issues such as denial of service (DOS) attack, rough base station attack, and small back-off window (SBW) attack etc. need to be focused on by researchers.

- **Efficient Medium Access Control (MAC) Protocol Design**

The performance of CRN depends on efficient spectrum sensing techniques as well as the design of medium access control (MAC) protocols. The execution of spectrum sensing task needs to be scheduled by the MAC protocols. Moreover, when a spectrum hole has been detected by more than one SU, the MAC protocol is responsible for making the decision about allocation. Therefore, MAC protocol design is essential for the successful network operation. In CRNs, the MAC protocol design faces multiple challenges. The challenge of

coexistence of SUs with the licensed users can be resolved by the flexible or adaptive MAC protocol design. The adaptive design can produce efficient sensing ability, adaptability, and resource allocation capability. On the other hand, to overcome hardware constraint, a hardware-constrained (HC) cognitive MAC protocol [71] has been introduced for the distributed network architecture. The MAC protocol designs should also consider channel interference and data handling capacity [72]. During the sensing process, CR nodes stop sending data packets to minimize system complexity. Hence, to minimize end-to-end delay due to long sensing duration, it is essential to adopt proper MAC protocols with optimum sensing durations [72]. A novel multichannel MAC protocol called time slotted channel reservation-based MAC protocol (TSCR-MAC) for CRNs was introduced in [73] to improve end-to-end delay and spectrum utilization. On the other hand, hidden terminal interference also degrades the performance of SUs. An underlay CR MAC protocol COMAC [74] has been introduced to minimize interference by allowing the SUs to access the licensed spectrum with active PUs at minimum transmit power. However, the hidden terminal interference challenge has not been overcome by COMAC MAC protocol [74]. Dynamic open spectrum sharing (DOSS) multichannel MAC protocol [75] has been introduced to solve the hidden and exposed terminal interference problem. In an underlay CRN, to enable shared access to the licensed spectrum, transmit power control at the secondary transmitter has emerged as an effective way to regulate the secondary interference. In [76], a scheme for the underlay SUs has been introduced to minimize the interference to the PUs. On the other hand, a CDMA-based underlay CR system [77] has focused on the secondary transmit power level increment to counter-balance the interference. However, all the mentioned MAC protocols have assumed the maximum allowed level of primary interference, although such situations rarely exist in practical implementations. There is still an open challenge towards the development of totally self-configuring MAC protocols that can meet the requirements of a wide range of applications.

Among these challenges, few are addressed in this thesis work. The next section has described the motivation behind this research work.

### 1.3 MOTIVATION

There are several factors in the area of underlay CRN where the scope of further research is present. One of the significant characteristics of the underlay CRNs is to use licensed spectrum even if the owner (PU) of that spectrum band is active. This characteristic can reduce the scarcity of free spectrum band for future wireless applications. Hence, this thesis has focused on the design of a cost-effective but reliable underlay CRN. However, the implementation process of a radio network needs to handle multiple design constraints. Amongst these design constraints, this thesis has focused on precise PU localization, optimum resource selection, and transmission power optimization for SUs.

The purpose of localization is to detect the accurate physical coordinates of the PUs in the CRNs. The specific location information of a PU is one of the essential requirements of an underlay CRU or SU to utilize licensed spectrum without causing severe interference to the primary receivers. Though a PU does not interact directly with a CRU during the localization process, the received signal strength indicator (RSSI) which gives a direct measure of the SNR can be used for localization. However, the RSSI measurement changes with the terrain conditions due to fading and shadowing effects on the channel for the same separation distance between the transmitter and the receiver. Besides, the internal noise of a radio receiver also influences the RSSI measurement. The uncertainty in the RSSI measurement leads to false detection and miss detection probabilities while decoding the signal transmitted by the PUs in an underlay CRN. Therefore, this thesis has focused on the mitigation of shadowing effects and radio receiver circuit generated internal noise during the localization process in an underlay CRN. However, it is very challenging for a single CR user to determine location coordinates of a mobile PU due to its random movement within the network. Therefore, a group of collaborative CRUs is considered to estimate the precise location coordinates of mobile PUs.

The principal motivation behind the research on channel selection scheme is the difficulty in finding a reliable channel frequency over time and space due to the coexistence of PUs as well as hidden terminals. One of the fundamental design problems is how the underlay CRUs will decide when and which licensed channel should be selected for

communication [78-80]. Hence, this thesis work has also focused on the design of a cost-effective optimum channel selection scheme.

However, during the cognitive communication on a selected channel frequency, the interference probability with the primary receivers is very high. Therefore, transmission power optimization for SUs is another significant area of research in the underlay CRNs.

## 1.4 SCOPE OF THE THESIS

CR is a very broad and highly multidisciplinary technology involving several fields of research such as smart antennas, hardware architectures, signal processing, communication theory, learning mechanisms, dynamic spectrum allocation methods, cognitive network security and protocol design. Moreover, cognition may take place in all the layers of a protocol stack of the open systems interconnection (OSI). However, the main focus of this thesis is on the development of reliable and rigid underlay CRN. Since the interference constraints are restrictive in the underlay CRN, not only the coverage area of the CRN is limited, but also the secondary transmit power is limited. Besides the transmit power limitation, the CRN is also subjected to distinct channel impairments such as fading and interference. Hence, it is very challenging to achieve a good quality of service (QoS) in a wireless channel due to the detrimental effects of fading. So, to enhance the performance of an underlay CRN, the goal of the thesis is the precise localization or detection of licensed users or PUs, optimum resource selection, and transmission power optimization.

The **first goal** of this thesis is to precisely determine the location coordinates of the PUs in the network for efficient underlay CR communication. Therefore, to locate a fixed as well as a mobile PU, a localization hypothesis has been proposed based on the RSSI measurement. However, the challenge of RSSI-based localization is its high sensitivity to the ambiance changes. The RSSI measurement changes with different terrain conditions for the same separation distance between a transmitter and a receiver. This variation in the RSSI value limits the accuracy of position estimation of an unknown PU using the weighted centroid localization (WCL) algorithm. Therefore, to improve the measurement accuracy of RSSI in different terrain conditions, the log-normal shadowing model with a correction factor has been introduced [81] [82]. On the other hand, the internal noise of a receiver circuit also

degrades the quality of the received signal which, in turn, reduces the localization accuracy. Therefore, this thesis work also has focused on the minimization of internal noise by designing a suitable FIR (Finite Impulse Response) filter after the demodulator stage of a CR receiver circuit. The modified CR receiver circuit has been emulated on the bench with a suitable setup to monitor the improvement of the received signal strength. However, localization of a mobile PU is more challenging to a single CRU due to its random movement within the network. Therefore, to overcome the limitations of a single CRU, a group of collaborative CRUs has been considered in [219] to localize a mobile PU precisely. In this scheme all the collaborative CRUs share its location coordinates and signal strength information which has been received from a mobile PU with each other. The WCL algorithm with filtered signal strength information has been used to compute location coordinates of the mobile PU. To enhance the accuracy, mean of the localization results which has been computed at the each of the collaborative CRUs has been considered. Therefore, after locating the accurate position of a PU in an underlay CRN, a channel selection is necessary to execute the underlay CR communication successfully.

The **second goal** of this thesis work is to develop a channel selection scheme for the underlay CRNs [83]. A channel selection hypothesis has been proposed to determine channel quality based on the strength of the received signal. Since the underlay CRUs use the partially occupied licensed spectrum band, the transmitted signal by the PU has been considered as an interfering factor along with the link noise and internal noise during the channel selection process. A circuit has been designed and tested to authenticate the proposed hypothesis. For testing purpose, the given spectrum (200 MHz to 400 MHz) is split into 'B' numbers of narrow bands (1 MHz). A channel with a given bandwidth (BW) has been selected randomly as per the principle of Hill Climbing algorithm [84]. Hereafter, the RSSI of the selected channel has been compared with the predefined system threshold ( $\lambda_{s/m}$ ). When the measured RSSI value of the selected channel is higher than or equal to the predefined system threshold ( $\lambda_{s/m}$ ) then the selected channel frequency BW is increased by 1 MHz. On the other hand, when the signal strength of the selected channel is less than the desired system threshold, the program will randomly choose another frequency slot to continue the same process. However, the selected channel frequency has to be scheduled for



use by the medium access control (MAC) protocols. Moreover, overhead time minimization, throughput maximization and controlling of the interference level at the primary receiver within the limit during the underlay CR communication, are also handled by the MAC protocols. Therefore, the MAC protocol design is also a critical issue to implement an underlay CRN successfully.

The **third goal** of this thesis is to develop an efficient MAC protocol to minimize interference from the hidden terminals, back-off waiting time, and interference with the PUs. The underlay CRUs are allowed to use licensed spectrum efficiently by keeping the resultant interference at the primary receiver below the predefined threshold. The interference with the transmission from hidden PUs also affects the data reception at the secondary receiver end. Therefore, a receiver-initiated (RI) MAC protocol [83] has been proposed to conduct data communication by the SUs efficiently. In this protocol, a secondary receiver starts the communication by sending locally sensed least noisy carrier frequency information through a command control frame. Hence, the receiver initiated channel selection scheme has reduced the collision probabilities with the hidden PUs. However, the RI MAC protocol cannot minimize the outage probability at the primary receiver due to the fixed secondary transmit power. Therefore, to keep interference level at the primary receiver within a limit, transmit power optimization of SU is necessary. Hence, a transmitter-initiated (TI) MAC protocol [85] with a flexible transmit power selection strategy has been proposed to minimize the outage probability at the primary receiver. In this protocol, the secondary transmit power level is set only after receiving channel quality information from the corresponding secondary receiver. A twin scan process of the selected channel at both ends (secondary transmitter and receiver) has been proposed to select an optimum transmit power. This process also can minimize the interference probability with the hidden terminals. A step-by-step transmit power adjustment concept has been established experimentally to maximize channel utilization and reliability for underlay CRNs. A power control circuit has been designed to implement this flexible power selection concept [85].

The next section provides an outline of the thesis organization with a brief summary.

## 1.5 ORGANIZATION OF THE THESIS

This thesis consists of six (6) chapters. The content of each chapter has been described here, in brief.

### **Chapter II:**

This chapter contains a literature review required for this thesis work. It starts with a brief survey on various localization issues and its importance in the CRNs. Survey also follows the different possible solutions proposed by the researchers. Hereafter, the survey focuses on the challenges and importance of MAC protocol design for CRN. Based on studies by different researchers on MAC protocols, a classification has been done considering critical characteristics and parameters. Further, transmit power control schemes of SUs have been reviewed.

### **Chapter III:**

A new analytical framework for RSSI based localization scheme to calculate the precise location coordinates of a fixed as well as a mobile PU in an underlay CRN has been described in this chapter. Based on the proposed localization hypothesis, the location coordinates of a fixed PU has been computed in different terrain conditions by applying the weighted centroid localization (WCL) algorithm. Subsequently, a collaborative localization scheme has been adopted to compute location coordinates of a mobile PU precisely. The internal noise mitigation scheme has also been proposed by designing a suitable FIR filter block after the demodulator stage of CR receiver circuit, to improve the accuracy of the localization.

### **Chapter IV:**

The concurrent channel selection strategy has been discussed in this chapter. The channel selection hypothesis has been proposed based on the received signal strength to determine the channel quality. Hereafter an interference temperature model has been considered to establish a relationship between signal power and noise temperature. Based on the strength of received

signal, a hardware circuit has been designed and tested to justify the proposed channel selection scheme along with the maximization of channel bandwidth using the principle of Hill Climbing algorithm.

#### **Chapter V:**

This chapter has proposed an efficient underlay MAC protocols to minimize interference with the hidden terminals, elimination of back-off waiting time and transmission power optimization of SUs. Since underlay cognitive communication takes place on a shared carrier frequency with the licensed PUs, the probability of interference with the primary transmission is very high. This affects the useful data reception at the secondary receiver end. If the received data is corrupted, retransmission attempts increase overhead time extremely and it reduces the system efficiency and throughput. Therefore, a receiver-initiated (RI) MAC protocol has been proposed to conduct data communication by the SUs efficiently. However, RI MAC protocol cannot minimize outage probability at the primary receivers due to fixed predefined transmit power of the SUs. Therefore, a transmitter-initiated (TI) MAC protocol has also been proposed to minimize the outage probability of primary receiver through flexible transmit power selection concept.

#### **Chapter VI:**

Finally, this chapter concludes the thesis and suggests some future research directions.



## CHAPTER II

---

# LITERATURE REVIEW

---

2.1	INTRODUCTION.....	21
2.2	LOCALIZATION.....	24
2.3	MAC PROTOCOL DESIGN.....	28
2.4	TRANSMIT POWER CONTROL IN UNDERLAY NETWORKS.....	37
2.5	DISCUSSION.....	39

### 2.1 INTRODUCTION

The traditional allocation policies of radio frequency (RF) have led to inefficient use of the precious RF spectrum. Also, the ever-growing demand for the spectrum resource due to the fast proliferation of wireless applications renders the fixed spectrum allocation policies inapplicable. Therefore, it is necessary to develop a new communication technology which can utilize the allocated underutilized spectrum more efficiently [6]. Hence the concept of cognitive radio (CR) was proposed in 1999 [7-8] by J. Mitola III *et.al.* at KTH (the Royal Institute of Technology in Stockholm). The CR technology is based on the principle of software-defined radio (SDR) [11]. The SDR adds the software configuration capability to

the radio hardware. As a result, the CR can operate on different RF bands by altering the relevant parameters. An SDR transceiver is capable enough to change its operating specifications according to the radio environment in which it operates. For example, an SDR enabled CR system can control the various communication factors like transfer speed, modulation schemes, power, frequency bands, etc. by sensing the state of the network and the activity of its surrounding users intelligently. CR may have a wide range of application domains. Some prospective areas namely, facility management, machine surveillance and preventive maintenance, precision agriculture, medicine and health, logistics, object tracking, telemetries, intelligent roadside, security, actuation and maintenance of complex systems, monitoring of indoor and outdoor environments etc. can use CR technology. In the battlefield or in disputed regions, an adversary may send jamming signals to disturb radio communication channels. In such situations, CR technology enabled device can apply handoff technique to use different frequency bands, thereby avoiding the frequency band with a jamming signal. In a health care system, numerous cognitive sensor nodes are placed on patients and they acquire critical data for remote monitoring by health care providers. In 2011, the IEEE 802.15 Task Group 6 approved a draft of a standard for body area network (BAN) [86] technology. On the other hand, the real-time surveillance applications namely, traffic monitoring, environmental monitoring, vehicle tracking etc. may suffer due to link failure. The CR enabled wireless systems can find a better channel or link to overcome such crisis. The IEEE 1609.4 standard proposes multi-channel operations in wireless access for vehicular environments (WAVE). The WAVE system operates with 75 MHz spectrum in the 5.9 GHz frequency band with one control channel and six service channels. However, the WAVE system also suffers from spectrum insufficiency problems [87]. Channel aggregation and the use of multiple channels concurrently are possible in CRN to increase the channel bandwidth [88].

A standard cognitive radio network (CRN) consists of primary users (PUs) and secondary users (SUs) that coexist within the same network. The PUs are allowed to operate on the allocated, licensed spectrum bands with higher priority. On the other hand, the SUs opportunistically access the licensed spectrum. The RF spectrum access by the secondary network depends on the network characteristics and regulatory constraints. Based on the spectrum utilization features, three main CRN paradigms are considered namely underlay,

overlay, and interweave. This thesis work has focused on the fundamental issues related to the underlay CRNs.

In the underlay CRNs, simultaneous cognitive and non-cognitive transmissions from secondary and primary users respectively are allowed on the same channel frequency as long as the level of the interference caused by the SU at the primary receiver is less than the maximum acceptable level. Therefore, the SUs do not have to wait to start data transmission on the licensed channels which are preoccupied by the PUs. However, keeping the secondary interference below the predefined tolerance limit at the primary receiver is a challenging task when the underlay spectrum access policy is considered. An underlay CRU can determine the instantaneous interference level at the primary receiver by overhearing transmission or feedback mechanisms. In [89], a method for adaptive allocation for SUs with limited number of feedback bits of PUs is suggested in order to minimize the inter-network interference. On the other hand, the secondary transmitter has to be very cautious while selecting transmission power level to ensure a minimum probability of interference. Since the interference constraints in underlay systems are typically quite restrictive, this limits the communication range of underlay SUs to a very short distance. The position information or awareness about a PU location is another fundamental requirement at the SUs to minimize interference in the underlay CRNs [90]. However, fading and shadowing effects reduce the accuracy of localization. It leads to the probability of miss-detection as well as false-detection of the primary signal. Therefore, a proper spectrum sensing mechanism is required to fulfill the localization task precisely in underlay CRN. The spectrum sensing is a method for obtaining data about the spectrum usage across multiple dimensions such as time, space, frequency and code. However, in any spectrum sensing process, the principal consideration is the prevention of performance degradation at any PU. It led to the evolution of medium access control (MAC) protocols for CRNs. In CRNs, MAC protocols perform a significant role for opportunistic allocation of the available RF spectrum. The MAC protocols also mitigate the interference probability with PUs and control the SUs either in a fixed manner or using random access mechanisms [91-92] for spectrum access. However, the MAC protocols which are designed for CRNs may suffer from severe performance degradation due to the multi-channel hidden terminal interference problem, sensing error, selection of common control channel, and network coordination problem [91].

This chapter has examined the fundamental operating principals of CR technology. In the underlay CRNs, transmit power selection is one of the essential criterions to minimize interference probability with the PUs. Therefore, it is necessary to evaluate the precise distance of a PU from the secondary transmitter for selecting optimum transmission power level of SU. The position information of a PU has also been used to enhance spectrum utilization. In section 2.2 a brief overview on the localization schemes used in CRNs is presented. The localization issue in CRN also involves the physical and MAC layer. A CR system behaves more accurately if the physical layer parameters are considered through proper MAC protocols. An overview and comparative survey on MAC protocols has been discussed in 2.3. Hereafter, the secondary transmission power optimization process and its importance in an underlay CRN have been addressed in section 2.4.

## 2.2 LOCALIZATION

The channel selection for the underlay CRNs is possible using the theory of compressive sensing (CS). Before channel selection, the underlay cognitive radio users (CRUs) must reliably detect accurate position coordinates of the licensed users or PUs in order to minimize interference. Precise localization is a difficult but important problem for successful operation of underlay CRNs. The objective of localization is to find the accurate physical coordinates of unknown nodes [90]. Therefore, to track PUs in a CRN, Bayesian technique has been presented in [93].

The localization schemes in CRNs have been classified into two broad categories: range-based [94] and range-free [95]. The range-free localization scheme depends on the connectivity information between the transmitter and receiver nodes which are involved in the localization process [96]. However, due to poor accuracy in the localization process, the range-free scheme is not suitable for underlay CRNs. On the other hand, range-based scheme depends on the measurement of distance or angle (range information) between the nodes to determine the location of an unknown node [97-98] with better accuracy, as compared to the range-free scheme. In the next subsection, range-based localization scheme has been discussed.



### 2.2.1 Range Based Localization

The range-based localization algorithms [99] consider the measured value of received signal to calculate the distance or angle between nodes (point-to-point measurement). Since the signal strength measurement during the localization process is used for range estimation, this scheme is termed as the range-based method. In the range-based method, localization of an unknown node is accomplished in two steps, namely ranging and then position computation. In the ranging step, the distance between the unknown PU and detector node or CRU can be determined by any of the methods, namely TOA (Time of Arrival), TDOA (Time difference of Arrival), RSSI (Received Signal Strength Indicator) or AOA (Angle of Arrival). In TOA and TDOA methods, the propagation time [99] is utilized to calculate the unknown distance. The AOA method measures the angle of the received signal to calculate the positions of unknown nodes. A hybrid localization scheme, based on RSSI and TOA or TDOA, has been addressed in [100]. However, it is very challenging to achieve timing synchronization with the TOA or TDOA in the CR systems. Moreover, TOA and TDOA methods require additional acoustic hardware. In the AOA method, an additional antenna array is required to implement the ranging step in the localization process. Hereafter, in the positioning step, the location coordinates of the unknown nodes are computed by Trilateration or Triangulation [101] methods. The localization accuracy achieved by this type of algorithms is high, but the resource cost is relatively high due to the requirement of additional hardware and optimum synchronization. Therefore, these algorithms are not suitable for localization in a large-scale network. An intelligent outdoor positioning scheme was proposed in [102] to calculate the position coordinates of an unknown node by distance measurement. The scheme uses the estimated distance to determine the position of the unknown node. Moreover, the scheme proposed in [102], uses only the received signal strength to compute distance and does not consider any location fingerprinting process in advance or location database. Experimental results of [102] show that the average localization error of the scheme is less than 3m, which is much smaller than the typical normal GPS localization error which is approximately 15m. Since RSSI-based localization is cost-efficient and does not require additional hardware, it is the simplest and yet a reliable approach among all the range-based measurement methods.

### 2.2.2 RSSI Based Localization

Measurement of the RSSI gives a clear idea about the condition of the received signal at the anchor nodes. It indicates the magnitude of electromagnetic wave energy received at a point in a media [103]. RSSI is used by multiple wireless communication networks and standards to determine the quality of the received signal. A novel, RSSI based uncertain data clustering, was proposed in [104] to calculate an unknown distance. The precision of the distance calculation has improved due to the use of a dynamic mapping strategy in [105]. The RSSI is inversely proportional to the distance and is affected by the ambient conditions of the environment. Therefore, when the distance between an unknown node and detector node increases, the RSSI value decreases and when the unknown node is closer to the detector node the RSSI value increases [106]. The distance calculations based on RSSI measurement considers path loss or signal attenuation factor. In real conditions with variable environmental and geographical terrain conditions, the path loss factor is also different. Therefore, path loss exponent is one of the significant parameters which affects distance calculation from RSSI measurement. In [107], a grid-based centralized localization method has been suggested which considers the path loss exponent in an environment to improve the localization accuracy. This method [107] considers all combinations of path loss exponent for each link and determines the target location by the averaging of all combinations.

Multipath fading effects on signal propagation between transmitter and receiver define the characteristics of RSSI. The electromagnetic waves travel in irregular paths and may get reflected multiple times. The reflection is due to the presence of different objects and obstacles in the path. The interaction among the reflected waves causes multipath fading which modulates the amplitude of the signal. Hence, the RSSI measurements are significantly affected by the location of the transmitter and receiver. In [108], the RSSI based new framework, called Sequential Monte-Carlo combined with shadow-fading estimation (SOLID) has been proposed to track the location of small-scale mobile PU accurately. The consideration of shadowing effects in SOLID considerably improves the performance accuracy of localization. Besides, by monitoring temporally-correlated shadow fading, SOLID accurately detects both manipulated and erroneous sensing reports, thus achieving high robustness. Another RSSI-based PU localization scheme, that uses distance calibration in an underlay CRN, was stated in [109]. Through MATLAB simulation, it shows that the proposed scheme can reduce the localization error. An RSSI-based distributed Bayesian

localization algorithm developed on the principal of message passing to solve the approximate interference problem has been discussed in [110]. However, localization attempts by individual nodes and high sensitivity to the ambient condition changes reduce the detection accuracy. The RSSI based localization can be classified into non-cooperative and cooperative schemes.

### 2.2.3 Non-cooperative and Cooperative Localization Schemes

Localization of non-cooperative object refers to the process of locating an object which is not intentionally participating in the localization process but still interferes with the RF spectrum. In [111], an approach to track multiple non-cooperative targets has been suggested. The suggested approach in [111] uses blind source node (BSS) algorithm to identify signal from the multiple identical targets. The RSSI based non-cooperative and cooperative schemes were applied in [112] to perform localization. For non-cooperative schemes, a novel Semi-Order Cone Programming (SOCP) based approach has been suggested in [113]. The SCOP approach seems to maintain an excellent trade-off between system performance and computational complexity. RSSI based non-collaborative localization refers to the individual nodes attempting to localize unknown location of a PU. On the other hand, in collaborative localization (CL) [114], the anchor nodes collaborate with each other to determine the positional information of an unknown node or a PU. In the collaborative localization scheme, the unknown locations of PUs can be determined concurrently by using an iterative method [114]. An RSSI-based cooperative localization method that estimates unknown coordinates of sensor nodes in a network has been recommended in [115]. This localization scheme has been tested and experimental results establish that this work provides an effective solution for localizing sensor nodes in unknown or dynamic environments.

### 2.2.4 Centroid Localization Algorithm

Centroid localization (CL) is a range-free technique which uses the knowledge of adjacent connected anchor nodes to determine the location of an unknown node or a PU [116]. The CL algorithm was developed by Bulusu et.al. [117] to determine the location coordinates of an unknown node using the known location coordinates of the anchor nodes which exist within the range of communication of the unknown node. The anchor node is defined as a secondary node which assists in the localization process by transmitting a beacon containing

its own location coordinates towards a secondary detector node or the detector CRU. The secondary detector node is responsible for estimating the location coordinates of an unknown PU. The location calculation, by using CL algorithm, is simple and economic but the calculated coordinates are not very reliable because of the probability of significant localization error. Therefore, weighted centroid localization (WCL) algorithm [118], an enhanced version of the CL method has been developed to compute the coordinates of unknown nodes. The WCL algorithm is based on RSSI which makes it simple, cost-effective, and transparent to the variation of the RF propagation environment. The RSSI values, corresponding to the transmitted signal from a PU and received at the respective anchor nodes, are defined as weights. The secondary detector node consider all the known location coordinates of anchor nodes and received signal strength information to estimate the unknown location coordinates of a PU. In [119], WCL algorithm has been recommended for outdoor localization scheme. The WCL algorithm involves lower computation complexity and minimum hardware cost but needs to compute the path loss and the distances between the unknown node and anchor nodes. In [120], H. Y. Shi proposed an anchor optimized, modified WCL algorithm based on RSSI. A weight-compensated WCL (WC-WCL) algorithm based on RSSI for an outdoor environment has also been stated in [121]. In WC-WCL algorithm, the unknown node position has been estimated by compensating the RSSI and the coordinates of anchor nodes. The theoretical analysis shows that the WC-WCL algorithm has the advantage of lower complexity, the minimum requirement of prior information, and lower power consumption. The simulation results show that the WC-WCL algorithm is better than WCL in terms of the localization accuracy.

In the next section a review on the importance, design requirement and classification of cognitive MAC protocols has been undertaken.

### **2.3 MAC PROTOCOL DESIGN**

MAC protocols are designed and implemented to provide the proper coordination during the spectrum access by a set of CRUs. The MAC protocol is responsible for effective and efficient communication. However, the CRUs must exchange the control information and spectrum information through a common control channel (CCC) before initiating data transmission. The MAC protocols support CRUs to access the CCC. The next subsection has

discussed the fundamental requirements for the development of an efficient cognitive MAC protocol.

### 2.3.1 Design Requirement of Cognitive MAC Protocol

In CRNs, MAC protocol design consists of two parts namely, sensing technique and access policy. Sensing techniques perform sensing operation to identify the set of available channels. After channel selection, the access policy determines access related issues such as whether to access the selected band or not [122]. However, in CRNs, the MAC protocol design faces various common challenges such as interference from hidden terminals, multipath effects, and parameters selection. Therefore, flexible or adaptive MAC protocol design is essential to maintain efficient sensing ability, adaptability and resource allocation capability of CRUs. The following criteria need to be considered while designing the MAC protocols for CRNs.

- **Accuracy in Cognitive Behaviour**

The accuracy of the cognitive operation depends on efficient spectrum sensing, proper analysis and finally precise channel selection [123]. However, improper spectrum sensing leads to false and miss detection probabilities about the presence or absence of PU signal which may cause harmful interference to PUs [124]. Therefore, the ability to sense the transmitted signal precisely from a PU is one of the fundamental requirements for an efficient MAC protocol [72] design for CRN. Hence, a MAC protocol needs to be designed to produce minimum negative effects on the system performance while at the same time meeting the accuracy and timing requirements.

- **Sensing Time**

An efficient MAC protocol should also consider channel interference and maximum data handling capacity of a channel. The data should be forwarded to a node which provides the highest margin for delay budget [72]. Furthermore, the MAC protocol needs to suspend all the communications within the CRN when spectrum sensing is carried out. This suspension condition is called quite sensing periods. So overall data transfer suffers and system throughput decreases. As a result, quite periods degrade the overall quality of service (QoS) of CRN. Hence, it is necessary to adopt suitable MAC protocols with optimum sensing durations [72].

- **Common Control Channel (CCC) Selection**

A MAC protocol needs exchange of control information through a common control channel (CCC) to establish data communication link among the CRUs. The CCC information must be available to all CR nodes for subsequent synchronization and data transmission. The control channels can either be static or dynamic. The use of the Industrial Scientific and Medical (ISM) band or underlay ultra-wideband frequency to exchange the control information is considered as a static approach. In [125-126] CRUs are assigned a control channel within the unlicensed band. On the other hand, the dynamic channel approach can be classified into two types, dedicated and non-dedicated CCC. A modified MAC protocol for decentralized CRNs was proposed in [127] without considering a dedicated CCC. A stable control channel was used in [127] to exchange control information among the CRUs. The concept of a stable control channel was accomplished by maintaining a status table of channels and updates about the status of the channels frequently at each CRU. However, this approach has stringent time requirement to select a stable control channel. On the other hand, in the centralized CRNs, a dedicated channel can be assigned as a CCC by the central administration for the CR users [128]. Classification of cognitive MAC protocols has been discussed in the next subsection.

### 2.3.2 Classification of MAC Protocol

The MAC protocols used in CRNs can be classified in terms of four parameters namely, architecture, spectrum sharing behaviour, spectrum sharing mode, and access mode. Those are depicted in Fig.2.1.

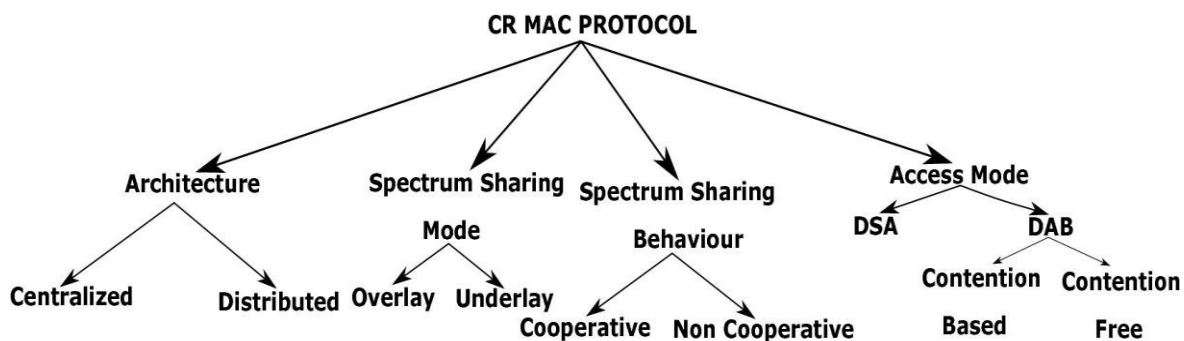


Figure 2.1: Classification of CR MAC Protocols

Depending on the CRN architectures, the MAC protocols are subdivided into two categories, one is meant for centralized network and the other one is for distributed network. In centralized networks, the central controller (fusion center) supports MAC protocols to coordinate the channel access mechanism. On the other hand, MAC protocols in the distributed networks execute channel access mechanism without a central coordinator. In [79], a detailed survey has been taken up on the dynamic access network architecture. In [92], MAC protocols for infrastructure-based and ad-hoc networks are differentiated according to the medium access scheme. The MAC protocol in the wireless regional area network (WRAN) based on the IEEE 802.22 standard [129-130] has been suggested for the centralized network architecture. A decentralized cognitive (DC) MAC protocol, based on a Partially Observable Markov Decision Process (POMDP) framework, is described in [51] to address hardware constraint, sensing error and channel availability. A hardware constraint (HC) MAC protocol [71] has been introduced within the distributed network architecture to minimize hardware constraint. In [131], a framework of a cognitive mesh network (COMNET) has been suggested to support opportunistic spectrum access (OSA) in wireless mesh distributed networks. Generally, centralized MAC protocols are highly dependent on the central controller. If the central controller fails, the whole network will fail. On the contrary, distributed MAC protocols are more resilient and scalable.

The MAC protocols are classified as overlay or underlay type in spectrum sharing mode. An underlay spectrum sharing based CR MAC protocol was recommended in [132] to investigate the dynamic spectrum sharing problem among PUs and SUs. In [76], a scheme of channel allocation for the SUs in underlay CRNs has been discussed. The proposed scheme in [76] minimizes the interference probability with the PUs. On the other hand, a CDMA-based underlay CR system [77] focuses on the increase of SUs transmit power to counter-balance the harmful interference. Another underlay MAC protocol, COMAC is described in [74]. COMAC allows SUs to transmit in the spectrum band of the PUs at low power levels to avoid harmful interference. The fundamental drawback of COMAC protocol is high probability of interference from the hidden terminals. It also faces a challenge when multiple users simultaneously access the control channel in the same network. Various overlay MAC protocols have also been suggested by researchers. The overlay access paradigm is investigated in [133] and is compared with the classical interweave approach. An Opportunistic spectrum access (OSA) overlay MAC protocol has

been introduced in [134] by considering synchronized transmission and hidden terminal problem. However, the fundamental drawback of OSA protocol is the requirement for a dedicated control channel.

Based on the access mode, MAC protocols are split into two categories namely direct access based (DAB) and dynamic spectrum allocation (DSA). In DAB protocols, without considering network optimization, each sender-receiver pair negotiates resource sharing using a traditional handshake procedure [135]. Moreover, each DAB protocol is classified further as contention based or coordination based. A contention-based MAC protocol, associated with the back-off process at the contending nodes, has been proposed in [136]. COMAC [74] is a contention-based protocol that tries to satisfy QoS constraint by limiting the number of channels per user. The DSA-driven MAC protocols exploit advanced optimization algorithms to realize intelligent, fair and efficient allocation of the available spectrum [135]. Various mathematical approaches such as graph theory [137], game theory [139], stochastic theory [51], genetic algorithm [140] etc. are considered to model the DSA network. Both DAB and DSA protocols can be deployed in centralized or distributed architectures. Table 2.1 shows a comparative survey on MAC protocols based on different parameters mentioned before.

In CRNs, secondary receiver performance degrades due to the path loss and fading effects. Moreover, interference or collisions may occur if multiple SUs transmit on the same channel at the same time. The MAC protocols are designed to minimize collisions amongst the SUs. Based on the principle of carrier sense multiple accesses with collision avoidance (CSMA/CA) [92], MAC protocols need not have to maintain time synchronization to perform collision detection. A CSMA based multichannel centralized MAC protocol was proposed in [140] to improve spectrum utilization and throughput performance. Single radio based statistical multi-channel allocation (SCA-MAC), a decentralized MAC protocol was suggested in [142] for efficient channel allocation. On the other hand, a CSMA based MAC protocol developed on the concept of a single transceiver and in-band signalling with simultaneous transmission of the CRUs was proposed in [147]. The presence of hidden and exposed terminals within the network is one of the fundamental reasons for interference or collision. A decentralized single transceiver based dynamic open spectrum sharing (DOSS) multichannel MAC protocol has been suggested in [75] to solve the problem of hidden and exposed terminals.



Table 2.1: Comparative Evaluation of MAC Protocols

MAC Protocol	CSMA MAC [140]	DNG MAC [141]	SCA MAC [142]	DOSS [75]	CREAM [143]	OC MAC [144]	A-MAC [127]	Game Theoretic DSA [138]	C-MAC [145]	OS MAC [146]	SYN MAC [92]	IEEE 802.22 [130]
Network Architecture	Centralized	x	x	x	x	x	x	✓	✓	✓	x	✓
	Distributed	x	✓	✓	✓	✓	✓	x	x	x	✓	x
Spectrum Sharing Behaviour	Cooperative	✓	x	x	✓	x	x	✓	✓	x	✓	✓
	Non-cooperative	x	✓	✓	✓	✓	✓	x	x	✓	x	x
Spectrum Mode	Overlay	x	✓	✓	✓	✓	x	✓	✓	✓	✓	✓
	Underlay	✓	x	x	x	x	✓	x	x	x	x	x
Access Mode	Contention free	D	x	✓	x	x	x	x	✓	x	x	✓
		A	x	x	x	x	x	x	✓	x	x	x
	Contention based	B	✓	✓	x	✓	✓	x	x	✓	✓	x
DSA		x	x	x	x	x	x	✓	x	x	x	x

Table 2.2: Comparative Study on MAC Protocols Based on Characteristics Features

MAC Protocol	CSMA MAC [140]	DNG MAC [141]	SCA MAC [142]	DOSS [75]	CREAM [143]	OC MAC [144]	A-MAC [127]	Game Theoretic DSA [138]	C-MAC [145]	OS MAC [146]	SYN MAC [92]	IEEE 802.22 [130]
Random Access	√	×	√	√	×	√	√	×	×	×	×	×
Time Slotted	×	√	×	×	×	×	×	×	√	×	×	√
Hybrid	×	×	×	×	√	×	×	√	×	√	√	×
Heterogeneous Network	√	√	×	√	×	√	×	√	×	×	×	×
Homogeneous Network	×	×	√	×	√	×	√	×	√	√	×	√
Single Radio	×	√	√	×	√	√	√	×	×	√	×	√
Multi Radio	√	×	×	√	×	×	×	√	√	×	√	×
Unlicensed CCC	×	×	√	√	√	√	×	×	×	√	×	×
Licensed CCC	√	√	×	×	×	×	√	√	√	×	√	√

A novel DSA-driven MAC protocol to achieve highly efficient spectrum usage and QoS provisioning was proposed in [148]. In this protocol [148], SUs are separated into various non-overlapping groups for dynamic channel allocation. However, the game-theoretic dynamic spectrum allocation (DSA) technique is a better approach to coordinate spectrum sharing among the CRUs. A novel multichannel time slotted channel reservation-based MAC protocol (TSCR-MAC) for CRNs was proposed in [73]. The TSCR-MAC protocol enhances spectrum utilization efficiency and throughput performance. Table 2.2 shows the comparative analysis of characteristic features of MAC protocols which are designed for CRNs

### **2.3.3 Learning Based Intelligent MAC Protocol**

Learning defines behaviour modification through practice, training, and experience. The ability of efficient learning capability is essential for intelligent behaviour. Thus, learning is indispensable to any cognitive system and must be at the foundation of CRNs. By implementing learning capability, a network system can classify, organize, synthesize and generalize information collected from the surroundings. Therefore, learning mechanisms help to build up knowledge and knowledge bases. The need for adaptive behaviours motivates the adoption of computational intelligence methods like machine learning in CRN. In the area of machine learning, Q-Learning is a simple yet powerful reinforcement learning technique widely used in applications, where an on-line optimal action-selection policy is required. A Q-learning-based dynamic spectrum access method for the industrial internet of things (IIoT) by introducing cognitive self-learning technical solution has been developed. It helps to solve the difficulty of distributed and ordered self-accessing for unlicensed terminals in [220]. In this work [220], a Q-learning based multi-channel access scheme was suggested for the unlicensed users migrating to other lower cells. The channel with the highest Q value is selected. A novel contention-based MAC protocol for wireless sensor networks, named QL MAC and based on a Q-learning approach, was proposed in [221]. The protocol aims to find an efficient wake-up strategy to reduce energy consumption on the basis of the actual network load of the neighbourhood. Moreover, it benefits from a cross-layer interaction with the network layer. It can, therefore, better understand the communication patterns and then to

significantly reduce energy consumption due to both idle listening and overhearing. An intelligent Medium Access Control (MAC) protocol selection scheme, based on machine learning in wireless sensor networks, has been proposed in [222]. The impact of the inherent behaviour of the cognitive system and variable external environments were considered in [222]. This scheme in [222] can benefit from the combination of the competitive protocols and non-competitive protocols and helps the network nodes to select the MAC protocol that suits the current network condition the best.

On the other hand, an adaptive MAC protocol selection scheme based on machine learning was proposed for cognitive radio networks in [223]. This scheme can combine the respective advantages of the competitive protocols and non-competitive protocols according to the network loads and can help the network nodes to select the MAC protocol that suits the current network circumstances the most. An opportunistic p-persistent carrier sense multiple access schemes for the underlay cognitive radio networks have been developed in [224]. This carrier sensing scheme opportunistically exploits wireless channel conditions while transmitting data to the secondary access point. Furthermore, to minimize collisions among SUs, an adaptive interference-level control technique has also been developed in [224]. To support heterogeneous wireless networks, a Deep-reinforcement Learning Multiple Access (DLMA) [225] has been developed based on the deep reinforcement learning (DRL) scheme. The framework of DLMA is formulated to achieve general  $\alpha$ -fairness among heterogeneous networks. Extensive simulation results show that DLMA can achieve near-optimal sum throughput and proportional fairness objectives. A novel and fully distributed MAC protocol, called S-LEARN, that allows sensor nodes in a CRSN to entwine their RF energy harvesting and data transmission activities has been developed. It addresses the issue of the disproportionate difference between the high power necessary for the node to transmit data packets and the small amount of power it can harvest wirelessly from the environment. The protocol was proposed in [226]. A short preamble cognitive medium access control (SPC-MAC) protocol which supports reliable and fast spectrum access while addressing the energy conservation problem in cognitive radio sensor networks (CRSNs) was introduced in [227]. The novelty of SPC-MAC lies in the combination of short preamble sampling and the opportunistic forwarding.

## 2.4 TRANSMIT POWER CONTROL IN UNDERLAY NETWORKS

The transmit power level control at the SUs is extremely important since an adequate power level is mandatory. Therefore, to maintain the specific quality of service (QoS), the power control for SUs has been considered as multiuser communication problem in [149]. The power control, based on game theory, has been studied in [150] with an interference constraint. However, in most of the approaches a constant power allocation (PA) policy has been considered. A spectrum sharing strategy based on a throughput model in a CRN has been proposed in [151]. In the proposed scheme [151], an optimization problem in the form of binary integer linear programming (BILP) is formulated, where it is assumed that every SU can access any available channel with a transmission range rather than cover the whole CRN. In [152], a joint beam-forming and power allocation for the CR network is considered to maximize transmit power level of SUs while keeping the interference at the PUs below a tolerable level.

To enhance the performance of underlay CRUs, different types of transmit power selection strategies for SUs have been studied. Optimal power control policies that maximize the achievable data transfer rates of underlay CR systems under either peak or average transmit power level have been discussed next.

- **Optimal Power Control Schemes to handle Outage Capacity Constraint**

Optimal power allocation strategy that maximize the ergodic capacity of an SU under either peak or average transmit power constraint was suggested in [153]. In [153], the computation of outage probability at the PU is based on the signal quality of the link between the primary transmitter and primary receiver. On the other hand, in [154] the optimal power control strategy that maximizes the ergodic capacity of the SU subject to peak/average transmit power constraint has been considered together with an upper limit on the outage capacity loss at the PU due to the secondary transmission. In [155], the impact of the transmit power level on fading severity and interference intensity under different practical constellations and Gaussian noise signals has also been investigated.

- **Optimal Power Control Schemes to handle Interference Temperature (IT) Constraint**

For underlay CRNs, a fundamental method to protect the PU is to impose interference power limits on the secondary transmit power level. The interfering power level at the primary receiver terminal due to the secondary transmission must be below a prescribed limit, also known as the interference temperature (IT) constraint [156]. Therefore, to minimize the outage probability at the PU, a maximum limit has been imposed over the secondary transmit power level in [153]. A distributed power control algorithm, based on Euclidean projection, has been suggested in [157] for minimizing total power transmitted by the SUs under the time-varying channel scenario. In this work, maximum transmit power constraint and the minimum SNR requirement for each SU, together with the IT constraint for each PU have been considered. The power allocation problem is transformed into a convex optimization problem without auxiliary variables and has been solved by the Lagrangian dual method [157].

In [158], from the information-theoretic perspective, the authors have proposed the use of the capacity requirement of PU instead of the IT constraint as a new criterion to regulate the SU transmission. The capacity constraint is directly related to the PU transmission and thus improves the spectrum sharing capability. However, to realize this capacity constraint, additional knowledge of the channel state information (CSI) is required at the SU transmitter. However, the additional CSI knowledge is not needed when the IT constraint apply.

- **Medium Access Protocol for Optimal Power Control**

Multiple access-based collision avoidance MAC protocols use fixed predefined transmit power level. Such protocols do not work when dynamic channel selection scheme is applied. MAC protocols with transmit power control functionality are explained in [159]. This work [159] addresses minimum transmit power selection scheme with request to send (RTS) and clear to send (CTS) command before exchanging packets to improve the channel reuse factor of the radio network. In the mobile ad hoc networks (MANETs), one essential issue is how to increase channel utilization while avoiding the hidden-terminal and exposed-terminal problems. A power control mechanism was proposed in [160]. The scheme in [160] allows a node 'A', to specify its current transmit power level in the transmitted RTS and allows

receiver node 'B' to include a desired transmit power level in the CTS sent back to node 'A'. On receiving the CTS, node 'A' then transmits DATA using the power level specified in the CTS. This scheme allows node 'B' to help node 'A' choose the appropriate power level, so as to maintain a desired signal-to-noise ratio. Transmit power is controlled according to packet size in [161]. The proposed scheme is based on the observation that reducing transmit power level can not only result in energy savings, but also can result in less errors. A higher bit error rate can lead to increased retransmissions, consuming more energy. Thus, the protocol in [161] chooses an appropriate power level based on the packet size. An adaptive scheme is also presented in [162] to choose MAC frame size based on the channel conditions.

## 2.5 DISCUSSION

This chapter presents a detailed review work on different localization schemes and MAC protocols used in CRNs. In a CRN, the positional information of an unknown PU is essential as it helps the SUs to use the available spectrum bands without causing harmful interference to the PUs. Several localization techniques have been developed to determine the unknown location coordinates of a PU in the CRN. The localization schemes used in the CRN are classified as range-free or range-based methods. As the range-based methods estimate the positional information of the PU accurately, this thesis work considers the range-based localization method to determine unknown location coordinates of both fixed and mobile PUs. Among the various range-based methods, the RSSI based localization scheme is quite reliable though it is relatively simple to implement and also cost-effective. Therefore, to perform precise localization, this thesis work has considered the RSSI based scheme. Additionally, for efficient channel selection and allocation, MAC protocol design is one of the significant criteria. Various types of MAC protocols have been designed and developed by the research community for CRNs. Different parameters and characteristics have to be considered while designing an efficient MAC protocol. A thorough study on the MAC protocols suitable for CRNs has also been undertaken here.





## CHAPTER III

---

# LOCALIZATION IN UNDERLAY COGNITIVE RADIO NETWORK

---

3.1	<b>INTRODUCTION</b> .....	41
3.2	<b>LOCALIZATION</b> .....	44
3.3	<b>LOCALIZATION OF A FIXED PRIMARY USER</b> .....	51
3.4	<b>LOCATION ESTIMATION OF A MOBILE PU</b> .....	59
3.5	<b>DISCUSSION</b> .....	76

### 3.1 INTRODUCTION

Cognitive radio users (CRUs) or secondary users (SUs) in an underlay cognitive radio network (CRN) are allowed to access the licensed radio frequency (RF) spectrum opportunistically without causing harmful interference to the primary users (PUs). Thus, knowledge about the location coordinates of any PU is required to ensure the effective use of

licensed spectrum. Hence, localization of PUs must be rapid and accurate enough for the successful operation of underlay CRNs. However, the localization issue in the underlay CRNs is generally different from localization in other applications such as wireless sensor network (WSN) and Global Positioning System (GPS) [163]. In an underlay CRN, a CRU can estimate the unknown location by detecting the transmitted signal from a PU. Therefore, to determine the unknown location, a CRU considers received signal-to-noise ratio (SNR) or received signal strength indicator (RSSI). A CRU needs to detect and locate a PU in the CRN even when the SNR of the received signal is less than the minimum requirement, so that the interference with the PUs is avoided. Many existing localization schemes attempt to calculate the position of the PUs accurately. The localization schemes may be classified into two broad categories, namely range-based [94] and range-free [95]. The range-free localization scheme only depends on the connectivity information between the nodes for localization without any extra hardware support [96]. Though this scheme is simple to implement with minimum energy consumption, it is not preferred in the underlay CRNs due to poor localization accuracy. On the other hand, range-based scheme depends on the measurement of distance or angle (range information) between the nodes to determine the location of an unknown node [97-98] with better accuracy, as compared to the range-free scheme. In this scheme, the distance or angle is measured by various techniques like received signal strength indicator (RSSI) [164], angle of arrival (AoA) [165], time difference of arrival (TDoA) [166], and time of arrival (ToA). However, RSSI based localization has been preferred over other techniques since AoA-based distance calculation involves costly hardware, ToA requires perfect synchronization, and TDoA is limited by localization coverage area [167]. A novel RSSI based uncertain data clustering was proposed in [104] to calculate the distance. The precision of the distance calculation has been improved by a dynamic mapping strategy [105]. However, RSSI-based localization is highly sensitive to the ambient condition changes, which reduce the detection accuracy. Therefore, to improve the localization accuracy, RSSI based collaborative localization scheme has been adopted in [168]. Collaborative localization (CL) [114] is an anchor-free localization technique, where the nodes collaborate with each other, to determine the position of an unknown node. A collaborative compressive sensing based approach has been introduced in [169] to calculate the location of any PU. In [170] a

statistical estimation framework, based on the collaborative spectrum sensing context, has been proposed to locate the position of a PU transmitter.

In this chapter, a RSSI based localization scheme for underlay CRNs has been proposed. Emulation and software simulation techniques have been mixed in this work to establish the proposed localization hypothesis. The weighted centroid localization (WCL) algorithm has been introduced in subsection 3.3.1 to compute precise coordinates of a fixed as well as a mobile PU. The RSSI parameter reflects the actual nature of signal reception due to variation in SNR at the CR receiver. However, accuracy of RSSI measurement varies with different terrain conditions for the same distance between a transmitter and a receiver. This variation in the RSSI value limits the accuracy of position estimation of an unknown PU using the WCL algorithm. Therefore, to improve the measurement accuracy of RSSI in different terrain conditions, the log-normal shadowing model along with a correction factor has been introduced in subsection 3.3.2. Hereafter, in subsection 3.3.3, a network scenario has been designed to calculate the accurate position coordinates of a fixed PU under different terrain conditions. However, localization of a mobile PU is more challenging to a single CRU due to its random movement within the network. Therefore, to overcome the limitations of localization by a single CRU, a range-based collaborative localization scheme has been proposed in section 3.4. However, the external or ambient noise effects and internal noise generated in the CR receiver circuit degrade the quality of the received signal, which in turn, reduces the localization accuracy. As the external noise effects in radio communication is unpredictable and unavoidable, the present work has focused on the minimization of internal noise of the radio receiver by designing suitable FIR (Finite Impulse Response) filters after the demodulator stage of a CR receiver. The modified CR receiver circuit has been emulated on the bench with a suitable setup to monitor the SNR improvement, which is described in subsection 3.4.3. Next, the WCL scheme has been applied with the improved strength of received signal to calculate the precise coordinates of a mobile PU collaboratively. This is discussed in detail in subsection 3.4.4.

## 3.2 LOCALIZATION

The objective of localization is to find the accurate physical coordinates of unknown nodes. These coordinates can be either global or relative. The localization is achieved with the help of anchor nodes which are either manually programmed with a physical position or using the global positioning system (GPS). Localization in a CRN refers to the determination of the physical position of an unknown PU using any coordinate system [90]. Therefore, to perform efficient localization, distance is measured between the transmitter and receiver nodes and then the measurement results are correlated with earlier reference measurements to determine the physical position. The information about PU location coordinates can enhance several capabilities of CRNs [171]. Hence, the SUs or CRUs need to detect and localize the unknown location of PUs in the coverage area even at values of RSSI [172] less than the threshold requirement. This section has introduced the significance of RSSI based localization scheme with a hypothesis.

### 3.2.1 Importance of RSSI in Localization Process

The performance reliability of a CR receiver depends on the variable level of the noise floor in the selected channel frequency. Therefore, for successful CR operation, the secondary receiver has to decode the received signal even in the presence of noise. The fundamental criterion for correct decoding is that the power of the received signal must be higher by a given margin with respect to the noise floor. The minimum separation between signal power level and noise power level for reliable radio performance as recommended in [173] is 18dB. The RSSI gives the direct measurement of the signal-to-noise ratio (SNR) of a communication channel together with the signal power and noise power. It is possible to predict the approximate physical distance between the communicating nodes based on the RSSI value which can be obtained by using the proper path loss model. However, the accuracy of path loss models is often very low due to the dynamic characteristics of the radio propagation environments [174-175]. To enhance the accuracy of measurement, a path loss model has been considered with a correction factor in this work. There are generally two fundamental approaches in the RSSI-based localization. The first approach assumes prior information on the environment, such as the Simultaneous Localization and Mapping

(SLAM) methods [176-177] and the second one is a two-step approach without any prior information.

In the two-step approach, there are two phases to complete the total localization process. Firstly, there is a learning phase, where data from the target area is collected and stored in the learning database. Secondly, there is a user localization phase, where localization is performed based on the data obtained from the learning phase. In this work, the two-step approach has been applied since no prior information is available except transmitted signal strength information of PU during the localization process. A RSSI-based localization hypothesis has been described in the next subsection.

### 3.2.2 Hypotheses on the PU Signaling Information

The CR enabled nodes sniffs the spectrum in the time domain. The decision statistics ( $D_{SI}$ ) [178] of received signal  $\{r(t)\}$  is given by-

$$D_{SI} = \frac{1}{N} \sum_{N-1}^N |r(t)|^2 dt \quad (3.1)$$

In equation (3.1),  $N$  is the sample size of the received signal  $\{r(t)\}$ .  $D_{SI}$ , is compared with the predefined system threshold ( $\lambda_{s/m}$ ) to determine presence or absence of PU signal.

$$H_a : D_{SI} < \lambda_{s/m} : \text{PU signal absent}$$

$$H_p : D_{SI} \geq \lambda_{s/m} : \text{PU signal present}$$

The hypothesis  $H_a$  becomes true when the transmitted signal from a PU is absent in the received signal  $\{r(t)\}$ . On the other hand, the hypothesis  $H_p$  becomes true when the received signal  $\{r(t)\}$  contains transmission from a PU. In case of hypothesis  $H_p$ , the strength  $\{P(t)\}$  of the transmitted signal by a PU is higher than the sum of the link noise ( $P_{ln}$ ) and internal noise ( $P_{in}$ ). However, during the localization process, if the strength of the noise is very high compared to the received signal strength from a PU then there will be a probability of miss or false detection.

Therefore, the signal to noise ratio ( $\gamma$ ) [179] is defined as the ratio of signal variance ( $\sigma_s^2$ ) to noise variance ( $\sigma_n^2$ ) as shown in equation (3.2).

$$\gamma = \frac{|h|^2 \sigma_s^2}{\sigma_n^2} \quad (3.2)$$

In equation (3.2),  $|h|$  represents the channel power gain. In the learning phase, when the sample size of received signals is large enough ( $N \geq 100$ ), then by central limit theorem (CLT), mean ( $E$ ) and variance ( $Var$ ) of  $E_{sI}$  under the hypothesis  $H_a$  are computed and denoted as  $N\sigma_n^2$  and  $N\sigma_n^4$  respectively. Similarly, under the hypothesis  $H_p$ , mean ( $E$ )  $N\sigma_n^2(1 + \gamma)$  and variance ( $Var$ )  $N\sigma_n^4(1 + 2\gamma)$  are also computed.

The  $Q(\cdot)$  function [180] is a complementary cumulative distribution function, which calculates the tail probability of a zero mean unit variance Gaussian variable. The function can be written as-

$$Q(x) = \frac{1}{\sqrt{2\pi}} \int_x^{\infty} \exp\left(-\frac{t^2}{2}\right) dt \quad (3.3)$$

$$\text{Probability of Successful Detection } (P_{sd}) = Q\left(\frac{\lambda_{s/m} - E(H_p)}{\sqrt{Var(H_p)}}\right) \quad (3.4)$$

In the above expression,  $E(H_p)$  and  $Var(H_p)$  are the mean and variance under hypothesis  $H_p$  respectively. Substituting the values of mean and variance in equation (3.4).

$$P_{sd} = Q\left\{\left(\frac{\lambda_{s/m}}{N\sigma_n^2} - 1 - \gamma\right) \sqrt{\frac{N}{(1 + 2\gamma)}}\right\} \quad (3.5)$$

$$\text{Probability of False Detection } (P_{fd}) = Q\left(\frac{\lambda_{s/m} - E(H_a)}{\sqrt{Var(H_a)}}\right) \quad (3.6)$$

In the above expression,  $E(H_a)$  and  $Var(H_a)$  are the mean and variance under hypothesis  $H_a$  respectively. Substituting the values of mean and variance in equation (3.6).

$$P_{fd} = Q\left\{\left(\frac{\lambda_{s/m}}{N\sigma_n^2} - 1\right) \sqrt{N}\right\} \quad (3.7)$$

Probability of Miss Detection ( $P_{md}$ ) =  $(1 - P_{sd})$

$$P_{md} = \left[ 1 - Q \left\{ \left( \frac{\lambda_{s/m}}{N\sigma_n^2} - 1 - \gamma \right) \sqrt{\frac{N}{(1+2\gamma)}} \right\} \right] \quad (3.8)$$

A pre-defined system threshold ( $\lambda_{s/m}$ ) is required to take decision about the presence or absence of adequate PU signal. Thus, the selection of the optimum system threshold ( $\lambda_{s/m}$ ) is very important to avoid false detection and miss-detection possibility during the localization process. The false detection happens when a CRU falsely detect the presence of a PU signal within the interference level. On the other hand, the miss-detection happens when a CRU takes a wrong decision about the absence of a PU signal due to interference on the same channel. False detection arises when the received signal at the radio receiver is affected by constructive fading. Miss-detection, on the other hand, may happen due to internal noise and fading effects.

Therefore, to minimize both false detection and miss-detection probabilities and enhance the successful detection probability, the system threshold ( $\lambda_{s/m}$ ) selection model has been described in the next subsection.

### 3.2.3 System Threshold Selection

Received signal power at CR receiver is affected by three factors, namely distance, average path loss and log-normal variation. The common practice of selecting the system threshold ( $\lambda_{s/m}$ ) is based on false detection probability. When the value of  $\lambda_{s/m}$  increases (or decreases), both  $P_{fd}$  and  $P_{md}$  decrease (or increase). Fig.3.1 shows that for a fixed signal-to-noise ratio (SNR), the probability of false detection ( $P_{fd}$ ) increases with decrease in the probability of miss-detection ( $P_{md}$ ). However, when the SNR is high,  $P_{md}$  is comparatively low. Fig.3.2 demonstrates a relationship between  $P_{sd}$  and  $P_{fd}$  for a fixed value of SNR. Therefore, the detection probability of  $P_{sd}$  and  $P_{fd}$  is directly proportional to each other.

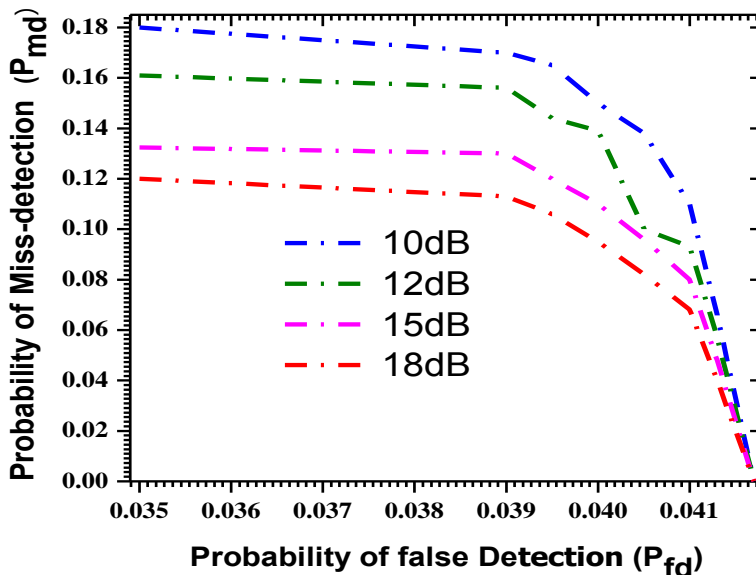


Figure 3.1: Relation between Miss Detection and False Detection Probabilities

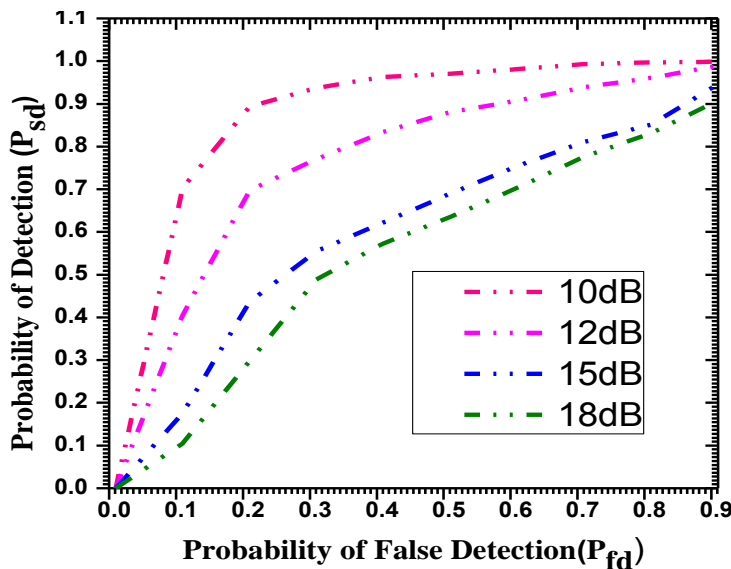


Figure 3.2: Relation between Successful Detection and False Detection Probabilities

Again, to achieve the high value of  $P_{sd}$ , the  $P_{md}$  must be kept very low. However, with time,  $P_{fd}$  may increase. Therefore, the optimum threshold selection can be viewed as the minimization of the total error probability ( $P_e$ ) [181] which is defined as-

$$P_e \cong P_{fd} + P_{md} = \left\{ P(H_a)P_{fd} + P(H_p)P_{md} \right\} \quad (3.9)$$



Hence, the optimum threshold  $(\lambda_{s/m}^*)$ [179] can be written as-

$$\lambda_{s/m}^* = \arg \min(P_e) = \arg \min \left\{ P(H_a)P_{fd} + P(H_p)P_{md} \right\} \quad (3.10)$$

In equation (3.10),  $P(H_a)P_{fd}$  is the probability of false detection of primary signal when primary transmission is absent and  $P(H_p)P_{md}$  is the probability of miss-detection of primary signal when primary transmission is present. Hence, both the terms can also be represented as complementary error function  $\{Erfc(\cdot)\}$ [180], as given below:

$$Erfc(x) = \frac{2}{\sqrt{\pi}} \int_x^{\infty} e^{-t^2} dt \quad (3.11)$$

The standard ' $Q$ ' function in terms of complementary error function can be written as-

$$Q(x) = \frac{1}{2} Erfc\left(\frac{x}{\sqrt{2}}\right) \quad (3.12)$$

Therefore, based on  $Erfc(\cdot)$ , both the error probability factors can be written as-

$$P(H_a)P_{fd} = Q(P_{fd})$$

$$\text{or, } P(H_a)P_{fd} = \left\{ \frac{1}{2} Erfc\left(\frac{P_{fd}}{\sqrt{2}}\right) \right\}$$

$$\text{or, } P(H_a)P_{fd} = \left[ \frac{1}{2} Erfc\left\{ \frac{1}{\sqrt{2}} \left( \frac{\lambda_{s/m}}{N\sigma_n^2} - 1 \right) \sqrt{N} \right\} \right] \text{ (Substitute } P_{fd} \text{ from equ.3.7)}$$

Multiplying both numerator and denominator by  $\sqrt{N}$

$$\text{or, } P(H_a)P_{fd} = \left\{ \frac{1}{2} Erfc\left(\frac{\lambda_{s/m} - N\sigma_n^2}{\sqrt{2N}\sigma_n^2}\right) \right\} \quad (3.13)$$

Similarly,

$$P(H_p)P_{md} = Q(P_{md}) = Q(1 - P_{sd})$$

$$\text{or, } P(H_p)P_{md} = \left\{ 1 - \frac{1}{2} Erfc\left(\frac{P_{sd}}{\sqrt{2}}\right) \right\}$$

$$\text{or, } P(H_p)P_{md} = \left[ 1 - \frac{1}{2} Erfc\left\{ \frac{1}{\sqrt{2}} \left( \left( \frac{\lambda_{s/m}}{N\sigma_n^2} - 1 - \gamma \right) \sqrt{\frac{N}{(1+2\gamma)}} \right) \right\} \right] \text{ (Substitute } P_{sd} \text{ from equ.3.5)}$$

Multiplying both numerator and denominator by  $\sqrt{N}$

$$\text{or, } P(H_p)P_{md} = \left[ 1 - \frac{1}{2} \text{Erfc} \left\{ \frac{\lambda_{s/m} - N\sigma_n^2(1+\gamma)}{\sqrt{2N}\sigma_n^2(1+2\gamma)} \right\} \right] \quad (3.14)$$

The optimum threshold ( $\lambda_{s/m}^*$ ) [179] for an AWGN (Additive White Gaussian Noise) fading channel, can be obtained by substituting equation (3.13) and (3.14) in equation (3.10).

$$\lambda_{s/m}^* = \arg \min \left[ 1 + \frac{1}{2} \text{Erfc} \left( \frac{\lambda_{s/m} - N\sigma_n^2}{\sqrt{2N}\sigma_n^2} \right) - \frac{1}{2} \text{Erfc} \left\{ \frac{\lambda_{s/m} - N\sigma_n^2(1+\gamma)}{\sqrt{2N}\sigma_n^2(1+2\gamma)} \right\} \right] \quad (3.15)$$

The optimum threshold ( $\lambda_{s/m}^*$ ) is achieved when  $\frac{\delta P_e(\lambda_{s/m}^*)}{\delta \lambda_{s/m}^*} = 0$ . After some algebraic manipulations, a simplified representation in the form of a quadratic equation of  $\lambda_{s/m}$  is obtained as given below:

$$\lambda_{s/m}^2 - N\sigma_n^2\lambda_{s/m} - \frac{N\sigma_n^4}{2} - \left( N\gamma + \frac{(1+2\gamma)\ln(1+2\gamma)}{\gamma} \right) = 0 \quad (3.16)$$

Therefore, the system threshold ( $\lambda_{s/m}$ ) [179] for any received signal with an acceptable SNR value can be derived as-

$$\lambda_{s/m} = \frac{N\sigma_n^2}{2} \left[ 1 \pm \sqrt{1 + 2\gamma \left\{ 1 + \frac{(1+2\gamma)\ln(1+2\gamma)}{N\gamma^2} \right\}} \right] \quad (3.17)$$

Since  $\lambda_{s/m} \geq 0$ , therefore for low SNR,  $\gamma \ll 1$ ,  $(1+2\gamma) \approx 1$  and  $\ln(1+2\gamma) \approx 0$ . Hence the equation (3.17) can be well-approximated [179] as-

$$\lambda_{s/m} = \frac{N\sigma_n^2}{2} \left[ 1 \pm \sqrt{1} \left\{ 1 + \frac{0}{N} \right\} \right]$$

$$\text{or, } \lambda_{s/m} = \frac{N\sigma_n^2}{2} [1+1]$$

$$\text{or, } \lambda_{s/m} = N\sigma_n^2 \quad (3.18)$$

Fig.3.3 shows the difference in successful detection probability for variable SNR values. The probability of successful detection increases with the increment in SNR values. The

maximum probability of successful detection is observed when the SNR value is greater than 15 dB.

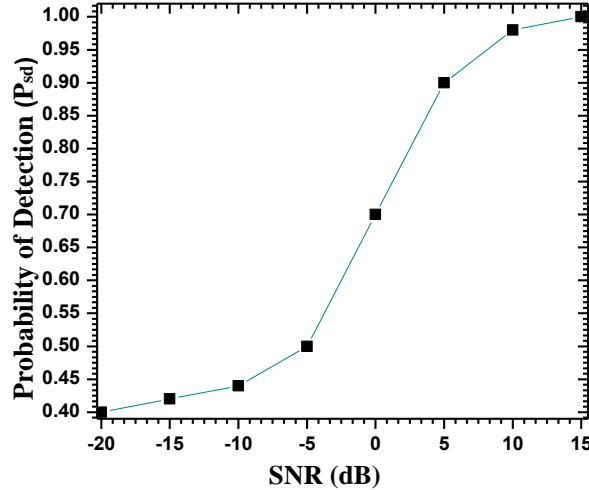


Figure 3.3: Variation of Successful Detection Probability with SNR

Therefore, system threshold selection is a significant criterion to execute the localization operation successfully. The localization of a PU has been conducted under AWGN fading channel condition, in this work. Therefore, a zero-mean Gaussian random variable with standard deviation has been introduced as a correction factor to select system threshold. An internal noise factor has also been proposed to consider the desensitization effects due to platform noise. Therefore, the real-time optimum system threshold can be written as-

$$\lambda_{s/m} \approx \left( N\sigma_n^2 + \sigma_G + P_{in} \right) \quad (3.19)$$

The system threshold ( $\lambda_{s/m}$ ) defined in equation (3.19) has been used to perform localization operation efficiently in an underlay CRN. A WCL scheme has been applied to locate the coordinates of a fixed PU under different propagation scenario in the next section.

### 3.3 LOCALIZATION OF A FIXED PRIMARY USER

The positional information of a PU is necessary to avoid harmful interference in the underlay CRNs. Therefore, a fixed PU localization scheme has been introduced in this section under

four different terrain conditions. The WCL algorithm has been stated in the next subsection to calculate location coordinates of a PU.

### 3.3.1 Weighted Centroid Localization (WCL) Scheme

Centroid localization (CL) [116], which is a range-free localization technique, uses the knowledge of adjacent connected anchor node to estimate the location of an unknown node or a PU. The CL algorithm was proposed by Bulusu *et.al.* [117] to determine the coordinates of an unknown node when the anchor nodes exist within the common range or scope of the communication. The anchor node is defined as a secondary node which assists in the localization process by transmitting a beacon containing its own location coordinates towards a secondary detector node or a detector CRU. The secondary detector node in the CL algorithm is responsible to estimate the location coordinates  $(X_{est}, Y_{est})$  of an unknown PU. In the CL algorithm, all the secondary detector nodes know the location coordinates and activities of all the neighboring anchor nodes or SUs which are located within the transmission range of a particular PU. The received location information from all the anchor nodes is used to find out centroid location coordinates of an unknown PU  $(X_{est}, Y_{est})$  by equation (3.20).

$$(X_{est}, Y_{est}) = \left( \frac{X_1 + \dots + X_A}{A}, \frac{Y_1 + \dots + Y_A}{A} \right) \quad (3.20)$$

In equation (3.20), 'A' represents number of adjacent connected anchor nodes or anchor SUs. The known  $(x, y)$  coordinates of the anchor nodes are represented by  $(X_K, Y_K)$ , where  $K = (1, 2, \dots, A)$ . The location estimation using CL method is simple and economic but the calculated coordinates contains high localization error and are not very reliable. Therefore, weighted centroid localization (WCL) algorithm [118], an improved version of CL method, has been considered in this work to calculate accurate location coordinates of PUs. The underlying idea of WCL algorithm is based on RSSI which makes it simple, cost effective, and transparent to the variation of the RF propagation environment. The RSSI of the signal transmitted by a PU and received at all the anchor nodes define weights and weighted sum of all the anchor nodes or anchor SUs is considered by the secondary detector

node to estimate the location coordinates of an unknown PU in WCL algorithm. Therefore, to compute the location coordinates  $\hat{P}(X_{est}, Y_{est})$  of an unknown node or a PU [90], WCL algorithm use the known coordinates  $(X_K, Y_K)$  of 'A' number of anchor SUs or anchor CRUs as shown in equation (3.21).

$$\hat{P}(X_{est}, Y_{est}) = \left\{ \frac{\sum_{K=1}^A W_K X_K}{W_{Ksum}}, \frac{\sum_{K=1}^A W_K Y_K}{W_{Ksum}} \right\} \quad (3.21)$$

$$W_K \text{ (Weight Factors of an anchor SU)} = \frac{(P_K - P_{min})}{\Delta P} \quad (3.22)$$

Where,  $P_K$  is the received power at the  $K^{th}$  anchor SU and  $P_{min}$  is the minimum received power in the considered group of anchor SUs.

$\Delta P = (P_{max} - P_{min})$ , where  $P_{max}$  is the maximum received power at an anchor SU in considered group. Sum of the weight factors ( $W_{Ksum}$ ) at all the anchor SUs in the considered group is  $\sum_{K=1}^A W_K$ .

Since strength of received power at any anchor SU depends on the distance between it and the PU, it is clear from equation (3.22) that the anchor SU node which is closest to the PU has a strong impact on location estimation.

Therefore, in the WCL scheme, PU localization depends on the precise measurement of RSSI at all the anchor nodes. However, the challenge of RSSI-based localization is its high sensitivity to the ambient changes. The possibility of variation in RSSI measurement limits the accuracy in the position estimation of an unknown PU. Hence, to improve localization accuracy, a radio propagation model has been considered with a correction factor in the next subsection.

### 3.3.2 Power Law Model with a Correction Factor

The RSSI which can be measured in decibel-milliwatts (dBm) is ten times the logarithm of the ratio of received signal power ( $P_r$ ) and a reference power ( $P_0$ ) [182] as shown in equation (3.23).

$$RSSI_{dBm} = 10 \log_{10} \left( \frac{P_r}{P_0} \right) \quad (3.23)$$

Equation (3.23) can be simplified as-  $RSSI_{dBm} = 10 \log_{10}(P_r)$  [Assuming  $P_0 = 1\text{mW}$ ] (3.24)

In radio receivers, received signal strength indicator (RSSI) gives a direct linear relationship with SNR (refer 3.1.1). The equation (3.24), can be written in terms of the SNR as-

$$SNR_{dB} = K \log_{10}(P_r) \quad [\text{Where, 'K' = constant}] \quad (3.25)$$

It is known that the received power, decreases with path distance [31]. As per Friis equation [106], the received signal power ( $P_r$ ) is inversely proportional to the square of the distance ( $d$ ) between the transmitter and the receiver antennas. Equation (3.26) shows the relationship between  $P_r$  and  $d$ .

$$P_r \propto \left( \frac{1}{d^2} \right) \quad (3.26)$$

The above relationship may be used to replace  $P_r$  in equation (3.24) resulting in equation (3.27), as shown below:

$$\begin{aligned} RSSI_{dBm} &\propto 10 \log_{10} \left( \frac{1}{d^2} \right) \\ \text{or, } RSSI_{dBm} &\propto -20 \log_{10}(d) \\ \text{or, } RSSI_{dBm} &= -K \log_{10}(d) \quad [\text{Where, } K = \text{Proportionality Constant}] \\ \text{or, } RSSI_{dBm} &= K \log_{10} \left( \frac{1}{d} \right) \quad (3.27) \end{aligned}$$

The equation (3.27), can be written in terms of the SNR as-

$$SNR_{dB} \propto \left( \frac{1}{d} \right) \quad (3.28)$$

The radio propagation models have been derived using a combination of theoretical and empirical models. However, both the theoretical and measurement-based propagation models indicate that the average received signal power decreases logarithmically with distance.

Therefore, a classical log-distance path loss model has been considered here for non-line of sight (NLOS) scenario [174] to measure the received power ( $P_r$ ) when the separation between the transmitter and the receiver is  $d_r$  (in meters). Therefore, the received power ( $P_r$ ) can be calculated as-

$$P_r = P_0 + 10n \log_{10} \left( \frac{d_r}{d_0} \right) \quad (3.29)$$

In equation (3.29),  $P_r$  and  $P_0$  represent the received and reference power levels in watts at any CR receiver. The distance between PU and CRU is denoted by  $d_r$  and  $d_0$  is the nominal reference distance corresponding to  $P_0$ . The factor ' $n$ ' is known as path loss exponent (PLE) or propagation environment characteristics and its value ranges between 1 and 5 depending upon the ambience and terrain characteristics. Thus, the accuracy of the RSSI measurement is affected by the different values of ' $n$ ' which varies with the terrain conditions. Fig.3.4 shows the RSSI measurement results under four different terrain conditions for the same separation distance  $d_r$  (m). The received power ( $P_r$ ) has been calculated by substituting different values of ' $n$ ' in the equation (3.29). The reference distance ( $d_0$ ) and reference power ( $P_0$ ) are assumed to be 1m and 1mW respectively. Hereafter, RSSI has been computed by substituting the results of equation (3.29) in equation (3.24).

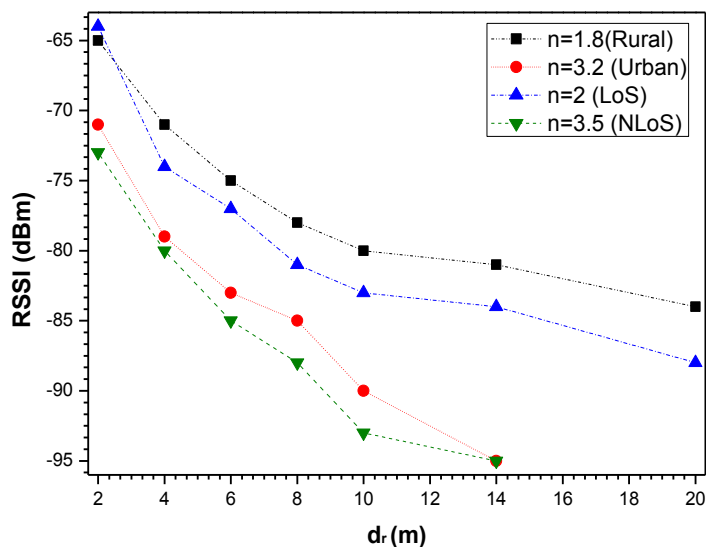


Figure 3.4: Effects of Path Loss Exponent on RSSI with Distance

Further, to improve accuracy of RSSI measurement under different terrain conditions, a correction factor ( $\sigma_G$ ) has been considered to enhance the accuracy of a path loss model. Therefore, log-distance path loss model has been transformed into log-normal path loss model and equation (3.29) can be rewritten as-

$$P_r = P_o + 10n \log_{10} \left( \frac{d_r}{d_0} \right) + (\sigma_G) \quad (3.30)$$

In equation (3.30), the standard deviation ( $\sigma_G$ ) is often estimated by empirical measurements whose range varies in between 6dB to 12dB depending on the terrain conditions. Therefore, to improve received power ( $P_r$ ) measurement accuracy, the PLE ( $n$ ) and the standard deviation ( $\sigma_G$ ) of the Gaussian random variable should be known precisely for an efficient CRN modelling. Table 3.1 shows the approximate values of ' $\sigma_G$ ' and ' $n$ ' for different terrains.

**Table 3.1: Network Modelling Factors**

Terrain Profiles	Standard Deviation ( $\sigma_G$ )	Path Loss Exponent ( $n$ )
Rural	6.5	1.8
Urban	9.3	3.2
Line-of-sight (LOS)	6.9	2
Non-Line-of-Sight (NLOS)	9.5	3.5

Further, the equation (3.30) can be simplified by substituting  $P_o = 1mW$  and  $d_0 = 1m$ .

$$P_r = 10n \log_{10}(d_r) + (\sigma_G) \quad (3.31)$$

The propagation paths between a transmitter and a receiver are different and random in the various terrain scenarios. The received signal strength value varies for the same separation distance between a transmitter and a receiver in different terrains. In the next subsection, an underlay CRN scenario has been considered with a fixed positioned PU and five CRUs. The WCL algorithm has been applied to compute location coordinates of a fixed PU in different terrain conditions.



3.3.3 Network Scenario

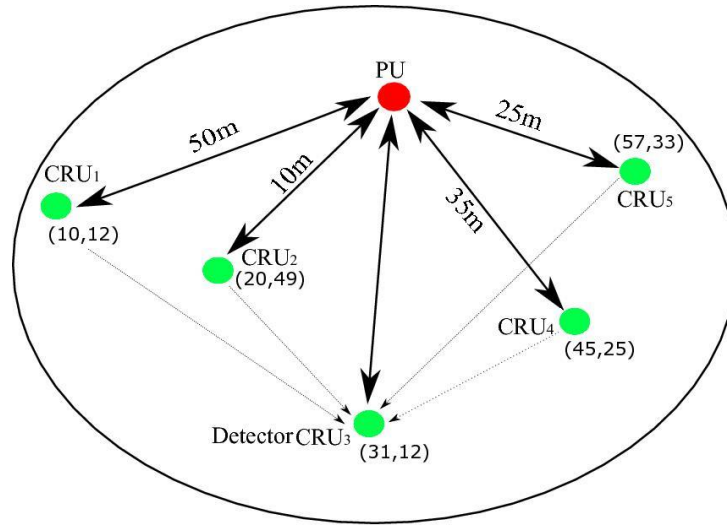


Figure 3.5: Network Scenario

Fig.3.5 shows an underlay CRN with five CRUs or SUs and a PU within the reception range. The CRUs have been placed at known coordinates with fixed distances from the PU. The CRU1, CRU2, CRU4, and CRU5 are defined as anchor nodes and CRU3 as a detector node. Since, the four anchor CRUs, are at different distances from the fixed PU, the RSSI of the PU transmitted signal are different. The received power ( $P_r$ ) at the anchor nodes has been measured using equation (3.29) for four different terrain conditions. The correction factor ( $\sigma_G$ ) and path loss exponent ( $n$ ) have been considered as per Table 3.1 for different terrains. Hereafter, The RSSI values at different anchor nodes are computed by substituting the result of equation (3.29) in equation (3.24). The results of equation (3.24) have been converted to millivolt.

Table 3.2: RSSI (mV) Measurement at the anchor CRUs

No. Of CRUs	Dist. (m)	LOS		NLOS		Rural		Urban	
		$RSSI_{wocf}$ (mV)	$RSSI_{wcf}$ (mV)	$RSSI_{wocf}$ (mV)	$RSSI_{wcf}$ (mV)	$RSSI_{wocf}$ (mV)	$RSSI_{wcf}$ (mV)	$RSSI_{wocf}$ (mV)	$RSSI_{wcf}$ (mV)
CRU1	50	1.05	1.45	0.6	1.39	1.15	1.44	0.74	1.44
CRU2	10	3.80	4.05	1.15	3.99	3.95	4.11	1.29	3.99
CRU4	35	1.92	2.30	0.91	2.29	2.09	2.33	1.05	2.21
CRU5	25	2.52	2.93	1.09	2.97	2.73	2.99	1.23	2.76

Table 3.2 shows the measurement of RSSI at all the anchor CRUs by considering both the correction factor ( $RSSI_{wcf}$ ) and without correction factor ( $RSSI_{wocf}$ ) for four different terrain conditions. The measured RSSI value at a given distance varies under four different terrain conditions when the correction factor ( $\sigma_G$ ) has not been considered. However, with the correction factor ( $\sigma_G$ ), approximately similar RSSI measurement has been observed at a given distance under different terrain conditions. Therefore, to compute the precise coordinates of the fixed PU, RSSI with the correction factor for each anchor CRU node has been considered by the detector node (CRU3). Each anchor CRU node transmits beacons which contain its location coordinates information and RSSI of the signal transmitted by the PU, for the secondary detector node or CRU3. The detector node performs certain housekeeping operation to update its lookup table with the information received from the anchor nodes. Hereafter, equation (3.21) of the WCL algorithm has been used to calculate the absolute coordinates of the fixed PU. Table 3.3 shows the computed PU location coordinates for different terrains. It has been observed that the location coordinates calculation of the fixed PU varies significantly when the correction factor is not considered during the RSSI measurement. On the other hand, with the correction factor, the variation in location coordinates is negligibly small. Hence, the minimum localization error has been achieved with the proposed correction factor.

**Table 3.3: Absolute Location Coordinates of a Fixed PU**

Terrain Profile	Fixed PU Coordinates $\hat{PU}(X_{est}, Y_{est})$	
	With Out Correction Factor	With Correction Factor
LOS	(44.66,64.22)	(39,67.91)
NLOS	(88.99,91)	(37.33,69.1)
Rural	(48.99,61.33)	(39.55,68.99)
Urban	(99.035,93.89)	(38.51,69)

The next section has introduced a collaborative localization of a mobile PU under NLOS scenario.

### 3.4 LOCATION ESTIMATION OF A MOBILE PU

The accurate location information of any PU is one of the essential requirements of underlay CRUs for an efficient use of licensed spectrum without causing any interference with the PU. Though a PU does not directly communicate with a CRU, the RSSI which gives a direct measure of the SNR has been used for localization process. However, due to random movement of mobile PUs, it is very challenging for a single CRU to determine the precise location coordinates. Therefore, a group of collaborative CRUs is required to estimate precise location coordinates of mobile PUs.

#### 3.4.1 Optimization of the Number of Collaborative Users

An adequate number of collaborative CRUs is necessary to ensure localization accuracy with minimum error. Hence, to optimize the number of collaborative users, a mapping algorithm based on Marcum-Q function [183-184] has been applied to calculate the number of collaborative CRUs. The accurate error probability performance has been plotted for 'c' number of collaborative CRUs based on this function.

The detection probability ( $Q_d$ ) of a PU has been formulated using Marcum-Q function [183-184], shown in (3.32).

$$Q_d = \frac{c \times P_{sd} \times (1 - P_{sd})^{(c-1)}}{(c-1)!} \quad (3.32)$$

In equation (3.32), 'c' represents the number of collaborative CRUs and  $P_{sd}$  is the successful detection probability which has been computed using incomplete Gamma function.

The occurrence probability of two error factors namely, probability of false detection and probability of miss-detection reduce the localization accuracy. The false alarm happens when CRUs falsely detect the presence of the PU signal. On the other hand, the miss-detection happens when CRUs fail to detect the presence of PU signal, mainly due to interference. Therefore, probability of false detection ( $Q_f$ ) and probability of miss-detection ( $Q_m$ ) in the presence of Additive White Gaussian Noise (AWGN) have been formulated by Marcum-Q function [183-184].

$$Q_f = \frac{c \times P_{fd} \times (1 - P_{fd})^{(c-1)}}{(c-1)!} \quad (3.33) \quad \text{and} \quad Q_m = (1 - Q_d) \quad (3.34)$$

In equation (3.33),  $P_{fd}$  has been calculated using incomplete gamma function [183-184].

Therefore, total localization error probability has been formulated as-

$$Q_{error} = (Q_f + Q_m) \quad (3.35)$$

This error probability varies with number of CRUs, which work in a group to perform PU localization collaboratively. The environment is simulated using MATLAB simulator and results are graphically represented in Fig.3.6 which establishes a relationship between the total error rate and number of CRUs. For this purpose, the number of CRU ( $c$ ) is varied from 1 to 10.

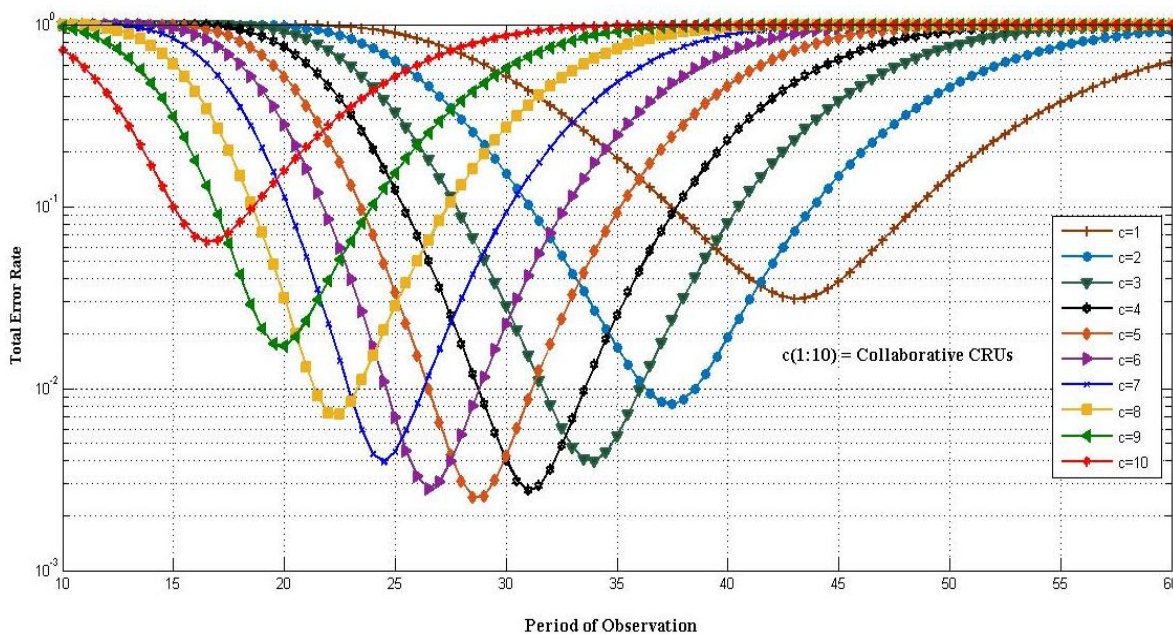


Figure 3.6: Variation of Detection Error with Number of CRUs

The simulation result shows that the detection error is high for both higher and lower number of CRUs. The error rate is minimum when ' $c$ ' varies in between 4 to 6. For simplicity, a group of four CRUs ( $c=4$ ) has been considered to conduct further experiments.

**3.4.2 Localization of a Mobile PU**

A network consisting of four collaborative CRUs placed at four corners of a square has been considered to perform precise localization of a mobile PU. Fig.3.7 shows the proposed (100m×100m) network scenario. All the collaborative CRUs have been placed in this network at the following coordinates.

CRU1: (0, 0), CRU2: (100, 0), CRU3: (100, 100), CRU4: (0, 100).

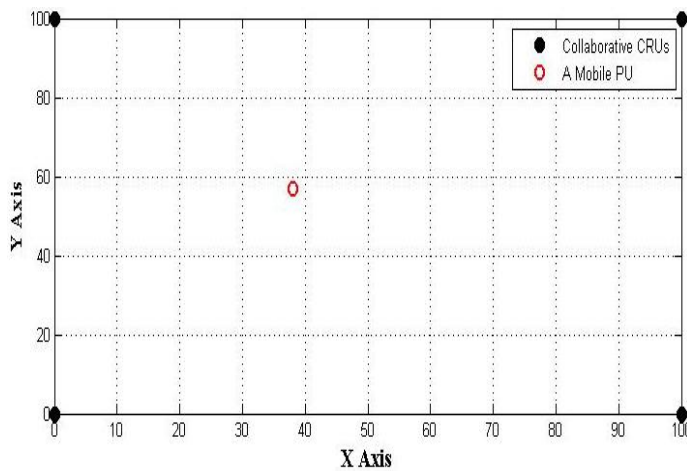


**Figure 3.7: Network Model**

A mobile PU has been placed within the network scenario at a true location coordinates. The mobile PU location changes between each iteration. Hence, the distance between the mobile PU and each of the collaborative CRU changes continuously. Table 3.4 shows the true location coordinates of a mobile PU for ten observations.

**Table 3.4: True Location Coordinates of a Mobile PU**

Observations	Coordinates (x, y)
1 <sup>st</sup>	(21.7,17)
2 <sup>nd</sup>	(91,88)
3 <sup>rd</sup>	(41,86.8)
4 <sup>th</sup>	(30.3,11.7)
5 <sup>th</sup>	(44.8,22)
6 <sup>th</sup>	(36.4,70)
7 <sup>th</sup>	(16,36)
8 <sup>th</sup>	(17.8,52.5)
9 <sup>th</sup>	(62.8,43)
10 <sup>th</sup>	(78,80.3)

An approximate probabilistic distance estimation of the mobile PU is obtained by network simulation using MATLAB simulator. Fig.3.8 shows the true and estimated location coordinates of a mobile PU for ten sample positions. The estimation error factor ( $\Delta d$ ) is obtained mathematically using Gaussian Newton method [185].

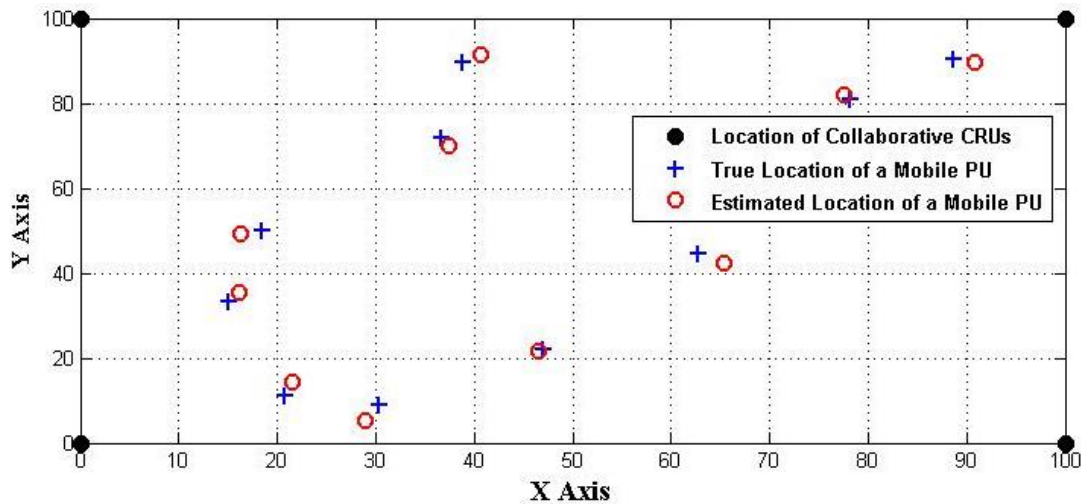


Figure 3.8: True and Estimated Location of a Mobile PU

Fig.3.8 shows estimated position information of the mobile PU from each of the collaborative CRUs. Therefore based on these ten observations, distance of the mobile PU from each of collaborative CRUs have been computed and plotted in Fig.3.9.

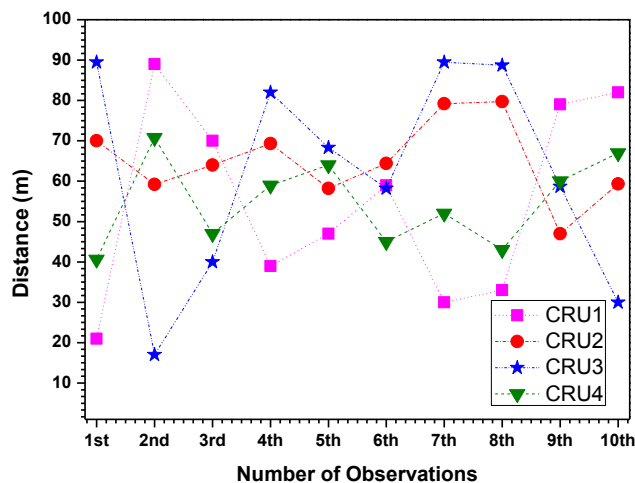


Figure 3.9: Distance Measurement at different CRUs with respect to the PU Movement within the Network

Distance variations of the mobile PU have been considered to compute the received power level at each collaborative CRU. In the simulation experiment, the path loss exponent ( $n$ ) and

the standard deviation ( $\sigma_G$ ) of the Gaussian random variable have been set at 3.5 and 9.5 respectively to establish NLOS communication. Fig.3.10 depicts a comparative analysis of received signal level or SNR for all the observations at different CRUs.

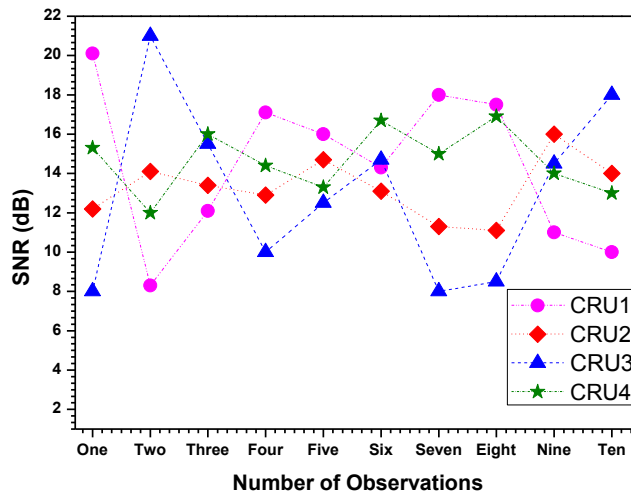


Figure 3.10: SNR Measurement at different CRUs with respect to the PU Movement within the Network

The complete simulation process, starting from collaborative user selection to distance and SNR calculation has been stated in a localization algorithm 3.1.

**Localization Algorithm. 3.1**

1. Measure,  $Q_d$  and  $Q_f$  [consider Eq. (3.32) and (3.33)]
2. Calculate,  $Q_m$  using  $Q_d$  [consider Eq. (3.34)]
3. Compute,  $Q_{error}$  [consider Eq. (3.35)]
4. Repeat step 3, for c (no of variable CRU) = 1 to 10 [optimize a group of collaborative CRUs]
5. Plot, estimated location with respect to the true locations for ten observations.
6. Compute, mobile PU distance from each collaborative CRU for ten observations using  $Dist(c.m) = \sum_{m=1}^1 \left[ \sum_{c=1}^4 \sqrt{\{Loc(c, x) - Loc(m, x)\}^2 + \{Loc(c, x) - Loc(m, y)\}^2} \right]$
7. Compute received signal strength or SNR using result of step 6 [consider Eq. (3.28)]

However, in the generalized CR receivers, the SNR of the received signal is not very reliable due to the presence of external and internal noise. It leads to an increase in the localization error probability of a PU. The localization capability of a radio receiver can be enhanced either by increasing the sensitivity or by using high gain antennas. In most of the cases, providing a directional high gain antenna in place of an omnidirectional antenna is not a practical solution. On the other hand, receiver sensitivity (SNR) is measured by the ratio of the received signal power and the total harmonic distortion (THD) respectively. If THD can be mitigated with suitable filter design, the SNR will definitely improve. It will also reduce the occurrence probabilities of miss and false detection. Therefore, a scheme to minimize a significant part of the internal noise which is generated by the receiver circuit itself has been described in the next subsection. It will improve the precision of localization in the underlay CRNs.

### **3.4.3 Internal Noise Mitigation**

Two critical factors which affect reliable and consistent reception in CR receivers are the random external noise and circuit generated internal noise. The external noise effects on radio communication are unpredictable and unavoidable. Therefore, this thesis work has focused on the minimization of the internal noise by designing a suitable FIR filter. The internal noise, which is generated mainly due to receiver circuit nonlinearity, interferes with the received signal and reduces SNR of the received signal. Hence the CR receiver circuit design has been modified by incorporating the proposed filter block after the demodulator stage. It enhances the overall SNR of the received signal.

#### **3.4.3.1 Modified Cognitive Radio Receiver**

In the data communication system, bit error rate (BER), which indicates the reliability of received data, is inversely proportional to the SNR. Therefore, if SNR can be improved, it will automatically lead to a fall in BER. Hence, the SNR improvement filtration block has been introduced in Fig.3.11 to minimize mainly the internal noise of a radio receiver.



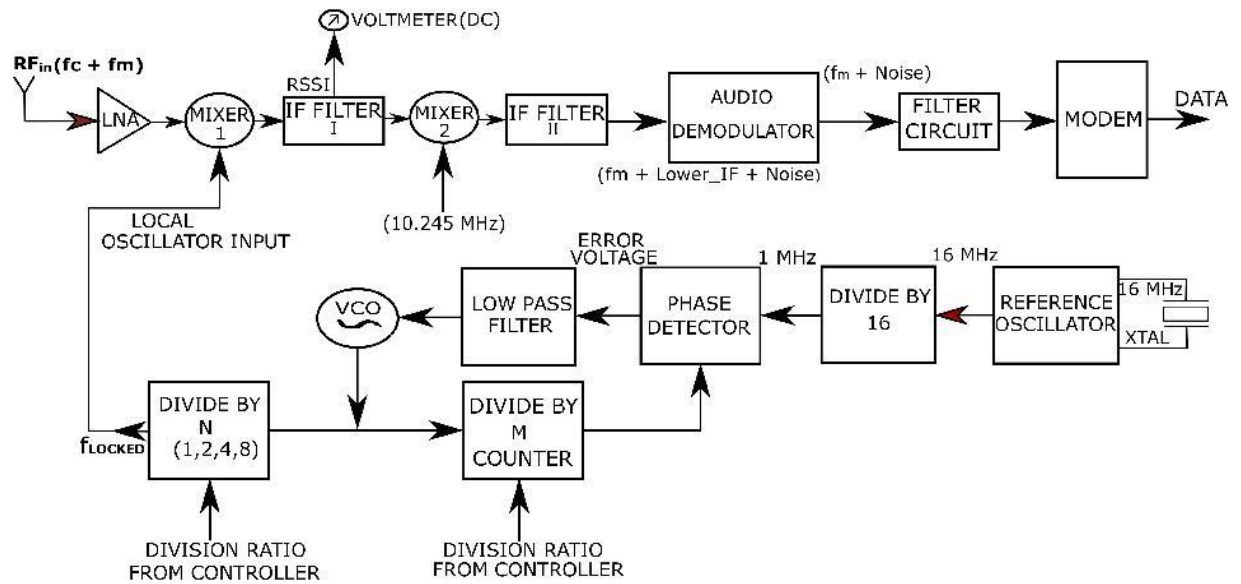
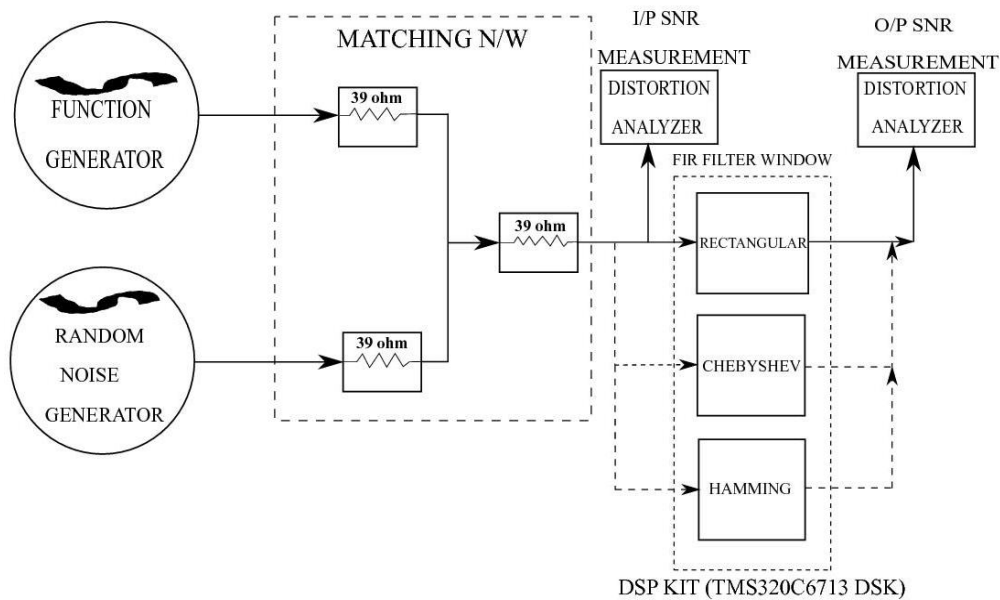


Figure 3.11: Operational Block of a Modified Cognitive Radio Receiver

The modulated signal ( $RF_{in}$ ) is picked up by the antenna from communication medium. The received signal is fed to a low noise amplifier (LNA) stage to amplify the desired band. The modulated carrier signal is amplified selectively in the LNA stage. Then the amplified signal is passed to a mixer block. The second input of this mixer is the local oscillator (LO) signal. The voltage controlled oscillator (VCO) determines the locked frequency to be used as the LO signal to the first mixer. Multiple steps are involved in the generation of the VCO signal. The reference oscillator produces a stable 16 MHz clock frequency with the help of a 16 MHz Xtal. This output is divided by 16 to produce a lower reference frequency of 1 MHz for the phase detector. The process of stepping down of reference frequency is necessary to ensure stable error correction. The second input to the phase detector comes from 'Divide By M' counter. The 'M' value is programmed by the controller. The error voltage from the phase detector is smoothed by the low pass filter (LPF) before it is applied to the VCO block for necessary frequency correction. The locked output of the VCO is divided by (N) to obtain final locked frequency ( $f_{LOCKED}$ ). This frequency is fed to the first mixer and acts as the local oscillator (LO) signal. The reference oscillator, divider, phase detector, LPF, counters and the VCO are all integrated into the PLL IC (NBC12429). The output of the mixer unit is down-converted by first intermediate frequency ( $f_m + first\_IF$  where,  $first\_IF$  is assumed as 10.7

MHz) stage. Then the output of the first IF is applied to the second mixer to convert to a lower intermediate frequency ( $f_m + lower\_IF$  where,  $lower\_IF$  is 455 KHz) by narrowband filtering. After the IF stages, the next operational block is the audio demodulator stage with a FM limiter. In this stage signal is first down converted to the baseband. The baseband signal is filtered in the main filter to attenuate other out of band signals and extract the modulating or message signal ( $f_m$ ). In a normal CR receiver circuit, the modulating signal is passed on to the modem to recover binary data. In the proposed system model, a filter block has been introduced after the demodulator stage of the CR receiver circuit to reduce the internal noise which in turn improves the localization accuracy. Three different filter types namely, Rectangular, Chebyshev, and Hamming were designed and tested in the audio frequency band on a reconfigurable DSP kit (TMS320C6713 DSK, details in Appendix A) to compare the relative improvements in the SNR of the demodulated signal. For final selection of the optimum filter type, a comparative analysis has been done on the results obtained with the three designed reconfigurable filters.

The output of the selected filter block is fed to the MODEM unit of the receiver for generation of the digital data.



**Figure 3.12: Proposed Experimental Block**

Testing of the modified receiver block (Fig.3.12) was carried out around a function generator (FG3MD, 3MHz) and a random noise source (AWG30, 30 MHz, details in Appendix A). The internal noise was generated by the random noise source (AWG30, 30 MHz) and the test signal or message signal ( $f_m$ ) was obtained from the function generator (FG3MD, 3MHz). The test signal was mixed with the variable output of AWG30 to generate the noisy signal. This analog noisy signal, which emulates the demodulated signal, was applied to the input of the designed filter unit through a matching network. The DSP kit (TMS320C6713 DSK) was programmed to realize three different types of FIR filter windows, one at a time, in the audio frequency range. All the three filters have been tested at a nominal frequency of 1 KHz since the audio signal attains maximum power level at 1 KHz (approx.). SNR of the input test signal improved after additional filtering since the designed filter reduced the internal noise effects. To measure the SNR a distortion analyzer (sm5027-details in Appendix A) was used.

#### 3.4.3.2 Operational Analysis

Fig.3.13 shows the experimental set up. The analog noisy signal was converted to digital signal by the analog to digital (ADC) unit of the DSP kit (TMS320C6713 DSK). The converted digital signal was processed by the designed FIR filters developed with the DSP kit. The filtered digital signal was transformed back to analog form using the digital to analog (DAC) unit of the DSP kit. The distortion analyzer (sm5027) was used to measure the SNR of both input and output signals of the DSP kit.

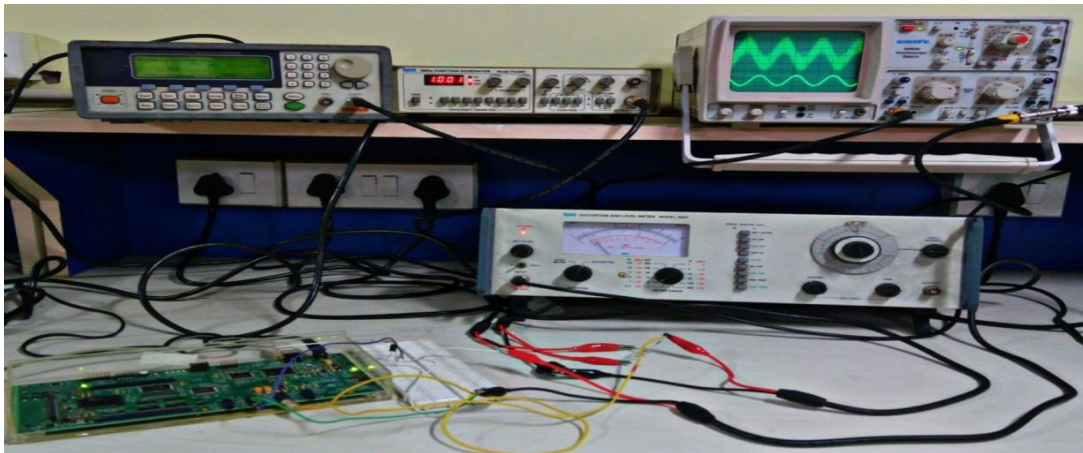


Figure 3.13: Hardware Setup

Variable noise levels have been generated from the random noise generator to make the analysis more realistic. The operational sequence of the experiment and the design code of digital filters are described in Fig. 3.14.

Step 1  $\Rightarrow$  The reconfigurable DSP kit (TMS320C6713CDSK) is initialized for three parallel filter windows.

Step 2  $\Rightarrow$  Test signal is fed to the initialized DSP kit along with the random noise.

Step 3  $\Rightarrow$  The analog noisy input signal is converted to digital form and is passed through a selected filter window.

Step 4  $\Rightarrow$  Filtered output is again converted back to analog signal by the DAC unit of DSP kit.

Step 5  $\Rightarrow$  Converted output signal is fed to the distortion analyser (sm5027) for measurement.

**a. Various Steps of Emulation of the Proposed Modification**

```
void main()
{
    DSK6713_AIC23_CodecHandle hCodec;
    Uint32 l_input, r_input, l_output, r_output;
    DSK6713_init ();
    hCodec = DSK6713_AIC23_openCodec(0,
    &config);
    DSK6713_AIC23_set Freq (hCodec, 1);
    while (1)
    while (!DSK6713_AIC23_read(hCodec,
    &l_input));
    while (!DSK6713_AIC23_read(hCodec,
    &r_input));
    l_output=(Int16)FIR_FILTER(&filter_Coeff
    ,l_input);
    r_output=l_output;
    while (!DSK6713_AIC23_write(hCodec,
    l_output));
    while (!DSK6713_AIC23_write(hCodec,
    r_output));
    }
    DSK6713_AIC23_close Codec (hCodec);
}
signed int FIR_FILTER(float * h, signed int x)
{
    int i=0;
    signed long output=0;
    in_buffer [0] = x; /* new input at buffer [0] */
    for (i=51;i>0;i--)
    in_buffer[i] = in_buffer[i-1]; /* shuffle the buffer
    */
    for (i=0;i<51;i++)
    output = output + h[i] * in_buffer[i];
    return (output);
}
```

**b. Corresponding Code for DSP Emulation**

**Figure 3.14: Operation Sequence and Filter Design Code**

The SNR, measured at the output port for each of the three filter windows, are tabulated in Table 3.5 with respect to the common SNR of the input test signal.

**Table 3.5: Performance Analysis of Different Filter Types at Variable Noise Levels**

Noise Level (mV)	Input SNR (dB)	Rectangular Filter Window		Chebyshev Filter Window		Hamming Filter Window	
		Output SNR (dB)	Improvement (dB)	Output SNR (dB)	Improvement (dB)	Output SNR (dB)	Improvement (dB)
5	21.0	21.8	0.8	22.7	1.7	21.7	0.7
10	20.4	21.1	0.7	22.0	1.6	21.1	0.7
20	19.0	19.8	0.8	20.5	1.5	19.8	0.8
50	18.9	19.5	0.6	20.5	1.6	19.8	0.9
100	18.0	18.8	0.8	19.7	1.7	18.7	0.7
150	17.6	18.3	0.7	19.1	1.5	18.4	0.8
200	17.5	18.3	0.8	19.0	1.5	18.3	0.8
300	16.6	17.4	0.8	18.2	1.6	17.4	0.8
350	16.4	17.1	0.7	18.1	1.7	17.2	0.8
450	16.3	17.1	0.8	18.0	1.7	17.2	0.9
600	15.5	16.3	0.8	17.2	1.7	16.2	0.7
650	15.0	15.7	0.7	16.5	1.5	15.7	0.7
700	14.7	15.6	0.9	16.4	1.7	15.5	0.8
750	14.2	15.1	0.9	16.0	1.8	14.9	0.7
800	13.9	14.5	0.6	15.6	1.7	14.5	0.6
850	13.5	14.0	0.5	15.3	1.8	14.2	0.7
900	13.4	14.1	0.7	15.1	1.7	13.9	0.5
950	13.2	14.0	0.8	15.0	1.8	13.5	0.3

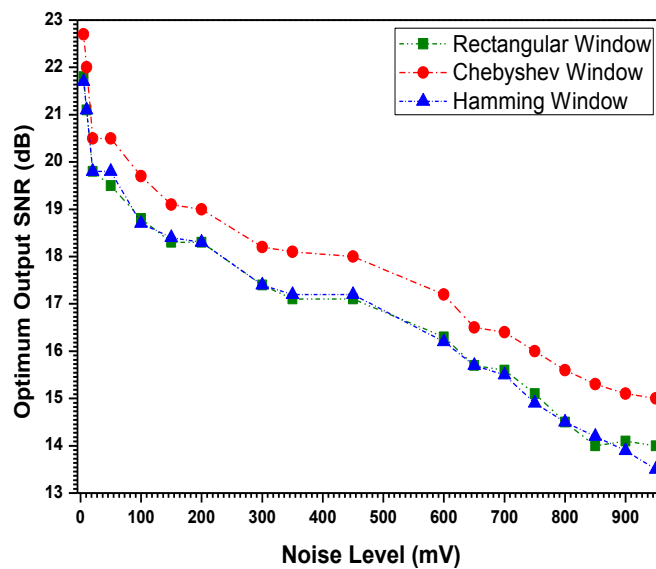


**Figure 3.15: Plot of Output SNR Vs Input Noise Level for Different Filter Types**

The outputs of the three filter windows have been plotted in Fig.3.15. It has been found from Table 3.5 that on the average, an improvement of 1.7 dB in the output SNR value over the corresponding input SNR is obtained with the Chebyshev filter, whereas, the Hamming and Rectangular filter types have achieved improvements up to a maximum of 0.7 dB to 0.9 dB in the output SNR respectively. Though the performances of all the three designed filters degrade at higher noise level, the performance of Chebyshev filter is better than those of the other two. Therefore, the Chebyshev filter has been selected as the optimum filter type for internal noise mitigation. The next subsection has described the computation scheme of precise coordinates of a mobile PU.

#### 3.4.4 Computation of Location Coordinates

The WCL algorithm [30] has been considered in this work to calculate precise location coordinates of a mobile PU. The fundamental principal of this algorithm is based on RSSI of signal received from the mobile PU. Therefore, in the proposed network scenario (refer Fig. 3.7), the CRUs have performed localization collaboratively for each observation. The Chebyshev filter has been introduced after demodulator stage to minimize system generated internal noise effects on received SNR. The variable SNR which has been obtained through MATLAB simulation (refer Fig. 3.10) of proposed network has been applied to the Chebyshev filter. Table 3.6 shows the improvement of SNR after filtration at each of the collaborative CRU with respect to the SNR before filtration.

**Table 3.6: SNR (dB) Improvement at Each of the Collaborative CRUs**

Observations	CRU1		CRU2		CRU3		CRU4	
	Without Filtration	With Filtration	Without Filtration	With Filtration	Without Filtration	With Filtration	Without Filtration	With Filtration
<b>First</b>	20.1	21.6	12.2	13.9	8	9.7	15.3	17
<b>Second</b>	8.3	9.8	14.1	15.8	21	22.6	12	13.7
<b>Third</b>	12.1	13.7	13.4	15	15.5	17.2	16	17.7
<b>Fourth</b>	17.1	18.8	12.9	14.6	10	11.7	14.4	16
<b>Fifth</b>	16	17.7	14.7	16.4	12.5	14.2	13.3	15
<b>Sixth</b>	14.3	16	13.1	14.8	14.7	16.4	16.7	18.4
<b>Seventh</b>	18	19.6	11.3	13	8	9.7	15	16.7
<b>Eighth</b>	17.5	19.2	11.1	12.8	8.5	10.2	16.9	18.6
<b>Ninth</b>	11	12.7	16	17.6	14.5	16.1	14	15.6
<b>Tenth</b>	10	11.6	14	15.7	18	19.7	13	14.7

SNR values before and after filtration have been converted to the mean received power ( $P_r$ ) for all the observations separately at each of the collaborative CRU using equation (3.25). Hereafter, equation (3.24) was used to compute RSSI. Hence RSSI with known coordinates of the anchor CRU nodes has been applied to the equation (3.21) to compute location coordinates of the mobile PU. Table 3.7 shows the RSSI value at each of the collaborative CRU for all the observations. Precision of RSSI values is fixed up to the first decimal place.

**Table 3.7: RSSI ( $\mu V$ ) at Each of the Collaborative CRUs without and with Filtering**

Observations	CRU1		CRU2		CRU3		CRU4	
	Without Filtration	With Filtration	Without Filtration	With Filtration	Without Filtration	With Filtration	Without Filtration	With Filtration
<b>First</b>	359.3	428.3	145	176.3	89.3	108.9	207.2	251.7
<b>Second</b>	92.6	110	181	248.3	398.9	480.3	141.5	172.4
<b>Third</b>	143.2	172.4	166.6	200	212.15	257.9	224.3	273.2
<b>Fourth</b>	254.8	309.7	157.1	191	112.4	168.5	186.9	224.3
<b>Fifth</b>	224.3	273.2	193.4	235.2	149.5	182.3	164.8	200
<b>Sixth</b>	184.71	224.3	160.2	195.72	217.4	235.1	243.6	296.2
<b>Seventh</b>	282.4	428.32	133.6	158.8	89.3	108.4	200	243.4
<b>Eighth</b>	267.05	408.8	128.6	156.7	94.7	115.3	249	302.8
<b>Ninth</b>	126.1	153.05	224.3	275.9	189.1	232	178.2	214.6
<b>Tenth</b>	112.4	135.6	178.2	216	282.4	385.9	158.8	193.4

In the proposed localization scheme, all the four CRUs, act as the detector node to localize coordinates of a mobile PU, within the period of observation. As per the WCL algorithm, when CRU1 act as a detector node, then CRU2, CRU3 and CRU4 perform the role of anchor nodes. The same procedure has been followed when other three CRUs act as the detector nodes. The anchor nodes share necessary information with the detector node for localization of the coordinates of a mobile PU. Each of the four detector nodes estimates the location coordinates on the basis of collected information from anchor nodes for ten common observations. The computation steps involved are listed in localization algorithm 3.2.

**Localization Algorithm. 3.2**

1. Choose the detector node among the four CRUs one by one.
2. After detector node selection, evaluate received RSSI and location coordinates information from the anchor nodes (A).
3. Consider,  $RSSI = P_{K=1:3}$  from the anchor nodes (A).
4. Determine,  $P_{\max}$  and  $P_{\min}$  from the results of step 3.
5. Calculate,  $\Delta P = P_{\max} - P_{\min}$
6. Consider anchor location coordinates  $(X_{K=1:4}, Y_{K=1:4})$
7. Compute,  $W_{K=1:3}$  [consider Eq. (3.22)]
8. Calculate,  $PU(X)_{possum} = (X)_{possum} + W_K \times (X_K)$
9. Calculate,  $PU(Y)_{possum} = (Y)_{possum} + W_K \times (Y_K)$
10. Compute,  $W_{Ksum} = \sum_{K=1}^A W_K$
11. Calculate,  $PU(X, Y)_{meanloc} = \frac{PU(X, Y)_{possum}}{W_{Ksum}}$

The location coordinates are estimated by using the proposed localization algorithm 3.2. The RSSI values with and without Chebyshev filtering of the received signal from the mobile PU have been separately considered. The given true location coordinates are compared with the estimated locations in both cases. The variation in the localization coordinates of the mobile PU with respect to each of the four CRUs are plotted one by one in the Fig. 3.16, Fig. 3.18, Fig. 3.20 and Fig. 3.22 respectively.



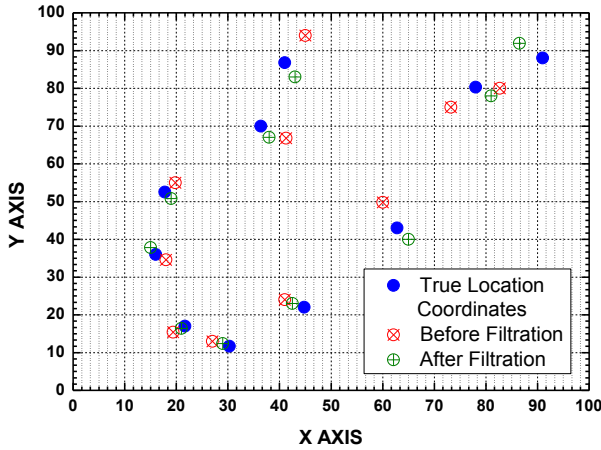


Figure 3.16: CRU1 as a Detector Node

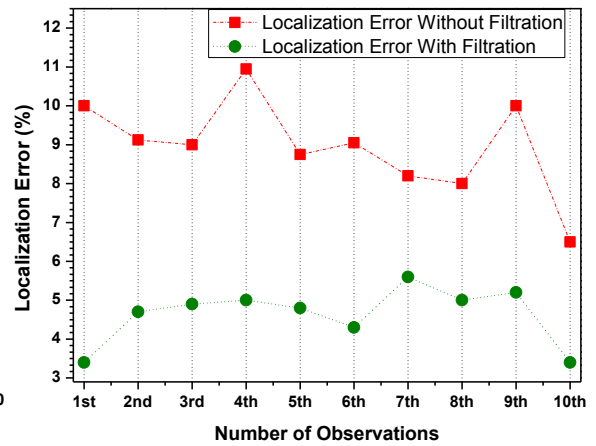


Figure 3.17: Error in Location Estimation by CRU1

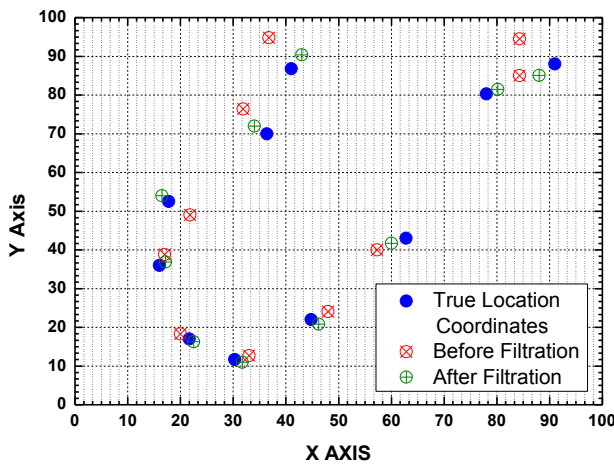


Figure 3.18: CRU2 as a Detector Node

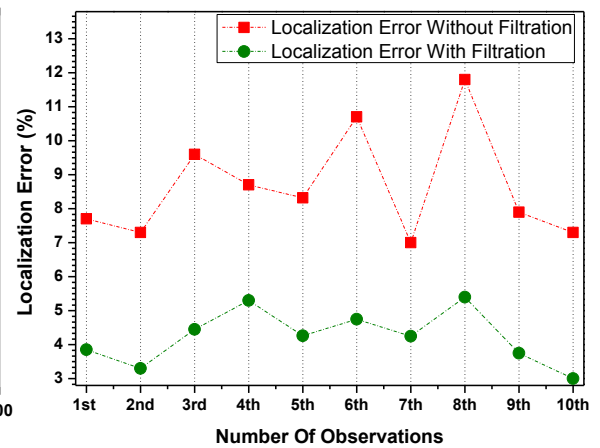


Figure 3.19: Error in Location Estimation by CRU2

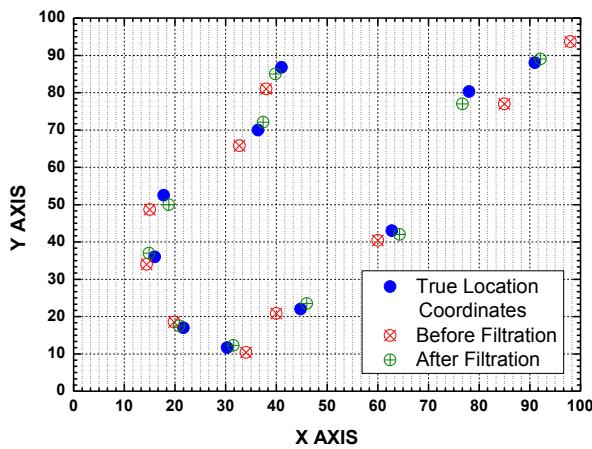


Figure 3.20: CRU3 as a Detector Node

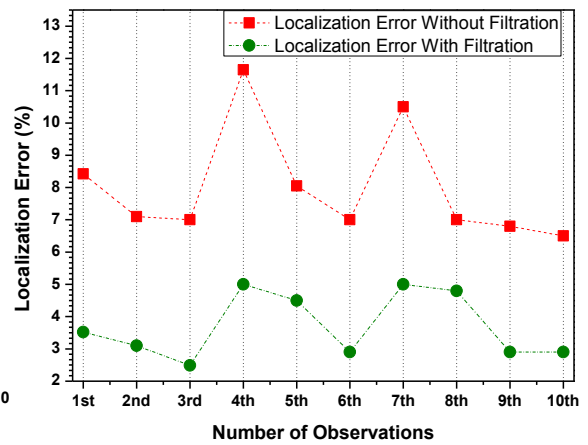


Figure 3.21: Error in Location Estimation by CRU3

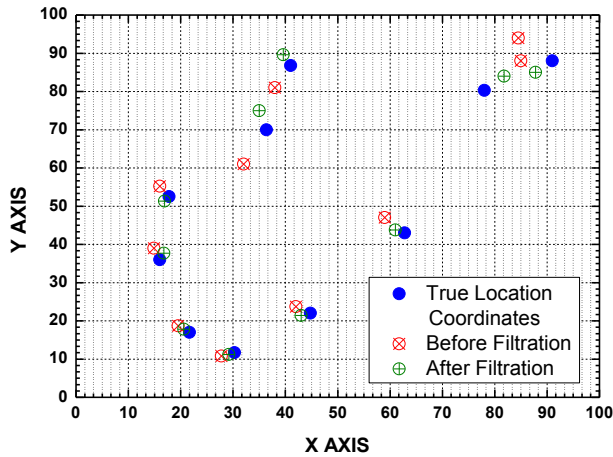


Figure 3.22: CRU4 as a Detector Node

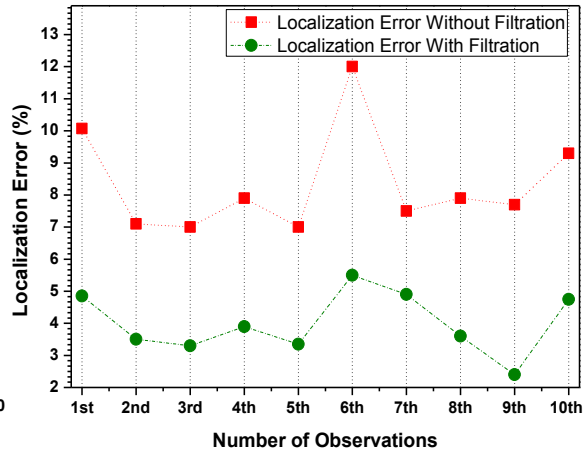


Figure 3.23: Error in Location Estimation by CRU4

The addition of Chebyshev filter minimizes the location estimation error. The percentage errors in location estimation without and with Chebyshev filter are shown graphically for CRU1 to CRU4 in the Fig. 3.17, Fig. 3.19, Fig 3.21 and Fig. 3.23 respectively within a common period of observation. It has been observed that the range of percentage error without filtration is (6.5–12) % and with Chebyshev filter the error percentage has come down to (2.4–5.6) %.

Table 3.8: Estimated Mean Location Coordinates

Observations	PU Coordinates ( $X_{mean}, Y_{mean}$ )
1 <sup>st</sup>	(21.2, 17)
2 <sup>nd</sup>	(88.6, 87.75)
3 <sup>rd</sup>	(41.4, 87.8)
4 <sup>th</sup>	(30.6, 11.9)
5 <sup>th</sup>	(44, 22.2)
6 <sup>th</sup>	(36.1, 71.7)
7 <sup>th</sup>	(15.7, 37.5)
8 <sup>th</sup>	(17.5, 51.7)
9 <sup>th</sup>	(62.5, 41.9)
10 <sup>th</sup>	(79.9, 80.1)

Further to improve localization accuracy of mobile users, collaborative scheme has been adopted in this work. The localization estimation results after filtration of all the four CRUs are considered together and the mean location coordinates of the mobile PU are calculated for each observation. Table 3.8 represents the estimated mean location coordinates of a

mobile PU for each observation. Fig. 3.24 shows a comparative study of estimated mean location coordinates with the true location coordinates.

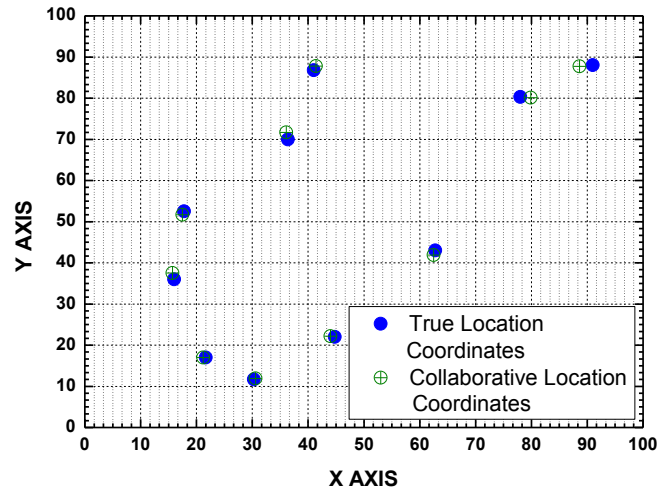


Figure 3.24: Estimated Mean Location Coordinates of Each Observation

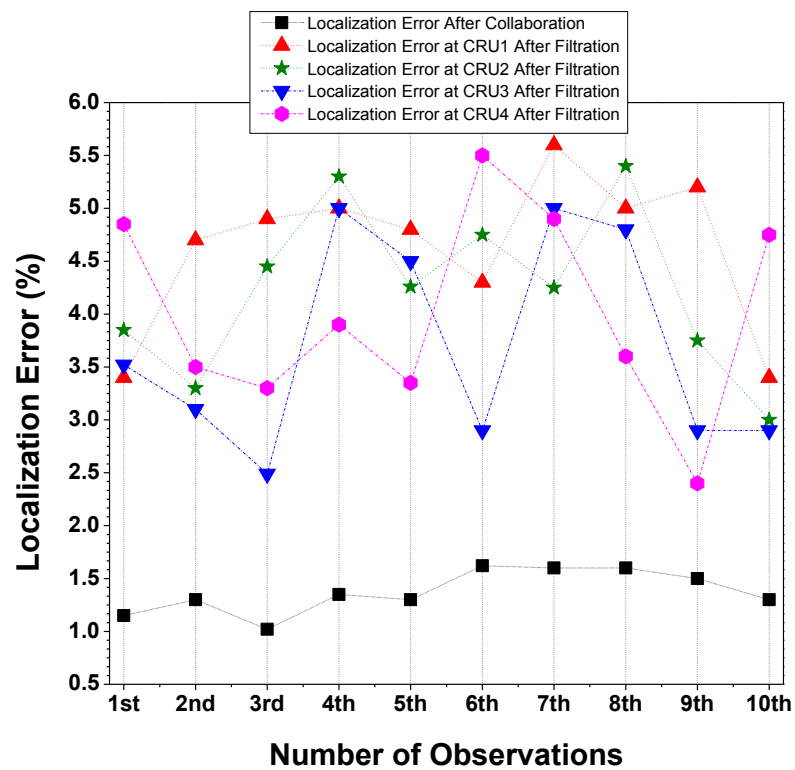


Figure 3.25: Error in Collaborative Location Estimation

Fig.3.25 shows the location estimation error after collaborative localization. It has been observed that the percentage error of collaborative estimation has come down to (1.3–1.62) % compared to (2.4–5.6) % location estimation error when each of the CRU performs localization individually.

### 3.5 DISCUSSION

This chapter has introduced a new analytical framework for RSSI based localization scheme to calculate the precise location coordinates of a fixed as well as a mobile PU in an underlay CRN. A localization hypothesis has been proposed to establish the RSSI based localization scheme. Subsequently, a mathematical model has been developed to optimize the system threshold for efficient PU localization. A well-known localization algorithm WCL, which considers only RSSI measurement at anchor nodes with known location information, has been applied to calculate the location coordinates of a fixed PU under different terrain conditions. It has been observed that RSSI measurement at the CRUs varies with different terrains for the same distance between the transmitter and the receiver. Therefore, a power law model has been considered with a correction factor to improve the accuracy of RSSI measurement under different terrain conditions. The precise location of a fixed PU has been calculated for all the given terrain conditions using the proposed power law model. However, localization of a mobile PU by a single CRU results in poor accuracy. Consequently, a range-based collaborative localization scheme has been introduced in this work to overcome the limitations of a single user localization scheme. In order to calculate the optimum number of collaborative CRUs, a mapping algorithm based on Marcum-Q function has been applied. The graphical analysis reveals that the detection error rate is minimal when four to six users are considered jointly to perform the localization task. For simplicity, a group of four fixed collaborative users has been chosen for experimentation. A rectangular network zone ( $100m \times 100m$ ) with the fixed CRUs placed at the four extremes of the lamina and a mobile PU inside the network zone have been considered as the simulation environment. However, several unpredictable factors such as random external noise effects as well as internal noise of the radio receiver affects reliable signal reception by the CRUs. Since external noise effects on radio communication are random and unavoidable, this chapter has focused on the mitigation of internal noise by modifying CR receiver circuit with the incorporation of a FIR

filter block after the demodulator stage. Three different filter types, namely, Rectangular, Chebyshev, and Hamming have been designed and tested using a programmable DSP kit. A comparative analysis among these three different filter types mentioned above has been done on the basis of their noise filtering performances. All the three filters have been tested at 1 KHz frequency since the audio signal attains maximum power level at 1 KHz (approx.). An average of 1.7 dB improvement in the output SNR value over the corresponding input SNR has been observed with the Chebyshev filter. Also Hamming and Rectangular filters both have achieved a moderate improvement up to a maximum of 0.7 dB to 0.9 dB in the output SNR respectively. Though the performances of all the three designed filters degrade at higher noise level, the Chebyshev filter performance is better than the other two. Therefore, the Chebyshev filter has been selected as an optimum filter type to perform internal noise mitigation. Hereafter, the simulated variable SNR which has been obtained at each of the collaborative CRU due to the movement of mobile PU have been applied to the Chebyshev filter. The SNR obtained with and without Chebyshev filtering have been converted to RSSI voltage for location coordinates calculation at each of the collaborative CRU. The converted RSSI finally determine the precise location of the given mobile PU. The WCL algorithm has been applied to find out the location coordinates of the mobile PU with respect to each collaborative CRU. The collaborative CRUs share its location coordinates and signal strength information, which has been received from a mobile PU, with each other. The received information from the collaborative CRUs has been used to compute location coordinates of the mobile PU for ten observations. The graphical analysis reveals that the coordinates of a mobile PU, obtained after filtering is more accurate as compared to the coordinates, obtained before filtering with respect to each CRU. To enhance the localization accuracy, mean of all the location coordinates of the ten common observations has been computed. The range of localization error after the calculation of mean location coordinates collaboratively has come down to (1.3–1.62) % from the earlier (2.4–5.6) % error when each CRU localizes coordinates individually after filtering. Precise localization capabilities reduce the interference probability with PUs. It also reduces the miss detection and false detection probabilities in the network. Hence, the overall spectrum utilization efficiency improves.



## CHAPTER IV

---

# CHANNEL SELECTION SCHEME FOR UNDERLAY COMMUNICATION

---

4.1	<b>INTRODUCTION</b> .....	79
4.2	<b>SELECTION PARAMETERS</b> .....	81
4.3	<b>OPTIMUM CHANNEL SELECTION SCHEME</b> ....	86
4.4	<b>DISCUSSION</b> .....	93

### 4.1 INTRODUCTION

The ever-increasing demand for radio resources poses new challenges for future wireless communication systems. The need for higher data rates is increasing as a result of the transition from voice-only communications to multimedia type applications. With the existing fixed spectrum assignment policy [1], it is very challenging to meet the demand for spectrum resources with the high data rate expected for future communication systems. However, the actual scenario points to under-utilization or partial-utilization of the pre-

assigned radio frequency (RF) channels by different wireless applications. Duration of underutilization of an RF channel varies with time, frequency and location resulting in spectrum opportunities which can be availed of by other devices. Therefore, a dynamic or variable channel frequency allocation scheme is necessary to meet the demand for secondary wireless applications which, in turn improves spectrum utilization. Hence, the cognitive radio (CR) technology [7] based on dynamic spectrum allocation or sharing policy has emerged. The cognitive technology enabled cognitive radio users (CRUs) or secondary users (SUs) can access the available unoccupied or partially occupied spectrum resource opportunistically. However, if the channel cannot be selected reasonably, the secondary data transmission performance may suffer. The resource or channel selection schemes have been classified into four different types namely, auction model [186], learning model [187], optimization model [188] and prediction [189] model. The channel selection scheme, based on the auction model [186] takes PU as sellers, SU as buyers and idle channel as products. Since the behavior of PUs is very unpredictable and non-cooperative in a practical environment, the auction model cannot ensure the best spectrum selection. Moreover, delay involved in the auction process causes huge system overhead time. In the learning model [187], for proper channel selection, the short term historical state information of spectral occupancy and availability are combined with long term historical information. However, this model faces a challenge during channel selection in a heterogeneous network. The performance indices, namely system time, throughput, maximum channel utilization time, and minimum system delay are considered during the channel selection by the optimization method [188]. The channel selection scheme based on the single object optimization is simple. However, the selection becomes very challenging when the multi-objective optimization is applied. The prediction model [189], considers a specific channel model to analyze the activity of PUs through environmental sensing. The prediction model enabled users can pre-select and switch to the target channel through historical information statistics or some predictive technique. The prediction capability enhances the efficiency of secondary data transmission. However, if the delay involved in periodic detection is high, the effectiveness of the scheme decreases. Thus, the prediction model is suitable for systems where PU activities are regular.

From the earlier discussion, it is clear that a channel selection scheme requires a high degree of flexibility. The radio channel environment is not consistent due to propagation



losses, interferences, and environmental noises. Hence, to handle this inconsistency, some spectrum analysis technique is required to determine the characteristics of the selected channel. After detection and analysis, the spectrum allocation decision (or spectrum assignment) function selects the radio frequency (RF) channel with maximum signal to noise ratio (SNR) for reliable operation of the CR receivers. Hence, a busy time ratio (BTR) metric was introduced in [190] to select the channel by characterizing its quality. A novel graph-theoretic matching algorithm has been proposed in [191] to solve the dynamic channel characteristics. On the other hand, the selection process, described in [192], uses the statistical information of the previous utilization pattern of the channels. It shows a considerably improved performance. In the underlay cognitive scenario, the interference probability with the PU signal is very high due to the simultaneous use of the same channel frequency. Therefore, to minimize interference probability a dynamic channel access strategy has been suggested in [193]. In [194], the utilization of multiuser channel quality information (CQI) has been introduced to allow underlay CRUs to access the licensed spectrum. A cooperative sensing method has been suggested in [195] to avoid collision between SUs and PUs.

A channel frequency selection scheme of the underlay cognitive radio networks (CRNs) has been suggested in this chapter. The channel frequency selection hypothesis has been proposed in subsection 4.2.1. A comparison between the predefined system threshold ( $\lambda_{s/m}$ ) and the RSSI of the selected channel is done to determine whether the channel can be used in an underlay CRN. A hardware module for channel selection scheme has been designed and tested in section 4.3. The hardware testing results have been tabulated in subsection 4.3.3 to justify the proposed hypothesis.

## 4.2 SELECTION PARAMETERS

In CRNs, SUs are temporary visitors to the licensed spectrum. Therefore, SUs should vacate the occupied spectrum when the owner or PU resumes operation. The frequent spectrum handoff process causes huge overhead for the SUs. To decrease the secondary overhead, it is necessary to reduce the number of connection disruptions in a channel. Hence, this thesis

work has considered underlay cognitive communication system, in which SUs operate simultaneously with the PUs on the same licensed channel. However, the selection of licensed channels in underlay CRNs depends on various parameters. Based on the utilization patterns, the licensed bands have been classified into three categories namely black spaces, gray spaces, and white spaces. The black spaces mean that in the occupied spectrum band, the interference level is very high. The gray spaces represent low intensity interference. The white spaces indicate spectrum hole or interference free spectrum. Amongst the three classified spaces, grey spaces are used by the underlay CRUs. However, the selection of grey space spectrum band depends on the proper spectrum sensing technique. The spectrum sensing is one of the essential features of CR enabled devices to become aware of the parameters related to spectrum availability, access policies, and radio channel characteristics like transmit power and noise [1]. The dynamic spectrum access operation of CR depends on two main components namely, spectrum sensing policy and techniques [196]. The spectrum sensing policy decides when and which frequency band to access and it may be implemented either individually or collaboratively. On the other hand, sensing techniques define the selection process for the desired frequency band.

The sensing techniques have been classified into non-cooperative and cooperative schemes. In the non-cooperative scheme, SUs perform sensing operation individually to take a decision about the availability of RF channels. In the cooperative method, multiple SUs share their locally sensed information to obtain an accurate channel selection result [10] [197]. Based on the collected information, the controller (spectrum manager) of the centralized network can reduce the complexity of the SU terminals by allocating the available channels. One fundamental objective of the central controller is to prevent overlapped spectrum sharing among the SUs. The next sub section describes the optimum channel selection hypothesis of Underlay CRN.

#### 4.2.1 Resource Selection Hypothesis

The SUs learn about the radio environment to select the optimum channels for cognitive communication. Fig.4.1 shows the cognitive communication in underlay scenario. The transmitter of a SU sends a supervisory tone  $S(t)$  on a licensed channel. In underlay scenario,

primary and secondary communication takes place on a common channel [198]. In this case, the primary signal  $\{PU(t)\}$  has been considered as an interfering factor along with the link noise ( $P_{ln}$ ) and system generated internal noise ( $P_{in}$ ). Hence, a hypothesis has been proposed to perform the selection operation efficiently. The SNR of the resultant signal,  $\{R(t)\}$  received by the secondary receiver is defined as-

$$SNR = \frac{S(t)}{\{PU(t) + P_{ln} + P_{in}\}} \quad (4.1)$$

SNR of the received signal is compared with a predefined system threshold ( $\lambda_{s/m}$ ) to determine the quality of the selected channel. The test statistics has been classified into two categories:

$$SNR \text{ of the received signal} < \lambda_{s/m} : H_0$$

$$SNR \text{ of the received signal} \geq \lambda_{s/m} : H_1$$

Therefore, hypothesis ( $H_0$ ) is true when the SNR of  $R(t)$  is less than  $\lambda_{s/m}$ . Otherwise, hypothesis ( $H_1$ ) is true.

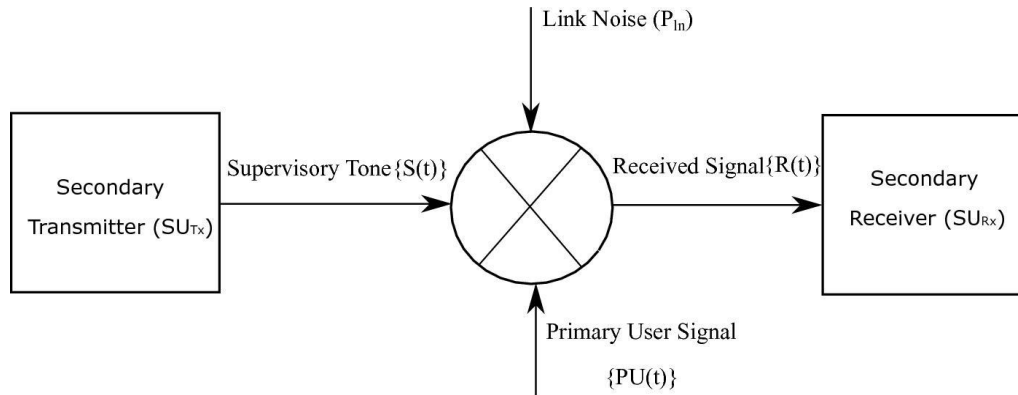


**Figure 4.1: Underlay Cognitive Communication**

Therefore, a channel has been selected ( $H_1$ ) when the SNR of the received signal  $\{R(t)\}$  meets the predefined condition of the channel quality. So, the selected channel reliability has been tested only in the presence of noise. Hence, the knowledge of noise power level ( $P_{ln} + P_{in}$ ) is essential to derive the reliability statistics for channel selection. But it is impossible to

measure the power level of random noise, separately. So, the receiver noise power is assumed to be known a priori in many channel selection methods. However, the noise power level may change over time, thus giving rise to the so-called noise uncertainty problem [57]. The noise uncertainty degrades the performance of the channel selection schemes. Therefore, controlling of interference is essential to achieve maximum performance level during channel selection in CRNs. The next subsection derives a relationship between the noise uncertainty factors and the received signal power.

#### 4.2.2 Interference Temperature Model

Interference temperature is defined as a measure of the RF power available at a radio receiver. More specifically, it is the temperature equivalent (measured in Kelvin) of the RF power available at a receiving antenna per unit of bandwidth [199]. In 2003, the federal communication commission (FCC) defined the interference temperature as-

$$T_{\text{int}} = \left\{ \frac{(I + N)}{KB} \right\} \quad (4.2)$$

In equation (4.2),  $(I + N)$  is the total noise power consists of interference ( $I$ ) and noise ( $N$ ) generated by undesired transmitters and other noise sources, ' $B$ ' is the bandwidth and ' $K$ ' is the Boltzmann's constant. Moreover, the interference temperature metric can be used to calculate the received interference power ( $P_{\text{int}}$ ) at the receiver, in watts [156].

$$T_{\text{int}}(f_c, B) = \frac{P_{\text{int}}(f_c, B)}{KB} \quad (4.3)$$

In equation (4.3) the average interference power  $\{P_{\text{int}}(f_c, B)\}$  and the corresponding absolute temperature  $\{T_{\text{int}}(f_c, B)\}$  are present in the center ( $f_c$ ) of any frequency channel with a specific BW ( $B$ ). Boltzmann's constant ( $K$ ) defines a relationship between the absolute temperature and kinetic energy. However, interference and noise behave distinctly. Interference is more deterministic and independent of bandwidth, whereas noise is not. The objective of this research is to define a single metric that fully captures both the properties of noise and interference. From equation (4.3),  $T_{\text{int}}$  can be specified as a function of  $B$  as-

$$T_{\text{int}}(f_c, B) = \frac{1}{KB} P_{\text{int}}(f_c, B) = \frac{1}{KB} \left( \frac{1}{B} \int_{f_c - \frac{B}{2}}^{f_c + \frac{B}{2}} S[f] df \right) \quad (4.4)$$

The  $S[f]$  represents power spectral density (PSD) [200] of the RF environment. For a given geographic area, the FCC specified an interference temperature limit ( $T_L$ ). This value would be a maximum amount of tolerable interference for a given frequency band in a particular location. Any unlicensed transmitter utilizing this band must guarantee that their transmissions together with the existing interference level must not exceed the interference temperature limit at a licensed receiver [201]. Therefore, optimization of transmission power of an unlicensed user is one of the important factors to control this interference. The SNR of the received signal can be used to determine the amount of energy required for any transmission. The interrelationship among interference temperature, BW, and received signal strength is a powerful factor during channel selection. It has been illustrated by-

$$SNR \propto \left\{ \frac{P_r}{(P_{\text{ln}} + P_{\text{in}})} \right\} = \left( \frac{P_r}{P_N} \right) \quad (4.5)$$

In equation (4.5),  $P_{\text{ln}}$  and  $P_{\text{in}}$  represent the link noise and internal noise, respectively. The total noise power ( $P_N$ ) can also be represented in terms of interference temperature ( $T_{\text{int}}$ ).

$$P_N = (KBT_{\text{int}}) \quad (4.6)$$

The interference temperature ( $T_{\text{int}}$ ) is caused by the presence of link noise and system generated internal noise. Therefore,  $T_{\text{int}}$  can be written as-

$$T_{\text{int}} = (T_l + T_e) \quad (4.7)$$

In equation (4.7),  $T_l$  and  $T_e$  are the unwanted interference temperature corresponding to the link noise and the internal noise temperature respectively. Therefore to establish interrelationship between interference temperature and received signal strength, the equation (4.5) can be rewritten as-

$$SNR \propto \left\{ \frac{P_r}{KB(T_l + T_e)} \right\} \quad (4.8)$$

Hence, overall SNR degrades when interference temperature factors increase. The fundamental criterion for an optimum channel selection is that the signal power of the selected channel must be higher than the noise floor level. The minimum signal to noise ratio (SNR) for reliable data communication is recommended as 18 dB [173]. For example, if the noise floor peak is -85 dBm, the signal power should be a minimum of -67 dBm to achieve reliable data communication. However, together with the signal and noise power, the RSSI voltage indicates the SNR of a communications signal in CRNs. Hence, the RSSI measurements are playing an important role in radio resource management like cellular systems as it is used to monitor the signal and noise levels [202] together. Therefore, in this work RSSI corresponding to the received signal SNR has been used as the channel selection parameter in an underlay CRN. The next section has introduced the RSSI based channel selection scheme.

### 4.3 OPTIMUM CHANNEL SELECTION SCHEME

A channel selection scheme has been finalized by designing a suitable hardware circuit. The circuit has been tested and analyzed based on the comparison between the RSSI of the selected channel and the predefined system threshold. The Hill Climbing (HC) method has been introduced in the next subsection to maximize the bandwidth (BW) of the selected channel.

#### 4.3.1 Maximizing Channel Bandwidth using Hill Climbing Method

Hill Climbing (HC) is a simple search and optimization algorithm for single objective functions. It is an iterative algorithm that starts with an arbitrary solution to a problem, then attempts to find a better solution by changing the previous selection incrementally. If a change produces a better solution, further incremental change is made to find a better solution than the previous one. Let's consider a target function  $f(x)$ , where 'x' represents a

continuous or a discrete variable depending upon the problem domain. The optimization algorithm modifies ' $x$ ' and determines whether the correction increases the value of  $f(x)$ . Any modification that increases the value of  $f(x)$  is accepted. The variable ' $x$ ' is defined as 'locally optimal' [203]. The idea of beginning with a sub-optimal solution is compared to starting from the base of the hill by a randomly chosen track and finally reaching the top of the hill through the best track. The process is compared with the maximizing some solution. Another possibility for selection using HC algorithm is to start with the worst possible variable [204].

In numerical analysis, HC is a mathematical optimization technique [205] which belongs to the family of local search. Mathematically, the HC algorithm is used to maximize or minimize a given real function by choosing values from the available inputs. The relative simplicity of the HC algorithm makes it a popular choice amongst optimizing algorithms for CR technology. It can often produce a better result than other optimization algorithms when the amount of time available to perform a search is limited. In CR technology, HC algorithm is used as a heuristic search function. A heuristic search function is a function that will rank all the possible alternatives at any branching step in a search algorithm based on the available information.

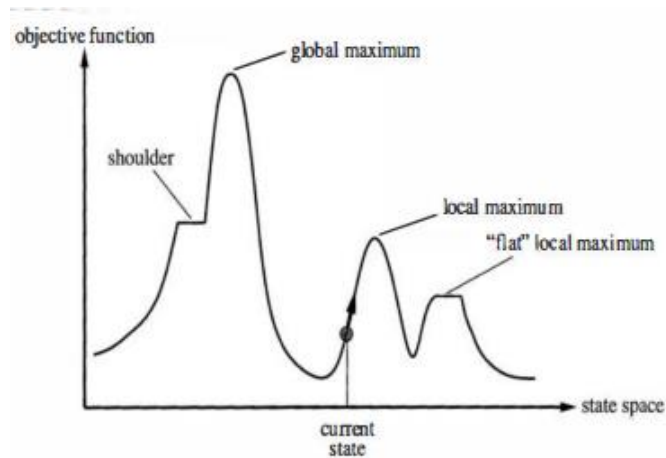
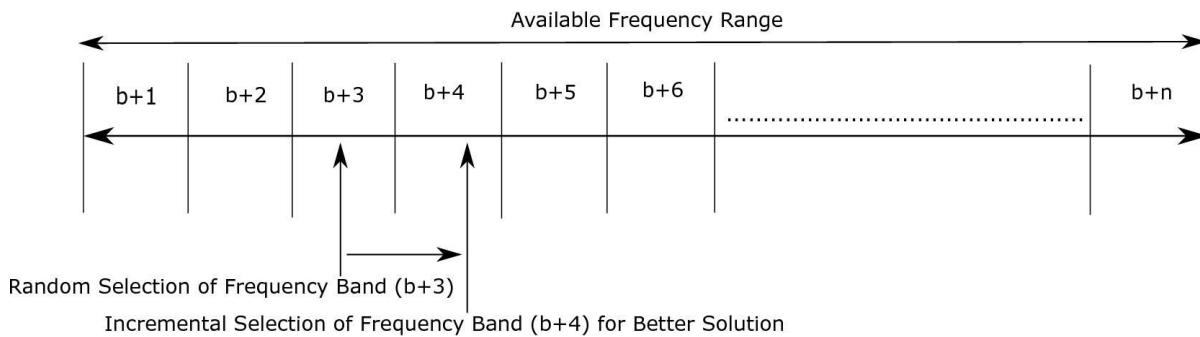


Figure 4.2: Hill-Climbing Optimization Algorithm [205]

Fig.4.2 shows state space diagram. It is a graphical representation which establishes a relation between the states of the search algorithm and the value of objective function. In Fig.4.2, the local maximum is a state which is better than the neighbor states. This local state is better because the value of an objective function is higher than its neighbors. HC algorithm

is good for finding a local optimum, but it is not guaranteed to find the global optimum out of the search space. This chapter has proposed an optimum channel selection scheme based on the principle of HC algorithm. In this scheme, after a random selection of channel BW as a solution, the system will try to find a better solution than the previous selection by increasing the BW with a step by step incremental process. During this process, if the signal to noise ratio (SNR) is poor for a given selection, compared to the previous one, the system will switch to another part of the spectrum randomly to continue the process. The process will continue until the cumulative BW is less than the allotted maximum channel BW. Once the channel BW is equal to the maximum frequency, the channel selection process will terminate.



**Figure 4.3: BW Selection as per Principle of Hill Climbing Algorithm**

Fig.4.3 shows a part of RF spectrum band that has been split into B numbers of narrow frequency bands of 1 MHz BW each. A narrow band can be selected randomly as per the principle of HC algorithm. Received signal strength indicator (RSSI), a dc voltage (output of the first IF processor IC) is linearly proportional to the signal power of selected channel frequency. The RSSI of the selected frequency band is compared with the predefined system threshold ( $\lambda_{s/m}$ ). The system threshold ( $\lambda_{s/m}$ ) has been chosen carefully to meet the requirement of minimum SNR for the reliable and consistent operation of CR receivers. Only when the RSSI of the selected channel frequency is greater than or equal to the predefined system threshold ( $\lambda_{s/m}$ ), the selection will be accepted and the selected channel frequency BW will be increased by 1MHz. The step by step BW increment will continue until the signal strength of the channel frequency is greater than or equal to the system threshold. Otherwise, some other portion of the frequency band will be selected randomly.



Fig.4.4 represents the operational flow of the proposed channel selection scheme for underlay cognitive communication.

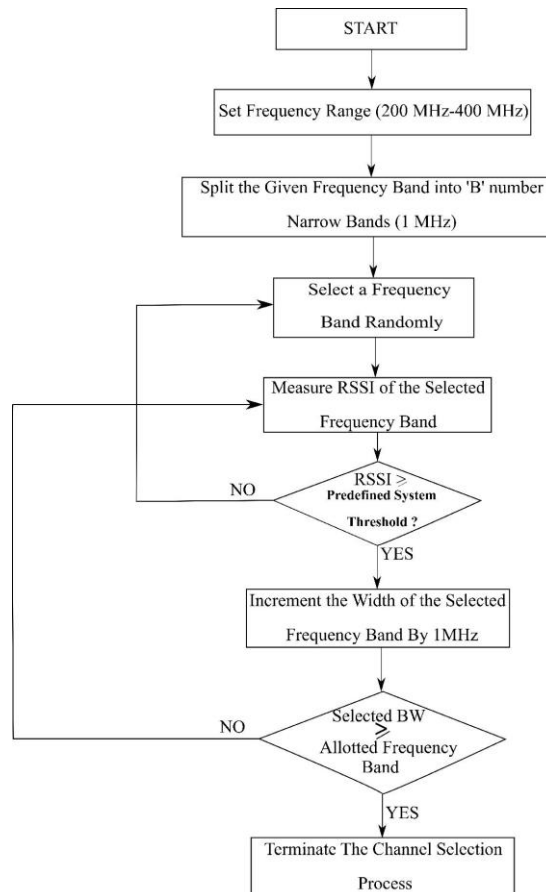


**Figure 4.4: Operational Flow Diagram of the Channel Selection Scheme**

### 4.3.2 Experimental Setup

Fig.4.5 represents the hardware scheme of channel selection for underlay communication. A variable voltage source has been used to emulate the RSSI of the selected channel. A DC comparator has been used to compare RSSI voltage with the predefined reference voltage. The output of the comparator has been connected to a voltage translator. The translator gives either 0 volt or 5-volt output. When the input is 5-volt, microcontroller instructs phase lock loop (PLL) IC to lock the selected channel frequency and the voltage controlled oscillator (VCO) of PLL IC increase the VCO frequency by 1 MHz under controller control. However, when the input is 0 volt, random selection of another channel frequency is instructed.

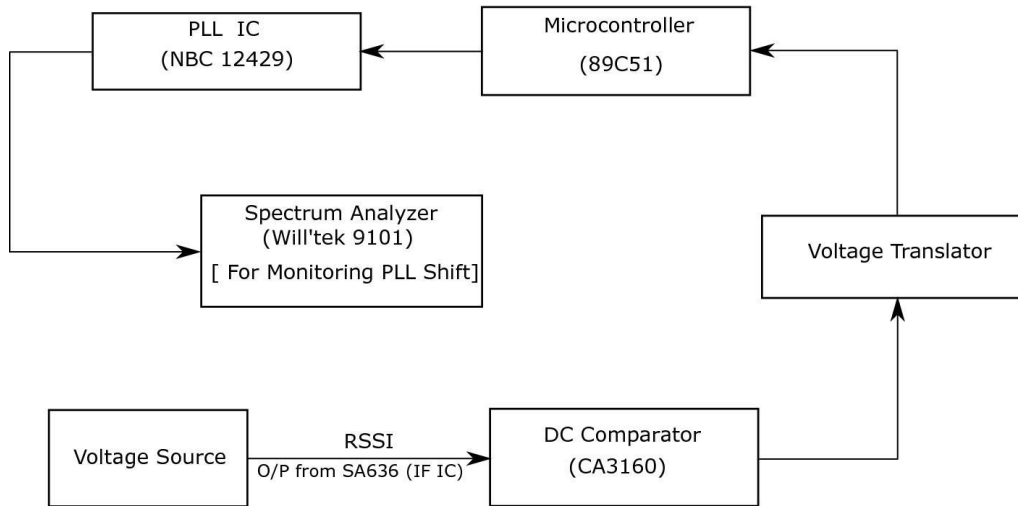


**Figure 4.5: Schematic Block of Channel Selection Scheme**

A frequency range of (200-400) MHz in the RF spectrum has been selected for the RSSI based channel selection scheme. The given spectrum band has been split into B number of narrow bands (refer Fig.4.3). After random selection of one sub-band out of the B bands, the quality of the selected channel frequency band is checked directly by comparison with the RSSI voltage, which has been obtained from the data sheet of the first IF processor IC SA 636 [206] (details in Appendix B). When the RSSI value is higher than or equal to the corresponding system threshold ( $\lambda_{s/m}$ ) value, the controller instructs the phase lock loop (PLL) IC to increase the BW of selected frequency band. On the other hand, if the RSSI of the selected channel frequency is less than the desired system threshold ( $\lambda_{s/m}$ ), the system selects another 1 MHz band of B to continue the same process. The operational amplifier (CA 3160-details in Appendix B) has been used to compare the RSSI of the selected channel frequency with the predefined reference voltage ( $V_{ref}$ ) of 0.8 V (System Threshold) through the voltage translator. The output of the comparator (CA3160) has been connected to a port (P0.0) of the microcontroller (89C51). The output ports of the 89C51 have been connected with the M [8:0], N [1:0], and P\_LOAD inputs of the PLL IC (NBC12429-details in Appendix B) [207]. M [8:0] pins are used to configure the PLL loop divider. M [8] is the MSB and M [0] is the LSB. N [1:0] pins are used to configure the output divider modules. P\_LOAD pin loads the configuration latches with the contents of the input. The M [8:0] and N [1:0] ports are set first and then the P\_LOAD is enabled by the microcontroller (89C51).

When the comparator output is high, controller changes 1 bit of M [8:0] to increase the frequency band by 1 MHz. The corresponding frequency is locked by the PLL within 20 ms [207]. The process will continue until the RSSI voltage value of the locked frequency band is greater or equal to the reference voltage. However, when the output of the comparator is low, the microcontroller gives a low state output. This causes the program to change M [8:0] in sequence, and the corresponding PLL output ( $F_{out}$ ) frequency is changed randomly within the range of (200-400) MHz. The frequency shift can be observed by a frequency domain instrument. In this work, the change in channel frequency was observed on the spectrum analyzer. Fig.4.6 shows the schematic diagram of the setup.

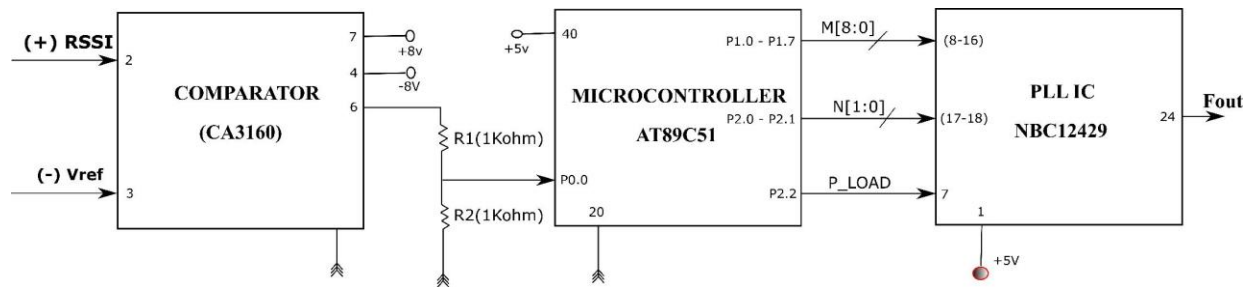
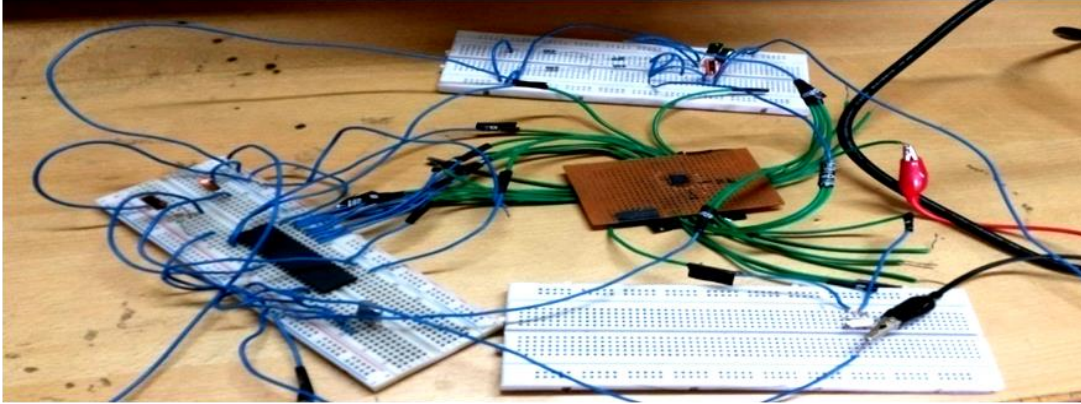


Figure 4.6: Experimental Setup of Channel Selection Scheme

In Fig.4.6, equivalent RSSI voltage corresponding to selected channel has been applied as an input to the comparator (CA3160) with a reference threshold voltage ( $V_{ref}$ ). When the RSSI voltage is greater than  $V_{ref}$ , the comparator output ( $C_{out}$ ) is 10V and when the RSSI value is less than  $V_{ref}$ , the comparator output ( $C_{out}$ ) is 0 V. Therefore, a voltage divider which is used to limit the comparator output ( $C_{out}$ ) within 5V, has been designed with  $R_1(1k\Omega)$  and  $R_2(1k\Omega)$ . The output of the voltage divider has been connected to the input port (P0.0) of a microcontroller (89C51). The microcontroller takes decisions about the selection or rejection of the selected channel frequency from the input voltage level (5V/0V). Thus, a given channel frequency band is selected automatically from the RSSI. The reference voltage ( $V_{ref}$ ) which has been obtained from the datasheet of the IF-IC [206] represents the minimum signal strength for the reliable network operation.

### 4.3.3 Emulated Results of Channel Selection Scheme

Fig.4.7 represents the laboratory setup of the experiment.



**Figure 4.7: Laboratory Setup of Experiment**

NBC12429, the general purpose PLL can be programmed for a frequency within 25 MHz and 400 MHz. The voltage-controlled oscillator (VCO) within the PLL operates over a frequency range of 200 MHz to 400 MHz. The output frequency ( $F_{out}$ ) of the PLL is represented mathematically [207] as-

$$F_{out} = [(F_{XTAL} \div 16) \times M] \div N \quad (4.9)$$

In equation (4.9),  $F_{XTAL}$  is the frequency of the crystal,  $M$  is the loop divider modulus, and  $N$  is the output divider modulus. 16 MHz crystal frequency is used as reference. If  $M$  is selected arbitrarily, the PLL will be unable to achieve loop lock. To avoid this, the selection of  $M$  value is limited within the VCO frequency range  $200 \text{ MHz} \leq VCO_f \leq 400 \text{ MHz}$ . The PLL output frequency step depends on the selection of  $N$ . Table 4.1 shows PLL output frequency range variation for four combinations of output divider modules.

**Table 4.1: Programmable Output Divider Function [207]**

N1	N0	N Divider	$F_{out}$	Output Frequency Range (MHz)	$F_{out}$ Step
0	0	$\div 1$	$M$	200-400	1 MHz
0	1	$\div 2$	$M \div 2$	100-200	500 KHz
1	0	$\div 4$	$M \div 4$	50-100	250 KHz
1	1	$\div 8$	$M \div 8$	25-50	125 KHz

Therefore, to get the desired PLL output ( $F_{out}$ ),  $M$  and  $N$  have been programmed properly. In this experiment, the division ratio of  $N$  [1:0] set as  $N = 1$ . Therefore, equation (4.9) can be written as-

$$F_{out} = \left[ \left\{ (16 \div 16) \times M \right\} \div 1 \right]$$

$$\text{or, } F_{out} = M \quad (4.10)$$

Therefore, if  $M$  changes by 1,  $F_{out}$  changes by 1 MHz. The test results have been tabulated in Table 4.2.

**Table 4.2: Emulated Results of Hardware Module**

$V_{ref}$	RSSI (Volt)	Microcontroller Port P2.3 Connection	$M$	$F_{out}$
0.8	1.1	5V DC	[011001011]	203MHz (Random)
0.8	1.3	5V DC	[011001100]	204 MHz (Increment)
0.8	0.5	Ground	[101000000]	320 MHz (Random)
0.8	0.8	5V DC	[101000001]	321 MHz (Increment)
0.8	1.3	5V DC	[101000010]	322 MHz (Increment)
0.8	1.3	5V DC	[101000011]	323 MHz (Increment)

#### 4.4 DISCUSSION

A channel selection scheme for the underlay CRNs has been developed in this work. One of the fundamental design problems is how the underlay CRUs decides when and which licensed channel should be selected for communication. A channel selection hypothesis has been proposed to determine channel quality based on the strength of the received signal. Since the underlay CRUs use the partially occupied licensed spectrum band, the transmitted signal by the PU has been counted as an interfering factor along with the link noise and internal noise during the channel selection process. The ability to select the optimum licensed channel would minimize the interference probability with the PUs in an underlay network. It also improves the utilization efficiency of licensed spectrum.



## CHAPTER V

---

# UNDERLAY COGNITIVE MAC PROTOCOL

---

5.1	<b>INTRODUCTION</b> .....	95
5.2	<b>OPPORTUNISTIC UNDERLAY NETWORK</b> .....	97
5.3	<b>RECEIVER-INITIATED (RI) MAC PROTOCOL</b> ....	103
5.4	<b>TRANSMITTER-INITIATED (TI) MAC PROTOCOL</b> .....	113
5.5	<b>FLEXIBLE TRANSMIT POWER SELECTION STRATEGY</b> .....	119
5.6	<b>DISCUSSION</b> .....	128

### 5.1 INTRODUCTION

The underlay cognitive radio users (CRUs) or secondary users (SUs) utilize the underutilized radio frequency spectrum dynamically and intelligently [208] without interfering with the licensed users or primary users (PUs). It is possible only when the SUs learn about the spectrum occupancy in real time [10]. After learning about the radio environment, SUs need to make appropriate decisions regarding the opportune moments for accessing the underutilized

parts of the channel spectrum. Therefore, the operational activities of SUs depend on efficient spectrum sensing techniques as well as effective medium access control (MAC) protocols. In CRNs, MAC protocols are required to exploit the spectrum opportunities, manage the interference with PUs, and coordinate the spectrum access amongst SUs either in a fixed manner or using random access mechanisms [91-92]. Hence the execution strategies of the spectrum sensing techniques need to be scheduled by MAC protocols. However, the performance of MAC protocols may suffer by the interference from the hidden terminals, sensing error, sensing delay, selection of common control channel, interference with PUs, and network coordination problem [91]. Therefore, CR specific MAC protocol design is a critical issue to implement the underlay CRNs successfully.

The underlay CRUs are allowed to use licensed spectrum efficiently by keeping the resultant interference at the primary receiver below the predefined threshold [22]. An underlay CR MAC protocol is proposed in [132] to investigate the dynamic spectrum sharing problem among PUs and SUs. In [76], a scheme for the underlay CRUs has been introduced to minimize the interference with the PUs. On the other hand, a CDMA-based underlay CR system [77] focuses on the increase transmit power of SUs to counter-balance the harmful interference. The collision with the hidden terminals degrades the received signal quality at the secondary receiver. A hidden node collision is also known as blind node collision which occurs when two nodes in the network are not able to see each other and communicate with a shared visible node. In an underlay CRN, the primary transmitter has been considered as a hidden terminal. Therefore, during the cognitive data communication, hidden primary transmitter can interfere with the transmitted data. The hidden terminal interference leads to corrupted data reception which subsequently leads to unsuccessful data transmission. Therefore, the secondary transmitter reattempts to transmit undelivered data to complete data transmission successfully. The waiting time duration increases exponentially with each retransmission attempts. It leads to a very high system overhead time. In [67], a mathematical model based on queuing theory has been derived to quantify the impact of the hidden terminal problem. A ranging based communication method has been recommended in [209] to minimize interference with the hidden terminals.

In section 5.2, a receiver-initiated (RI) MAC protocol is proposed to minimize hidden terminal interference problem and end-to-end delay. In the RI MAC protocol, a secondary



receiver establish a communication link by sending locally sensed least noisy carrier frequency information over a command control frame. The receiver initiated channel selection scheme has minimized the collision probabilities with the hidden terminals. Since the back-off waiting period due to the multiple failures in data transmission is not a factor at all, system overhead time is less compared to conventional MACA or MACA-BI protocols. Simulation results in subsection 5.2.3 are used to analyze the throughput and system efficiency in case of multiple retransmission attempts. However, the secondary transmissions may degrade the performance of a primary receiver due to the simultaneous usage of the same licensed spectrum. Therefore, to keep probability of interference level at the primary receiver within acceptable limit, optimization of secondary transmit power is necessary. In section 5.3, a transmitter-initiated (TI) MAC protocol with a flexible transmit power selection strategy is proposed to minimize the outage probability at the primary receiver. In this protocol, secondary transmitter initiates data transmission only after receiving channel quality information from the corresponding secondary receiver. Hence, a twin scan of the selected channel at both ends (secondary transmitter and receiver) has been proposed in this protocol to eliminate hidden terminal interference during data communication. A step-by-step transmit power adjustment concept has been established experimentally to maximize channel utilization and reliability for underlay CRNs. During this process, if the secondary transmit power reaches the limit to cause interference at the PU, then without wasting any time, SU opportunistically switches to another licensed channel to continue the secondary transmission. It not only improves the system throughput and efficiency but also overcomes interference possibility with the PUs.

## 5.2 OPPORTUNISTIC UNDERLAY NETWORK

Underlay CR brings the concept of a well regarded agile technology that allows concurrent opening up of the frequency bands to the users in a non-interfering mode. These radios should possess at least, minimum information about their surrounding non-cognitive users to make spectrum sharing possible. Exceeding the predefined tolerable interference limit may degrade the performance efficiency of the licensed users dramatically.

### 5.2.1 Channel Model

Fig.5.1 shows a point to point underlay cognitive communication environment. Here, simultaneous operation of a primary (Licensed) and a secondary (Cognitive) user pair (Transmitter  $T_x$ –Receiver  $R_x$ ) is examined [198]. The licensed channel is open to SUs for their use to achieve higher spectral efficiencies. In Fig.5.1 primary and secondary users are indexed by suffixes  $p$  and  $s$  respectively.  $h_{ss}$ , represents a link between secondary  $T_x$  and primary  $R_x$  and  $h_{pp}$  represents a link between primary  $T_x$  and primary  $R_x$ . The channel state information (CSI) is obtained from the classic spectrum sensing techniques. The SU adjusts transmit power depending on the sensing outcomes.

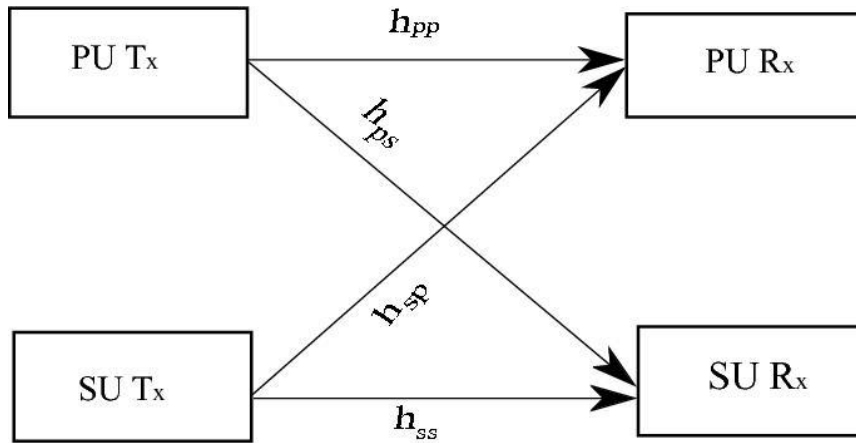


**Figure 5.1: Underlay Channel Model**

The channels are assumed to be AWGN (Additive White Gaussian Noise) type whose gains are random but constant during transmission. The corresponding input-output relation ( $Y_{sp}$ ) of the link ( $h_{sp}$ ) between the secondary  $T_x$  and primary  $R_x$  is given by-

$$Y_{sp} = \left( \sqrt{g_{sp}} X_{sp} + n \right) \quad (5.1)$$

In equation (5.1),  $X_{sp}$  and  $n$  represent secondary transmission on the channel link ( $h_{sp}$ ) and path loss exponent respectively. The channel power gain ( $g_{sp}$ ) of the link  $h_{sp}$  can be written as-

$$g_{sp} = d_{sp}^{-\alpha} |h_{sp}|^2 \quad (5.2)$$

In the equation (5.2),  $d_{sp}$  represents the distance between secondary  $T_x$  and primary  $R_x$  and  $\alpha$  is the attenuation power-law exponent. Channel gains are modelled as Zero Mean Circular Symmetric Gaussian (ZMCSCG) random entries, so that  $h_{sp} \sim N(0,1)$ , a normal distribution with mean 0 and variance 1. Now, during the licensed communication between a primary  $T_x$  and primary  $R_x$ , channel power gain will be  $g_{pp}$ . Hence the input output relation ( $Y_{pp}$ ) of the link  $h_{pp}$  can be written as-

$$Y_{pp} = \left( \sqrt{g_{pp}} X_{pp} + n + Y_{sp} \right) \geq \lambda_{PU} \quad (5.3)$$

Where,  $\lambda_{PU}$  is the predefined interference threshold limit at primary  $R_x$  and  $X_{pp}$  is the primary transmission on the channel link ( $h_{pp}$ ). The channel power gain ( $g_{pp}$ ) of the primary link ( $h_{pp}$ ) can be obtained as per equation (5.2). The input output relation ( $Y_{ss}$ ) of the link ( $h_{ss}$ ) between the secondary  $T_x$  and the secondary  $R_x$  can be defined likewise.

The outage handling capacity of PU is defined as the maximum capacity that can be achieved over all the fading channels for a specified outage probability. In [210], based on the statistical CSI, primary outage probability has been considered as a new criterion to measure the QoS. It has been assumed that a PU transmits with constant power and rate, denoted by  $P_p$  and  $r_p$  respectively. When the secondary transmission is not present on this licensed channel, then the transmission outage probability ( $\varepsilon_a$ ) [211] can be written as-

$$\varepsilon_a = P_r \left[ \frac{g_{pp} P_p}{n_p B} < \lambda_{PU} \right] \quad (5.4)$$

Where,  $P_r(\cdot)$  denotes the probability of a given transmission rate  $r_p$ . In the equation (5.4),  $n_p$  is assumed to be an independent random variable of the AWGN channel with a normal distribution having zero mean and variance  $N_0$ . The channel bandwidth is represented by  $B$ . The ergodic channel capacity of a SU is investigated by Bala *et al.* [212] using soft sensing information of PU activity in a shared channel under joint peak transmit power and average

received interference power constraints. This capacity defines the maximum achievable rate averaged over all fading states. Therefore, if the SU transmission presents on the same licensed channel then the transmission outage probability  $(\varepsilon_p)$  [211] can be written as-

$$\varepsilon_p = P_r \left[ \frac{g_{pp} P_p}{g_{sp} P_s + n_p B} < \lambda_{PU} \right] \quad (5.5)$$

The transmit power of the SU is denoted by  $P_s$ . Hence, to meet optimum SNR at primary  $R_x$ , the transmission outage probability  $(\varepsilon_p)$  always must be less than or equal to  $(\varepsilon_a)$  i.e.

$$\varepsilon_a \geq \varepsilon_p \quad (5.6)$$

The next sub-section introduces basic MAC protocols for secondary data communication by maintaining maximum interference with the PU within a predefined limit.

### 5.2.2 Basic Communication Protocols

A medium access control (MAC) protocol [213-214] allocates available channel resources among the SUs to avoid collision with the PUs. Handshaking procedure is used before initiating any data transmission. It creates a physical link between the two parties [215]. Thus four cycles are required to complete successful data transmission with conventional MACA protocol [216]. In multiple access with collision avoidance (MACA) protocol, a secondary  $T_x$  initiates communication by sending a command signal, known as request-to-send (RTS). If the recipient is in a condition to receive, it responds with the clear-to-send (CTS) command. After receiving confirmation from the secondary  $R_x$ , data transmission begins on a selected channel by the secondary  $T_x$ .

A receiver-initiated MACA-BI (By Invitation) protocol was proposed in [217] to minimize system overhead and transmission delay. In this protocol, a secondary  $R_x$  initiates communication by sending the ready-to-receive (RTR) command frame. After the reception of the RTR command, secondary  $T_x$  starts sending data on the locally selected channel. Communication session is over after receiving an acknowledgment (ACK) command from the corresponding secondary  $R_x$  node.

However, in an underlay CRN, the secondary  $T_x$  selects channel for data communication based on local sensing information. If the received signal strength at the secondary  $R_x$  is less than the predefined system threshold ( $\lambda_{s/m}$ ) then the received data can get corrupted. On reception of corrupted data, the secondary  $R_x$  does not respond to the secondary  $T_x$  with ACK command. Therefore, secondary  $T_x$  needs to retransmit the same data after a period of waiting time. This waiting time due to multiple retransmission attempts increases exponentially and results in huge overhead. It reduces overall system throughput and efficiency. Fig.5.2 and Fig.5.3 represent the retransmission timing sequence of the two conventional MAC protocols, respectively.

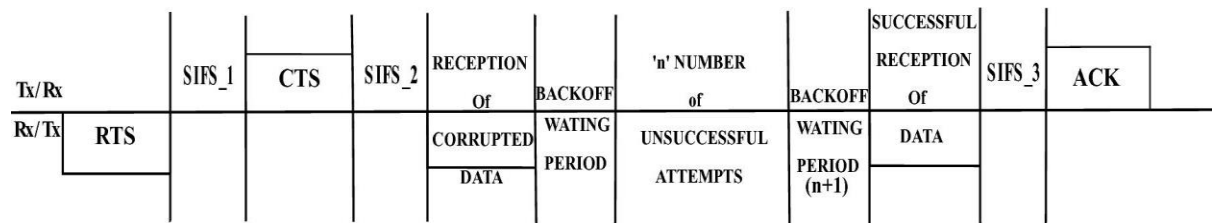


**Figure 5.2: Data Transmission Scheme under MACA Protocol**

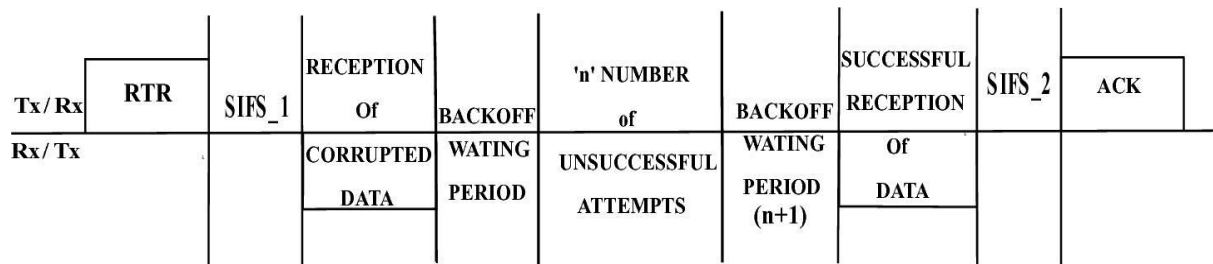


**Figure 5.3: Data Transmission Scheme under MACA-BI Protocol**

The shortest inter frame space (SIFS\_1, SIFS\_2,....., SIFS\_n) represents the system computation time ( $\tau_{comp}$ ) for processing, comparison and response. The lengths of the RTS and CTS control frames are 20 and 15 bytes long respectively. The RTR frame length is 16 bytes long. A common control channel is used to exchange command control frames between transmitter and receiver. Fig.5.4 shows the structure of the command control frames. Both the RTS and RTR frames consist of 6 bytes of destination ID or receiver address and 6 bytes of source ID

or transmitter address. The CTS frame simply gets the transmitter address of the RTS frame and set it to receiver address of 6 bytes. The RTS frame also consists of the information about the total number of packets which will be transmitted after receiving the required acknowledgment from the receiver unit. The CTS frame has the packet length information of two bytes. On the other hand, the RTR frame gives information about both the length and packet ID which the receiver wishes to receive from the corresponding secondary  $T_x$ .

<b>6</b>	<b>6</b>	<b>2</b>	<b>4</b>	<b>2</b>
Destination ID	Source ID	Frame Control	FCS	Number of Packets

(a) Request-to-Send (RTS)

<b>6</b>	<b>6</b>	<b>1</b>	<b>2</b>
Destination ID	Source ID	Control Bits	Packet Length

(b) Clear-to Send (CTS)

<b>6</b>	<b>6</b>	<b>1</b>	<b>2</b>	<b>1</b>
Destination ID	Source ID	Control Bits	Packet Length	Packet ID

(c) Ready-to-Receive (RTR)

**Figure 5.4: Command Control Frame Structure**

In a dense traffic condition, multiple collisions usually occur which may increase transmission delay exponentially. As a result, retransmission attempts for the same data packet degrade the overall system throughput and efficiency. Hence, a receiver-initiated (RI) MAC [83] protocol scheme has been proposed in the next section to minimize interference with the hidden terminals and maximize system efficiency.

### 5.3 RECEIVER-INITIATED (RI) MAC PROTOCOL

Underlay Cognitive communication takes place on a licensed carrier frequency along with the PUs. During the data communication, interference with the PU signal degrades the performance of an underlay CRN. In the proposed scheme, the secondary  $R_x$  initiates communication on the locally sensed, least noisy carrier frequency. In this protocol, data transmission completes within only three cycles for successful first attempt transmission. However, for each failure of data transmission, the receiver selects another channel frequency for retransmission and initiate communication without waiting for retransmission attempt from the corresponding secondary  $T_x$  on the previously selected licensed channel frequency. This is the fundamental difference from other conventional receiver initiated protocol such as MACA-BI. Since the back-off waiting period is not a limiting factor in the proposed RI MAC protocol, system overhead time will be less compared to conventional MACA or MACA-BI protocols.

#### 5.3.1 Timing Sequence of Data Transmission Scheme

The primary reason for implementing this technique is to minimize collisions with hidden terminals and improve data transmission efficiency. Therefore, to initiate communication, secondary  $R_x$  sends carrier-to receive (CTR) command with a desired secondary  $T_x$  address. CTR is a 21 bytes long control frame and contains preamble bits (for synchronization), control bits (source-destination information) and checksum bits.

6	6	2	4	2	1
Destination ID	Source ID	Control Bits	FCS	Packet Length	CI

Figure 5.5: Carrier-to-Receive (CTR) Frame Structure

Fig.5.5 shows the basic structure of the CTR command frame. It consists of frame control bits of two bytes, six bytes of a destination ID or a receiver address (RA), six bytes of a source ID or a transmitter address (TA), four bytes frame check sequence (FCS) and two

bytes of packet length information. The channel information (CI) of one byte will carry information about the suitable channel frequency. The corresponding secondary  $T_x$  will respond with data transmission on the receiver selected carrier frequency. Fig.5.6 represents the flow of handshaking procedure between secondary  $R_x$  and  $T_x$ .

For the concurrent transmission along with a PU on a licensed channel, the failure probability during data transmission is very high. Hence, when the received signal strength of the transmitted data from the corresponding secondary  $T_x$  is less than the predefined system threshold ( $\lambda_{s/m}$ ), the secondary  $R_x$  cannot recover the original information from the received data sequence. This unrecovered data sequence has been termed as corrupted data. On the reception of corrupted data, secondary  $R_x$  will instantly scan the available channels to select a different carrier frequency. Hereafter, without waiting for retransmission attempt from the corresponding secondary  $T_x$ , secondary  $R_x$  sends another CTR command frame with new carrier frequency information for data communication.

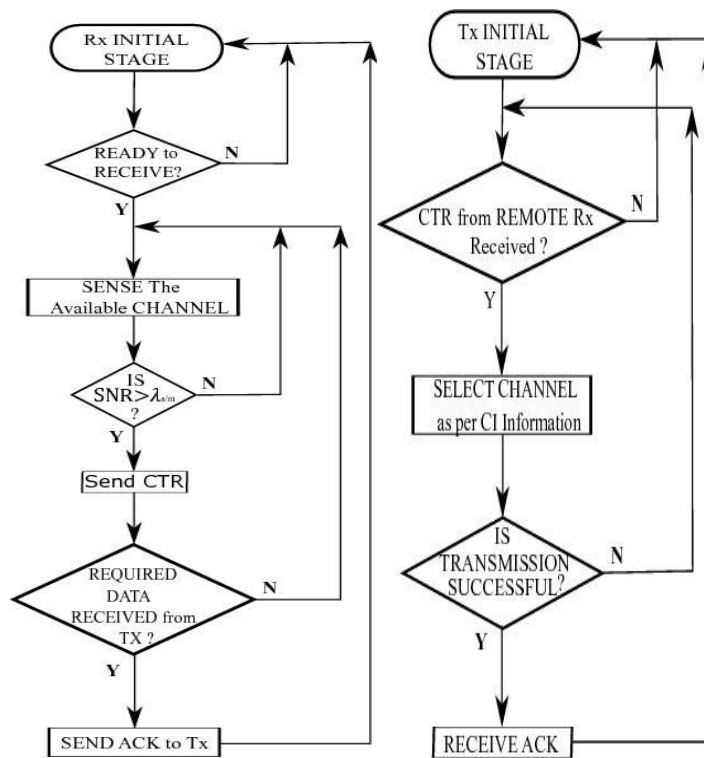
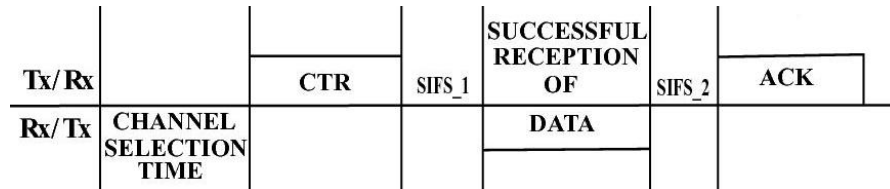


Figure 5.6: Operation Flow Diagram of the Proposed Protocol



The data transmission scheme has been classified into two binary hypotheses  $H_{sd}$  and  $H_{fd}$  corresponding to successful and failed data transmission. Fig.5.7 shows the successful data transmission scheme at first attempt under hypothesis  $H_{sd}$ . Here, a secondary  $T_x$  transmits required data after receiving the CTR command from a secondary  $R_x$ . On the reception of data successfully, secondary  $R_x$  responds with the ACK command. Therefore, successful data transmission completes within three cycles.

$$H_{sd} : \text{Signal Strength of the Received Data} \geq \lambda_{s/m}$$



**Figure 5.7: Scheme of Data Transfer under Hypothesis  $H_{sd}$**

However, the possibility of interference with the PU leads to high failure probability in secondary data transmission. Unsuccessful or failed data transmission scheme at first attempt has been shown in Fig.5.8 under hypothesis  $H_{fd}$ . Failure probability occurs when the received data signal strength is less than the predefined required system threshold ( $\lambda_{s/m}$ ). In this hypothesis, if corrupted data is received, then the receiver resends the CTR command. Therefore, transmitter reattempts to send the undelivered data on a different channel frequency selected by the receiver. The retransmission attempts may fail again, but it eliminates exponential back-off waiting time in data communication.

$$H_{fd} : \text{Signal Strength of the Received Data} < \lambda_{s/m}$$

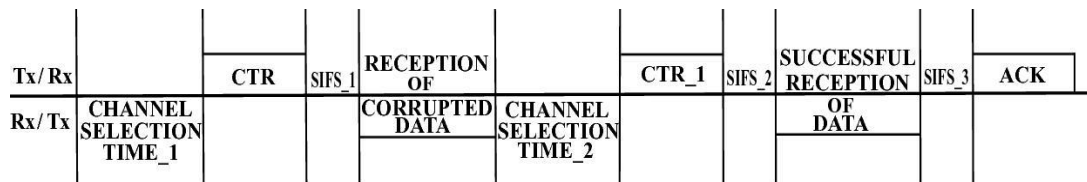


**Figure 5.8: Scheme of Data Transfer under Hypothesis  $H_{fd}$**

### 5.3.2 System Throughput and Efficiency

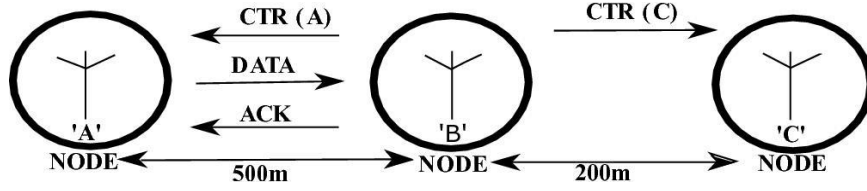


Figure 5.9: Data Transmission Scheme using RI MAC Protocol

Fig.5.9 shows a data transmission scheme for a network of three cognitive transceiver nodes. Here, the distance between node 'A' and 'B' is 500 meters whereas the distance between the node 'B' and 'C' is 200 meters. The receiver node 'B' initiates communication by generating CTR command with the address of node 'A'. Since both the nodes ('A' and 'C') receive carrier information simultaneously, only the node 'A' responds by sending data packets.

In this scheme, the sender ( $T_x$ ) starts sending data packets whenever it receives CTR command from any receiver. Here, a dedicated control channel has been assigned to exchange overhead command control frames ( $O_{cf}$ ) at a fixed transmission rate ( $R_{control}$ ). Therefore, the transmission time ( $\tau_{TC}$ ) of the control command with reliable channel selection and processing time can be calculated as-

$$\tau_{TC} = i \left( \tau_{comp} \right) + \frac{i \left( O_{cf} \right)}{R_{control}} \quad (5.7)$$

The minimum receiver computational time for scanning, comparison, and selection of reliable channel frequency is represented as  $\tau_{comp}$ . In equation (5.7), 'i' is the positive integer that represents the number of retransmissions of CTR frame. In the worst case scenario, system computation time ( $\tau_{comp}$ ) calculation depends on PLL locking time (20ms) [207], RSSI generation time by the IF processor IC SA 636 (10 ms) [206] and the program execution time. In this scheme, 16 MHz clock (duration of 60ns) has been considered. After the reception of CTR command, the transmitter changes channel frequency as per CI sent from the receiver. Hence the total data transmission time ( $\tau_{TD}$ ) between  $T_x - R_x$  can be calculated as-

$$\tau_{TD} = \left\{ \left( \frac{S}{\delta} \right) + T_p + T_t + \tau_{TC} \right\} \quad (5.8)$$

In the above equation, first term represents the time to forward all the bits on the link. Here,  $S$  is the combination of {control bits + data frame (M) bits} and  $\delta$  represents the uniform data transmission rate. To evaluate the maximum data rate over a given communication link or channel, Claude E. Shannon's Equation [218] for channel capacity  $(C) = B \log_2 \left( 1 + \frac{S}{N} \right)$  has been considered. The channel capacity (C) is related to the channel bandwidth and signal to noise ratio (SNR). Effective data rate ( $\delta$ ) is given by-  $\delta = \frac{\eta}{100} \times C$ . The transmission efficiency ( $\eta$ ) is evaluated as-

$$\eta = \frac{\text{Actual data}}{\text{Total no. of transmitted data}} \times 100\% \quad (5.9)$$

Second and third terms in equation (5.8) denote propagation delay time ( $T_p$ ) and channel processing time ( $T_i$ ) respectively.

The system throughput ( $Th_s$ ) is measured either in bits per second (bps) or in packets per second (pps) and is defined as the rate at which packets or bits are successfully delivered over a selected channel. Hence,  $Th_s$  can be computed as-

$$Th_s = \left( \frac{S}{\tau_{TD}} \right) \quad (5.10)$$

In equation (5.10),  $S$  and  $\tau_{TD}$  represent total data (control bits + message bits) and transmission time respectively.

### 5.3.3 System Performance Analysis

A comparative study has been done among RI MAC protocol and conventional MACA and MACA-BI protocols to analyse the performance of an underlay CRN. The transmit power of the SU has been set at 0.01 mW for network simulation. Gains and heights of the secondary transmitter/receiver antenna have been programmed as 1 and 0.1 meter respectively. The distance between a secondary  $T_x$  and the corresponding secondary  $R_x$  has been maintained at 500 meters along with the fixed data packet size of 100 bytes and slot duration of 10 ms.

To conduct experiment, channels of the industrial scientific and medical (ISM) band have been considered for secondary data communication. Based on the six numbers of re-

transmission attempts, the performance of various parameters like overhead time, throughput and system efficiency have been plotted. The proposed scheme switches channel frequency among the different channels of ISM band to support six retransmission attempts as shown in Table 5.1.

**Table 5.1: Channel Frequency for Multiple Retransmission Attempts**

Attempts	Channel Frequency
First	2.454 GHz
Second	2.4 GHz
Third	2.484 GHz
Fourth	2.424 GHz
Fifth	2.454 GHz
Sixth	2.4 GHz

In Fig.5.10, variations of overhead time with the number of attempts have been plotted for three different MAC protocols. The link establishment time for successful data transmission is equivalent to the overhead time of the system. The overhead time increases exponentially for MACA or MACA-BI protocol. However, MACA-BI protocol performs slightly better than the MACA protocol. On the contrary, the system overhead time in the RI MAC protocol is very low and nearly constant for multiple retransmission attempts.

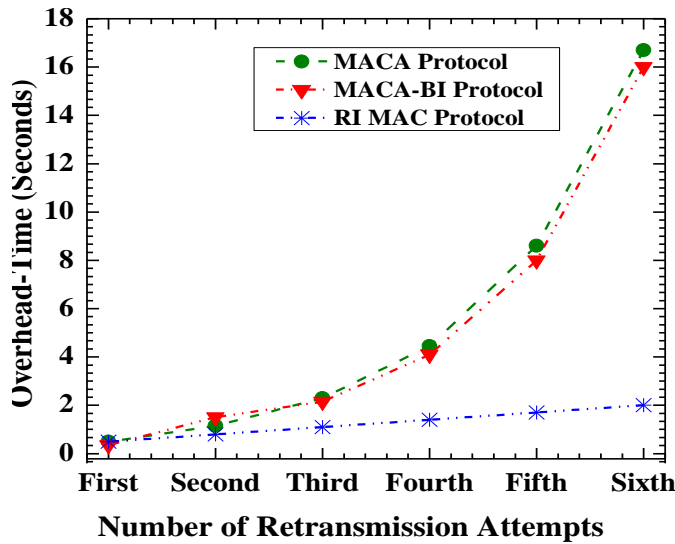


**Figure 5.10: Variation of Overhead Time with the Number of Attempts**

Fig.5.11 depicts the system throughput( $Th_s$ ) variation in a situation of multiple retransmissions with transmission range of 500 meters and 100 bytes packet length. With the MACA-

BI protocol, the system has achieved the maximum throughput compared to other MAC protocols at the first attempt as it completes the successful data transmission with minimum number of three cycles. But after the failure in data transmission at the first attempt, throughput falls sharply. On the contrary, even for multiple retransmission attempts, relatively high and stable throughput is achieved with the RI MAC protocol. The system throughput performance with the MACA and MACA-BI protocol is very poor due to generation of huge overhead time before each retransmission attempts as shown in Fig. 5.11.

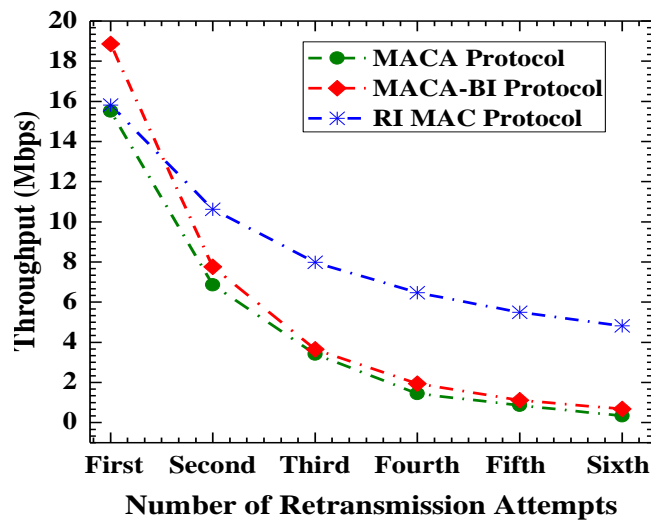


Figure 5.11: Throughput Performance with the Number of Attempts

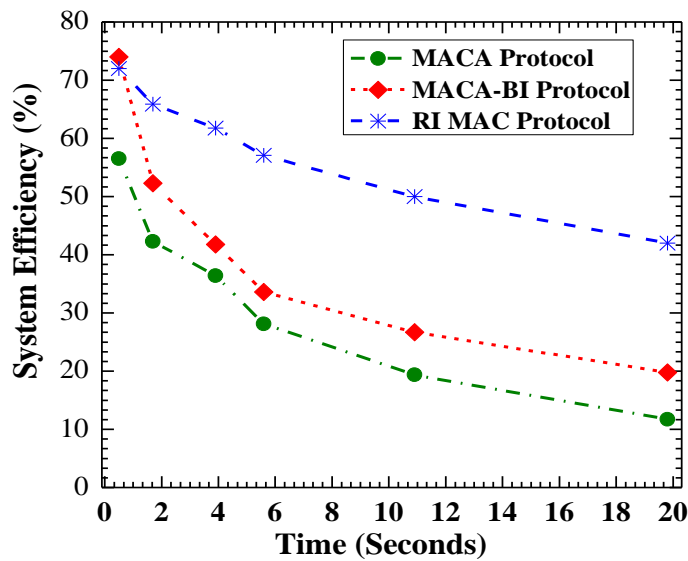


Figure 5.12: System Efficiency with Time

Fig.5.12 shows the system efficiency ( $\eta$ ) for a given period of observation during data communication. A comparative study has been undertaken among the conventional MAC protocols and RI MAC protocol. It is observed that the minimum system efficiency with RI MAC protocol is 43.4%. On the other hand, for MACA and MACA-BI, the system efficiency can go down to 18% and 22% respectively. Moreover, the average system efficiency of RI MAC protocol is higher than those of the MACA and MACA-BI protocols. Hence, the proposed MAC protocol is definitely much more efficient for underlay cognitive communication system. In the next subsection, performance of RI MAC protocol has been compared with the opportunistic matched filter-based (OMF) MAC protocol [228].

### 5.3.4 A Comparative Study

OMF-MAC protocol [228] uses a distributed coordination function (DCF) based contention process. The OMF MAC protocol distinguishes between the primary and secondary signals by applying short sensing intervals. When a signal transmitted by a primary user (PU) is detected on the channel by secondary users (SUs), all SUs must remain silent until the channel becomes free again. The silent period increases the time delay in data transmission and reduces secondary system efficiency. Additionally, the back off waiting period causes a delay if interference occurs during connection establishment or data transfer. Hence, cognitive radio network operation will be affected if the OMF MAC protocol is used.

In the proposed scheme, the secondary receiver initiates communication on the locally sensed, least noisy carrier frequency. In the RI MAC protocol, data transmission completes within only three cycles if the first attempt transmission is successful. However, for each failure of data transmission, the receiver selects another channel frequency for retransmission and initiates data transmission without waiting for a retransmission attempt from the corresponding secondary transmitter on the previously selected licensed channel frequency where transmission failed. This is the fundamental difference from the OMF MAC protocol. The receiver initiated channel selection scheme has minimized the collision probabilities with the hidden terminals. Since the back-off waiting period due to multiple failures in data transmission is not a factor at all, system overhead time is less compared to the OMF MAC protocol.

The channels of the ISM band have been considered for secondary data communication to analyze performance comparison between RI MAC and OMF MAC protocol. The overhead time and overall system efficiency have been plotted. The RI MAC protocol switches channel frequency among the different channels of the ISM band to support six retransmission attempts as shown in Table 5.1. The simulation parameters represent in Table 5.2.

**Table 5.2: Simulation Parameters**

Parameters	Value
Fixed Data Packet Size	100 bytes
Slot Duration	10 ms
Distance Between Secondary $T_x$ and $R_x$	500 meter
Secondary Transmit Power	0.01 mW
Secondary Antenna Height	0.1 meter
Gain	1

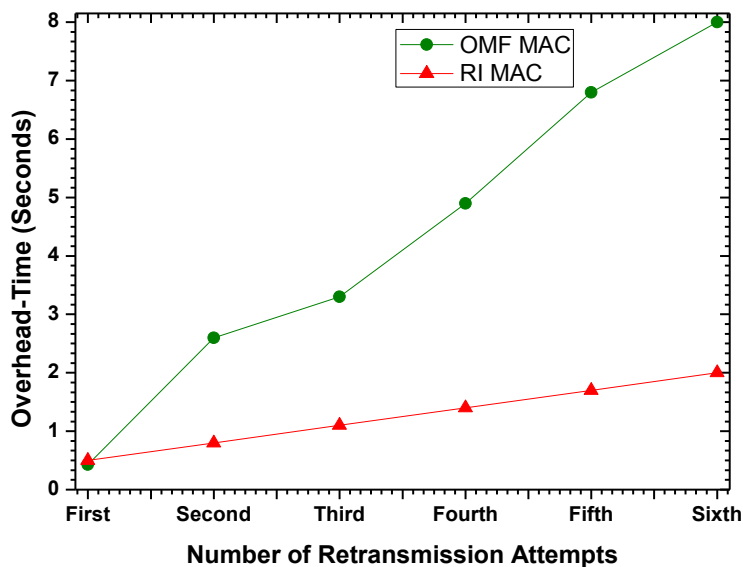


**Figure 5.13: System Overhead Time during Data Transmission**

Fig.5.13 and Fig.5.14 show the variations of overhead time with the number of attempts and the system efficiency ( $\eta$ ) for a given period of observation for the two protocols under comparison. The overhead time increases exponentially for the OMF MAC protocol because, after every silent period, a secondary receiver needs to establish a link to initiate data transmission on the same channel. On the contrary, the system overhead time in the RI MAC protocol is nearly constant after multiple retransmission attempts. This is due to the initiation of the channel switching process after each failure in data transmission. The channel switching

scheme eliminates silent period and link establishment time. The comparative study also shows that system efficiency over time varies from 71.2% to 43.4% for the RI MAC protocol. However, system efficiency goes down to 23.8% for the OMF MAC protocol. Hence, the proposed RI MAC protocol is much more efficient for the underlay cognitive communication system.

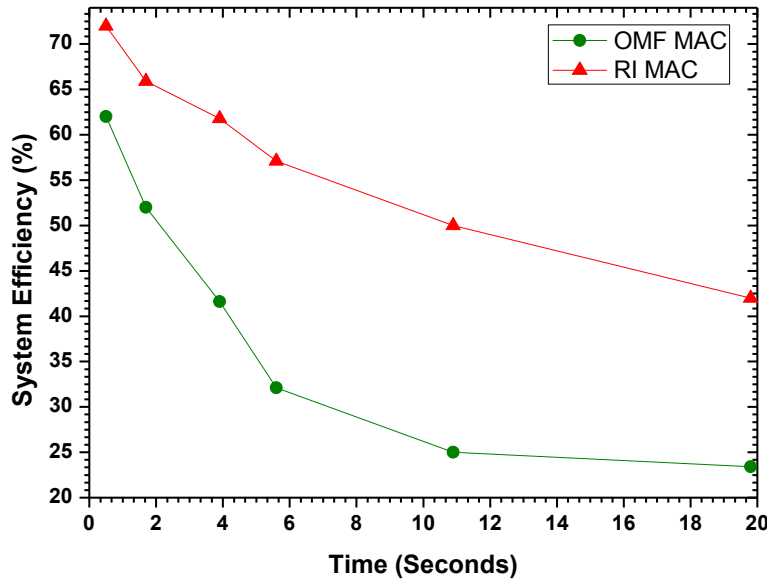


Figure 5.14: Overall System Efficiency

However, as per the proposed RI MAC protocol, it may so happen that the intended transmitter is already busy when it receives the CTR command from any receiver. Hence, the initiating receiver will switch to back-off waiting mode until the corresponding transmitter responds with the expected data. It may also be possible that the transmitter does not wish to communicate with the initiating receiver. Therefore, retransmission attempts of the CTR command after a period of waiting time may lead to huge overhead data. On the other hand, the primary criterion of underlay communication is the simultaneous usage of licensed spectrum by primary and secondary users. But, in RI MAC protocol, on each reception of corrupted data, the receiver retransmits the CTR command with a different channel frequency switching request. This is not the efficient utilization of radio spectrum from CR perspective. Therefore, to overcome the drawbacks of the RI MAC protocol a transmitter-initiated (TI) MAC [85] protocol has been proposed in the next section. In an underlay CRN, the foremost



objective is to keep the outage probability at primary  $R_x$  within a predefined limit. Hence, a flexible transmit power selection scheme for secondary  $T_x$  has been introduced in the TI MAC [85] protocol to minimize the outage probability of primary  $R_x$ . A twin channel sensing strategy at both ends of the corresponding SUs has also been adopted to minimize hidden terminal interference.

## 5.4 TRANSMITTER-INITIATED (TI) MAC PROTOCOL

A TI MAC [85] protocol is proposed to improve secondary data transmission efficiency. In this approach, transmit power level selection at secondary  $T_x$  depends on the received SNR or RSSI level of the selected channel from the secondary  $R_x$ .

### 5.4.1 Optimum Transmit Power Adaptation

The optimum transmit power control policies that maximize the achievable rates of underlay CR systems with an arbitrary input distributions under average transmit power and interference power constraints have been developed by Ozcan *et al.*[155]. Therefore, to satisfy the PU outage constraint given by equation (5.6), the secondary transmit power constraint has been considered. It has been categorized into two general types – (a) Flexible Transmit Power Constraint (b) Peak Transmit Power Constraint.

In the TI MAC protocol, the flexible transmit power constraint which depends on the outcome of the sensing result has been adopted. Hence, based on the CSI of the selected licensed channel, optimum transmit power level has been selected by keeping primary interference within the maximum limit. The selection has shown by equation (5.11).

$$E[P_s g_{sp}] \leq \lambda_{PU} \quad (5.11)$$

In equation (5.11),  $P_s$  denotes the secondary transmit power and  $g_{sp}$  is the channel power gain (refer Fig.5.1) and  $\lambda_{PU} = \left( \frac{Y_{pp} - Y_{sp}}{Y_{sp}} \right)$  defines interference limiting factor or SNIR (Signal

to Noise and Interference Ratio) at primary  $R_x$  due to transmission by the secondary  $T_x$  on the same channel. Therefore, in the TI MAC protocol during the secondary transmit power selection, the equation (5.11) has been modified as-

$$E[P_{s\_flx}] \leq P_{pk} \quad (5.12)$$

In the above equation  $E[\cdot]$  denotes the expected secondary flexible transmit power level and  $P_{pk}$  is the peak transmit power which ensures the maximum allowable secondary interference (SI) at Primary  $R_x$ . On the other hand, the secondary  $R_x$  receives signal on a channel selected by the secondary  $T_x$ . The received signal power at secondary  $R_x$  is  $|h|^2 P_{s\_flx}$ , where  $|h| = a$ , represents the propagation loss between secondary  $T_x$  and  $R_x$ . The probability of error due to high noise factor is

$$P(e) = P_r \left( a < \frac{1}{\sqrt{SNR}} \right) = 1 - e^{-\frac{1}{SNR}} \quad (5.13)$$

Therefore, in the next subsection a data transmission scheme based on TI MAC protocol has been introduced.

#### 5.4.2 Scheme of Data Transmission

In this scheme, the secondary  $T_x$  initiate communication by sending locally sensed least noisy carrier frequency information for the secondary  $R_x$ . The secondary  $R_x$ , in turn, checks and responds with the SNR of the selected carrier frequency. The data transmission starts on a channel selected by the secondary  $T_x$ , only after receiving the channel quality information from the secondary  $R_x$  end as well.

Therefore, two hypotheses ( $H_{fp\_sf}, H_{fp\_sm}$ ) have been proposed to implement a data transmission scheme. The hypothesis  $H_{fp\_sf}$  is true, only when successful data transmission is completed in the first attempt. Otherwise, hypothesis  $H_{fp\_sm}$  occurs, when more than one attempt are required to transmit same data successfully with the flexible selection of transmit power for each retransmission attempts.

$$H_{fp\_sf} : P_{s\_flx} \leq P_{pk} : \text{Successful Transmission at First Attempt}$$

$$H_{fp\_sm} : P_{(s\_flx)_i} \leq P_{pk} : \text{Successful Transmission after Multiple Attempts}$$

[  $i$  = Number of Retransmission Attempts (Positive Integer)]

Fig.5.15 shows the data transmission scheme of  $H_{fp\_sf}$  hypothesis.

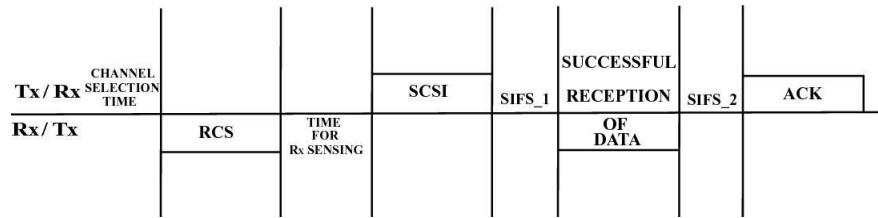


**Figure 5.15: Data Transfer Scheme for SUs under Hypothesis  $H_{fp\_sf}$**

In this scheme, after performing local sensing operation, the secondary  $T_x$  sends a channel switching request to a secondary  $R_x$  using request-to-carrier-switch (RCS) control command. On the reception of the RCS command, a supervisory tone is used by the secondary  $R_x$  to determine the SNR of the switched channel frequency. The signal strength information of the switched channel is sent back to the corresponding secondary  $T_x$  by using the switched carrier strength information (SCSI) command. Hereafter, to initiate data transmission, a flexible transmit power is selected based on the received signal strength information from the corresponding secondary  $R_x$ . Fig.5.16 has shown the frame structures of the RCS and SCSI command. The RCS frame consists of the channel frequency information (CFI) of one 1 byte. On the other hand SCSI frame contains channel quality information (CQI) of one byte. Both the frames also allot 6 bytes of destination ID or transmitter address and 6 bytes of source ID or receiver address. The number of packets information of two bytes and packet length information of two bytes are also present in the RCS and SCSI frame structures respectively.

<b>6</b>	<b>6</b>	<b>2</b>	<b>4</b>	<b>2</b>	<b>1</b>
Destination ID	Source ID	Frame Control	FCS	Number of Packets	CFI

(a) Request-to-Carrier Switch (RCS)

<b>6</b>	<b>6</b>	<b>1</b>	<b>2</b>	<b>1</b>
Destination ID	Source ID	Control Bits	Packet Length	CQI

(b) Switched Carrier Strength Information (SCSI)

**Figure 5.16: Structure of Command Control Frame**

Hence, the data is transmitted only after the selections of optimum transmit power. If the signal strength of the received data is less than the predefined system threshold ( $\lambda_{s/m}$ ), then instead of waiting for retransmission attempt from the corresponding secondary  $T_x$ , the secondary  $R_x$  sends step-up transmit power (SUTP) command. The SUTP command frame structure has been shown in Fig.5.17. This frame consists of one byte of frame control bits, six bytes of source ID or receiver address (RA) and 6 bytes of destination ID or transmitter address (TA). The transmit power level step-up instruction contains one byte information. This step-up instruction has been used to control the flexible transmit power of the secondary  $T_x$ .

<b>6</b>	<b>6</b>	<b>1</b>	<b>1</b>
Destination ID	Source ID	Control Bits	Tx Power Level Step_UP_Info

**Figure 5.17: Step-Up Transmit Power (SUTP) Frame Structure**

Whenever the secondary  $T_x$  receives the power level increment command from the corresponding secondary  $R_x$ , it increases the transmit power level and re-transmits the same data sequence. The process will continue until the transmitted data satisfies the receiver requirement. Fig.5.18 shows the data transmission scheme under hypothesis  $H_{fp-sm}$ . As per the defined algorithm in the next section, transmit power is increased step by step towards peak

transmit power till ‘ACK’ is received. However, even after reaching the peak transmit power ( $P_{pk}$ ), if the received signal strength is less than the system threshold, a different channel frequency is selected by the secondary  $T_x$  for data communication. The complete process is repeated until data has been transmitted successfully.

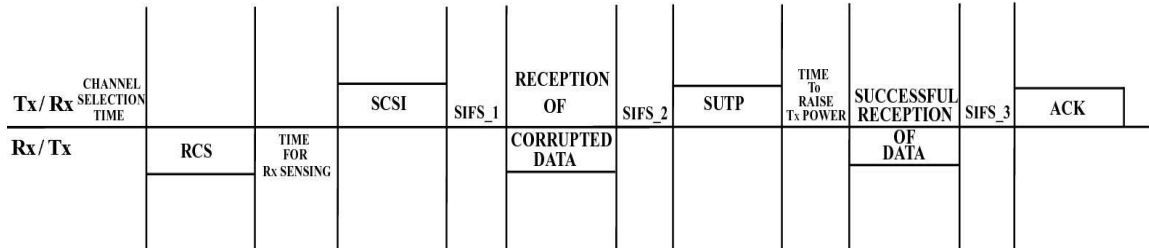


Figure 5.18: Data Transmission Scheme for SUs under Hypothesis  $H_{fp-sm}$

A comparative analysis between the RI and TI MAC protocols in terms of system throughput and efficiency has been undertaken in the next subsection.

### 5.4.3 Comparative Analysis of Proposed MAC Protocols

In this section, a comparative study has been done between RI MAC and TI MAC protocols. The simulation parameters have been considered as per previous simulation parameters (refer 5.2.3) to execute this comparative task. The mathematical model which is derived in section 5.2.2 has been considered to calculate system efficiency and throughput for both the proposed MAC protocols.

A plot of number of retransmission attempts vs overhead time is depicted in Fig.5.19 which shows the linearly increasing overhead time of RI MAC protocol compared to almost flat variation for TI MAC protocol after considering multiple retransmission attempts. In the TI MAC protocol, the maximum number of cycles which are required to complete successful data transmission is greater than the RI MAC protocol. However, in the RI MAC protocol, different channel selection times are required after each failure in data transmission. This channel selection is not required with the TI MAC protocol after each failure in transmission. Therefore, with the TI MAC protocol, system requires less overhead time even after multiple retransmissions.

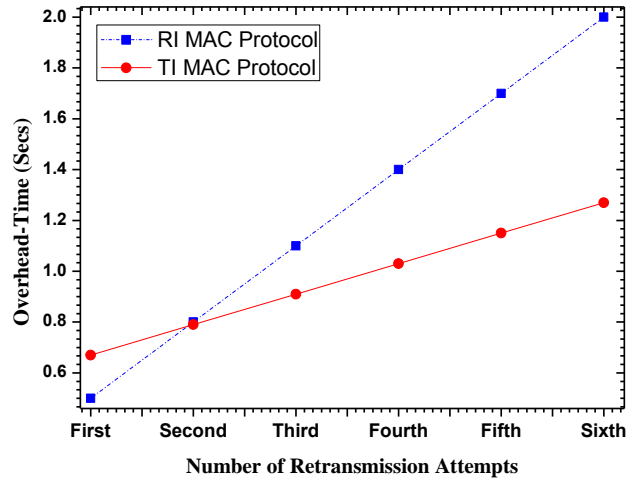


**Figure 5.19: Overhead-Time Variation with the Number of Attempts**

The system throughput variation for multiple retransmission attempts has been plotted in Fig.5.20. The requirement of less number of cycles and minimum overhead data to complete data transfer gives better throughput performance with RI MAC protocol as compared to the TI MAC protocol after the first attempt successful transmission. However, after multiple retransmission attempts, the system throughput falls almost linearly for the RI MAC protocol. On the other hand, TI MAC protocol gives better throughput performance compared to RI MAC protocol in the same condition.

Fig.5.21 shows the system efficiency for a given period of observations. The secondary system has achieved better efficiency with the TI MAC protocol than with the RI MAC protocol.

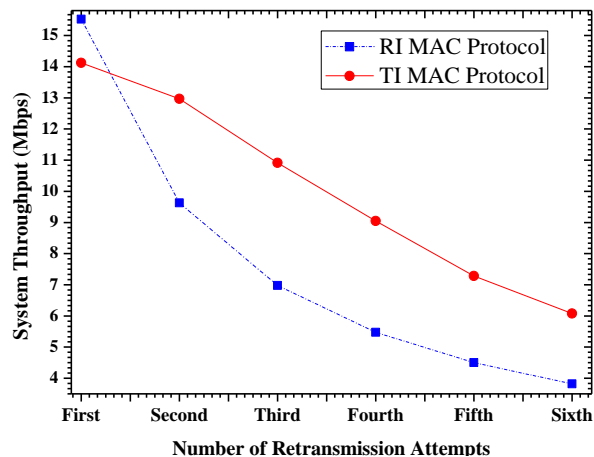


**Figure 5.20: Throughput Performance Variation with the Number of Attempts**

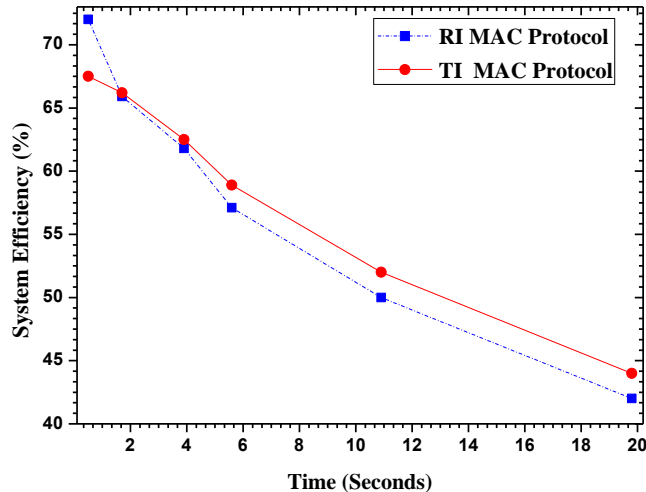


Figure 5.21: System Efficiency Variation with the Period of Observations

The next section presents an optimum transmit power selection concept which has been tested with a designed power control circuit.

## 5.5 FLEXIBLE TRANSMIT POWER SELECTION STRATEGY

The precise transmit power selection is very crucial in an underlay CRN to avoid interference with licensed users (primary  $R_x$ ). Therefore, a flexible transmit power selection scheme is proposed in this section. A power control circuit has been designed to implement the flexible selection procedure.

### 5.5.1 Optimum Power Selection

The received signal quality at the secondary  $R_x$  is expressed in terms of SNR and is measurable by the RSSI voltage. The fundamental criterion of an underlay CRN is to allow the SUs to operate on licensed spectrum without degrading the receiver performance of PUs. Therefore, selection of an optimum secondary transmit power level is essential for the SUs so as not to cause unacceptable interference at the PUs. Here, SNR is used as a reference to select the transmit power level for the SUs. The selection starts at a power level corresponding to a SNR level, which is 3dB lower than the SNR value sensed at the corresponding secondary  $R_x$  end on the selected channel. Hereafter, secondary transmit power level is increased in

steps based on the command instructions received from the corresponding secondary  $R_x$ . Secondary  $T_x$  sets transmit power, as per the condition defined in equation (5.14).

$$\begin{aligned}
 P_{s\_flx} &\leq \left( T_{xp} \right)_j - 3dB \leq P_{pk} \\
 P_{(s\_flx)j} &\leq \overline{T_{xp}} \leq P_{pk}
 \end{aligned}
 \tag{5.14}$$

In the equation (5.14),  $(T_{xp})_j$  represents the required power level to attain the desired signal strength at the secondary  $R_x$  and 'j' is positive binary integer ( $0000 \leq j < 1111$ ) which is used as an index to different power level ranges illustrated in Table 5.3. The data transmission starts at a power level, which is 3dB below the level required to attain the threshold on the selected channel at the corresponding secondary  $R_x$ . However, on the reception of corrupted data due to poor signal strength the corresponding secondary  $R_x$  responds with SUTP command instruction. The transmit power increases in steps of 0.5dB till it reaches the maximum limit ( $P_{pk}$ ). Therefore,  $\overline{T_{xp}} = \left[ (T_{xp})_j - 3dB \right] + iK$ , where 'K' = 0.5dB and 'i' is the number of re-transmission step. Algorithm.5.1 has been used to execute the flexible secondary transmit power selection scheme.

**Secondary Transmit Power Selection Algorithm.5.1**

1. RCS command is sent to the corresponding secondary  $R_x$ .
2. From the secondary  $R_x$  end, SCSI command has been generated after performing SNR measurement on the switched channel frequency.
3. The secondary  $T_x$  initiate data transmission on flexible selected transmit power using eq. (5.14).
4. When received signal strength  $\leq \lambda_{s/m}$ , SUTP command has been generated.
5. Otherwise, ACK command has been sent by the secondary  $R_x$ .
6. On the reception of SUTP command secondary  $T_x$  increase the transmit power to the next level and retransmit the same undelivered data.



**Table 5.3: Flexible Power Steps**

Binary Code	Range of Transmit Power Level (mW)
0000	3.19-3.89
0001	4.0-4.79
0010	4.8-5.62
0011	5.63-6.15
0100	6.17-7.9
0101	7.9-10
0110	10.23-12.59
0111	12.6-15.42
1000	15.80-19.5
1001	20-24.94
1010	25-31.6
1011	31.62-39.81
1100	39.90-50.04
1101	50.11-63.09
1110	64.6-85.11
1111	85.31-100

**Table 5.4: SNR Corresponding to Binary Code**

Binary	SNR Range (dB)
0000	5.051-5.9
0001	6.021-6.8
0010	6.81-7.5
0011	7.51-7.89
0100	7.9-8.974
0101	8.975-10
0110	10.1-11
0111	11.004-11.881
1000	11.987-12.9
1001	13.01-13.97
1010	13.979-14.994
1011	15-16
1100	16.01-16.994
1101	17-18
1110	18.1-19.3
1111	19.31-20

Table 5.4 shows the mapping of binary codes with the receiver performance (in terms of SNR) on any channel (assumed) selected by the secondary  $T_x$ . As per the channel SNR, the binary code will be sent to the secondary  $T_x$  using the proposed transmit power step up command.

The flexible secondary transmit power selection scheme has been implemented by designing a power control unit in the next subsection.

### 5.5.2 Power Control Unit

Fig.5.22 shows the hardware set-up for checking the flexible transmit power scheme. The RSSI voltage, which is directly proportional to the SNR, is available from the IF processor IC (SA 639) datasheet. This voltage has been used as a test input in the experiment.

In this circuit, the analog DC output of SA 639 has been digitized with the help of the 4-bit analog-to-digital converter (ADC 0804, details in Appendix C). The ADC outputs connect with a controller 89C51. This controller is pre-loaded with a look-up table (refer Table 5.3) of all the binary combinations corresponding to the range of possible RF power levels. The selection of the RF power level depends on the input RSSI value.

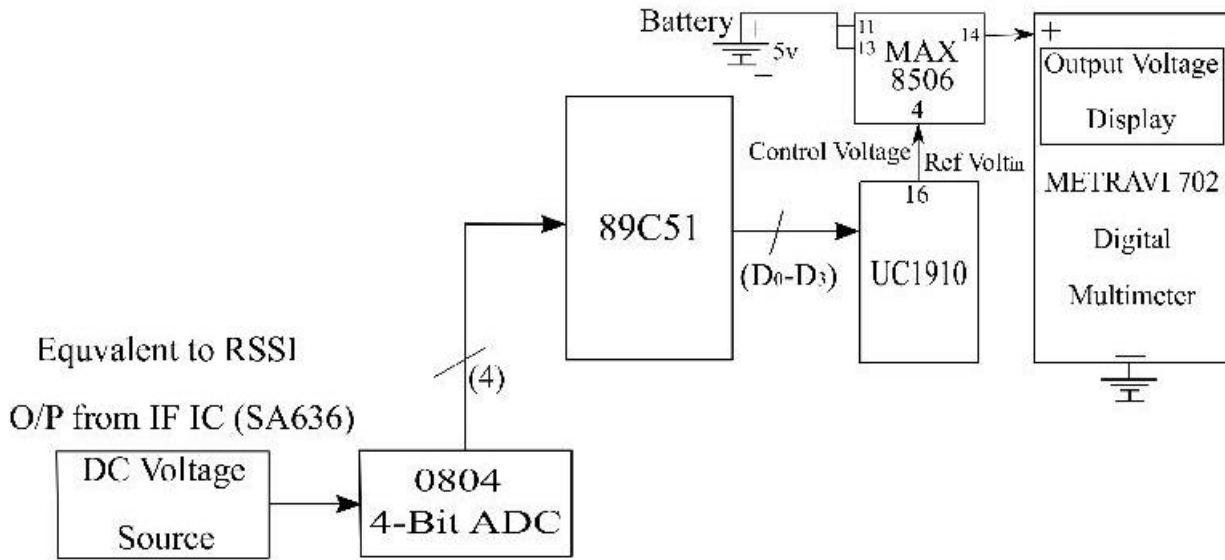


Figure 5.22: Power Control Hardware Module

The objective of this present scheme is to control the biasing voltage of the power amplifier stage rather than controlling the driver stage. Here, the RSSI voltage, after ADC conversion, is compared with the pre-programmed matching binary values in the controller. If the RSSI voltage is lower than the given network threshold, the secondary  $R_x$  executes the RF power step-up decision with the help of Table 5.3. This power control table has been programmed with the required 4-bit binary data within (0000-1111). Each of the binary entry corresponds to a range of transmit power level. The binary pattern corresponding to the desired transmit power level is applied to a voltage monitoring unit (IC UC1910). The DC control voltage from IC UC1910 (details in Appendix C) is used to control the DC-to-DC converter MAX8506 (details in Appendix C). The output of MAX8506 controls the biasing voltage of the RF power amplifier. The variation of the biasing voltage with respect to input reference voltage has been tabulated in Table 5.5.

**Table 5.5: Variable Biasing Voltage to Control Transmit Power**

Input Reference Voltage (UC1910 Output)	Biasing Voltage (MAX8506 Output)	Approximate Transmit power level
3.5 Volts	0.75 Volts	3.19-3.89
3.4 Volts	0.80 Volts	4.0-4.79
3.3 Volts	0.86 Volts	4.8-5.62
3.2 Volts	0.90 Volts	5.63-6.15
3.1 Volts	0.98 Volts	6.17-7.9
3.0 Volts	1.1 Volts	7.9-10
2.9 Volts	1.2 Volts	10.23-12.59
2.8 Volts	1.5 Volts	12.6-15.42
2.7 Volts	1.8 Volts	15.80-19.5
2.6 Volts	2.0 Volts	20-24.94
2.5 Volts	2.1 Volts	25-31.6
2.4 Volts	2.3 Volts	31.62-39.81
2.3 Volts	2.5 Volts	39.90-50.04
2.2 Volts	2.8 Volts	50.11-63.09
2.1 Volts	3.0 Volts	64.6-85.11
2.0 Volts	3.4 Volts	85.31-100

In the TI MAC protocol, the secondary  $R_x$  forwards the SUTP command frame to the corresponding secondary  $T_x$  when received data has been corrupted due to poor signal strength. On the reception of SUTP command, corresponding transmitter increase the transmit power level by one step and retransmit the previously transmitted data. The SNR for the corresponding transmit power level is also stored in the transmitter controller. Table 5.3 and Table 5.4 represents the flexible transmit power levels corresponding to variable SNR range. This proposed scheme maintains optimum transmit power level to minimize distortion at the PUs due to secondary interference. The Table 5.6 shows the selection of flexible transmit power level as per equation (5.14) for measured SNR at the secondary  $R_x$  end before initiating data transmission.

**Table 5.6: Transmit Power Variation Corresponding to the SNR at the Receiver End**

CSI at the Receiver End SNR (dB)	Corresponding Transmit Power Level (mW)	Corresponding Binary Code
13.5	11.22	0110
11	6.30	0100
17.3	26.92	1010
18	31.62	1011
18.5	35.48	1011
8	3.16	0000
15	15.89	1000

Fig.5.23 shows the step by step, transmit power increment process up to the maximum limit. This limit has been set by the SNR of the switched channel frequency at the secondary  $R_x$  end. Hence, it has been observed that whenever maximum limit of transmit power is reached, the secondary  $T_x$  switches to another channel frequency. This process continues till the optimum solution is achieved.

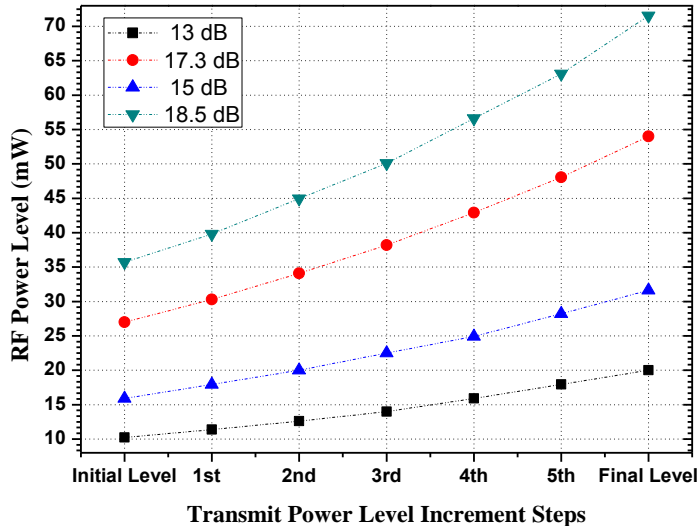


**Figure 5.23: Transmit Power Increment till the Maximum Interfering Limit**

In the next subsection, primary outage probability due to secondary transmission in underlay cognitive scenario has been emulated and analysed graphically.

### 5.5.3 Performance Analysis with Flexible Transmit Power

Here, the unlicensed channel in ISM band is considered for data communication between primary and secondary node pairs concurrently. The primary transmit power has been varied from 0.03mW to 0.09mW to observe the variation in secondary transmit power adaptability by maintaining the minimum level of interference at primary  $R_x$ . Distance among nodes (Secondary  $T_x - R_x$  and Primary  $T_x - R_x$ ) has been kept at 5 meters. Table 5.7 has listed the important parameters for network simulation.

Table 5.7: Simulation Parameters

Parameters	Value
Available Channel frequency	2.4 GHz, 2.432 GHz, 2.454 GHz, 2.481 GHz
Distance Among Nodes	5 meter
Separation Distance between Primary $R_X$ and Secondary $T_X$	10 meter
Tx-Rx Antenna Height (Secondary-Primary Unit)	0.1 meter
Gain	1
Primary Transmit Power	0.03mW to 0.09mW

Fig.5.24 shows the variations of primary outage probability with the flexible transmit power level of the secondary  $T_X$ . For the three different primary transmit power levels, outage probability of the primary receiver has been observed. Therefore, the precise selection of secondary transmit power is very important in an underlay CRN to keep outage probability within the predefined maximum limit.

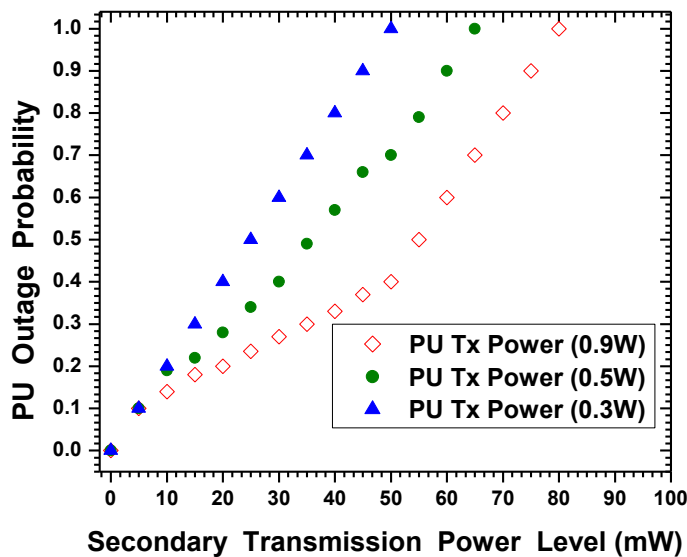


Figure 5.24: Outage Probability of PUs with the Flexible Transmit Power

Fig.5.25 shows, a linear increment of secondary channel capacity with increment of the interference threshold limit of the primary  $R_X$ . However, simulated channel capacity is less than the theoretical channel capacity. It happens since, in CR communication, the presence of link noise and circuit generated internal noise reduces the received signal SNR. It has been ob-

served that higher is the value of secondary transmit power, higher is the outage probability of primary  $R_x$ . It results in lower channel capacity of SUs. Therefore, channel capacity increases if the interference threshold limit in the primary  $R_x$  is high.

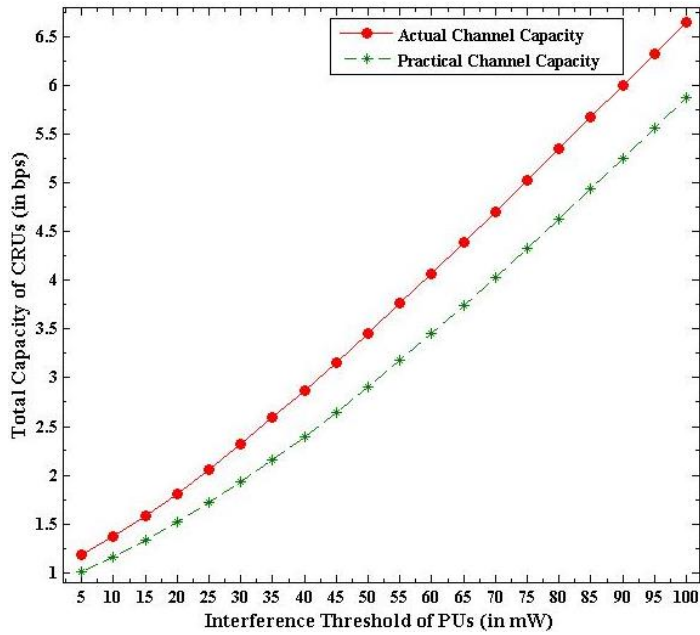


Figure 5.25: Channel Capacity of SUs

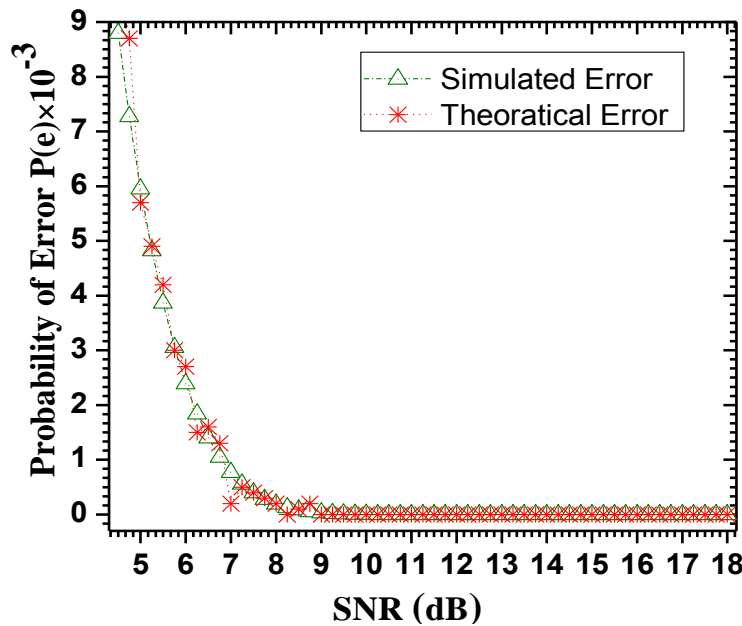


Figure 5.26: Secondary Error Probability Variation with SNR (dB) Levels

Fig.5.26 exhibits the error probability ( $P_e$ ) with the variable SNR. It is logical that the error probability ( $P_e$ ) of SUs goes down as SNR increases since the reliability of successful secondary transmission improves with high SNR value. The error probability ( $P_e$ ) reduces to almost 0 when the SNR is greater than 10dB (approx.). The simulation result differs from the theoretical calculation because of the presence of noise, as described.

In an underlay CRN, secondary transmit power level needs to be chosen carefully to minimize outage probability at primary  $R_X$ . Hence, in Fig.5.27 a relationship has been shown between the error probabilities ( $P_e$ ) of the primary  $R_X$  and transmit power levels of the secondary  $T_X$ . It can be observed that  $P_e$  comes down with the increase in the power level of the secondary  $T_X$  until it is less than or equal to the interference limit at the primary  $R_X$ . Therefore, it has been observed in Fig.5.27 that with the increment of the transmit power level more than the interference limit, the outage probability of primary  $R_X$  is increased. This phenomenon has been justified by the upward trend of the error probability ( $P_e$ ) when the secondary power level crosses the predefined interference limit of any primary  $R_X$  as shown in Fig.5.27.

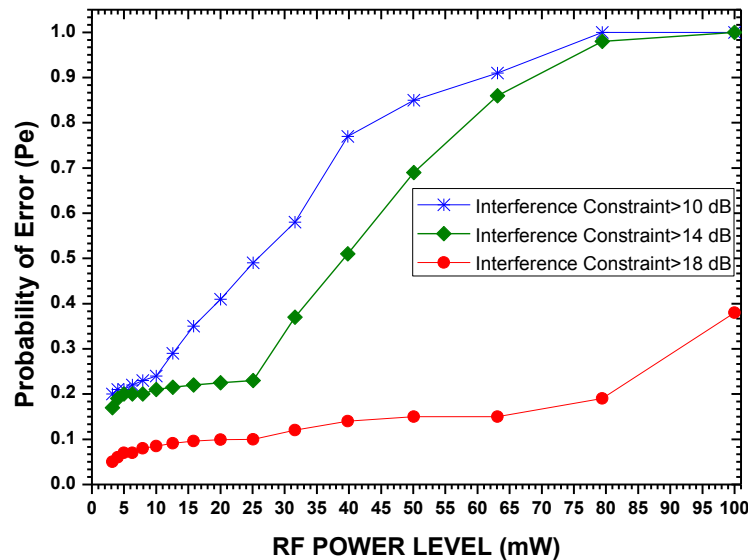


Figure 5.27: Primary Error Probability Variation for Interference Limits

## 5.6 DISCUSSION

Underlay CR communication takes place on a licensed channel frequency shared with the PUs. In the underlay network, interference with the hidden terminals degrades the performance of the secondary  $R_x$ . Therefore, to minimize interference probability with the hidden terminals, a receiver-initiated (RI) MAC protocol has been proposed in this work. Successful data transmission with the RI MAC protocol has been completed within three cycles on a channel selected by the secondary  $T_x$ . Since the back-off waiting period due to the multiple failures in data transmission is not a factor at all, system overhead time is less compared to conventional MACA or MACA-BI protocols. The simulation results are analyzed to plot the system throughput and efficiency for multiple retransmission attempts. Approximately consistent system throughput and efficiency have been achieved with RI MAC protocol even with multiple retransmission attempts. Concurrent spectrum allocation to the underlay CRUs has also been achieved with the proposed RI MAC protocol. However, the RI MAC protocol cannot minimize the outage probability of primary receiver due to predefine fixed secondary transmit power. It may also happen that this protocol faces the problem of long waiting period if the corresponding secondary transmitter does not respond after receiving a data transmission request from a secondary receiver. Therefore, a transmitter-initiated (TI) MAC protocol has been proposed to minimize the outage probability at the primary receiver and to reduce the overhead time during an underlay CR communication. In this protocol, secondary transmitter selects the transmit power level only after receiving channel quality information from the corresponding secondary receiver. A twin scan process of the selected channel at both ends ( $T_x - R_x$ ) has been introduced in the TI MAC protocol for transmit power selection. This process can also minimize the hidden terminal interference problem during data communication in an underlay CRN. A step-by-step flexible transmit power selection scheme has been introduced to maximize channel utilization and reliability for underlay CRNs. A power control circuit has been designed and tested to implement this flexible power selection concept. It improves data transmission efficiency and spectrum utilization by keeping interference probability within a tolerable limit at the primary  $R_x$ .



## CHAPTER VI

---

# CONCLUSIONS AND FUTURE WORK

---

6.1	<b>SUMMARY OF RESULTS</b> .....	130
6.2	<b>FUTURE SCOPE</b> .....	134

Limited availability of usable radio frequency (RF) spectrum and current rigid frequency allocation policies have resulted in the apparent scarcity of the RF spectrum even though the overall spectrum utilization is still very low. The cognitive radio (CR) technology improves the spectrum efficiency by allowing secondary users (SUs) or cognitive radio users (CRUs) to share the underutilized licensed spectrum by keeping interference level at the primary users (PUs) below the allowed limits. This thesis presents the precise localization, optimum resource selection and efficient resource allocation strategies for underlay cognitive radio networks (CRNs). The secondary transmission power optimization scheme has also been introduced to minimize interference probability with the PUs. A combination of emulation

and simulation has been performed to justify the proposed hypotheses. This concluding chapter has summarized all the key findings of the thesis and suggests several interesting future research directions.

## 6.1 SUMMARY OF RESULTS

In **Chapter III**, a received signal strength indicator (RSSI) based localization scheme for an underlay CRN has been proposed. The weighted centroid localization (WCL) algorithm has been applied to compute precise coordinates of fixed as well as mobile PUs. In the WCL scheme, PU localization depends on the precise measurement of RSSI. However, it has been observed that RSSI measurement at the CRUs varies with different terrains for the same distance between transmitter and receiver. The variation possibility of the RSSI measurement limits the accuracy in position estimation of the unknown PU. Hence, to improve the measurement accuracy of RSSI in different terrain conditions, the log-normal shadowing model with a correction factor has been introduced. To analyze the improvement, location coordinates of a fixed PU has been calculated under four different terrain conditions (LOS, NLOS, Urban and Rural). It has been observed that the calculation of location coordinates of the fixed PU varies significantly when the correction factor is not considered during the RSSI measurement. On the other hand, with the correction factor, the variation in the estimated location coordinates is negligibly small. Hence, minimum localization error has been achieved with the proposed correction factor. However, localization of a mobile PU is more challenging to a single CRU due to its random movement within the network. Therefore, to overcome the limitations of localization by a single CRU, a range-based collaborative localization scheme has been considered in this work. The graphical analysis reveals that the detection error rate is minimal when four to six users are involved together to perform the localization task. For simplicity, a group of four collaborative users have been experimentally considered to perform the localization task. A rectangular network zone ( $100m \times 100m$ ) has been designed with the fixed CRUs placed at the four extremes of the lamina and the mobile PU is placed inside the network zone. Several unpredictable factors such as random external noise as well as internal noise affect the reliable signal reception by the CRUs. Since external

noise effects on radio communication are random and unavoidable, this chapter has focused on the mitigation of internal noise by modifying CR receiver circuit with the incorporation of a FIR filter block after the demodulator stage. Three suitable filter types namely Rectangular, Chebyshev, and Hamming have been designed using a programmable DSP kit. All the designed FIR filters, after the demodulator stage, have been tested, one by one, with 1 KHz modulating signal mixed with signal from noise generator. An average of 1.7 dB signal to noise ratio (SNR) improvement has been achieved with the designed Chebyshev filter. Also, Hamming and Rectangular filters both have achieved a moderate improvement up to a maximum of 0.7 dB to 0.9 dB in the output SNR respectively. Though the performances of all the three designed filters degrade at higher noise level, the graphical analysis reveals that the Chebyshev filter performance is better than the other two. Therefore, the Chebyshev filter has been selected as an optimum filter type to perform internal noise mitigation. Hereafter, the simulated variable SNR which has been obtained at each of the collaborative CRUs, due to random movement of the mobile PU, has been applied to the Chebyshev filter. The SNR obtained with and without Chebyshev filtering have been converted to RSSI voltage for location coordinates calculation at each of the collaborative CRUs. The converted RSSI finally determine the precise location of the mobile PU. The WCL algorithm has been applied to find out the location coordinates of the mobile PU with respect to each collaborative CRU. The collaborative CRUs share its location coordinates and signal strength information received from the mobile PU with each other. The received information from the collaborative CRUs has been used to compute location coordinates of the mobile PU for ten observations. The graphical analysis reveals that the coordinates of a mobile PU, obtained after filtering is more accurate as compared to the coordinates, obtained before filtering with respect to each CRU. To enhance the localization accuracy, mean of all the location coordinates of the ten common observations has been computed. The range of localization error after the calculation of mean location coordinates collaboratively has come down to (1.3–1.62) % from the earlier (2.4–5.6) % error when each CRU localizes coordinates individually after filtering. Precise localization information reduces the interference probability with PUs. It also reduces miss detection and false detection probabilities in the network. Hence, the overall spectrum utilization efficiency improves.

In **Chapter IV**, a novel optimum channel selection scheme based on the RSSI measurement is presented. A channel selection hypothesis based on the strength of the received signal has been proposed. Since the underlay CRUs use the partially occupied licensed spectrum band, the transmitted signal by the PU has been counted as an interfering factor along with the link noise and internal noise during the channel selection process. A circuit has been designed and tested to authenticate the proposed hypothesis. Therefore, for testing purposes, the given spectrum (200 MHz to 400 MHz) is split into 'B' numbers of narrow bands (1 MHz). A channel with a given bandwidth (BW) has been selected randomly as per the principle of the hill-climbing (HC) algorithm. After a random selection of one sub-band out of the B bands, the controller instructs the phase lock loop (PLL) IC on the basis of the quality of the selected channel. The quality of the selected channel frequency has been checked directly by comparing the RSSI of the selected channel with the predefined system threshold ( $\lambda_{s/m}$ ). The system threshold has been chosen by the minimum requirement of SNR or signal strength for reliable radio communication. The RSSI value has been emulated using a DC voltage source, obtained from the first IF processor IC SA 636 datasheet. When the measured RSSI value of the selected channel is higher than or equal to the predefined system threshold, the controller instructs the PLL to increase the selected channel frequency BW by 1 MHz. However, when the signal strength of the selected channel is less than the desired system threshold, the program will randomly choose another frequency band to continue the same process. The emulation results have been tabulated to justify the proposed channel selection scheme. The ability for optimum selection of a licensed channel can minimize the interference probability with the PUs and improve the utilization efficiency of the licensed spectrum.

In **Chapter V**, an efficient MAC protocol which attempts to minimize interference of hidden terminals, back-off waiting time, and interference with the PUs, has been proposed. Underlay cognitive-communication takes place on a shared carrier frequency with a PU and collision with the hidden terminals and interference with the primary transmission affects the data reception at the secondary receiver end. When the received data is corrupted, retransmission attempts increase huge overhead time and overhead data which, in turn, reduce the system efficiency and throughput. Therefore, a receiver-initiated (RI) MAC protocol has been proposed to conduct data communication by the SUs efficiently. In the RI

MAC protocol, a secondary receiver initiates communication by sending locally sensed least noisy carrier frequency information over a command control frame. The corresponding secondary transmitter starts data transmission on the channel frequency selected by the secondary receiver. Successful data transmission with the RI MAC protocol is completed within three cycles. However, when the received signal strength corresponding to the data transmitted from the paired secondary transmitter is less than the predefined system threshold ( $\lambda_{s/m}$ ), the secondary receiver is not able to recover the original information from the received data sequence. This unrecovered data sequence has been termed as corrupted data. On the reception of corrupted data, a secondary receiver will instantly scan the available channels to select a different channel frequency. Hereafter, without waiting for a retransmission attempt from the corresponding secondary transmitter, the secondary receiver sends another command control frame with new carrier frequency information for data communication. Since the back-off waiting period due to the multiple failures in data transmission is not a factor in this protocol, system overhead time is less compared to conventional MACA or MACA-BI protocols. The graphical analysis shows that approximately consistent throughput and system efficiency can be achieved with RI MAC protocol even with multiple retransmission attempts. Concurrent spectrum allocation to the underlay CRUs has also been achieved with the proposed RI MAC protocol. However, the RI MAC protocol cannot minimize the outage probability at the primary receiver due to predefined fixed secondary transmit power. It may also happen that this protocol faces the problem of long waiting period if the corresponding secondary transmitter does not respond after receiving a data transmission request from a secondary receiver. Therefore, a transmitter-initiated (TI) MAC protocol has been proposed to minimize the outage probability at the primary receiver and to reduce the overhead time during an underlay CR communication. A twin scan scheme of the selected channel at both ends (secondary transmitter and receiver) has been adopted in the TI MAC protocol for optimum selections of secondary transmit power level. This process also can minimize the hidden terminal interference problem during data communication in an underlay CRN. In the TI MAC protocol, the secondary transmitters set transmit power only after receiving channel quality information from the corresponding secondary receiver. An incremental, flexible transmit power selection scheme has been introduced to maximize channel utilization and reliability

for underlay CRNs. A power control circuit has been designed and tested to implement this flexible power selection concept. It improves data transmission efficiency and spectrum utilization by keeping interference probability within a tolerable limit at the primary receiver.

## 6.2 FUTURE SCOPE

CRs are fully programmable wireless devices that can sense its operational environment and adapt transmission waveform, channel access method, spectrum use, and networking protocols dynamically for good network and application performance. The research contributions presented in this thesis have unveiled several new areas for future investigation which has been summarized below.

Chapter III has introduced the localization scheme under additive white Gaussian noise (AWGN) fading channel condition. Raleigh and Rician fading channels may be studied in the future to perform localization scheme in real-time conditions. Furthermore, during the location estimation process, the system computational time has not been taken into consideration in this thesis work. The delay associated with the detection process may increase overhead time and reduce system efficiency. Therefore, in the future, researchers may consider the optimization of detection time for RSSI based localization scheme to maximize the system efficiency. In this thesis work, to reduce computational complexity, one active PU has been considered at a time. Hence, to emulate real-time conditions, researchers may be examined the presence of more than one PU at a time.

Chapter IV has discussed the optimum channel frequency selection scheme. A cost-effective simple hardware setup has been designed to accomplish the channel selection process. A fixed predefined system threshold value has been considered during the selection process. To handle the variable channel traffic conditions, an adaptive threshold selection scheme should be developed to utilize the frequency spectrum more efficiently.

Moreover, employment of machine learning techniques may be studied to enhance the performance of CR technology.

---

# BIBLIOGRAPHY

---

- [1] Haykin, S. (2005, February). Cognitive radio: brain-empowered wireless communications. *IEEE Journal on Selected Areas in Communications*, 23(2), 201-220.
- [2] Islam, M. H., Koh, C. L., Oh, S. W., Qing, X., Lai, Y. Y., Wang, C., & Toh, W. (2008, May). Spectrum survey in Singapore: Occupancy measurements and analyses. 3rd International Conference on Cognitive Radio Oriented Wireless Networks and Communications, 1-7.
- [3] Datla, D., Wyglinski, A. M., & Minden, G. J., (2009, October). A spectrum surveying framework for dynamic spectrum access networks. *IEEE Transactions on Vehicular Technology*, 58(8), 4158-416.
- [4] FCC, (2013, Accessed on: 2nd July) Before the Federal Communications Commission Washington DC, USA 20554, <http://www.cs.ucdavis.edu/liu/2891/Material/FCC-03-322A1>.
- [5] Estimated spectrum bandwidth requirements for the future development of IMT-2000 and IMT-Advanced, International Telecommunication Union, 2010. <http://www.itu.int/pub/R-REP-M.2078>.
- [6] Akyildiz, I., Altunbasak, Y., Fekri, F., & Sivakumar, R. (2004, March). AdaptNet: an adaptive protocol suite for the next-generation wireless Internet. *IEEE Communications Magazine*, 42(3), 128-136.
- [7] Mitola, J., & Maguire, G. Q. (1999, August). Cognitive radio: making software radios more personal. *IEEE Personal Communications*, 6(4), 13-18.
- [8] Mitola, J. (2000). Cognitive radio an integrated agent architecture for software defined radio (Doctoral dissertation. Royal Institute of Technology (KTH) Stockholm, Sweden.
- [9] Gomez-Cuba, F., Asorey-Cacheda, R., & Gonzalez-Castano, F. J. (2012, Third Quarter). A survey on cooperative diversity for wireless networks. *IEEE Communications Surveys & Tutorials*, 14(3), 822-835.
- [10] Yucek, T., & Arslan, H. (2009, First Quarter). A survey of spectrum sensing algorithms for cognitive radio applications. *IEEE Communications Surveys & Tutorials*, 11(1), 116-130.
- [11] Mitola, J. (1993, April). Software radios: Survey, critical evaluation and future directions. *IEEE Aerospace and Electronic Systems Magazine*, 8(4), 25-36.
- [12] Sousa, E. S., Sadler, B. M., Hossain, E., & Jafar, S. A. (2009, April). Cognitive radio: A path in the evolution of public wireless networks. *Journal of Communications and Networks*, 11(2), 99-103.

- [13] Jabbari, B., Pickholtz, R., & Norton, M. (2010, August). Dynamic spectrum access and management. *IEEE Wireless Communications*, 17(4), 6-15.
- [14] Song, M., Xin, C., Zhao, Y., & Cheng, X. (2012, February). Dynamic spectrum access: from cognitive radio to network radio. *IEEE Wireless Communications*, 19(1), 23-29.
- [15] Lu, X., Wang, P., Niyato, D., & Hossain, E. (2014, April). Dynamic spectrum access in cognitive radio networks with RF energy harvesting. *IEEE Wireless Communications*, 21(3), 102-110.
- [16] Biglieri, E., Goldsmith, A. J., Greenstein, L. J., Poor, H. V., & Mandayam, N. B. (2013). *Principles of cognitive radio*. Cambridge University Press, ISBN: 978-1-107-02875-3.
- [17] Zhao, Q., & Sadler, B. M. (2007, May). A survey of dynamic spectrum access. *IEEE Signal Processing Magazine*, 24(3), 79-89.
- [18] Hossain, E., Niyato, D., & Han, Z. (2009). *Dynamic spectrum access and management in cognitive radio networks*. Cambridge University Press, ISBN: 978-0-521-89847-8.
- [19] Buddhikot, M. M. (2007, April). Understanding dynamic spectrum access: models, taxonomy and challenges. 2nd IEEE International Symposium on New Frontiers in Dynamic Spectrum Access Networks, 649-663.
- [20] Hatfield, D. N., & Weiser, P. J. (2005, November). Property rights in spectrum: Taking the next step. In *First IEEE International Symposium on New Frontiers in Dynamic Spectrum Access Networks*, 43-55.
- [21] Naeem, M., Anpalagan, A., Jaseemuddin, M., & Lee, D. C. (2014, May). Resource allocation techniques in cooperative cognitive radio networks. *IEEE Communications Surveys & Tutorials*, 16(2), 729-744.
- [22] Le, L. B., & Hossain, E. (2008, December). Resource allocation for spectrum underlay in cognitive radio networks. *IEEE Transactions on Wireless communications*, 7(12), 5306-5315.
- [23] Chen, Y., Lei, Q., & Yuan, X. (2014, December). Resource allocation based on dynamic hybrid overlay/underlay for heterogeneous services of cognitive radio networks. *Wireless Personal Communications*, 79(3), 1647-1664.
- [24] Oh, J., & Choi, W. (2010, September). A hybrid cognitive radio system: A combination of underlay and overlay approaches. In *2010 IEEE 72nd Vehicular Technology Conference-Fall*, 1-5.
- [25] Berlemann, L., & Mangold, S. (2009, March). *Cognitive radio and dynamic spectrum access*. John Wiley & Sons, ISBN: 978-0-470-51167-1.
- [26] Buljore, S., Harada, H., Houze, P., Tsagkaris, K., Ivanov, V., Nolte, K. & Stamatelatos, M. (2008, July). IEEE P1900. 4 Standard: Reconfiguration of multi-radio systems. *International Conference on Computational Technologies in Electrical and Electronics Engineering*, 413-417.



- [27] IEEE Standard for Information Technology- Local and Metropolitan Area Networks- Specific Requirements- Part 11: Wireless LAN Medium Access Control (MAC) and Physical Layer (PHY) Specifications Amendment 3: 3650–3700 MHz Operation in USA, IEEE STD 802-11y-2008, Nov. 3, 2008, 1-90.
- [28] IEEE Standard for Local and Metropolitan Area Networks Part 16: Air Interface for Broadband Wireless Access Systems Amendment 2: Improved Coexistence Mechanisms for License-Exempt Operation, IEEE Std 802.16h-2010, Jul. 30, 2010, 1-223.
- [29] Stevenson, C. R., Chouinard, G., Lei, Z., Hu, W., Shellhammer, S. J., & Caldwell, W. (2009, February). IEEE 802.22: The first cognitive radio wireless regional area network standard. *IEEE Communications Magazine*, 47(1), 130-138.
- [30] Sherman, M., Mody, A. N., Martinez, R., Rodriguez, C., & Reddy, R. (2008). IEEE standards supporting cognitive radio and networks, dynamic spectrum access, and coexistence. *IEEE Communications Magazine*, 46(7), 72-79.
- [31] "Cognitive wireless RAN medium access control (MAC) and physical layer (PHY) specifications: Policies and procedures for operations in the TV bands", IEEE std802.22-2011, 1-680, 2011.
- [32] Standard for Wireless Regional Area Networks (WRAN) - Specific requirements - Part 22: Cognitive Wireless RAN Medium Access Control (MAC) and Physical Layer (PHY) Specifications: Policies and procedures for operation in the TV Bands, The Institute of Electrical and Electronics Engineering, Inc. Std. IEEE 802.22.
- [33] Draft Supplement to STANDARD FOR Telecommunications and Information Exchange Between Systems - LAN/MAN Specific Requirements- Part 11: Wireless Medium Access Control (MAC) and physical layer (PHY) specifications: Specification for Radio Resource Measurement, The Institute of Electrical and Electronics Engineering, Inc. Std. IEEE 802.11k/D0.7, 2003, October.
- [34] Harada, H., Alemseged, Y., Filin, S., Riegel, M., Gundlach, M., Holland, O. & Grande, L. (2013, March). IEEE dynamic spectrum access networks standards committee. *IEEE Communications Magazine*, 51(3), 104-111.
- [35] "IEEE 802.19 wireless coexistence working group (WG)", (2011, December). <http://ieee802.org/19/>.
- [36] "IEEE std. 802.11af: Wireless LAN in the TV white space", (2011, December). [http://www.ieee802.org/11/Reports/tgaf\\_update.htm](http://www.ieee802.org/11/Reports/tgaf_update.htm).
- [37] Mueck, M., Piiipponen, A., Kalliojarvi, K., Dimitrakopoulos, G., Tsagkaris, K., Demestichas, P., & Filin, S. (2010, September). ETSI reconfigurable radio systems: status and future directions on software defined radio and cognitive radio standards. *IEEE Communications Magazine*, 48(9), 78-86.

- [38] Wyglinski, A. M., Nekovee, M., & Hou, T. (Eds.). (2009, November). Cognitive radio communications and networks: Principles and Practice. Academic Press, ISBN: 978-0-12-374715-0.
- [39] Flores, A. B., Guerra, R. E., Knightly, E. W., Ecclesine, P., & Pandey, S. (2013, October). IEEE 802.11 af: A standard for TV white space spectrum sharing. *IEEE Communications Magazine*, 51(10), 92-100.
- [40] Lehman, J. F., Laird, J. E., & Rosenbloom, P. S. (1996, April). A gentle introduction to Soar, an architecture for human cognition. *Invitation to Cognitive Science*, 4, 212-249.
- [41] Sloman, A. (2003, October). The cognition and affect project: Architectures, architecture-schemas, and the new science of mind. Tech. rep., School of Computer Science, University of Birmingham, 3-31.
- [42] Heise E., Westermann R. (1989) Anderson's Theory of Cognitive Architecture (ACT\*). In: Westmeyer H. (eds) *Psychological Theories from a Structuralist Point of View. Recent Research in Psychology*, Springer, 103-127, ISBN: 978-3-540-51904-1.
- [43] Brehmer, B. (2005, June). The dynamic OODA loop: Amalgamating Boyd's OODA loop and the cybernetic approach to command and control. In *Proceedings of the 10th International Command and Control Research Technology Symposium*, 365-368.
- [44] Chen, T., Zhang, H., Maggio, G. M., & Chlamtac, I. (2007, June). Topology management in CogMesh: a cluster-based cognitive radio mesh network. *IEEE International Conference on Communications*, 6516-6521.
- [45] Bouabdallah, N., Ishibashi, B., & Boutaba, R. (2011, January). Performance of cognitive radio-based wireless mesh networks. *IEEE Transactions on Mobile Computing*, 10(1), 122-135.
- [46] Liu, K. R., Sadek, A. K., Su, W., & Kwasinski, A. (2009). *Cooperative communications and networking*. Cambridge University Press, ISBN: 978-0-521-89513-2.
- [47] Letaief, K. B., & Zhang, W. (2009, May). Cooperative communications for cognitive radio networks. *Proceedings of the IEEE*, 97(5), 878-893.
- [48] Zhao, Q., Tong, L., & Swami, A. (2005, November). Decentralized cognitive MAC for dynamic spectrum access. In *First IEEE International Symposium on New Frontiers in Dynamic Spectrum Access Networks*, 224-232.
- [49] Chen, C. Y., Chou, Y. H., Chao, H. C., & Lo, C. H. (2012, August). Secure centralized spectrum sensing for cognitive radio networks. *Wireless Networks*, 18(6), 667-677.
- [50] Chen, Y., Zhou, H., Kong, R., Zhu, L., & Mao, H. (2017, March). Decentralized blind spectrum selection in cognitive radio networks Considering Handoff Cost. *Future Internet*, 9(2), 10.

- [51] Zhao, Q., Tong, L., Swami, A., & Chen, Y. (2007, April). Decentralized cognitive MAC for opportunistic spectrum access in ad hoc networks: A POMDP framework. *IEEE Journal on Selected Areas in Communications*, 25(3), 589-600.
- [52] Zhao, J., & Yuan, J. (2013, October). An improved centralized cognitive radio network spectrum allocation algorithm based on the allocation sequence. *International Journal of Distributed Sensor Networks*, 9(10), 875342.
- [53] Dhifallah, O., Dahrouj, H., Al-Naffouri, T. Y., & Alouini, M. S. (2017, April). Decentralized SINR balancing in cognitive radio networks. *IEEE Transactions on Vehicular Technology*, 66(4), 3491-3496.
- [54] Kang, X., Liang, Y. C., Garg, H. K., & Zhang, L. (2009, October). Sensing-based spectrum sharing in cognitive radio networks. *IEEE Transactions on Vehicular Technology*, 58(8), 4649-4654.
- [55] Federal Communications Commission. (2008, November). In the Matter of Unlicensed Operation in the TV Broadcast Bands: Second Report and Order and Memorandum Opinion and Order. Document 08-260.
- [56] Sachs, J., Maric, I., & Goldsmith, A. (2010, April). Cognitive cellular systems within the TV spectrum. *IEEE Symposium on New Frontiers in Dynamic Spectrum*, 1-12.
- [57] Tandra, R., & Sahai, A. (2005, June). Fundamental limits on detection in low SNR under noise uncertainty. *International Conference on Wireless Networks, Communications and Mobile Computing*, 1, 464-469.
- [58] Tandra, R., & Sahai, A. (2008, February). SNR walls for signal detection. *IEEE Journal of Selected Topics in Signal Processing*, 2(1), 4-17.
- [59] Sonnenschein, A., & Fishman, P. M. (1992, July). Radiometric detection of spread-spectrum signals in noise of uncertain power. *IEEE Transactions on Aerospace and Electronic Systems*, 28(3), 654-660.
- [60] Sahai, & D. Cabric. (2005, November). A tutorial on spectrum sensing: fundamental limits and practical challenges. *Proceeding of IEEE Symposium on New Frontiers in Dynamic Spectrum Access Networks*, Baltimore, 8-11.
- [61] Xu, E., & Labeau, F. (2015, November). Impact evaluation of noise uncertainty in spectrum sensing under middleton class a noise. *IEEE 12th Malaysia International Conference on Communications*, 36-40.
- [62] Chen, D., Li, J., & Ma, J. (2008, October). Cooperative spectrum sensing under noise uncertainty in cognitive radio. *4th International Conference on Wireless Communications, Networking and Mobile Computing*, 1-4.

- [63] Lehtomaki, J. J., Juntti, M., Saarnisaari, H., & Koivu, S. (2005, November). Threshold setting strategies for a quantized total power radiometer. *IEEE Signal Processing Letters*, 12(11), 796-799.
- [64] Charan, C., & Pandey, R. (2016, August). Eigenvalue based double threshold spectrum sensing under noise uncertainty for cognitive radio. *International Journal for Light and Electron Optics*, 127(15), 5968-5975.
- [65] Zhang, R., Lim, T. J., Liang, Y. C., & Zeng, Y. (2010, January). Multi-antenna based spectrum sensing for cognitive radios: A GLRT approach. *IEEE Transactions on Communications*, 58(1), 84-88.
- [66] Sun, M., Zhao, C., Yan, S., & Li, B. (2017, May). A novel spectrum sensing for cognitive radio networks with noise uncertainty. *IEEE Transactions on Vehicular Technology*, 66(5), 4424-4429.
- [67] Reddy, B. Y. (2012). Solving hidden terminal problem in cognitive networks using cloud technologies. 6<sup>th</sup> International Conference on Sensor Technologies and Applications, 235-240.
- [68] Min, A. W., Shin, K. G., & Hu, X. (2009, October). Attack-tolerant distributed sensing for dynamic spectrum access networks. 17th IEEE International Conference on Network Protocols, 294-303.
- [69] Chen, R., & Park, J. M. (2006, September). Ensuring trustworthy spectrum sensing in cognitive radio networks. 1st IEEE Workshop on Networking Technologies for Software Defined Radio Networks, 110-119.
- [70] Chen, R., Park, J. M., & Reed, J. H. (2008, January). Defense against primary user emulation attacks in cognitive radio networks. *IEEE Journal on Selected Areas in Communications*, 26(1), 25-37.
- [71] Jia, J., Zhang, Q., & Shen, X. S. (2008, January). HC-MAC: A hardware-constrained cognitive MAC for efficient spectrum management. *IEEE Journal on Selected Areas in Communications*, 26(1), 106-117.
- [72] Aijaz, A., Ping, S., Akhavan, M. R., & Aghvami, A. H. (2014, December). CRB-MAC: A receiver-based MAC protocol for cognitive radio equipped smart grid sensor networks. *IEEE Sensors Journal*, 14(12), 4325-4333.
- [73] Wu, J., Wang, Y., & Deng, J. (2014, August). TSCR-MAC: Time-slotted channel reservation based cognitive MAC. In 9th International Conference on Communications and Networking in China, 666-671.
- [74] Salameh, H. B., Krunz, M., & Younis, O. (2009, October). MAC protocol for opportunistic cognitive radio networks with soft guarantees. *IEEE Transactions on Mobile Computing*, 8(10), 1339-1352.

- [75] Ma, L., Han, X., & Shen, C. C. (2005, November). Dynamic open spectrum sharing MAC protocol for wireless ad hoc networks. In *First IEEE International Symposium on New Frontiers in Dynamic Spectrum Access Networks*, 203-213.
- [76] Elezabi, A., Kashef, M., Abdallah, M., & Khairy, M. M. (2009, June). Cognitive interference-minimizing code assignment for underlay CDMA networks in asynchronous multipath fading channels. *International Conference on Wireless Communications and Mobile Computing: Connecting the World Wirelessly*, 1279-1283.
- [77] Wang, B., & Zhao, D. (2008, November). Performance analysis in CDMA-based cognitive wireless networks with spectrum underlay. *IEEE Global Telecommunications Conference*, 1-6.
- [78] Akyildiz, I. F., Lee, W. Y., & Chowdhury, K. R. (2009, July). CRAHNs: Cognitive radio ad hoc networks. *AD Hoc Networks*, 7(5), 810-836.
- [79] Krishna, T. V., & Das, A. (2009, June). A survey on MAC protocols in OSA networks. *Computer Networks*, 53(9), 1377-1394.
- [80] Cormio, C., & Chowdhury, K. R. (2009, September). A survey on MAC protocols for cognitive radio networks. *Ad Hoc Networks*, 7(7), 1315-1329.
- [81] Chatterjee, S., & Banerjee, P. (2015, July). Non cooperative primary users-localization in cognitive radio networks. *IEEE 2nd International in Recent Trends in Information Systems*, 68-75.
- [82] Chatterjee, S., Banerjee, P., & Nasipuri, M. (2015, January). Enhancing accuracy of localization for primary users in cognitive radio networks. *IEEE International Conference on Computational Intelligence & Networks*, 74-79.
- [83] Chatterjee, S., Banerjee, P., & Nasipuri, M. (2018, August). A new protocol for concurrently allocating licensed spectrum to underlay cognitive users. *Digital Communications and Networks*, 4(3), 200-208.
- [84] Chatterjee, S., & Banerjee, P. (2014, January). Hill-Climbing approach for optimizing receiver bandwidth. *IEEE International Conference in Electronics, Communication and Instrumentation*, 1-4.
- [85] Chatterjee, S., Banerjee, P., & Nasipuri, M. (2017, September). Optimized flexible power selection for opportunistic underlay cognitive radio networks. *Wireless Personal Communications*, 96(1), 1193-1213.
- [86] IEEE 802.15 WPAN™ Task Group 6 (TG6) Body Area Networks. IEEE Standards Association (2013, May). <http://www.ieee802.org/15/pub/TG6.html>.

- [87] Di Felice, M., Doost-Mohammady, R., Chowdhury, K. R., & Bononi, L. (2012, June). Smart radios for smart vehicles: Cognitive vehicular networks. *IEEE Vehicular Technology Magazine*, 7(2), 26-33.
- [88] Gao, B., Yang, Y., & Park, J. M. (2011, June). Channel aggregation in cognitive radio networks with practical considerations. *IEEE International Conference on Communications*, 1-5.
- [89] Kibria, M. G., Yuan, F., & Kojima, F. (2016, February). Feedback bits allocation for interference minimization in cognitive radio communications. *IEEE Wireless Communications Letters*, 5(1), 104-107.
- [90] Sithamparanathan, K., & Giorgetti, A. (2012). *Cognitive radio techniques: spectrum sensing, interference mitigation, and localization*. Artech House, ISBN: 9781608072040.
- [91] Liang, Y. C., Chen, K. C., Li, G. Y., & Mahonen, P. (2011, September). Cognitive radio networking and communications: An overview. *IEEE Transactions on Vehicular Technology*, 60(7), 3386-3407.
- [92] Cormio, C., & Chowdhury, K. R. (2009, September). A survey on MAC protocols for cognitive radio networks. *Ad Hoc Networks*, 7(7), 1315-1329.
- [93] Kandeepan, S., Reisenfeld, S., Aysal, T. C., Lowe, D., & Piesiewicz, R. (2009, April). Bayesian tracking in cooperative localization for cognitive radio networks. In *VTC Spring 2009-IEEE 69th Vehicular Technology Conference*, 1-5.
- [94] Langendoen, K., & Reijers, N. (2003, November). Distributed localization in wireless sensor networks: a quantitative comparison. *Computer networks*, 43(4), 499-518.
- [95] He, T., Huang, C., Blum, B. M., Stankovic, J. A., & Abdelzaher, T. (2003, September). Range-free localization schemes for large scale sensor networks. *9th Annual International Conference on Mobile Computing and Networking*, 81-95.
- [96] Gui, L., Val, T., Wei, A., & Taktak, S. (2014, January). An adaptive range-free localization protocol in wireless sensor networks, *International Journal of Ad Hoc and Ubiquitous Computing*, 15(1/2/3), 38-56.
- [97] Kumar, P., Reddy, L., & Varma, S. (2009, December). Distance measurement and error estimation scheme for RSSI based localization in wireless sensor networks. *Fifth International Conference on Wireless Communication and Sensor Networks*, 1-4.
- [98] Kovavisaruch, L. O., & Ho, K. C. (2005, March). Alternate source and receiver location estimation using TDOA with receiver position uncertainties. *IEEE International Conference on Acoustics, Speech, and Signal Processing*, (4), 1065-1068.
- [99] Singh, A. K., & Singh, A. K. (2016, January). Range-based primary user localization in cognitive radio networks. *Procedia Computer Science*, 93, 199-206.

- [100] Catovic, A., & Sahinoglu, Z. (2004, October). The Cramer-Rao bounds of hybrid TOA/RSS and TDOA/RSS location estimation schemes. *IEEE Communications Letters*, 8(10), 626-628.
- [101] Lim, H., Kung, L. C., Hou, J. C., & Luo, H. (2005). Zero-configuration, robust indoor localization: Theory and experimentation. *25th IEEE International Conference on Computer Communications*, 1-12.
- [102] Stoyanova, T., Kerasiotis, F., Efstathiou, K., & Papadopoulos, G. (2010, July). Modeling of the RSS uncertainty for RSS-based outdoor localization and tracking applications in wireless sensor networks. *Fourth International Conference on Sensor Technologies and Applications*, 45-50.
- [103] Chao, C. H., Chu, C. Y., & Wu, A. Y. (2008, October). Location-constrained particle filter human positioning and tracking system. *IEEE Workshop on Signal Processing Systems*, 73-76.
- [104] Luo, Q., Peng, Y., Peng, X., & Saddik, A. (2014, April). Uncertain data clustering-based distance estimation in wireless sensor networks. *Sensors*, 14(4), 6584-6605.
- [105] Liu, S., Chen, Y., Trappe, W., & Greenstein, L. J. (2009, February). Non-interactive localization of cognitive radios based on dynamic signal strength mapping. *Sixth International Conference on Wireless On-Demand Network Systems and Services*, 85-92.
- [106] Friis, H. T. (1946, May). A note on a simple transmission formula. *Proceedings of the IRE*, 34(5), 254-256.
- [107] Shirahama, J., & Ohtsuki, T. (2008, May). RSS-based localization in environments with different path loss exponent for each link. In *VTC Spring 2008-IEEE Vehicular Technology Conference*, 1509-1513.
- [108] Min, A. W., & Shin, K. G. (2013, April). Robust tracking of small-scale mobile primary user in cognitive radio networks. *IEEE Transactions on Parallel and Distributed Systems*, 24(4), 778-788.
- [109] Lee, Y. D., & Koo, I. (2014, August). A Received Signal Strength-based Primary User Localization Scheme for Cognitive Radio Sensor Networks Using Underlay Model-based Spectrum Access. *KSII Transactions on Internet and Information Systems*, 8(8), 2663-2674.
- [110] Abouzar, P., Michelson, D. G., & Hamdi, M. (2016, October). RSSI-based distributed self-localization for wireless sensor networks used in precision agriculture. *IEEE Transactions on Wireless Communications*, 15(10), 6638-6650.
- [111] Zhu, Y., Vikram, A., Fu, H., & Guan, Y. (2014, November). On non-cooperative multiple-target tracking with wireless sensor networks. *IEEE Transactions on Wireless Communications*, 13(11), 6496-6510.

- [112] Tomic, S., Beko, M., & Dinis, R. (2015, May). RSS-based localization in wireless sensor networks using convex relaxation: Noncooperative and cooperative schemes. *IEEE Transactions on Vehicular Technology*, 64(5), 2037-2050.
- [113] Tomic, S., Beko, M., & Dinis, R. (2014, October). Distributed RSS-based localization in wireless sensor networks based on second-order cone programming. *Sensors*, 14(10), 18410-18432.
- [114] Mirza, D., & Schurgers, C. (2007, September). Collaborative localization for fleets of underwater drifters. In *OCEANS, IEEE*, 1-6.
- [115] Jiang, J. A., Chuang, C. L., Lin, T. S., Chen, C. P., Hung, C. H., Wang, J. Y., & Lai, T. Y. (2010, January). Collaborative localization in wireless sensor networks via pattern recognition in radio irregularity using omnidirectional antennas. *Sensors*, 10(1), 400-427.
- [116] HE Yan Li. (2011, May). Research on centroid localization algorithm for wireless sensor networks based RSSI. *Computer Simulation, Wireless Sensor Network*, 165-168.
- [117] Bulusu, N., Heidemann, J., & Estrin, D. (2000, October). GPS-less low-cost outdoor localization for very small devices. *IEEE Personal Communications*, 7(5), 28-34.
- [118] Blumenthal, J., Grossmann, R., Golatowski, F., & Timmermann, D. (2007, October). Weighted centroid localization in zigbee-based sensor networks. In *international Symposium on Intelligent Signal Processing*, 1-6.
- [119] Xianhao, S., & Jiazhi, Y. (2010, October). Node self-localization algorithm based on rssi in wireless sensor networks outdoor. In *International Conference on Intelligent System Design and Engineering Application*, (1), 1010-1012.
- [120] Shi, H. (2012, June). A new weighted centroid localization algorithm based on RSSI. In *IEEE International Conference on Information and Automation*, 137-141.
- [121] Dong, Q., & Xu, X. (2014, March). A novel weighted centroid localization algorithm based on RSSI for an outdoor environment. *Journal of Communications*, 9(3), 279-285.
- [122] Bayhan, S. (2010, June). MAC layer design in cognitive radio networks. In *International Symposium on "A World of Wireless, Mobile and Multimedia Networks"*, 1-2.
- [123] Shah, G. A., Gungor, V. C., & Akan, O. B. (2012, June). A cross-layer design for QoS support in cognitive radio sensor networks for smart grid applications. In *International Conference on Communications*, 1378-1382.
- [124] Gungor, V. C., & Sahin, D. (2012, June). Cognitive radio networks for smart grid applications: A promising technology to overcome spectrum inefficiency. *IEEE Vehicular Technology Magazine*, 7(2), 41-46.



- [125] Kondareddy, Y. R., & Agrawal, P. (2008, May). Synchronized MAC protocol for multi-hop cognitive radio networks. In International Conference on Communications, 3198-3202.
- [126] Salameh, H. A. B., & Krunz, M. (2009, July). Channel access protocols for multihop opportunistic networks: challenges and recent developments. *IEEE network*, 23(4), 14-19.
- [127] Joshi, G. P., Kim, S. W., & Kim, B. S. (2009, September). An efficient MAC protocol for improving the network throughput for cognitive radio networks. In Third International Conference on Next Generation Mobile Applications, Services and Technologies, 271-275.
- [128] Ren, P., Wang, Y., Du, Q., & Xu, J. (2012, February). A survey on dynamic spectrum access protocols for distributed cognitive wireless networks. *EURASIP Journal on Wireless Communications and Networking*, 1(60), 1-21.
- [129] Htike, Z., & Hong, C. S. (2011). Overview of 802.22 WRAN Standard and Research Challenges. *OSIA Standards & Technology Review*, 24(2), 57-64.
- [130] Cordeiro, C., Challapali, K., Birru, D., & Shankar, S. (2005, November). IEEE 802.22: the first worldwide wireless standard based on cognitive radios. In First IEEE International Symposium on New Frontiers in Dynamic Spectrum Access Networks, 328-337.
- [131] Chowdhury, K. R., & Akyildiz, I. F. (2008, January). Cognitive wireless mesh networks with dynamic spectrum access. *IEEE Journal on Selected Areas in Communications*, 26(1), 168-181.
- [132] Kim, D. I., Le, L. B., & Hossain, E. (2008, December). Joint rate and power allocation for cognitive radios in dynamic spectrum access environment. *IEEE Transactions on Wireless Communications*, 7(12), 5517-5527.
- [133] Srinivasa, S., & Jafar, S. A. (2007, May). Cognitive radios for dynamic spectrum access-the throughput potential of cognitive radio: A theoretical perspective. *IEEE Communications Magazine*, 45(5), 73-79.
- [134] Le, L., & Hossain, E. (2008, March). A MAC protocol for opportunistic spectrum access in cognitive radio networks. In Wireless Communications and Networking Conference, 1426-1430.
- [135] De Domenico, A., Strinati, E. C., & Di Benedetto, M. G. (2012, March). A survey on MAC strategies for cognitive radio networks. *IEEE Communications Surveys & Tutorials*, 14(1), 21-44.
- [136] Sharma, G., Ganesh, A., & Key, P. (2009, April). Performance analysis of contention based medium access control protocols. *IEEE Transactions on Information Theory*, 55(4), 1665-1682.

- [137] Wang, F., Younis, O., & Krunz, M. (2006, April). GMAC: A game-theoretic MAC protocol for mobile ad hoc networks. In 4th International Symposium on Modeling and Optimization in Mobile, Ad Hoc and Wireless Networks, 1-9.
- [138] Zou, C., & Chigan, C. (2008, May). A game theoretic DSA-driven MAC framework for cognitive radio networks. In International Conference on Communications, 4165-4169.
- [139] El Nainay, M. Y., Friend, D. H., & MacKenzie, A. B. (2008, October). Channel allocation & power control for dynamic spectrum cognitive networks using a localized island genetic algorithm. In 3rd IEEE Symposium on New Frontiers in Dynamic Spectrum Access Networks, 1-5.
- [140] Tan, L. T., & Le, L. B. (2014, June). Joint cooperative spectrum sensing and MAC protocol design for multi-channel cognitive radio networks. EURASIP Journal on Wireless Communications and Networking, 2014(1), 101.
- [141] Shah, M. A., Zhang, S., & Maple, C. (2013, February). An analysis on decentralized adaptive MAC protocols for cognitive radio networks. International Journal of Automation and Computing, 10(1), 46-52.
- [142] Hsu, A. C. C., Wei, D. S., & Kuo, C. C. J. (2007, March). A cognitive MAC protocol using statistical channel allocation for wireless ad-hoc networks. In IEEE Wireless Communications and Networking Conference, 105-110.
- [143] Zhang, X., & Su, H. (2011, February). CREAM-MAC: Cognitive radio-enabled multi-channel MAC protocol over dynamic spectrum access networks. IEEE Journal of Selected Topics in Signal Processing, 5(1), 110-123.
- [144] Hung, S. Y., Cheng, Y. C., Wu, E. K., & Chen, G. H. (2008, May). An opportunistic cognitive MAC protocol for coexistence with WLAN. In IEEE International Conference on Communications, 4059-4063.
- [145] Cordeiro, C., & Challapali, K. (2007, April). C-MAC: A cognitive MAC protocol for multi-channel wireless networks. In 2nd IEEE International Symposium on New Frontiers in Dynamic Spectrum Access Networks, 147-157.
- [146] Hamdaoui, B., & Shin, K. G. (2008, August). OS-MAC: An efficient MAC protocol for spectrum-agile wireless networks. IEEE Transactions on Mobile Computing, 7(8), 915-930.
- [147] Lien, S. Y., Tseng, C. C., & Chen, K. C. (2008, May). Carrier sensing based multiple access protocols for cognitive radio networks. In IEEE International Conference on Communications, 3208-3214.
- [148] Song, H., & Lin, X. (2009, July). A novel DSA-driven MAC protocol for cognitive radio networks. Wireless Sensor Network, 1(2), 61-121.

- [149] Xing, Y., Mathur, C. N., Haleem, M. A., Chandramouli, R., & Subbalakshmi, K. P. (2007, April). Dynamic spectrum access with QoS and interference temperature constraints. *IEEE Transactions on Mobile Computing*, 6(4), 423-433.
- [150] Yang, C. G., Li, J. D., & Tian, Z. (2010, May). Optimal power control for cognitive radio networks under coupled interference constraints: A cooperative game-theoretic perspective. *IEEE Transactions on Vehicular Technology*, 59(4), 1696-1706.
- [151] Wang, W., Lv, T., Ren, Z., Gao, L., & Liu, W. (2009, September). A novel spectrum sharing algorithm based on the throughput in cognitive radio networks. In *5th International Conference on Wireless Communications, Networking and Mobile Computing*, 1-4.
- [152] Choi, S., Park, H., & Hwang, T. (2014, January). Optimal beamforming and power allocation for sensing-based spectrum sharing in cognitive radio networks. *IEEE Transactions on Vehicular Technology*, 63(1), 412-417.
- [153] Kang, X., Zhang, R., Liang, Y. C., & Garg, H. K. (2011, February). Optimal power allocation strategies for fading cognitive radio channels with primary user outage constraint. *IEEE Journal on Selected Areas in Communications*, 29(2), 374-383.
- [154] Kang, X., Zhang, R., Liang, Y. C., & Garg, H. K. (2009, June). Optimal power allocation for cognitive radio under primary user's outage loss constraint. In *IEEE International Conference on Communications*, 1-5.
- [155] Ozcan, G., & Gursoy, M. C. (2015, August). Optimal power control for underlay cognitive radio systems with arbitrary input distributions. *IEEE Transactions on Wireless Communications*, 14(8), 4219-4233.
- [156] Kolodzy, P. J. (2006, March). Interference temperature: a metric for dynamic spectrum utilization. *International Journal of Network Management*, 16(2), 103-113.
- [157] Yongjun, X., & Xiaohui, Z. (2013, October). Optimal power allocation for multiuser underlay cognitive radio networks under QoS and interference temperature constraints. *China Communications*, 10(10), 91-100.
- [158] Vu, M., Devroye, N., Sharif, M., & Tarokh, V. (2007, August). Scaling laws of cognitive networks. In *2nd International Conference on Cognitive Radio Oriented Wireless Networks and Communications*, 2-8.
- [159] Wu, S. L., Tseng, Y. C., & Sheu, J. P. (2000, September). Intelligent medium access for mobile ad hoc networks with busy tones and power control. *IEEE Journal on Selected Areas in Communications*, 18(9), 1647-1657.
- [160] Pursley, M. B., Russell, H. B., & Wysocarski, J. S. (2000). Energy-efficient transmission and routing protocols for wireless multiple-hop networks and spread-spectrum radios. In *IEEE/AFCEA EUROCOMM 2000. Information Systems for Enhanced Public Safety and Security (Cat. No. 00EX405)*, 1-5.

- [161] Ebert, J. P., Stremmel, B., Wiederhold, E., & Wolisz, A. (2000, September). An energy-efficient power control approach for WLANs. *Journal of Communications and Networks*, 2(3), 197-206.
- [162] Lettieri, P., & Srivastava, M. B. (1998, March). Adaptive frame length control for improving wireless link throughput, range, and energy efficiency. In *Proceedings. IEEE INFOCOM'98*, 2, 564-571.
- [163] Wang, J., Urriza, P., Han, Y., & Cabric, D. (2011, October). Weighted centroid localization algorithm: theoretical analysis and distributed implementation. *IEEE Transactions on Wireless Communications*, 10(10), 3403-3413.
- [164] Alippi, C., & Vanini, G. (2006, March). A RSSI-based and calibrated centralized localization technique for wireless sensor networks. In *Fourth Annual IEEE International Conference on Pervasive Computing and Communications Workshops*, 5-305.
- [165] Niculescu, D., & Nath, B. (2003, March). Ad hoc positioning system (APS) using AOA. *Twenty-second Annual Joint Conference of the IEEE Computer and Communications Societies*, 3, 1734-1743.
- [166] Cheng, E., Lin, X., Chen, S., & Yuan, F. (2016, September). A TDoA localization scheme for underwater sensor networks with use of multilinear chirp signals. *Mobile Information Systems*, 2016, 1-11.
- [167] Sayed, A. H., Tarighat, A., & Khajehnouri, N. (2005, July). Network-based wireless location: challenges faced in developing techniques for accurate wireless location information. *IEEE Signal Processing Magazine*, 22(4), 24-40.
- [168] Sahoo, P. K., & Hwang, I. (2011, October). Collaborative localization algorithms for wireless sensor networks with reduced localization error. *Sensors*, 11(10), 9989-10009.
- [169] Liu, L., Han, Z., Wu, Z., & Qian, L. (2011, December). Collaborative compressive sensing based dynamic spectrum sensing and mobile primary user localization in cognitive radio networks. In *IEEE Global Telecommunications Conference*, 1-5.
- [170] Sayrac, B., Gueguen, L., Trang, C. C., & Serrano, A. M. G. (2013, May). Point-process based localization of primary users in collaborative dynamic spectrum access. In *ICT*, 1-5.
- [171] Celebi, H., & Arslan, H. (2007, August). Utilization of location information in cognitive wireless networks. *IEEE Wireless Communications*, 14(4), 6-13.
- [172] Wang, J., Chen, J., & Cabric, D. (2013, March). Cramer-Rao bounds for joint RSS/DoA-based primary-user localization in cognitive radio networks. *IEEE Transactions on Wireless Communications*, 12(3), 1363-1375.
- [173] Lee, W. C. (1993, February). *Mobile communications design fundamentals*. John Wiley & Sons, ISBN: 978-0-471-57446-0.

- [174] Rappaport, T. S. (1996, January). *Wireless communications: Principles and practice*. Upper Saddle River, NJ: Prentice Hal, ISBN: 0133755363.
- [175] Seybold, J. S. (2005, September). *Introduction to RF propagation*. John Wiley & Sons, ISBN: 9780471655961.
- [176] Durrant-Whyte, H., & Bailey, T. (2006, June). Simultaneous localization and mapping: part I. *IEEE Robotics & Automation Magazine*, 13(2), 99-110.
- [177] Bailey, T., & Durrant-Whyte, H. (2006, September). Simultaneous localization and mapping (SLAM): Part II. *IEEE Robotics & Automation Magazine*, 13(3), 108-117.
- [178] Quan, Z., Cui, S., & Sayed, A. H. (2008, February). Optimal linear cooperation for spectrum sensing in cognitive radio networks. *IEEE Journal of Selected Topics in Signal Processing*, 2(1), 28-40.
- [179] Liu, X., Jia, M., & Tan, X. (2013, January). Threshold optimization of cooperative spectrum sensing in cognitive radio networks. *Radio Science*, 48(1), 23-32.
- [180] Atapattu, S., Tellambura, C., & Jiang, H. (2011, June). Spectrum sensing via energy detector in low SNR. In *IEEE International Conference on Communications*, 1-5.
- [181] Zhang, W., Mallik, R. K., & Letaief, K. B. (2009, December). Optimization of cooperative spectrum sensing with energy detection in cognitive radio networks. *IEEE Transactions on Wireless Communications*, 8(12), 5761-5766.
- [182] Parameswaran, A. T., Husain, M. I., & Upadhyaya, S. (2009, September). Is RSSI a reliable parameter in sensor localization algorithms: An experimental study. In *Field failure Data Analysis Workshop (F2DA09) (Vol. 5)*.
- [183] J. I. Marcum (1950, January) , "Table of Q functions," Rand Corporation, Santa Monica, CA, U.S. Air Force Project RAND Research Memorandum M-339, ASTIA Document AD 1165451.
- [184] Morales-Jimenez, D., Lopez-Martinez, F. J., Martos-Naya, E., Paris, J. F., & Lozano, A. (2014, February). Connections between the generalized Marcum Q-function and a class of hypergeometric functions. *IEEE Transactions on Information Theory*, 60(2), 1077-1082.
- [185] Golub, G. H., & Pereyra, V. (1973, April). The differentiation of pseudo-inverses and nonlinear least squares problems whose variables separate. *SIAM Journal on Numerical Analysis*, 10(2), 413-432.
- [186] ZHANG Sen. (2010, January). *Research of dynamic spectrum sharing and power allocation in cognitive radio networks*. Beijing University of Posts and Telecommunications.
- [187] W.-J. Feng., C. Zhou., & W-H. Jiang. (2010, November). Channel selection based on EWA game abstraction in cognitive radio network. *Journal of Applied Sciences*, 28(6), 580-584.

- [188] Wang, L. C., Wang, C. W., & Adachi, F. (2011, April). Load-balancing spectrum decision for cognitive radio networks. *IEEE Journal on Selected Areas in Communications*, 29(4), 757-769.
- [189] Li, L., Deng, Y. N., Yuan, Y., & Feng, W. J. (2015, March). Research on channel selection algorithms in cognitive radio networks. *Journal of Networks*, 10(3), 159-164.
- [190] G.-H. Yang, H. Zheng, J. Zhao, & V.O.K. Li. (2006 June). Adaptive channel selection through collaborative sensing. In *Proc. IEEE International Conference on Communications*, 3753–3758.
- [191] Swami, S., Ghosh, C., Dhekne, R. P., Agrawal, D. P., & Berman, K. A. (2008, December). Graph theoretic approach to QoS-guaranteed spectrum allocation in cognitive radio networks. *International Performance, Computing and Communications Conference*, 354-359.
- [192] Wellens, M., de Baynast, A., & Mahonen, P. (2008, March). Exploiting historical spectrum occupancy information for adaptive spectrum sensing. *IEEE Wireless Communications and Networking Conference*, 717-722.
- [193] Jalali, E., Balapuwaduge, I. A., Li, F. Y., & Pla, V. (2015, February). A dynamic channel access strategy for underlay cognitive radio networks: Markov modelling and performance evaluation. *Transactions on Emerging Telecommunications Technologies*, 28(1).
- [194] Yi, N., Ma, Y., & Tafazolli, R. (2010, June). Underlay cognitive radio with full or partial channel quality information. *International Journal of Navigation and Observation*, (2010), 1-12.
- [195] Hu, F., Chen, B., Zhai, X., & Zhu, C. (2016, November). Channel selection policy in multi-SU and multi-PU cognitive radio networks with energy harvesting for internet of everything. *Mobile Information Systems*, (2016), 1-12.
- [196] Axell, E., Leus, G., Larsson, E. G., & Poor, H. V. (2012, May). Spectrum sensing for cognitive radio: State-of-the-art and recent advances. *IEEE Signal Processing Magazine*, 29(3), 101-116.
- [197] Haykin, S., Thomson, D. J., & Reed, J. H. (2009, May). Spectrum sensing for cognitive radio. *Proceedings of the IEEE*, 97(5), 849-877.
- [198] Goldsmith, A. J., Greenstein, L. J., Mandayam, N. B., & Poor, H. V. (2012). *Principles of cognitive radio*. Cambridge University Press, ISBN: 978-1-107-02875-3.
- [199] Force, S. (2002, November). Spectrum policy task force report. *Federal Communications Commission ET Docket 02*, vol. 135.

- [200] Clancy, T. C. (2006). Dynamic spectrum access in cognitive radio networks (Doctoral Dissertation).
- [201] Clancy, T., & Arbaugh, W. (2006, June). Measuring interference temperature. In Virginia Tech Symposium on Wireless Personal Communications, 1-10.
- [202] Kyriazakos, S. A., & Karetzos, G. T. (2004, May). Practical radio resource management in wireless systems. Artech House, ISBN: 978-1580536325.
- [203] Russell, Stuart J., & Norvig, Peter (2003), Artificial Intelligence: A Modern Approach (2nd ed.), Upper Saddle River, New Jersey: Prentice Hall, ISBN: 0-13-103805-2.
- [204] Torbaghan, M. K., Kazemi, S. M., Zhiani, R., & Hamed, F. (2013, February). Improved hill climbing and simulated annealing algorithms for size optimization of trusses. In Proceedings of World Academy of Science, Engineering and Technology, 7(2), 135-138.
- [205] Talbi, E. G., & Muntean, T. (1993, January). Hill-climbing, simulated annealing and genetic algorithms: a comparative study and application to the mapping problem. Twenty-sixth Hawaii International Conference on System Sciences, (2), 565-573.
- [206] SA636, NXP B.V. 2012, 5 (2012, December), 1-3.
- [207] NBC12429, Semiconductor Components Industries, LLC, (2003, January)-Rev.2, NBC12429/D, 1-20.
- [208] Akyildiz, I. F., Lee, W. Y., Vuran, M. C., & Mohanty, S. (2006, September). NeXt generation/dynamic spectrum access/cognitive radio wireless networks: A survey. Computer Networks, 50(13), 2127-2159.
- [209] Wang, Y., Song, M., Zhang, Y., Zhang, Y., & Xing, Y. (2012, February). A method of avoiding interference with hidden terminal in cognitive radio network. 14th International Conference on Advanced Communication Technology, 23-27.
- [210] Lan, P., Chen, L., Zhang, G., & Sun, F. (2015, December). Optimal resource allocation for cognitive radio networks with primary user outage constraint. EURASIP Journal on Wireless Communications and Networking, 2015(1), 239.
- [211] Kang, X., Liang, Y. C., Nallanathan, A., Garg, H. K., & Zhang, R. (2009, February). Optimal power allocation for fading channels in cognitive radio networks: Ergodic capacity and outage capacity. IEEE Transactions on Wireless Communications, 8(2), 940-950.
- [212] Bala, I., Bhamrah, M. S., & Singh, G. (2017, February). Capacity in fading environment based on soft sensing information under spectrum sharing constraints. Wireless Networks, 23(2), 519-531.
- [213] Hu, S., Yao, Y. D., & Yang, Z. (2014, February). MAC protocol identification using support vector machines for cognitive radio networks. IEEE Wireless Communications, 21(1), 52-60.

- [214] Xia, F., & Rahim, A. (2015, June). MAC protocols for cyber-physical systems. Springer, 1-89, ISBN: 978-3-662-46360-4.
- [215] Yadav, R., Varma, S., & Malaviya, N. (2009, August). A survey of MAC protocols for wireless sensor networks. *UbiCC Journal*, 4(3), 827-833.
- [216] Karn, P. (1990, September). MACA-a new channel access method for packet radio. In *ARRL/CRRL Amateur Radio 9th Computer Networking Conference*, (140), 134-140.
- [217] Talucci, F., & Gerla, M. (1997, October). MACA-BI (MACA by invitation). A wireless MAC protocol for high speed ad hoc networking. *6th International Conference on Universal Personal Communications*, (2), 913-917.
- [218] Costello, D. J., & Forney, G. D. (2007, June). Channel coding: The road to channel capacity. *Proceedings of the IEEE*, 95(6), 1150-1177.
- [219] Chatterjee, S., Banerjee, P., & Nasipuri, M. Enhancing localization accuracy of collaborative cognitive radio users by internal noise mitigation. *Telecommunication Systems*. (Under Review).
- [220] Li, F., Lam, K. Y., Sheng, Z., Zhang, X., Zhao, K., & Wang, L. (2018, September). Q-learning-based dynamic spectrum access in cognitive industrial Internet of Things. *Mobile Networks and Applications*, 23(6), 1636-1644.
- [221] Galzarano, S., Liotta, A., & Fortino, G. (2013, December). QL-MAC: A Q-learning based MAC for wireless sensor networks. In *International Conference on Algorithms and Architectures for Parallel Processing*, 267-275.
- [222] Qiao, M., Zhao, H., Huang, S., Zhou, L., & Wang, S. (2018, November). An intelligent MAC protocol selection method based on machine learning in wireless sensor networks. *KSII Transactions on Internet & Information Systems*, 12(11), 5425-5448.
- [223] Qiao, M., Zhao, H., Wang, S., & Wei, J. (2016, November). MAC protocol selection based on machine learning in cognitive radio networks. *19th International Symposium on Wireless Personal Multimedia Communications*, 453-458.
- [224] Jung, B. C., & Lee, W. (2018, April). Performance analysis of opportunistic CSMA schemes in cognitive radio networks. *Wireless Networks*, 24(3), 833-845.
- [225] Yu, Y., Wang, T., & Liew, S. C. (2019, May). Deep-reinforcement learning multiple access for heterogeneous wireless networks. *IEEE Journal on Selected Areas in Communications*, 37(6), 1277-1290.
- [226] Hawa, M., Darabkh, K. A., Al-Zubi, R., & Al-Sukkar, G. (2016, January). A self-learning MAC protocol for energy harvesting and spectrum access in cognitive radio sensor networks. *Journal of Sensors*, 2016, 1-18.



- 
- [227] Zheng, M., Du, M., Chen, L., Liang, W., & Yu, H. (2018, April). SPC-MAC: A short preamble cognitive MAC protocol for cognitive radio sensor networks. In *Wireless Communications and Networking Conference*, 1-6.
- [228] Oo, T. Z., Tran, N. H., Dang, D. N. M., Han, Z., Le, L. B., & Hong, C. S. (2016). OMF-MAC: an opportunistic matched filter-based MAC in cognitive radio networks. *IEEE transactions on vehicular technology*, 65(4), 2544-2559.



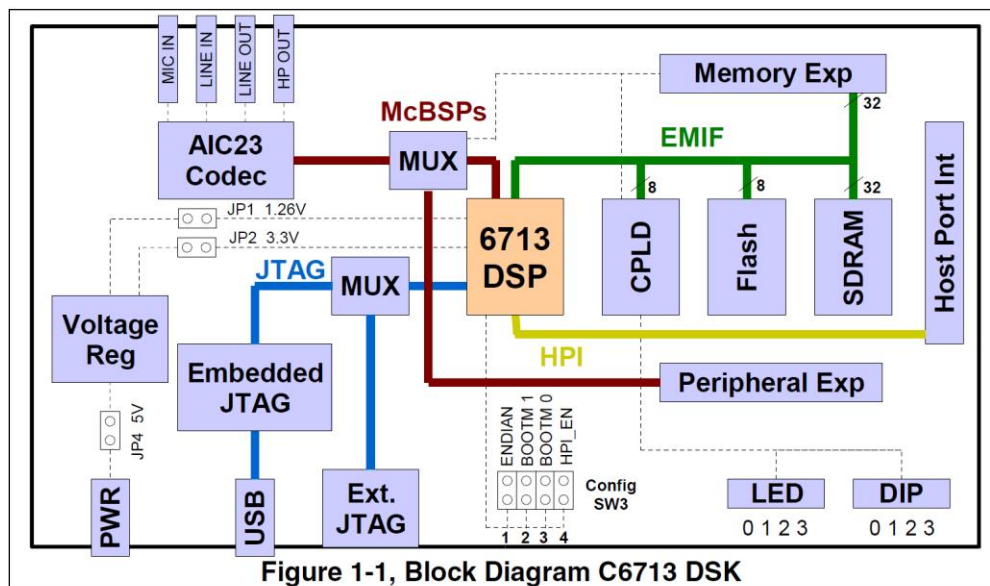
# APPENDIX



# TMS320C6713 DSK

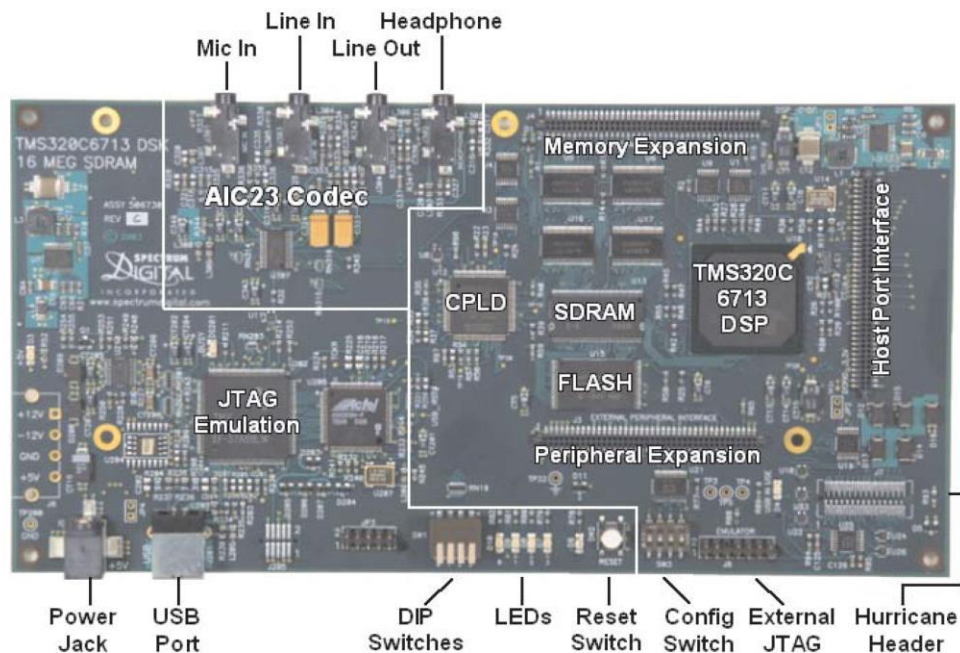
## Key Features

The C6713 DSK is a low-cost standalone development platform that enables users to evaluate and develop applications for the TI C67xx DSP family. The DSK also serves as a hardware reference design for the TMS320C6713 DSP. Schematics, logic equations and application notes are available to ease hardware development and reduce time to market.



The DSK comes with a full complement of on-board devices that suit a wide variety of application environments. Key features include:

- A Texas Instruments TMS320C6713 DSP operating at 225 MHz.
- An AIC23 stereo codec
- 16 Mbytes of synchronous DRAM
- 512 Kbytes of non-volatile Flash memory (256 Kbytes usable in default configuration)
- 4 user accessible LEDs and DIP switches
- Software board configuration through registers implemented in CPLD
- Configurable boot options
- Standard expansion connectors for daughter card use
- JTAG emulation through on-board JTAG emulator with USB host interface or external emulator
- Single voltage power supply (+5V)



### Functional Overview of the TMS320C6713 DSK

The DSP on the 6713 DSK interfaces to on-board peripherals through a 32-bit wide EMIF (External Memory InterFace). The SDRAM, Flash and CPLD are all connected to the bus. EMIF signals are also connected daughter card expansion connectors which are used for third party add-in boards.

The DSP interfaces to analog audio signals through an on-board AIC23 codec and four 3.5 mm audio jacks (microphone input, line input, line output, and headphone output). The codec can select the microphone or the line input as the active input. The analog output is driven to both the line out (fixed gain) and headphone (adjustable gain) connectors. McBSP0 is used to send commands to the codec control interface while McBSP1 is used for digital audio data. McBSP0 and McBSP1 can be re-routed to the expansion connectors in software.

A programmable logic device called a CPLD is used to implement glue logic that ties the board components together. The CPLD has a register based user interface that lets the user configure the board by reading and writing to its registers.

The DSK includes 4 LEDs and a 4 position DIP switch as a simple way to provide the user with interactive feedback. Both are accessed by reading and writing to the CPLD registers.

An included 5V external power supply is used to power the board. On-board switching voltage regulators provide the +1.26V DSP core voltage and +3.3V I/O supplies. The board is held in reset until these supplies are within operating specifications.

## 30MHz Arbitrary Waveform Signal Generator



### FEATURES

- 4.3" High Resolution TFT LCD Display
- Two Independent Channels Output, Same Characteristic
- 1 $\mu$ Hz Frequency Resolution for whole range
- 120 MSa/s Sampling Rate, 14 Bits Vertical Resolution
- 5 Standard Waveforms, 50 Built-in and 5 User-defined Arbitrary Waveforms
- FM, AM, PM, PWM, Sum, FSK, BPSK and SUM Modulation, Sweep and Burst Function
- Channel Coupling and Combine Features On CHB
- Build in 350MHz Frequency Counter
- Arbitrary Waveform Edit PC Software
- Standard Interface: USB Host, USB Device and RS-232

## Technical Specifications

<b>Frequency</b>		
Range	Sine	1 $\mu$ Hz ~ 30MHz.
	Square, Pulse	1 $\mu$ Hz ~ 10MHz.
	Others	1 $\mu$ Hz ~ 5MHz.
Resolution		1 $\mu$ Hz.
Accuracy		$\pm$ (50ppm+1 $\mu$ Hz).
<b>Waveform</b>		
Type	Standard	Sine, Square, Ramp, Pulse, Noise.
	Arbitrary	50 built-in waveforms + 5 user-defined waveforms
Sine	Harmonic Distortion	$\leq$ 60dBc (F<5MHz).
		$\leq$ 50dBc (F $\geq$ 5MHz).
	Total Distortion	$\leq$ 0.1% (20Hz ~ 20kHz, 20Vpp).
Square	Edge Time	$\leq$ 20ns.
Pulse	Overshoot	$\leq$ 10%.
	Duty Cycle	0.1% ~ 99.9%.
	Pulse Width	50ns ~ 2000s.
Ramp	Symmetry	0.0% ~ 100.0%.
Arbitrary	Length	4096 points.
	Sampling Rate	120 MSa/s.
	Vertical Resolution	14 bits (CHA); 10bits (CHB).
<b>Amplitude</b>		
Range		0.1mVpp ~ 10Vpp (50 $\Omega$ ), 0.2mVpp ~ 20Vpp (Open circuit).
Resolution		1mVpp (Amplitude $\geq$ 1Vpp), 0.1mVpp (Amplitude <1Vpp).
Accuracy		$\pm$ (1% of setting+1mVpp).
<b>DC Offset</b>		
Range		$\pm$ 5V DC (50 $\Omega$ ), $\pm$ 10V DC (High Z).
Accuracy		$\pm$ (1% of setting + 1mV DC).
<b>Modulation (CHA)</b>		
FM, AM, PM, PWM, SUM	Carrier Waveform	Sine, Square, Ramp, etc. (only Pulse for PWM).
	Modulating Waveform	Sine, Square, Ramp, etc.
	Modulating Frequency	1 $\mu$ Hz ~ 100kHz.
FSK, BPSK	Carrier Waveform	Sine, Square, Ramp, etc.
	Hope Frequency	1 $\mu$ Hz ~ 30MHz.
	Hope Rate	1 $\mu$ Hz ~ 100kHz.
<b>Sweep (CHA)</b>		
Carrier Waveforms		Sine, Square, Ramp, etc.
Sweep Mode		Linear or Logarithmic.
Sweep Time		5ms ~ 500s.
List Sweep		Length : 600, Stop Time : 5ms to 500s, Hold Time: 0 to 500s.
<b>Burst (CHA)</b>		
Burst Waveform		Sine, Square, Ramp, etc.
Burst Count		1 ~ 1000000.
<b>Frequency Counter</b>		
Frequency Range		0.01Hz ~ 350MHz, resolution : 6 digits/s.
Period, Pulse Width		100ns ~ 20s.
Duty Cycle		1% ~ 99%.
<b>General Characteristics</b>		
Power		AC 100 ~ 240V, 45 ~ 65Hz, <30VA.
Dimension		256 x 102 x 322 mm.
Weight		Approx. 3 Kg.
<b>Standard Accessories</b>		
Power Cord		1 No.
BNC Cable		1 No.
CD (Software+User's Guide)		1 No.



**Distortion and Level Meter****Features**

- ★ Distortion Measurement for Frequency Range 30Hz to 300KHz
- ★ Distortion Level 0.3% to 100% FSD
- ★ High Fundamental Rejection Capabilities
- ★ Low Residual Distortion
- ★ Minimum Input Level for Distortion Measurement, 300mV rms for 100% Set Level
- ★ Level Meter Range from 1mV to 300V rms Full Scale
- ★ Frequency Response upto 3MHz
- ★ O/P BNC Terminal for Monitoring Fundamental Freq. waveform & Distortion on Oscilloscope

**Description**

APLAB's Distortion & Level Meter Model 2007 are versatile instruments useful for testing audio & communication equipments.

Harmonic distortion is one of many types of distortions created in audio and communication equipments. Harmonic related frequencies caused by non linear elements in amplifiers, create a poor distorted signal to the listener. Aplab's Distortion & Level Meter Model 2007 help to measure the total of this distorted frequency components present in the signal, quickly and very easily in a frequency range of 30Hz to 300KHz. Thus it is used as an ideal test equipment in electronics labs & in production test setup. It can also be used as an AC voltmeter for general purpose voltage & gain measurements over a wide range of level & frequency.

The accuracy of distortion mode & very low measurements upto 0.3% are the features which make the instrument very useful in harmonic distortion measurement application.

## Specifications

### DISTORTION METER

Range	: From 0.3% to 100% full scale in six ranges of 0.3, 1, 3, 10, 30 & 100%.
Frequency Range	: 30Hz to 300KHz in eight ranges.
Input Level	: 300mV to 10V max.
Input Impedance	: Approx. 600 ohms or 10K ohms (HI) unbalanced.
Filter Characteristics (Second Harmonic Accuracy)	: Better than $\pm 0.6$ dB for fundamental freq. range of 30Hz to 300Hz. Better than $-0.8$ dB for fundamental freq. range of 300Hz to 3KHz. Better than $-1$ dB for fundamental freq. range of 3KHz to 30KHz. Better than $-2$ dB for fundamental freq. range of 30KHz to 100KHz. Better than $-3$ dB for fundamental freq. range of 100KHz to 300KHz.
Distortion Introduced	: $< 0.05\%$ .
Meter Indication	: Proportional to average value of the waveform.
Dial Calibration Accuracy	: Better than $\pm 3\%$ from 300Hz to 300KHz. Better than $\pm 5\%$ from 30Hz to 300Hz.

### LEVEL MEASUREMENT

Voltage Range	: From 1mV to 300V full scale in twelve ranges in 1-3-10 sequence.
dB Range	: $+50$ dBm to $-60$ dBm in 12 ranges of 10dB steps.
Accuracy of Indication	: Within $\pm 3\%$ of f.s.d. at 10KHz.
Frequency Range	: 20Hz to 3MHz.
Frequency Response	: <i>1mV to 30mV ranges</i> : $\pm 0.3$ dB from 30Hz to 1MHz. $\pm 0.5$ dB from 20Hz to 30Hz & 1MHz to 3MHz. <i>100mV to 3V ranges</i> : $\pm 0.5$ dB of f.s.d. from 30Hz to 500KHz $\pm 1$ dB of f.s.d. from 20Hz to 30Hz & 500KHz to 3MHz. <i>10V &amp; above ranges</i> : $\pm 0.5$ dB of f.s.d. from 20Hz to 100KHz
Meter Calibration	: The meter circuit is average reading type, calibrated in rms value for sinewave input. Two linear voltage scales provided are 0 to 3V and 0 to 10V. The dB scale is calibrated from $-20$ dB to $+2$ dB.
Input Impedance	: Approx. 10M ohms // 40pF nominal.
Residual Noise	: $< -80$ dB & $< 0.05$ mV
Output	: 130mV rms $\pm 10\%$ for full scale deflection at 10KHz.
Output Impedance	: Approx 2.2K ohms.

### GENERAL

Power	: 230V AC $\pm 10\%$ , 47-53Hz. Optional 115V AC $\pm 10\%$ , 57-63Hz.
Dimensions	: 420 (W) x 145 (H) x 235 (D) mm approx.
Weight	: 4.3 Kg. approx.
Standard Accessories	: Instruction Manual - 1 No. BNC(M) to BNC(M) Cable - 1 No. BNC(M) to Alligator Clip - 1 No. Mains Cord - 1 No.

## Low voltage high performance mixer FM IF system with high-speed RSSI

**SA636****DESCRIPTION**

The SA636 is a low-voltage high performance monolithic FM IF system with high-speed RSSI incorporating a mixer/oscillator, two limiting intermediate frequency amplifiers, quadrature detector, logarithmic received signal strength indicator (RSSI), voltage regulator, wideband data output and fast RSSI op amps. The SA636 is available in 20-lead SSOP (shrink small outline package).

The SA636 was designed for high bandwidth portable communication applications and will function down to 2.7 V. The RF section is similar to the famous SA605. The data output has a minimum bandwidth of 600 kHz. This is designed to demodulate wideband data. The RSSI output is amplified. The RSSI output has access to the feedback pin. This enables the designer to adjust the level of the outputs or add filtering.

SA636 incorporates a power-down mode which powers down the device when Pin 8 is LOW. Power down logic levels are CMOS and TTL compatible with high input impedance.

**FEATURES**

- Wideband data output (600 kHz min.)
- Fast RSSI rise and fall times
- Low power consumption: 6.5 mA typ. at 3 V
- Mixer input to >500 MHz
- Mixer conversion power gain of 11 dB at 240 MHz
- Mixer noise figure of 12 dB at 240 MHz
- XTAL oscillator effective to 150 MHz (L.C. oscillator to 1 GHz local oscillator can be injected)
- 92 dB of IF Amp/Limiter gain
- 25 MHz limiter small signal bandwidth
- Temperature compensated logarithmic Received Signal Strength Indicator (RSSI) with a dynamic range in excess of 90 dB
- RSSI output internal op amp
- Internal op amps with rail-to-rail outputs
- Low external component count; suitable for crystal/ceramic/LC filters
- Excellent sensitivity: 0.54  $\mu$ V into 50  $\Omega$  matching network for 12 dB SINAD (Signal to Noise and Distortion ratio) for 1 kHz tone with RF at 240 MHz and IF at 10.7 MHz
- ESD hardened
- 10.7 MHz filter matching (330  $\Omega$ )
- Power-down mode ( $I_{CC} = 200 \mu$ A)

**ORDERING INFORMATION**

DESCRIPTION	TEMPERATURE RANGE	ORDER CODE	DWG #
20-Pin Plastic Shrink Small Outline Package (Surface-mount)	-40 °C to +85 °C	SA636DK	SOT266-1

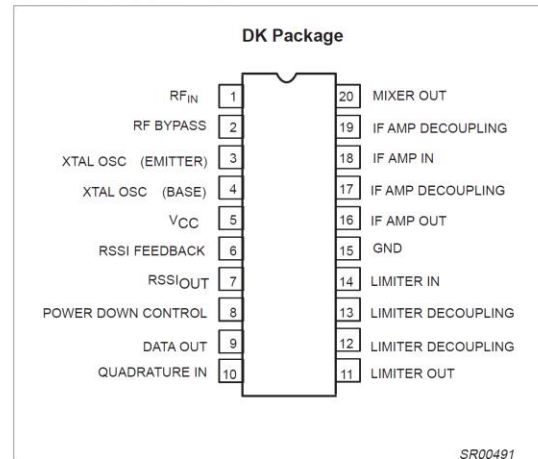
**PIN CONFIGURATION**

Figure 1. Pin configuration

**APPLICATIONS**

- DECT (Digital European Cordless Telephone)
- Digital cordless telephones
- Digital cellular telephones
- Portable high performance communications receivers
- Single conversion VHF/UHF receivers
- FSK and ASK data receivers
- Wireless LANs

Low voltage high performance mixer FM  
IF system with high-speed RSSI

SA636

**BLOCK DIAGRAM**

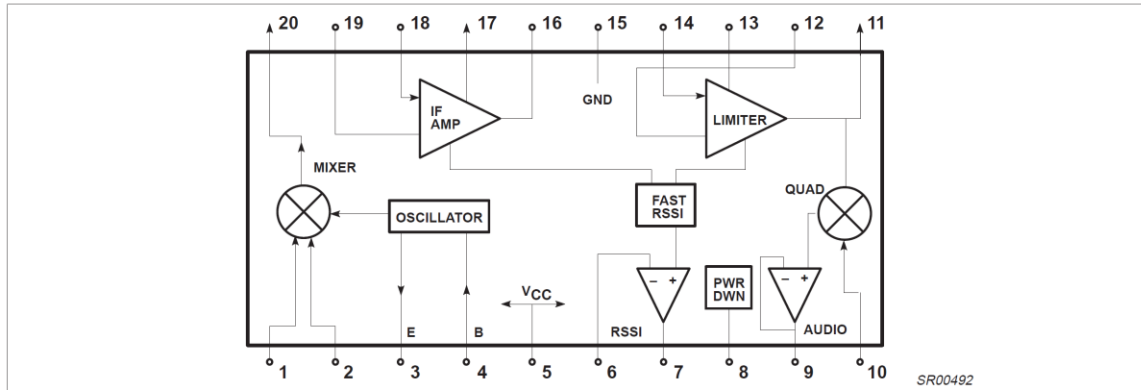


Figure 2. Block diagram

**ABSOLUTE MAXIMUM RATINGS**

SYMBOL	PARAMETER	RATING	UNITS
$V_{CC}$	Single supply voltage	0.3 to 7	V
$V_{IN}$	Voltage applied to any other pin	-0.3 to ( $V_{CC}+0.3$ )	V
$T_{stg}$	Storage temperature range	-65 to +150	°C
$T_{amb}$	Operating ambient temperature range SA636	-40 to +85	°C
$\theta_{JA}$	Thermal impedance (DC package)	117	°C/W

**DC ELECTRICAL CHARACTERISTICS**

$V_{CC} = +3\text{ V}$ ,  $T_{amb} = 25\text{ °C}$ ; unless otherwise stated.

SYMBOL	PARAMETER	TEST CONDITIONS	LIMITS			UNITS
			MIN	TYP	MAX	
$V_{CC}$	Power supply voltage range		2.7	3.0	5.5	V
$I_{CC}$	DC current drain	Pin 8 = HIGH	5.5	6.5	7.5	mA
	Input current	Pin 8 LOW	-10		10	μA
		Pin 8 HIGH	-10		10	μA
	Input level	Pin 8 LOW	0		$0.3V_{CC}$	V
		Pin 8 HIGH	$0.7V_{CC}$		$V_{CC}$	V
$I_{CC}$	Standby	Pin 8 = LOW		0.2	0.5	mA
$t_{ON}$	Power-up time	RSSI valid (10% to 90%)		10		μs
$t_{OFF}$	Power-down time	RSSI invalid (90% to 10%)		5		μs

## Low voltage high performance mixer FM IF system with high-speed RSSI

SA636

### AC ELECTRICAL CHARACTERISTICS

$T_{amb} = 25\text{ }^{\circ}\text{C}$ ;  $V_{CC} = +3\text{V}$ , unless otherwise stated. RF frequency = 240.05 MHz + 14.5 dBV RF input step-up; IF frequency = 10.7 MHz; RF level = -45 dBm; FM modulation = 1 kHz with  $\pm 125$  kHz peak deviation. Audio output with C-message weighted filter and de-emphasis capacitor. Test circuit Figure 1. The parameters listed below are tested using automatic test equipment to assure consistent electrical characteristics. The limits do not represent the ultimate performance limits of the device. Use of an optimized RF layout will improve many of the listed parameters.

SYMBOL	PARAMETER	TEST CONDITIONS	LIMITS			UNITS
			MIN	TYP	MAX	
<b>Mixer/Osc section (ext LO = 160mV<sub>RMS</sub>)</b>						
$f_{IN}$	Input signal frequency			500		MHz
$f_{OSC}$	External oscillator (buffer)			500		MHz
	Noise figure at 240 MHz			12		dB
	Third-order input intercept point	Matched $f_1=240.05$ MHz; $f_2=240.35$ MHz		-16		dBm
	Conversion power gain	Matched 14.5 dBV step-up	8	11	14	dB
	RF input resistance	Single-ended input		700		$\Omega$
	RF input capacitance			3.5		pF
	Mixer output resistance	(Pin 20)		330		$\Omega$
<b>IF section</b>						
	IF amp gain	330 $\Omega$ load		38		dB
	Limiter gain	330 $\Omega$ load		54		dB
	Input limiting -3dB	Test at Pin 18		-105		dBm
	AM rejection	80% AM 1 kHz		50		dB
	Data level	$R_{LOAD} = 100$ k $\Omega$	120	130		mV <sub>RMS</sub>
	3 dB data bandwidth		600	700		kHz
	SINAD sensitivity	RF level = -111 dBm		16		dB
THD	Total harmonic distortion			-43	-38	dB
S/N	Signal-to-noise ratio	No modulation for noise		60		dB
	IF RSSI output with buffer	IF level = -118 dBm		0.2	0.5	V
		IF level = -68 dBm	0.3	0.6	1.0	V
		IF level = -10 dBm	0.9	1.3	1.8	V
	IF RSSI output rise time (10kHz pulse, no 10.7MHz filter) (no RSSI bypass capacitor)	IF frequency = 10.7 MHz RF level = -56 dBm		1.2		$\mu\text{s}$
		RF level = -28 dBm		1.1		$\mu\text{s}$
	IF RSSI output fall time (10 kHz pulse, no 10.7 MHz filter) (no RSSI bypass capacitor)	IF frequency = 10.7 MHz RF level = -56 dBm		2.0		$\mu\text{s}$
		RF level = -28 dBm		7.3		$\mu\text{s}$
	RSSI range			90		dB
	RSSI accuracy			$\pm 1.5$		dB
	IF input impedance			330		$\Omega$
	IF output impedance			330		$\Omega$
	Limiter input impedance			330		$\Omega$
	Limiter output impedance			300		$\Omega$
	Limiter output level with no load			130		mV <sub>RMS</sub>
<b>RF/IF section (int LO)</b>						
	System RSSI output	RF level = -10 dBm		1.4		V
	System SINAD	RF level = -106 dBm		12		dB

**CA3160**

4MHz, BiMOS Operational Amplifier with MOSFET Input/CMOS Output

FN976  
Rev 5.00  
June 2004

The CA3160 is an operational amplifier that combines the advantages of both CMOS and bipolar transistors on a monolithic chip. The CA3160 series are frequency compensated versions of the popular CA3130 series.

Gate protected P-Channel MOSFET (PMOS) transistors are used in the input circuit to provide very high input impedance, very low input current, and exceptional speed performance. The use of PMOS field effect transistors in the input stage results in common-mode input voltage capability down to 0.5V below the negative supply terminal, an important attribute in single supply applications.

A complementary symmetry MOS (CMOS) transistor-pair, capable of swinging the output voltage to within 10mV of either supply voltage terminal (at very high values of load impedance), is employed as the output circuit.

The CA3160 Series circuits operate at supply voltages ranging from 5V to 16V, or  $\pm 2.5V$  to  $\pm 8V$  when using split supplies, and have terminals for adjustment of offset voltage for applications requiring offset null capability. Terminal provisions are also made to permit strobing of the output stage.

**Ordering Information**

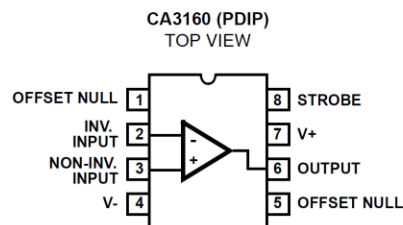
PART NUMBER	TEMP. RANGE (°C)	PACKAGE	PKG. NO.
CA3160E	-55 to 125	8 Ld PDIP	E8.3

**Features**

- MOSFET Input Stage Provides:
  - Very High  $Z_i$  . . . . .  $1.5T\Omega$  ( $1.5 \times 10^{12}\Omega$ ) (Typ)
  - Very Low  $I_i$  . . . . . 5pA (Typ) at 15V Operation
  - . . . . . 2pA (Typ) at 5V Operation
- Common-Mode Input Voltage Range Includes Negative Supply Rail; Input Terminals Can Be Swung 0.5V Below Negative Supply Rail
- CMOS Output Stage Permits Signal Swing to Either (or Both) Supply Rails

**Applications**

- Ground Referenced Single Supply Amplifiers
- Fast Sample Hold Amplifiers
- Long Duration Timers/Monostables
- High Input Impedance Wideband Amplifiers
- Voltage Followers (e.g., Follower for Single Supply D/A Converter)
- Wien-Bridge Oscillators
- Voltage Controlled Oscillators
- Photo Diode Sensor Amplifiers

**Pinout**

NOTE: CA3160 Series devices have an on-chip frequency compensation network. Supplementary phase compensation or frequency roll-off (if desired) can be connected externally between Terminals 1 and 8.

## CA3160

## Absolute Maximum Ratings

Supply Voltage (Between V+ and V- Terminals)	+16V
Differential Mode Input Voltage	.8V
Input Voltage	(V+ +8V) to (V- -0.5V)
Input Current	1mA
Output Short Circuit Duration (Note 2)	Indefinite

## Thermal Information

Thermal Resistance (Typical, Note 1)	$\theta_{JA}$ (°C/W)	$\theta_{JC}$ (°C/W)
PDIP Package	115	N/A
Maximum Junction Temperature (Plastic Package)	150°C	
Maximum Storage Temperature Range	-65°C to 150°C	
Maximum Lead Temperature (Soldering 10s)	300°C	

## Operating Conditions

Temperature Range	-55°C to 125°C
-------------------	----------------

**CAUTION:** Stresses above those listed in "Absolute Maximum Ratings" may cause permanent damage to the device. This is a stress only rating and operation of the device at these or any other conditions above those indicated in the operational sections of this specification is not implied.

## NOTES:

- $\theta_{JA}$  is measured with the component mounted on an evaluation PC board in free air.
- Short Circuit may be applied to ground or to either supply.

Electrical Specifications  $T_A = 25^\circ\text{C}$ ,  $V_+ = 15\text{V}$ ,  $V_- = 0\text{V}$ , Unless Otherwise Specified

PARAMETER	SYMBOL	TEST CONDITIONS	CA3160			UNITS
			MIN	TYP	MAX	
Input Offset Voltage	$ V_{IO} $	$V_S = \pm 7.5\text{V}$	-	6	15	mV
Input Offset Current	$ I_{IO} $	$V_S = \pm 7.5\text{V}$	-	0.5	30	pA
Input Current	$I_I$	$V_S = \pm 7.5\text{V}$	-	5	50	pA
Large-Signal Voltage Gain	$A_{OL}$	$V_O = 10V_{P,P}$ , $R_L = 2k\Omega$	50	320	-	kV/V
			94	110	-	dB
Common-Mode Rejection Ratio	CMRR		70	90	-	dB
Common-Mode Input-Voltage Range	$V_{ICR}$		0	-0.5 to 12	10	V
Power-Supply Rejection Ratio	PSRR	$\Delta V_{IO}/\Delta V_S$ , $V_S = \pm 7.5\text{V}$	-	32	320	$\mu\text{V/V}$
Maximum Output Voltage	$V_{OM+}$	$R_L = 2k\Omega$	12	13.3	-	V
	$V_{OM-}$		-	0.002	0.01	V
	$V_{OM+}$	$R_L = \infty$	14.99	15	-	V
	$V_{OM-}$		-	0	0.01	V
Maximum Output Current	$I_{OM+}$	$V_O = 0\text{V}$ (Source)	12	22	45	mA
	$I_{OM-}$	$V_O = 15\text{V}$ (Sink)	12	20	45	mA
Supply Current (Note 3)	$I_+$	$V_O = 7.5\text{V}$ , $R_L = \infty$	-	10	15	mA
		$V_O = 0\text{V}$ , $R_L = \infty$	-	2	3	mA
Input Offset Voltage Temperature Drift		$\Delta V_{IO}/\Delta T$	-	8	-	$\mu\text{V}/^\circ\text{C}$

Electrical Specifications For Design Guidance,  $V_{SUPPLY} = \pm 7.5\text{V}$ ,  $T_A = 25^\circ\text{C}$ , Unless Otherwise Specified

PARAMETER	SYMBOL	TEST CONDITIONS		TYP	UNITS
Input Offset Voltage Adjustment Range		10k $\Omega$ Across Terminals 4 and 5 or Terminals 4 and 1		$\pm 22$	mV
Input Resistance	$R_I$			1.5	T $\Omega$
Input Capacitance	$C_I$	$f = 1\text{MHz}$		4.3	pF
Equivalent Input Noise Voltage	$e_N$	BW = 0.2MHz	$R_S = 1M\Omega$	40	$\mu\text{V}$
			$R_S = 10M\Omega$	50	$\mu\text{V}$
Equivalent Input Noise Voltage	$e_N$	$R_S = 100\Omega$	1kHz	72	$\text{nV}/\sqrt{\text{Hz}}$
			10kHz	30	$\text{nV}/\sqrt{\text{Hz}}$
Unity Gain Crossover Frequency	$f_T$			4	MHz
Slew Rate	SR			10	V/ $\mu\text{s}$

## NBC12429, NBC12429A

### 3.3V/5V Programmable PLL Synthesized Clock Generator

25 MHz to 400 MHz

#### Description

The NBC12429 and NBC12429A are general purpose, Phase-Lock-Loop (PLL) based synthesized clock sources. The VCO will operate over a frequency range of 200 MHz to 400 MHz. The VCO frequency is sent to the N-output divider, where it can be configured to provide division ratios of 1, 2, 4, or 8. The VCO and output frequency can be programmed using the parallel or serial interfaces to the configuration logic. Output frequency steps of 125 kHz, 250 kHz, 500 kHz, or 1.0 MHz can be achieved using a 16 MHz crystal, depending on the output dividers. The PLL loop filter is fully integrated and does not require any external components.

#### Features

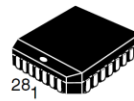
- Best-in-Class Output Jitter Performance,  $\pm 20$  ps Peak-to-Peak
- 25 MHz to 400 MHz Programmable Differential PECL Outputs
- Fully Integrated Phase-Lock-Loop with Internal Loop Filter
- Parallel Interface for Programming Counter and Output Dividers During Powerup
- Minimal Frequency Overshoot
- Serial 3-Wire Programming Interface
- Crystal Oscillator Interface
- Operating Range:  $V_{CC} = 3.135$  V to 5.25 V
- CMOS and TTL Compatible Control Inputs
- Pin and Function Compatible with Motorola MC12429 and MPC9229
- 0°C to 70°C Ambient Operating Temperature (NBC12429)
- -40°C to 85°C Ambient Operating Temperature (NBC12429A)
- Pb-Free Packages are Available



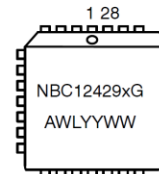
ON Semiconductor®

<http://onsemi.com>

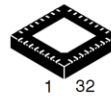
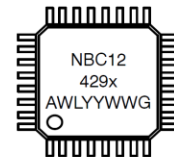
#### MARKING DIAGRAMS



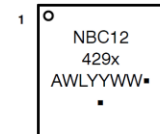
PLCC-28  
FN SUFFIX  
CASE 776



LQFP-32  
FA SUFFIX  
CASE 873A



QFN32  
MN SUFFIX  
CASE 488AM



x = Blank or A  
 A = Assembly Location  
 WL, L = Wafer Lot  
 YY, Y = Year  
 WW, W = Work Week  
 G or ■ = Pb-Free Package  
 (Note: Microdot may be in either location)

#### ORDERING INFORMATION

See detailed ordering and shipping information in the package dimensions section on page 18 of this data sheet.



**NBC12429, NBC12429A**

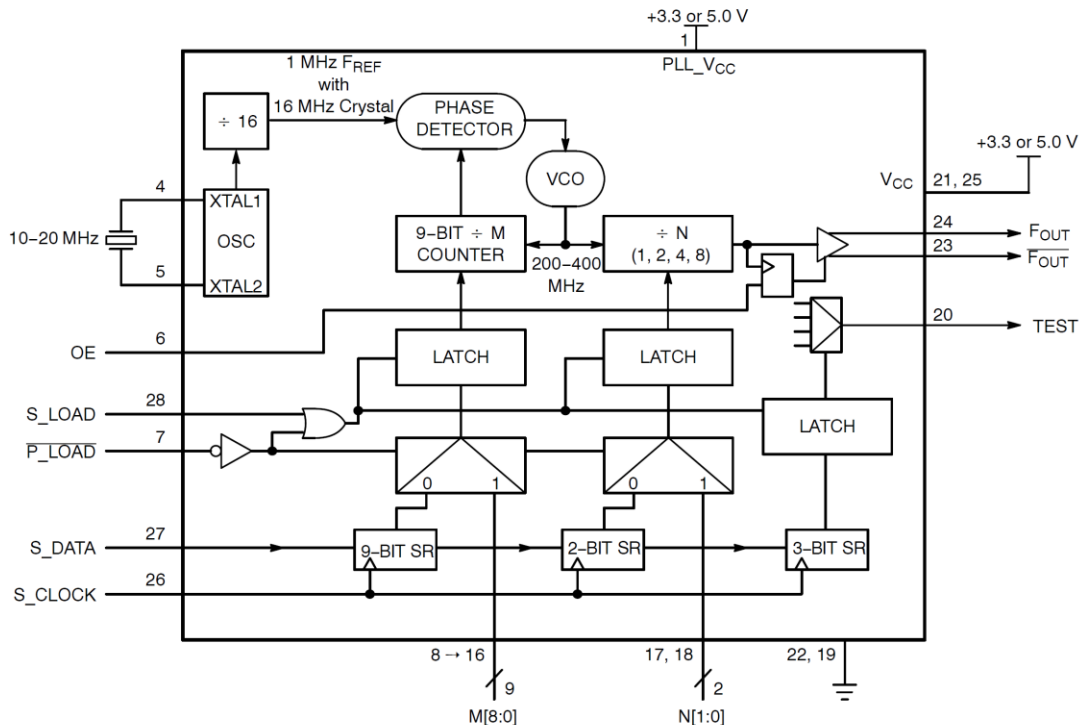


**Figure 1. Block Diagram (PLCC-28)**

**NBC12429, NBC12429A**

The following gives a brief description of the functionality of the NBC12429 and NBC12429A Inputs and Outputs. Unless explicitly stated, all inputs are CMOS/TTL compatible with either pullup or pulldown resistors. The PECL outputs are capable of driving two series terminated 50 Ω transmission lines on the incident edge.

**Table 3. PIN FUNCTION DESCRIPTION**

Pin Name	Function	Description
<b>INPUTS</b>		
XTAL1, XTAL2	Crystal Inputs	These pins form an oscillator when connected to an external series-resonant crystal.
S_LOAD*	CMOS/TTL Serial Latch Input (Internal Pulldown Resistor)	This pin loads the configuration latches with the contents of the shift registers. The latches will be transparent when this signal is HIGH; thus, the data must be stable on the HIGH-to-LOW transition of S_LOAD for proper operation.
S_DATA*	CMOS/TTL Serial Data Input (Internal Pulldown Resistor)	This pin acts as the data input to the serial configuration shift registers.
S_CLOCK*	CMOS/TTL Serial Clock Input (Internal Pulldown Resistor)	This pin serves to clock the serial configuration shift registers. Data from S_DATA is sampled on the rising edge.
P_LOAD**	CMOS/TTL Parallel Latch Input (Internal Pullup Resistor)	This pin loads the configuration latches with the contents of the parallel inputs. The latches will be transparent when this signal is LOW; therefore, the parallel data must be stable on the LOW-to-HIGH transition of P_LOAD for proper operation.
M[8:0]**	CMOS/TTL PLL Loop Divider Inputs (Internal Pullup Resistor)	These pins are used to configure the PLL loop divider. They are sampled on the LOW-to-HIGH transition of P_LOAD. M[8] is the MSB, M[0] is the LSB.
N[1:0]**	CMOS/TTL Output Divider Inputs (Internal Pullup Resistor)	These pins are used to configure the output divider modulus. They are sampled on the LOW-to-HIGH transition of P_LOAD.
OE**	CMOS/TTL Output Enable Input (Internal Pullup Resistor)	Active HIGH Output Enable. The Enable is synchronous to eliminate possibility of runt pulse generation on the F <sub>OUT</sub> output.

**OUTPUTS**

$F_{OUT}$ , $\overline{F_{OUT}}$	PECL Differential Outputs	These differential, positive-referenced ECL signals (PECL) are the outputs of the synthesizer.
TEST	CMOS/TTL Output	The function of this output is determined by the serial configuration bits T[2:0].

**POWER**

$V_{CC}$	Positive Supply for the Logic	The positive supply for the internal logic and output buffer of the chip, and is connected to +3.3 V or +5.0 V.
PLL_ $V_{CC}$	Positive Supply for the PLL	This is the positive supply for the PLL and is connected to +3.3 V or +5.0 V.
GND	Negative Power Supply	These pins are the negative supply for the chip and are normally all connected to ground.
-	Exposed Pad for QFN-32 only	The Exposed Pad (EP) on the QFN-32 package bottom is thermally connected to the die for improved heat transfer out of package. The exposed pad must be attached to a heat-sinking conduit. The pad is electrically connected to GND.

\* When left Open, these inputs will default LOW.

\*\* When left Open, these inputs will default HIGH.

**FUNCTIONAL DESCRIPTION**

The internal oscillator uses the external quartz crystal as the basis of its frequency reference. The output of the reference oscillator is divided by 16 before being sent to the phase detector. With a 16 MHz crystal, this provides a reference frequency of 1 MHz. Although this data sheet illustrates functionality only for a 16 MHz crystal, Table 9, any crystal in the 10 MHz – 20 MHz range can be used, Table 11.

The VCO within the PLL operates over a range of 200 to 400 MHz. Its output is scaled by a divider that is configured by either the serial or parallel interfaces. The output of this loop divider is also applied to the phase detector.

The phase detector and the loop filter force the VCO output frequency to be M times the reference frequency by adjusting the VCO control voltage. Note that for some values of M (either too high or too low), the PLL will not achieve loop lock.

The output of the VCO is also passed through an output divider before being sent to the PECL output driver. This output divider (N divider) is configured through either the serial or the parallel interfaces and can provide one of four division ratios (1, 2, 4, or 8). This divider extends the performance of the part while providing a 50% duty cycle.

The output driver is driven differentially from the output divider and is capable of driving a pair of transmission lines terminated into 50  $\Omega$  to  $V_{CC} - 2.0$  V. The positive reference

for the output driver and the internal logic is separated from the power supply for the PLL to minimize noise induced jitter.

The configuration logic has two sections: serial and parallel. The parallel interface uses the values at the M[8:0] and N[1:0] inputs to configure the internal counters. Normally upon system reset, the  $\overline{P\_LOAD}$  input is held LOW until sometime after power becomes valid. On the LOW-to-HIGH transition of  $\overline{P\_LOAD}$ , the parallel inputs are captured. The parallel interface has priority over the serial interface. Internal pullup resistors are provided on the M[8:0] and N[1:0] inputs to reduce component count in the application of the chip.

The serial interface logic is implemented with a fourteen bit shift register scheme. The register shifts once per rising edge of the S\_CLOCK input. The serial input S\_DATA must meet setup and hold timing as specified in the AC Characteristics section of this document. With P\_LOAD held high, the configuration latches will capture the value of the shift register on the HIGH-to-LOW edge of the S\_LOAD input. See the programming section for more information.

The TEST output reflects various internal node values and is controlled by the T[2:0] bits in the serial data stream. See the programming section for more information.

**NBC12429, NBC12429A****Table 9. PROGRAMMING VCO FREQUENCY FUNCTION TABLE WITH 16 MHZ CRYSTAL**

VCO Frequency (MHz)	M <sub>Count</sub> Divisor	256	128	64	32	16	8	4	2	1
		M8	M7	M6	M5	M4	M3	M2	M1	M0
200	200	0	1	1	0	0	1	0	0	0
201	201	0	1	1	0	0	1	0	0	1
202	202	0	1	1	0	0	1	0	1	0
203	203	0	1	1	0	0	1	0	1	1
•	•	•	•	•	•	•	•	•	•	•
•	•	•	•	•	•	•	•	•	•	•
•	•	•	•	•	•	•	•	•	•	•
397	397	1	1	0	0	0	1	1	0	1
398	398	1	1	0	0	0	1	1	1	0
399	399	1	1	0	0	0	1	1	1	1
400	400	1	1	0	0	1	0	0	0	0

**PROGRAMMING INTERFACE**

Programming the NBC12429 and NBC12429A is accomplished by properly configuring the internal dividers to produce the desired frequency at the outputs. The output frequency can be represented by this formula:

$$F_{OUT} = (F_{XTAL} \div 16) \times M \div N \quad (\text{eq. 1})$$

where  $F_{XTAL}$  is the crystal frequency, M is the loop divider modulus, and N is the output divider modulus. Note that it is possible to select values of M such that the PLL is unable to achieve loop lock. To avoid this, always make sure that M is selected to be  $200 \leq M \leq 400$  for a 16 MHz input reference.

Assuming that a 16 MHz reference frequency is used the above equation reduces to:

$$F_{OUT} = M \div N \quad (\text{eq. 2})$$

Substituting the four values for N (1, 2, 4, 8) yields:

**Table 10. Programmable Output Divider Function**

N1	N0	N Divider	F <sub>OUT</sub>	Output Frequency Range (MHz)*	F <sub>OUT</sub> Step
0	0	÷ 1	M	200–400	1 MHz
0	1	÷ 2	M ÷ 2	100–200	500 kHz
1	0	÷ 4	M ÷ 4	50–100	250 kHz
1	1	÷ 8	M ÷ 8	25–50	125 kHz

\*For crystal frequency of 16 MHz.

The user can identify the proper M and N values for the desired frequency from the above equations. The four output frequency ranges established by N are 200 MHz – 400 MHz, 100 MHz – 200 MHz, 50 MHz – 100 MHz and 25 MHz – 50 MHz, respectively. From these ranges, the user will establish the value of N required. The value of M can then be calculated based on Equation 1. For example, if an output frequency of

131 MHz was desired, the following steps would be taken to identify the appropriate M and N values. 131 MHz falls within the frequency range set by an N value of 2; thus, N [1:0] = 01. For N = 2,  $F_{OUT} = M \div 2$  and  $M = 2 \times F_{OUT}$ . Therefore,

$$M = 131 \times 2 = 262, \text{ so } M[8:0] = 10000110.$$

Following this same procedure, a user can generate any whole frequency desired between 25 and 400 MHz. Note that for  $N > 2$ , fractional values of  $F_{OUT}$  can be realized. The size of the programmable frequency steps (and thus, the indicator of the fractional output frequencies achievable) will be equal to  $F_{XTAL} \div 16 \div N$ .

For input reference frequencies other than 16 MHz, see Table 11, which shows the usable VCO frequency and M divider range.

The input frequency and the selection of the feedback divider M is limited by the VCO frequency range and  $F_{XTAL}$ . M must be configured to match the VCO frequency range of 200 MHz to 400 MHz in order to achieve stable PLL operation.

$$M_{\min} = f_{VCO\min} \div (f_{XTAL} \div 16) \text{ and} \quad (\text{eq. 3})$$

$$M_{\max} = f_{VCO\max} \div (f_{XTAL} \div 16) \quad (\text{eq. 4})$$

The value for M falls within the constraints set for PLL stability. If the value for M fell outside of the valid range, a different N value would be selected to move M in the appropriate direction.

The M and N counters can be loaded either through a parallel or serial interface. The parallel interface is controlled via the  $\overline{P\_LOAD}$  signal such that a LOW to HIGH transition will latch the information present on the M[8:0] and N[1:0] inputs into the M and N counters. When the  $\overline{P\_LOAD}$  signal is LOW, the input latches will be transparent and any changes on the M[8:0] and N[1:0] inputs will affect the  $F_{OUT}$  output pair. To use the serial port, the

S\_CLOCK signal samples the information on the S\_DATA line and loads it into a 14 bit shift register. Note that the P\_LOAD signal must be HIGH for the serial load operation to function. The Test register is loaded with the first three bits, the N register with the next two, and the M register with the final nine bits of the data stream on the S\_DATA input. For each register, the most significant bit is loaded first (T2, N1, and M8). A pulse on the S\_LOAD pin after the shift register is fully loaded will transfer the divide values into the counters. The HIGH to LOW transition on the S\_LOAD input will latch the new divide values into the counters. Figures 5 and 6 illustrate the timing diagram for both a parallel and a serial load of the device synthesizer.

M[8:0] and N[1:0] are normally specified once at powerup through the parallel interface, and then possibly

again through the serial interface. This approach allows the application to come up at one frequency and then change or fine-tune the clock as the ability to control the serial interface becomes available.

The TEST output provides visibility for one of the several internal nodes as determined by the T[2:0] bits in the serial configuration stream. It is not configurable through the parallel interface. The T2, T1, and T0 control bits are preset to '000' when P\_LOAD is LOW so that the PECL F<sub>OUT</sub> outputs are as jitter-free as possible. Any active signal on the TEST output pin will have detrimental affects on the jitter of the PECL output pair. In normal operations, jitter specifications are only guaranteed if the TEST output is static. The serial configuration port can be used to select one of the alternate functions for this pin.



**ADC0803, ADC0804**

Data Sheet

August 2002

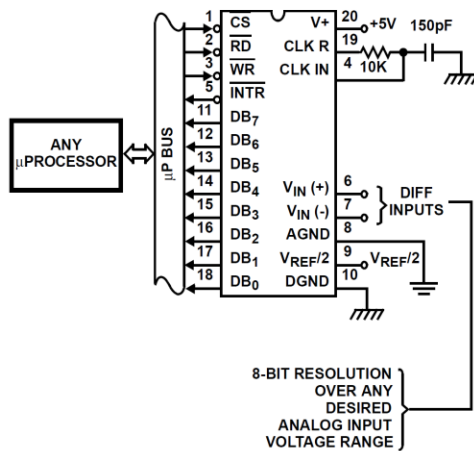
FN3094.4

**8-Bit, Microprocessor-Compatible, A/D Converters**

The ADC080X family are CMOS 8-Bit, successive-approximation A/D converters which use a modified potentiometric ladder and are designed to operate with the 8080A control bus via three-state outputs. These converters appear to the processor as memory locations or I/O ports, and hence no interfacing logic is required.

The differential analog voltage input has good common-mode-rejection and permits offsetting the analog zero-input-voltage value. In addition, the voltage reference input can be adjusted to allow encoding any smaller analog voltage span to the full 8 bits of resolution.

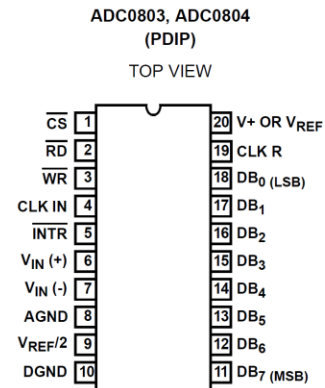
**Typical Application Schematic**



**Features**

- 80C48 and 80C80/85 Bus Compatible - No Interfacing Logic Required
- Conversion Time ..... <100μs
- Easy Interface to Most Microprocessors
- Will Operate in a "Stand Alone" Mode
- Differential Analog Voltage Inputs
- Works with Bandgap Voltage References
- TTL Compatible Inputs and Outputs
- On-Chip Clock Generator
- Analog Voltage Input Range (Single + 5V Supply) ..... 0V to 5V
- No Zero-Adjust Required
- 80C48 and 80C80/85 Bus Compatible - No Interfacing Logic Required

**Pinout**



**Ordering Information**

PART NUMBER	ERROR	EXTERNAL CONDITIONS	TEMP. RANGE (°C)	PACKAGE	PKG. NO
ADC0803LCN	±1/2 LSB	V <sub>REF/2</sub> Adjusted for Correct Full Scale Reading	0 to 70	20 Ld PDIP	E20.3
ADC0804LCN	±1 LSB	V <sub>REF/2</sub> = 2.500V <sub>DC</sub> (No Adjustments)	0 to 70	20 Ld PDIP	E20.3

## ADC0803, ADC0804

## Absolute Maximum Ratings

Supply Voltage	6.5V
Voltage at Any Input	-0.3V to (V <sup>+</sup> + 0.3V)

## Operating Conditions

Temperature Range	0°C to 70°C
-------------------	-------------

## Thermal Information

Thermal Resistance (Typical, Note 1)	$\theta_{JA}$ (°C/W)
PDIP Package	80
Maximum Junction Temperature	
Plastic Package	150°C
Maximum Storage Temperature Range	-65°C to 150°C
Maximum Lead Temperature (Soldering, 10s)	300°C

CAUTION: Stresses above those listed in "Absolute Maximum Ratings" may cause permanent damage to the device. This is a stress only rating and operation of the device at these or any other conditions above those indicated in the operational sections of this specification is not implied.

## NOTE:

- $\theta_{JA}$  is measured with the component mounted on a low effective thermal conductivity test board in free air. See Tech Brief TB379 for details.

## Electrical Specifications (Notes 2, 8)

PARAMETER	TEST CONDITIONS	MIN	TYP	MAX	UNITS
<b>CONVERTER SPECIFICATIONS</b> V <sup>+</sup> = 5V, T <sub>A</sub> = 25°C and f <sub>CLK</sub> = 640kHz, Unless Otherwise Specified					
Total Unadjusted Error					
ADC0803	V <sub>REF/2</sub> Adjusted for Correct Full Scale Reading	-	-	±1/2	LSB
ADC0804	V <sub>REF/2</sub> = 2.500V	-	-	±1	LSB
V <sub>REF/2</sub> Input Resistance	Input Resistance at Pin 9	1.0	1.3	-	kΩ
Analog Input Voltage Range	(Note 3)	GND-0.05	-	(V <sup>+</sup> ) + 0.05	V
DC Common-Mode Rejection	Over Analog Input Voltage Range	-	±1/16	±1/8	LSB
Power Supply Sensitivity	V <sup>+</sup> = 5V ±10% Over Allowed Input Voltage Range	-	±1/16	±1/8	LSB
<b>CONVERTER SPECIFICATIONS</b> V <sup>+</sup> = 5V, 0°C to 70°C and f <sub>CLK</sub> = 640kHz, Unless Otherwise Specified					
Total Unadjusted Error					
ADC0803	V <sub>REF/2</sub> Adjusted for Correct Full Scale Reading	-	-	±1/2	LSB
ADC0804	V <sub>REF/2</sub> = 2.500V	-	-	±1	LSB
V <sub>REF/2</sub> Input Resistance	Input Resistance at Pin 9	1.0	1.3	-	kΩ
Analog Input Voltage Range	(Note 3)	GND-0.05	-	(V <sup>+</sup> ) + 0.05	V
DC Common-Mode Rejection	Over Analog Input Voltage Range	-	±1/8	±1/4	LSB
Power Supply Sensitivity	V <sup>+</sup> = 5V ±10% Over Allowed Input Voltage Range	-	±1/16	±1/8	LSB
<b>AC TIMING SPECIFICATIONS</b> V <sup>+</sup> = 5V, and T <sub>A</sub> = 25°C, Unless Otherwise Specified					
Clock Frequency, f <sub>CLK</sub>	V <sup>+</sup> = 6V (Note 4)	100	640	1280	kHz
	V <sup>+</sup> = 5V	100	640	800	kHz
Clock Periods per Conversion (Note 5), t <sub>CONV</sub>		62	-	73	Clocks/Conv
Conversion Rate In Free-Running Mode, CR	$\overline{INTR}$ tied to $\overline{WR}$ with $\overline{CS} = 0V$ , f <sub>CLK</sub> = 640kHz	-	-	8888	Conv/s
Width of $\overline{WR}$ Input (Start Pulse Width), t <sub>W(WR)</sub>	$\overline{CS} = 0V$ (Note 6)	100	-	-	ns
Access Time (Delay from Falling Edge of $\overline{RD}$ to Output Data Valid), t <sub>ACC</sub>	C <sub>L</sub> = 100pF (Use Bus Driver IC for Larger C <sub>L</sub> )	-	135	200	ns
Three-State Control (Delay from Rising Edge of $\overline{RD}$ to HI-Z State), t <sub>1H</sub> , t <sub>0H</sub>	C <sub>L</sub> = 10pF, R <sub>L</sub> = 10K (See Three-State Test Circuits)	-	125	250	ns
Delay from Falling Edge of $\overline{WR}$ to Reset of $\overline{INTR}$ , t <sub>WJ</sub> , t <sub>RI</sub>		-	300	450	ns
Input Capacitance of Logic Control Inputs, C <sub>IN</sub>		-	5	-	pF
Three-State Output Capacitance (Data Buffers), C <sub>OUT</sub>		-	5	-	pF



**UC1910**  
**UC2910**  
**UC3910**

## 4-Bit DAC and Voltage Monitor

### FEATURES

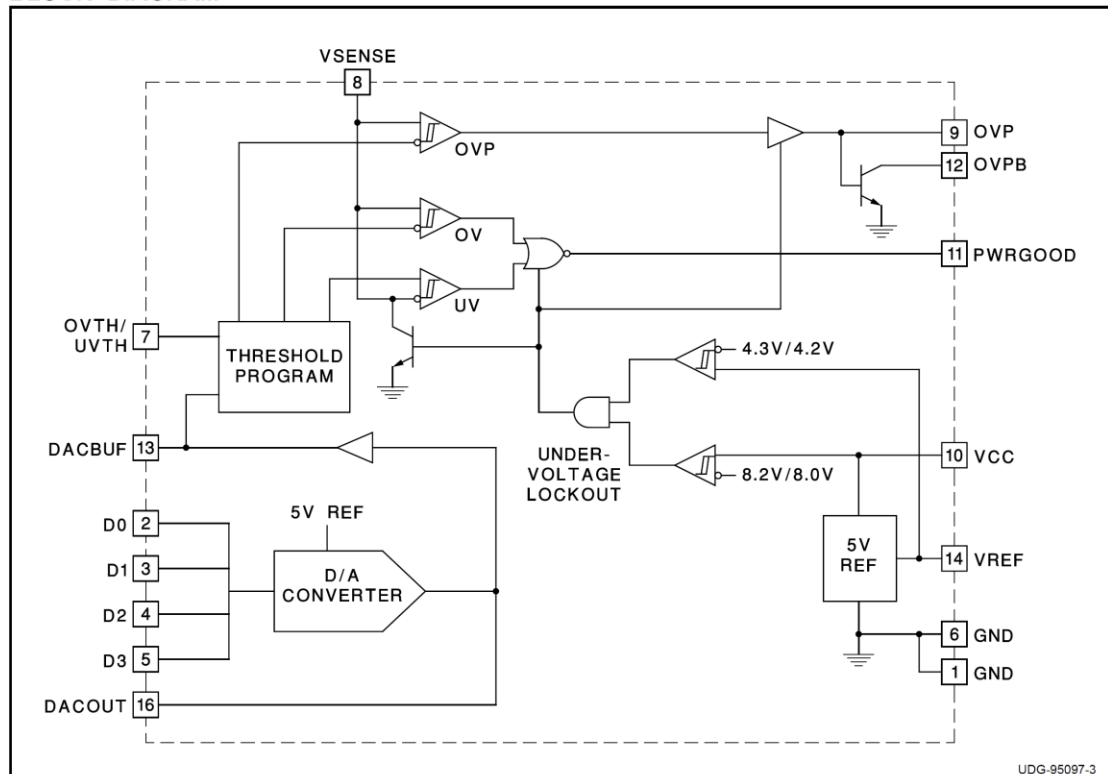
- Precision 5V Reference
- 4-Bit Digital-to-Analog (DAC) Converter
- 0.5% DAC/Reference Combined Error
- Programmable Undervoltage and Overvoltage Fault Windows
- Overvoltage Comparator with Complementary SCR Driver and Open Collector Outputs
- Undervoltage Lockout

### DESCRIPTION

The UC3910 is a complete precision reference and voltage monitor circuit for Intel Pentium® Pro and other high-end microprocessor power supplies. It is designed for use in conjunction with the UC3886 PWM. The UC3910 together with the UC3886 converts 5VDC to an adjustable output ranging from 2.0VDC to 3.5VDC in 100mV steps with 1% DC system accuracy.

The UC3910 utilizes thin film resistors to ensure high accuracy and stability of its precision circuits. The chip includes a precision 5V voltage reference which is capable of sourcing 10mA to external circuitry. The output voltage of the DAC is derived from this reference, and the accuracy of the DAC/reference combination is 0.5%. Programmable window comparators monitor the supply voltage to indicate that it is within acceptable limits. The window is programmed as a percentage centered around the DAC output. An overvoltage protection comparator is set at a percentage 2 times larger than the programmed lower overvoltage level and drives an external SCR as well as provides an open collector output. Undervoltage lockout protection assures the correct logic states at the outputs during power-up and power-down.

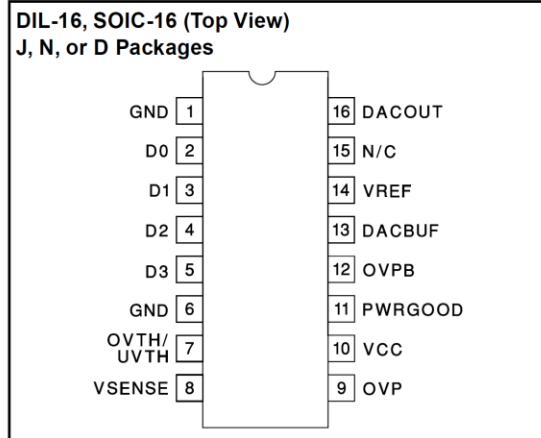
### BLOCK DIAGRAM



3/97

UC1910  
UC2910  
UC3910

### CONNECTION DIAGRAM



**ELECTRICAL CHARACTERISTICS** Unless otherwise specified, VCC = 12V, VSENSE = 3.5V,  $V_{OVTH/UVTH} = 1.26V$ ,  $V_{D0} = V_{D1} = V_{D2} = V_{D3} = 0V$ ,  $0^{\circ}C < T_A < 70^{\circ}C$  for the UC3910,  $-25^{\circ}C < T_A < 80^{\circ}C$  for the UC2910,  $-55^{\circ}C < T_A < 125^{\circ}C$  for the UC1910  $T_A = T_J$ .

PARAMETER	TEST CONDITIONS	MIN	TYP	MAX	UNITS
<b>Undervoltage Lockout</b>					
V <sub>IN</sub> UVLO Turn-on Threshold		7	8	9	V
UVLO Threshold Hysteresis		50	200	500	mV
<b>Supply Current</b>					
I <sub>IN</sub> Startup	VCC = 5V		2	3.5	mA
I <sub>IN</sub>	VCC = 12V		10	12	mA
<b>DAC/Reference</b>					
DACOUT Voltage Accuracy	Line, Load, $0^{\circ}C < T_A < 70^{\circ}C$ (Note 1)	-0.9		0.9	%
	Line, Load, $-55^{\circ}C < T_A < 125^{\circ}C$	-1.5		1.5	%
D0-D3 Voltage High	Dx Pin Floating	4.6	4.85		V
D0-D3 Input Bias Current	Dx Pin Tied to GND	-140	-105		$\mu A$
VREF Output Voltage	I <sub>VREF</sub> = 0mA, $0^{\circ}C < T_A < 70^{\circ}C$	4.97	5	5.03	V
VREF Total Variation	Line, Load, $0^{\circ}C < T_A < 70^{\circ}C$ (Note 1)	4.96	5	5.04	V
	Line, Load, $-55^{\circ}C < T_A < 125^{\circ}C$	4.925	5	5.075	V
VREF Sourcing Current	VREF = 0V	10			mA
<b>DAC Buffer</b>					
Input Offset Voltage	I <sub>DACBUF</sub> = -1mA, $0^{\circ}C < T_A < 70^{\circ}C$	-25		25	mV
Output Sourcing Current		-12		-1	mA
<b>Monitor Circuitry (Note 2)</b>					
VSENSE UV Threshold Voltage	Code 0, Ratio = 0.45 (Note 3)	3.174	3.237	3.3	V
	Code 0, Ratio = 0.9	2.87	2.975	3.08	V
	Code 15, Ratio = 0.45	1.816	1.85	1.884	V
	Code 15, Ratio = 0.9	1.635	1.7	1.765	V
VSENSE OV Threshold Voltage	Code 0, Ratio = 0.45	3.7	3.763	3.826	V
	Code 0, Ratio = 0.9	3.92	4.025	4.13	V
	Code 15, Ratio = 0.45	2.116	2.15	2.184	V
	Code 15, Ratio = 0.9	1.635	2.3	2.365	V



UC1910  
UC2910  
UC3910

**ELECTRICAL CHARACTERISTICS (cont.)** Unless otherwise specified, VCC = 12V, VSENSE = 3.5V, VO<sub>VTH</sub>/UV<sub>VTH</sub> = 1.26V, V<sub>D0</sub> = V<sub>D1</sub> = V<sub>D2</sub> = V<sub>D3</sub> = 0V, 0°C < T<sub>A</sub> < 70°C for the UC3910, -25°C < T<sub>A</sub> < 80°C for the UC2910, -55°C < T<sub>A</sub> < 125°C for the UC1910 T<sub>A</sub> = T<sub>J</sub>.

PARAMETER	TEST CONDITIONS	MIN	TYP	MAX	UNITS
<b>Monitor Circuitry (Note 2) (cont.)</b>					
VSENSE OVP Threshold Voltage	Code 0, Ratio = 0.45	3.937	4.025	4.113	V
	Code 0, Ratio = 0.9	4.41	4.55	4.69	V
	Code 15, Ratio = 0.45	2.235	2.3	2.365	V
	Code 15, Ratio = 0.9	2.505	2.6	2.695	V
OV, UV Comparator Hysteresis	Code 0, Ratio = 0.9	70	88	120	mV
	Code 15, Ratio = 0.45	15	25	40	mV
OVP Comparator Hysteresis	Code 0, Ratio = 0.9	160	218	300	mV
	Code 15, Ratio = 0.45	40	62	85	mV
Input Common Mode Range	OV, UV, OVP Comparators	0		5	V
Propagation Delay	OV, UV Comparators			5	μs
	OVP Comparator			5	μs
<b>PWRGOOD, OVP, OVPB Outputs</b>					
PWRGOOD Voltage Low	IPWRGOOD = 10mA			0.4	V
OVP Sourcing Current	VOVP = 1.4V	65			mA
OVPB Voltage Low	IOVPB = 1mA			0.4	V

Note 1: "Line, Load" implies that the parameter is tested at all combinations of the conditions:  
10.8V < VCC < 13.2V, -2mA < I<sub>VREF</sub> < 0mA.

Note 2: These are the actual voltages on VSENSE which will cause the OVPB and PWRGOOD outputs to switch, assuming the DACOUT voltage is perfect. These limits apply for 0°C < T<sub>A</sub> < 70°C.

Note 3: "Code 0" means pins D0 - D4 are all low; "Code 15" means they are all floating or high (See Table 1). "Ratio" is the divider ratio of the resistor string between DACBUF and OVTH/UVTH (See Figure 1).

## PIN DESCRIPTIONS

**D0-D3 (DAC Digital Input Control Codes):** These are the DAC digital input control codes, with D0 representing the least significant bit (LSB) and D3, the most significant bit (MSB) (See Table 1). A bit is set low by being connected to GND; a bit is set high by floating it, or connecting it to a 3V to 5V voltage source. Each control pin is pulled up to approximately 4.8V by an internal 40μA current source.

**DACBUF (Buffered DACOUT Voltage):** This pin provides a buffered version of the DACOUT voltage to allow external programming of the OV/UV thresholds (see OVTH/UVTH below).

**DACOUT (Digital-to-Analog Converter Output Voltage):** This pin is the output of the 4-bit digital to analog (DAC) converter. Setting all input control codes low produces 3.5V at DACOUT; setting all codes high produces 2.0V at DACOUT. The LSB step size (i.e. resolution) is 100mV (See Table 1). The DACOUT source impedance is typically 3kΩ and must therefore drive a high impedance input. Bypass DACOUT at the driven input with a 0.01μF, low ESR, low ESL capacitor for best circuit noise immunity.

**GND (Signal Ground):** All voltages are measured with

Decimal Code	D3	D2	D1	D0	DACOUT Voltage
15	1	1	1	1	2.0
14	1	1	1	0	2.1
13	1	1	0	1	2.2
12	1	1	0	0	2.3
11	1	0	1	1	2.4
10	1	0	1	0	2.5
9	1	0	0	1	2.6
8	1	0	0	0	2.7
7	0	1	1	1	2.8
6	0	1	1	0	2.9
5	0	1	0	1	3.0
4	0	1	0	0	3.1
3	0	0	1	1	3.2
2	0	0	1	0	3.3
1	0	0	0	1	3.4
0	0	0	0	0	3.5

Table 1. Programming the DACOUT Voltage

respect to GND. The two GND pins are connected together internally but should also be connected externally using a short PC board trace. Bypass capacitors on the VCC and VREF pins should be connected directly to the ground plane near one of the signal ground

**PIN DESCRIPTIONS (cont.)**

pins.

**OVP (Overvoltage Comparator Output):** This output pin drives an external SCR circuit with up to 65mA when the voltage on VSENSE rises above its nominal value by a percentage set by the voltage on the OVTH/UVTH pin (see below). The OVP comparator hysteresis is a function of both the DACBUF voltage and the OV/UV percentage programmed.

**OVPB (Overvoltage Comparator Complementary Output):** This output is a complement to the OVP output (see above) and provides an open collector capable of sinking 1mA when the voltage on VSENSE rises above its nominal value by a percentage set by the voltage on the OVTH/UVTH pin (see below).

**OVTH/UVTH (Undervoltage and Lower Overvoltage Threshold Input):** This pin is used to program the window thresholds for the OV and UV comparators. The OV-UV window is centered around the DACBUF voltage and can be programmed from  $\pm 5\%$  to  $\pm 15\%$  about DACBUF. Connect a resistor divider between DACBUF and GND to set the percentage. The threshold for the OVP comparator is internally set to a percentage 2 times larger than the programmed OV percentage; therefore, its range extends from 10% to 30% above DACBUF.

**PWRGOOD (Undervoltage/Lower Overvoltage Out-**

**put):** This pin is an open collector output which is driven low to reset the microprocessor when VSENSE rises above or falls below its nominal value by a percentage programmed by OVTH/UVTH. The OV and UV comparators' hysteresis is a function of the DACBUF voltage and the OV/UV programmed percentage.

**VCC (Positive Supply Voltage):** This pin supplies power to the chip. Connect VCC to a stable voltage source of at least 9V and capable of sourcing at least 15mA. The OVP and PWRGOOD outputs are held low, the OVPB output is in a high impedance state, and the VSENSE pin is pulled low until VCC exceeds the upper undervoltage lockout threshold. This pin should be bypassed directly to the GND pin with a 0.1 $\mu$ F low ESR, low ESL capacitor.

**VREF (Voltage Reference Output):** This pin provides an accurate 5V reference, capable of delivering up to 10mA to external circuitry, and is internally short circuit current limited. For best reference stability, bypass VREF directly to the GND pin with a 0.1 $\mu$ F, low ESR, low ESL capacitor.

**VSENSE (Output Voltage Sensing Input):** This pin is the input to the OVP and PWRGOOD comparators and is connected to the system output voltage through a lowpass filter. When choosing the resistor value for this filter, make sure that no more than 500 $\mu$ A will flow

19-2918; Rev 1; 1/04

**MAXIM**

## PWM Step-Down DC-DC Converters with 75mΩ Bypass FET for WCDMA and cdmaOne Handsets

### General Description

The MAX8506/MAX8507/MAX8508 integrate a PWM step-down DC-DC regulator and a 75mΩ (typ) bypass FET to power the PA in WCDMA and cdmaOne™ cell phones. The supply voltage range is from 2.6V to 5.5V, and the guaranteed output current is 600mA. One megahertz PWM switching allows for small external components.

The MAX8506 and MAX8507 are dynamically controlled to provide varying output voltages from 0.4V to 3.4V. The MAX8508 is externally programmed for fixed 0.75V to 3.4V output. Digital logic enables a high-power (HP) bypass mode that connects the output directly to the battery for all versions. The MAX8506/MAX8507/MAX8508 are designed so the output settles in less than 30μs for a full-scale change in output voltage and load current.

The MAX8506/MAX8507/MAX8508 are offered in 16-pin QFN packages (4mm x 4mm thin QFN packages (0.8mm max height).

### Applications

WCDMA/NCDMA Cell Phones  
Wireless PDAs, Palmtops, and Notebook Computers  
Wireless Modems

cdmaOne is a trademark of CDMA Development Group.

### Features

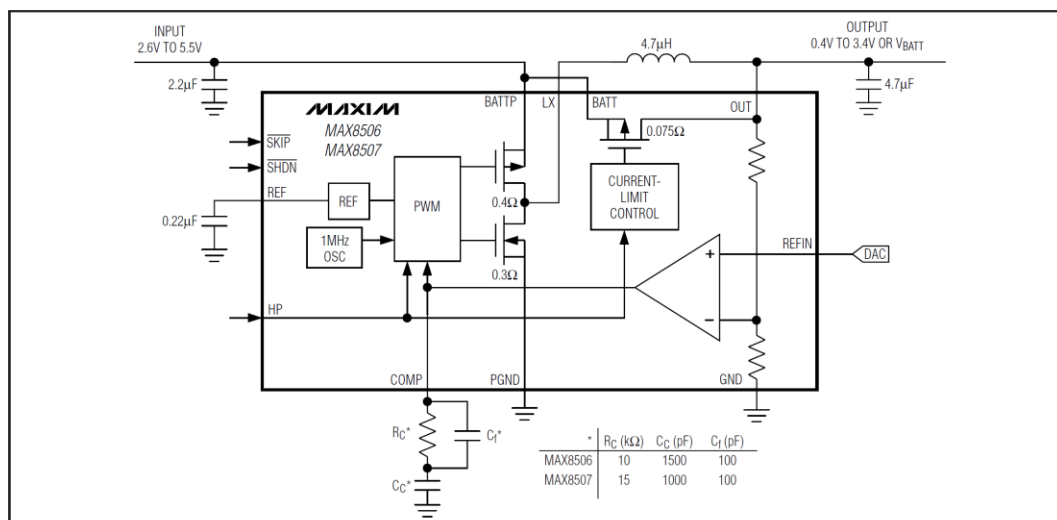
- ◆ Integrated 75mΩ (typ) Bypass FET
- ◆ 38mV Dropout at 600mA Load
- ◆ Up to 94% Efficiency
- ◆ Dynamically Adjustable Output from 0.4V to 3.4V (MAX8506, MAX8507)
- ◆ Externally Fixed Output from 0.75V to 3.4V (MAX8508)
- ◆ 1MHz Fixed-Frequency PWM Switching
- ◆ 600mA Guaranteed Output Current
- ◆ Shutdown Mode 0.1μA (typ)
- ◆ 16-Pin Thin QFN (4mm x 4mm, 0.8mm max Height)

### Ordering Information

PART	TEMP RANGE	PIN-PACKAGE
MAX8506ETE	-40°C to +85°C	16 Thin QFN
MAX8507ETE	-40°C to +85°C	16 Thin QFN
MAX8508ETE	-40°C to +85°C	16 Thin QFN

Pin Configurations appear at end of data sheet.

### Typical Application Circuits (MAX8506/MAX8507)



Typical Application Circuits continued at end of data sheet.

**MAX8506/MAX8507/MAX8508**

**ABSOLUTE MAXIMUM RATINGS**BATT<sub>P</sub>, BATT, OUT, SHDN, SKIP, HP, REFIN,

FB to GND	-0.3V to +6V
PGND to GND	-0.3V to +0.3V
BATT to BATT <sub>P</sub>	-0.3V to +0.3V
OUT, COMP, REF to GND	-0.3V to (V <sub>BATT</sub> + 0.3V)
LX Current (Note 1)	1.6A
OUT Current (Note 1)	3.2A
Output Short-Circuit Duration	Continuous

Continuous Power Dissipation (T<sub>A</sub> = +70°C)

16-Pin Thin QFN (derate 16.9mW/°C above +70°C)	1.349W
Operating Temperature Range	-40°C to +85°C
Junction Temperature	+150°C
Storage Temperature Range	-65°C to +150°C
Lead Temperature (soldering, 10s)	+300°C

**Note 1:** LX has internal clamp diodes to PGND and BATT. Applications that forward bias these diodes should take care not to exceed the IC's package power-dissipation limits.

Stresses beyond those listed under "Absolute Maximum Ratings" may cause permanent damage to the device. These are stress ratings only, and functional operation of the device at these or any other conditions beyond those indicated in the operational sections of the specifications is not implied. Exposure to absolute maximum rating conditions for extended periods may affect device reliability.

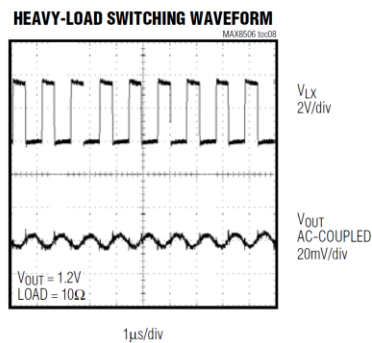
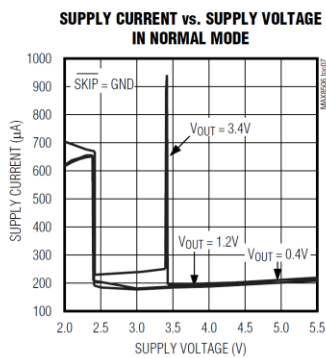
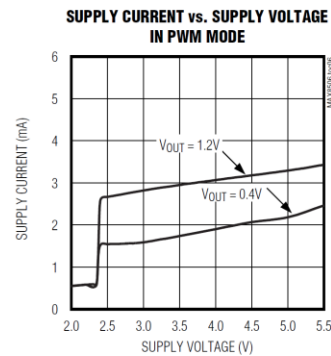
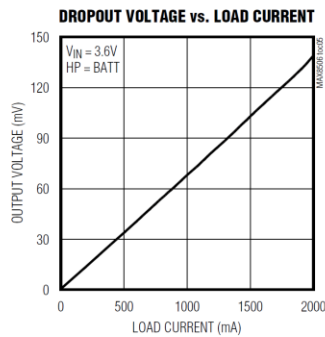
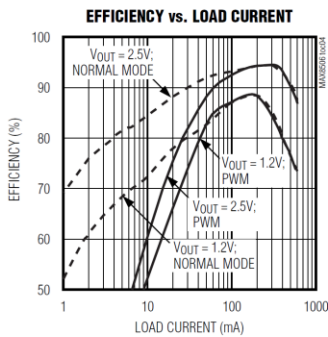
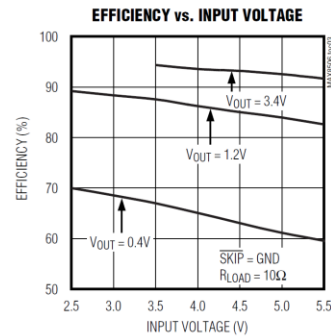
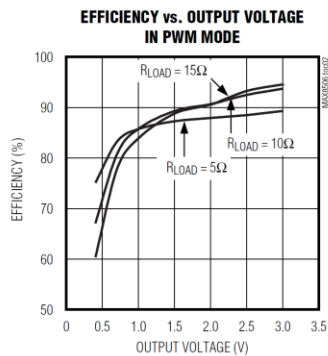
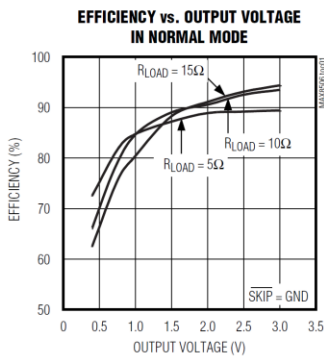
**ELECTRICAL CHARACTERISTICS**

(V<sub>BATT</sub> = V<sub>BATT<sub>P</sub></sub> = 3.6V, SHDN = SKIP = BATT, HP = GND, V<sub>REFIN</sub> = 1.932V (MAX8506), V<sub>REFIN</sub> = 1.70V (MAX8507), C<sub>REF</sub> = 0.22μF, T<sub>A</sub> = -40°C to +85°C, unless otherwise noted. Typical values are at T<sub>A</sub> = +25°C.) (Note 2)

PARAMETER	CONDITIONS	MIN	TYP	MAX	UNITS
Input BATT Voltage		2.6		5.5	V
Undervoltage Lockout Threshold	V <sub>BATT</sub> rising	2.150	2.35	2.575	V
Undervoltage Lockout Hysteresis			40		mV
Quiescent Current	SKIP = GND (normal mode)		180	250	μA
	SKIP = BATT, 1MHz switching		1750		
Quiescent Current in Dropout	HP = BATT		775	1000	μA
Shutdown Supply Current	SHDN = GND		0.1	5	μA
OUT Voltage Accuracy	V <sub>REFIN</sub> = 1.932V, I <sub>OUT</sub> = 0 to 600mA (MAX8506)	3.375	3.40	3.425	V
	V <sub>REFIN</sub> = 0.426V, I <sub>OUT</sub> = 0 to 30mA (MAX8506)	0.740	0.75	0.760	
	V <sub>REFIN</sub> = 1.700V, I <sub>OUT</sub> = 0 to 600mA (MAX8507)	3.375	3.40	3.425	
	V <sub>REFIN</sub> = 0.375V, I <sub>OUT</sub> = 0 to 30mA (MAX8507)	0.740	0.75	0.760	
OUT Input Resistance	MAX8506	250	485		kΩ
	MAX8507	275	535		
REFIN Input Current		-1	0.1	+1	μA
REFIN to OUT Gain	MAX8506		1.76		V/V
	MAX8507		2.00		
Reference Voltage		1.225	1.25	1.275	V
Reference Load Regulation	10μA < I <sub>REF</sub> < 100μA		2.5	8.5	mV
Reference Bypass Capacitor		0.1	0.22		μF
FB Voltage Accuracy	FB = COMP (MAX8508)	0.7275	0.75	0.7725	V
FB Input Current	V <sub>FB</sub> = 1V (MAX8508)		0.03	0.175	μA
P-Channel On-Resistance	I <sub>LX</sub> = 180mA	V <sub>BATT</sub> = 3.6V	0.4	0.825	Ω
		V <sub>BATT</sub> = 2.6V	0.5		
N-Channel On-Resistance	I <sub>LX</sub> = 180mA	V <sub>BATT</sub> = 3.6V	0.3	0.5	Ω
		V <sub>BATT</sub> = 2.6V	0.35		
HP/Bypass P-Channel On-Resistance	I <sub>OUT</sub> = 180mA, V <sub>BATT</sub> = 3.6V		0.075	0.110	Ω

**Typical Operating Characteristics**

( $V_{BATT} = V_{BATTP} = 3.6V$ ,  $SHDN = \overline{SKIP} = BATT$ ,  $HP = GND$ ,  $T_A = +25^\circ C$ , unless otherwise noted.) (See the *Typical Application Circuits*.)



**Pin Description**

PIN		NAME	FUNCTION
MAX8506 MAX8507	MAX8508		
1	1	$\overline{\text{SHDN}}$	Shutdown Control Input. Drive low for shutdown mode. Connect to BATT or logic high to enable the IC.
2	2	GND	Ground. Connect to PGND and directly to EP.
3	3	REF	Reference Output. Output of the internal 1.25V reference. Bypass to GND with a 0.22 $\mu$ F capacitor.
4	—	REFIN	External Reference Input. Connect to the output of a digital-to-analog converter for dynamic adjustment of the output voltage.
5	5	COMP	Compensation. Connect a compensation network from COMP to GND to stabilize the regulator. See the <i>Typical Application Circuits</i> .
6	6	HP	High-Power Bypass Control Input. Drive low for OUT to regulate to the voltage set by REFIN (MAX8506/MAX8507) or the external resistors on FB (MAX8508). Drive HP high for OUT to be connected to BATT by an internal bypass PFET.
7	7	N.C.	No Connection. Connect to PGND.
8	8	PGND	Power Ground. Connect to GND.
9	9	LX	Inductor Connection to the Drains of the Internal Power MOSFETs. LX is high impedance in shutdown mode.
10	10	BATTP	Supply Voltage Input. Connect to a 2.6V to 5.5V source. Bypass BATTP to PGND with a low-ESR 2.2 $\mu$ F capacitor. Connect BATTP to BATT.
11, 13, 15	11, 13, 15	BATT	Supply Voltage Input. Connect all BATT pins to BATTP.
12, 14	12, 14	OUT	Regulator Output. Connect both OUT pins directly to the output voltage.
16	16	$\overline{\text{SKIP}}$	Skip Control Input. Connect to GND or drive low to enable pulse skipping under light loads. Connect $\overline{\text{SKIP}}$ to BATT or logic high for forced-PWM mode.
—	4	FB	Output Feedback Sense Input. To set the output voltage, connect FB to the center of an external resistive voltage-divider between OUT and GND. FB voltage regulates to 0.75V when HP is low.
—	—	EP	Exposed Pad. Connect directly to GND underneath the IC.

# Optimized Flexible Power Selection for Opportunistic Underlay Cognitive Radio Networks

Sabyasachi Chatterjee<sup>1</sup>  · Prabir Banerjee<sup>1</sup> · Mita Nasipuri<sup>2</sup>

© Springer Science+Business Media New York 2017

**Abstract** A flexible transmit power selection concept for underlay cognitive users is proposed in this paper. We have employed an opportunistic, sensing based spectrum sharing method. Besides the power constraint to avoid interference at PU, the transmit power constraints of secondary user is also considered. Received Signal Strength Indicator based carrier selection method has been adopted. To resolve hidden terminal problem, twin scan concept is used at both ends (secondary transmitter and receiver) with same carrier frequency. Secondary transmitter selects suitable carrier frequency to initiate communication with the minimum power level as defined by the proposed algorithm. If received signal strength at the corresponding secondary receiver is below the predefined required receiver threshold, then power level is stepped up automatically. To maximize secondary user channel capacity, we have considered flexible power selection strategy as per channel state information. If the cognitive receiver is unable to recover the received information, even with the peak transmit power, it will again perform the frequency scanning operation. This is repeated till the best result is achieved. A power control circuit is designed to check the power selection concept.

**Keywords** Channel state information · Flexible transmitter power · Power control circuit · Received signal strength indicator · Spectrum sharing · Underlay cognitive radio

---

✉ Sabyasachi Chatterjee  
sabyasachi.chatterjee@heritageit.edu

Prabir Banerjee  
prabir.banerjee@heritageit.edu

Mita Nasipuri  
mnasipuri@cse.jdvu.ac.in

<sup>1</sup> Heritage Institute of Technology, Kolkata, India

<sup>2</sup> Jadavpur University, Kolkata, India

# 1 Introduction

Recently, the rapid development of wireless services and applications has overcrowded the radio spectrum. Therefore, efficient allocation of the scarce radio spectrum is a key challenge for new generation radio communication systems. Cognitive Radio (CR) technology is a new way to overcome the spectrum shortage problem. It allows smart and dynamic spectrum management [1]. Basically, there are three paradigms for the operation of CRs. Opportunistic Spectrum Access (OSA), also known as spectrum overlay [2] have unlicensed users, also known as Secondary Users (SUs) and operate on the licensed spectrum opportunistically when Primary Users' (PUs) transmission is detected to be idle. Spectrum Sharing (SS) or spectrum underlay allows the SUs to use licensed spectrum even when the owner of that licensed spectrum is active (PU). It is permitted on the condition that the resultant interference at the PU receiver is below the prescribed threshold [3]. In the third paradigm, sensing based spectrum sharing [4] or inter-wave approach allows the SUs to sense the status of channel first and then select appropriate carrier frequency based on the sensed result. If the PU is detected to be active, Secondary Cognitive Users (SUCs) use licensed spectrum simultaneously by keeping interference level below the tolerance limit [3]. Otherwise, the SU works in spectrum overlay approach where there is an active cooperation between PUs and SUs. Hybrid schemes, using a combination of all these paradigms [5], have a great potential to improve the efficiency of spectrum sharing. Each of them requires a different level of cognition about the surrounding environment.

A distributed power control algorithm based on Euclidean projection to keep the interference level at PU below the interference temperature threshold is proposed in [6]. The outage probability of all cognitive users and primary users should be reduced by distributed probabilistic power algorithm [7]. QoS (Quality of Service) sensitivity based admission control algorithm [8] for the optimal power allocation strategy was proposed for underlay-based CRN with PU's statistical delay [9]. A convex optimization problem has been solved by Gu et al. [10] to allocate power to SUs. Secondary throughput is maximized under power constraints by an optimum value of the relay amplification factor [11]. A new resource allocation method based on dynamic allocation of hybrid sharing transmission mode of overlay and underlay (Dy-HySOU) is proposed in [12]. A hybrid CR system where the switching from an overlay mode to an underlay mode is probabilistically controlled is not only used to maximize the departure rate of the SU [13] but also enable energy-efficient transmission [14]. Optimal power allocation and relay selection (PARS) under the QoS constraint of the PU transmission is presented in [15]. In a non-cooperative network, overlay based on combination of underlay/overlay based hybrid spectrum sharing system is difficult to implement since data sequence of PUs' is unknown which motivated us to focus on underlay cognitive radio network. Here it is very important to measure received signal strength in terms of SNR (Signal to Noise Ratio). This approach also checks the interference level as is investigated in [16]. To allocate the available spectrum for maintaining minimum SNR and to achieve acceptable QoS, a geometric programming technique was proposed by Xing et al. [17]. Generally, PUs operates at constant transmission power with fixed data rate. To keep the outage probability of PUs below a desired target, a new type of constraint has been imposed over the underlay secondary transmission [18]. A new Genetic Algorithm (GA) based power allocation scheme is used to achieve maximum system utility [19] and to maximize the total throughput of underlay cognitive radio network [20]. Spectrum and energy-efficient routing (SEER) protocol improves transmission efficiency and balances in energy consumption [21].



We have proposed optimized flexible transmit power control algorithm for Cognitive SUs under Opportunistic sensing based spectrum sharing environment. The proposed scheme not only improves the throughput of the secondary network but also guarantees the QoS (Quality of Service) of the primary network. The following are the main highlights of this paper:

- RSSI based dual scanning concept for reliable channel selection has been introduced to take care of the optimum transmitter power level and any local interference at the SU.
- In underlay scheme, an optimization between transmit power control and high SNR at the SU receiver is required. Hence, we have proposed a flexible transmission power concept to keep the interference level at the primary receivers below the critical limit.
- We have considered handshaking techniques to establish a communication link and optimal power allocation. A new receiver initiated transmitter power control command protocol is proposed for secondary cognitive users.
- The linear variation of transmitter power is generally controlled by the bias voltage of the RF amplifier. Therefore, we have designed a power control circuit, based on feedback mechanism, to control the bias voltage. The feedback signal is derived from the RSSI signal.

The remainder of the paper is organized as follows: Sect. 2 explains the underlay network in an opportunistic sensing based environment. This section provides a detailed analysis of the actual channel model and power allocation strategy based on received signal strength. Section 3 defines a mathematical model for optimized receiver threshold allocation scheme. The proposed receiver initiated handshaking protocol is presented in Sect. 4. Section 5 highlights the design of the power control circuit. Section 6 concludes the paper.

## 2 Opportunistic Underlay Sensing Network

Cognitive radio brings a concept of a well regarded agile technology that allows opening up the frequency bands to concurrent operating users in a non-interfering mode. These radios should possess a minimum of information about their surrounding non cognitive users to make spectrum sharing possible. Exceeding the predefined tolerable interference threshold may degrade the efficiency of the primary users dramatically.

### 2.1 Channel Model

We consider an underlay Cognitive point to point wireless communication environment in which a Primary (licensed) and Secondary (Cognitive) user pair (Transmitter [ $T_x$ ]-Receiver [ $R_x$ ]) concurrently operates on a common spectrum band. Here, the licensed channel is open to be used by Cognitive Users to achieve higher spectral efficiencies. We assume frequency flat fading channels with ergodic time varying gains. Figure 1 represents Primary and Secondary links as  $i$  and  $j$  respectively.  $h_{ij}$  represents link between secondary  $T_x$  and secondary  $R_x$  and  $h_{ji}$  represents link between Primary  $T_x$  and Primary  $R_x$ . Channel State Information (CSI) can be obtained based on the classic spectrum sensing information. The secondary users adapt its transmission power depending on the value of sensing metric.

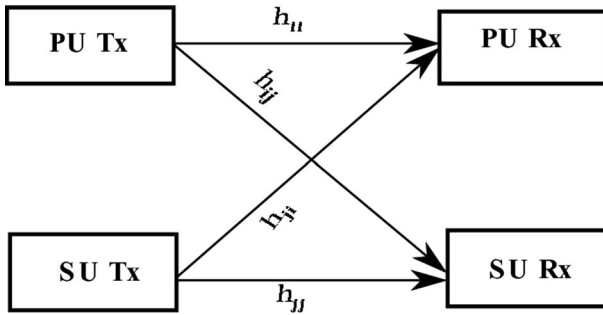


**Fig. 1** Underlay channel model

The channels are assumed to be AWGN (Additive White Gaussian Noise) type whose gains are random but constant during transmission. The corresponding input–output relation of the link  $h_{ji}$  between nodes Secondary Tx and Primary Rx is given by

$$y_i = \sqrt{g_{ji}}x_j + n \quad (1)$$

The channel power gain  $g_{ji}$  of link  $h_{ji}$  absorbs both Rayleigh fading and path loss effects so

$$g_{ji} = d_{ji}^{-\alpha} |h_{ji}|^2 \quad (2)$$

where, the distance between Secondary Tx and Primary Rx is represented by  $d_{ji}$ . Path loss exponent ( $\alpha$ ) and channel gains are modelled as Zero Mean Circular Symmetric Gaussian (ZMCSCG) random entries, so that  $h_{ji} \sim N(0, 1)$ . Now during the licensed communication, channel power gain will be  $g_{ii}$

$$\hat{y}_i = \sqrt{g_{ii}}x_i + y_i \geq \lambda_{PU} \quad (3)$$

where,  $\lambda_{PU}$  is the predefined SNR limit at Primary Rx. Another channel power gain  $h_{jj}$  can be defined likewise.

## 2.2 SNR Adaptation for Licensed Communication

The outage capacity is one of the capacity notions of fading channels. The outage capacity is defined as the maximum constant rate that can be maintained for a specified outage probability. Based on the statistical CSI, primary outage probability has been considered as a new criterion to measure the QoS in [22]. We assume that the licensed user transmits with constant transmitter power and rate denoted by  $P_p$  and  $r_p$  respectively. Supposing that the SU transmission is not present on this licensed spectrum, the transmission outage probability of the PU channel [23]—where  $P_r(\cdot)$  denotes the probability.

$$\varepsilon_0 = P_r \left[ \frac{g_{ji}P_p}{N_0B} < \lambda_{PU} \right] \quad (4)$$

The ergodic channel capacity for a secondary user is investigated using soft sensing information about primary user activity in a shared channel under joint peak transmit power and average received interference power constraints by Bala et al. [24]. This capacity is defined as the maximum achievable rate averaged over all fading states. Here

we have considered the effects of the SU transmission on the same licensed spectrum. The transmission outage probability can be written as [23]

$$\epsilon_p^{(c)} = P_r \left[ \frac{g_{ii}P_p}{g_{ij}P_s + N_0B} < \lambda_{PU} \right] \tag{5}$$

The transmitted power used by the SU is denoted as  $P_s$ . To meet optimum SNR at PU Rx, desired outage probability always must be

$$\epsilon_0 \geq \epsilon_p^{(c)} \tag{6}$$

### 2.3 Optimum $T_x$ Power Adaptation at SU Transmitter

The secondary transmitter must adapt its transmit power from the CSI (Channel State Information) of the licensed channel. Optimal power control policies that maximize the achievable rates of underlay cognitive radio systems with arbitrary input distributions under both peak/average transmit power and peak/average interference power constraints have been developed by Ozcan et al. [25]. Now to satisfy PU outage constraint given by Eq. (6), we also consider the SU’s own transmit power constraint which can be categorized into two general types—(a) Flexible Transmit Power Constraint, (b) Peak Transmit Power Constraint.

The secondary transmitter adapts its transmitter power level depending on the outcome of the sensing module. RSSI information will help to select the best possible predefined power level proposed by flexible transmit power constraints.

$$E[P_s \_flx] \leq P_{pk} \tag{7}$$

where  $E[\cdot]$  denotes the expected Secondary flexible transmit power limiting within the peak transmit power to satisfy SI (Secondary Interference) at Primary Rx is below the predefined limit  $E[P_s g_{ji}] \leq \gamma_i$ , where  $\gamma_i = \frac{\hat{y}_i - y_i}{y_i}$  defines interference limiting factor or SNIR (Signal to Noise and Interference Ratio) at PU Rx due to transmission by the secondary Tx.

### 3 Optimized Threshold Selection

Threshold allocation in Underlay Cognitive Network (UCN)for Secondary Users (SUs) is very crucial in terms of successful data transmission without creating any harmful interference at the Primary Receiver end. Reliable simultaneous licensed channel selection at the SU Tx end depends on this predefined threshold as per CSI. The energy static or decision static of received signal energy is given by [26]

$$E_{SI} = \frac{1}{N} \sum_{N-1}^N |r_i(t)|^2 dt \tag{8}$$

Comparing  $E_{SI}$  with the pre-set threshold  $\lambda_i$  of CR enabled nodes, the absence or presence of primary user signal can be determined by [26]

$$\begin{aligned} H_0 &: E_{SI} < \lambda_i \\ H_1 &: E_{SI} \geq \lambda_i \end{aligned}$$

The signal to noise ratio (SNR) is defined as the ratio of the signal variance to the noise variance, given as [27]

$$\gamma = \frac{h_i^2 \sigma_s^2}{\sigma_n^2} \quad (9)$$

The received energy by the underlay cognitive users is taken as a decision statistic [28] which follows central and non-central Chi squared distribution each with  $2\mu$  degree of freedom and a non-centrality parameter-for the later one.

$$E_{si} \sim \begin{cases} \chi^2 2\mu \\ \chi^2 2\mu(2\gamma) \end{cases} \quad (10)$$

When the sample size of received signal is large enough ( $N \geq 100$ ), then by central limit theorem (CLT), mean and variance of  $E_{SI}$  under the hypothesis  $H_0$  are  $N\sigma_n^2$  and  $N\sigma_n^4$  respectively. Similarly, under hypothesis  $H_1$ , mean is  $N\sigma_n^2(1 + \gamma)$  and variance is  $N\sigma_n^4(1 + 2\gamma)$ . The  $Q(\cdot)$  function can be written as [29]

$$Q(x) = \frac{1}{\sqrt{2\pi}} \int_x^\infty \exp\left(-\frac{t^2}{2}\right) dt \quad (11)$$

Successful Detection:  $H_1$  true, decide  $H_1$ : Probability ( $H_1$  true, decide  $H_1$ )

$$= p_{sd} = Q\left(\frac{\lambda_{i1} - \mu H_1}{\sigma H_1}\right) p_{sd} = Q\left(\left(\frac{\lambda}{N\sigma_n^2} - 1 - \gamma\right) \sqrt{\frac{N}{1 + 2\gamma}}\right) \quad (12)$$

False Detection:  $H_0$  true, decide  $H_1$ : Probability ( $H_0$  true, decide  $H_0$ )

$$= P_{fd} = Q\left(\frac{\lambda_{i1} - \mu H_0}{\sigma H_0}\right) P_{fd} = Q\left(\left(\frac{\lambda}{N\sigma_n^2} - 1\right) \sqrt{N}\right) \quad (13)$$

Miss Detection:  $H_1$  true, decide  $H_0$  : Probability ( $H_1$  true, decide  $H_0$ ) =  $P_{md} = 1 - P_{sd}$  (14)

A pre-defined threshold  $\lambda_i$  is a common parameter which varies from 0 to  $\infty$ . It is required for the decision whether the PU signal is absent or present. Thus selection of operating threshold is very important in the context of Cognitive Radio Networks (CRNs). [27] The false alarm happens when Secondary Cognitive Users (SCUs) falsely detects the presence of the PU signal within the interfering level. The misdetection happens when SCUs mistakenly take a decision about the absence of the PU signal mainly due to interference on the same channel. False alarm condition arises when the radio receiver suffers mainly from constructive fading. Misdetection, on the other hand, may happen due to desensitization and fading due to interference. These two error probabilities reflect the spectrum utilization of Cognitive Radio (CR) nodes. Therefore, the goal of the threshold optimization is to decrease both the false alarm and misdetection probabilities. The common practice of setting the threshold is based on the false alarm probability. When the  $\lambda_i$  increases (or decreases), both  $P_{fd}$  and  $P_{md}$  decrease (or increase). Now, to achieve a high  $P_{sd}$ , the  $P_{md}$  must be kept very low while with time probability of  $P_{fd}$  increase. Therefore, the optimal threshold selection can be viewed as the minimization of the total error rate,

defined as [30]  $P_e \cong P_{fd} + P_{md}$ . The error detection probability of  $CR_i$  can be written as [29]

$$P_{ei} = P(H_0)P_{fd} + P(H_1)P_{md} \tag{15}$$

Figure 2 shows that probability of false detection ( $P_{fd}$ ) increases with decrease in the probability of misdetection ( $P_{md}$ ). If the Received Signal Strength (RSS) is high, the probability of misdetection is very low.

Figure 3 shows that probability of false detection ( $p_{fd}$ ) increases linearly if the Received Signal Strength (RSS) is closer to threshold value as per (12). Maximum probability 1 of successful detection ( $P_{sd}$ ) is achieved when probability of false detection is absent. This nature of  $P_{sd}$  has been plotted against  $P_{fd}$  in Fig. 3. The conventional method is to maximize the detection probability while minimizing the total error. The optimal threshold can be written as [26]

$$\lambda^* = \arg \min p_e(\lambda) \tag{16}$$

For an AWGN (Additive White Gaussian Noise) fading channel, the optimal threshold is given by [29]

$$\lambda^* = \arg \min \left( 1 + \frac{1}{2} \operatorname{Erfc} \left( \frac{\lambda - N\sigma_n^2}{\sqrt{2\pi}\sigma_n} \right) - \frac{1}{2} \operatorname{Erfc} \left( \frac{\lambda - N\sigma_n^2(1 + \gamma)}{\sqrt{2N(1 + \gamma)}\sigma_n} \right) \right) \tag{17}$$

Here,  $P_{fd} = \frac{1}{2} \operatorname{Erfc} \left( \frac{\lambda - N\sigma_n^2}{\sqrt{2N}\sigma_n} \right)$  and  $P_{sd} = \frac{1}{2} \operatorname{Erfc} \left( \frac{\lambda - N\sigma_n^2(1 + \gamma)}{\sqrt{2N}\sigma_n} \right)$  respectively,  $\operatorname{Erfc}(\cdot)$  is the complementary error function which is defined as [29]  $\operatorname{Erfc}(z) = \frac{2}{\sqrt{\pi}} \int_z^\infty e^{-t^2} dt$  and standard Q function  $Q(z) = \frac{1}{2} \operatorname{Erfc} \left( \frac{z}{\sqrt{2}} \right)$ .

Therefore, the optimal threshold for any received signal with acceptable SNR value can be derived as [29]

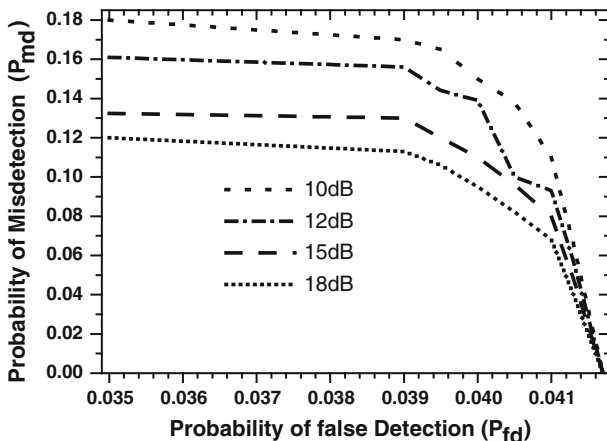
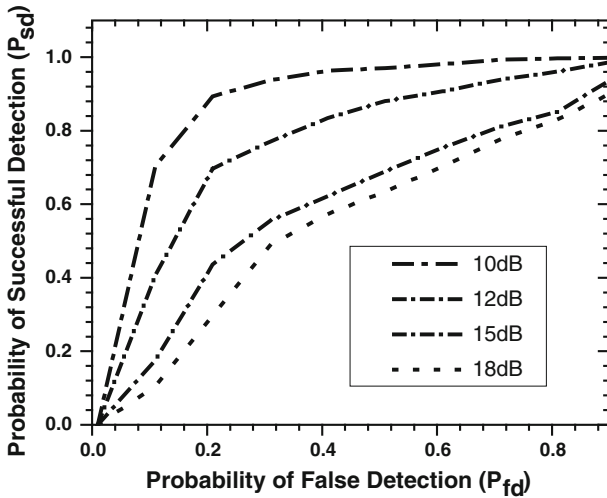


Fig. 2 Relation between misdetection and false detection probability



**Fig. 3** Linear relationship between successful detection and false detection probabilities

$$\lambda^* = \frac{N\sigma_n^2}{2} \left( 1 + \sqrt{1 + 2\gamma \left( 1 + \frac{(1 + 2\gamma) \ln(1 + 2\gamma)}{N\gamma^2} \right)} \right) \quad (18)$$

When the received signal strength (SNR) is very low, i.e.  $\gamma \ll 1$ ,  $(1 + 2\gamma) \approx 1$  and the optimal threshold can be well-approximated as [29]

$$\lambda^* \approx \frac{N\sigma_n^2}{2} (1 + \sqrt{1 + 2\gamma}) \approx N\sigma_n^2 \quad (19)$$

Figure 4 shows probability of successful detection with respect to variable SNR results. Detection probability improves with higher SNR values. Maximum detection probability is is

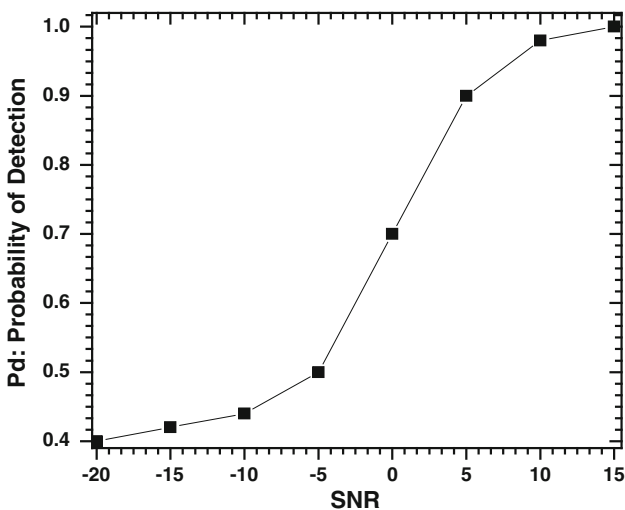


**Fig. 4** Variation of  $p_d$  with SNR

achieved when SNR value is more than 15 dB. In our work, we have examined channel condition in terms of received signal in variable conditions. We have considered AWGN fading channel performance to justify our work. If one is to model an accurate CR environment, the shadowing effects cannot be neglected. If the shadowing effect is neglected, the Path Loss behaviour represents an unrealistic straight line curve. For consideration of shadowing effect, a zero-mean Gaussian random variable with standard deviation  $-\sigma$  can be assumed. It is a variable with positive value or negative value. It signifies that the optimal threshold of received signal will have a deviation, either positive or negative, in real time RF (Radio Frequency) propagation environment. Along with this, to consider internal desensitization effects due to platform noise, we have considered internal noise factor  $\lambda_{\text{int}}$ . It is a correction factor to determine local instantaneous threshold value. In Eq. (15), it has been shown mathematically that the probability of total error rate depends on false detection (positive deviation) and misdetection (negative deviation) probability. Therefore, the real time optimal receiver threshold for received signal (SNR) can be written as-

$$\lambda_i^* \approx (N\sigma_n^2 \pm \sigma \cdot G + \lambda_{\text{int}}) \quad (20)$$

The challenge is to obtain, optimum threshold for SNR to satisfy the system performance requirement. We can find out analytically the desired SNR in an omni-directional antenna system. As a typical example, we can compare underlay cognitive radio system with conventional cellular system where the same frequency is reused. In a cellular system, the specified SNR is 18 dB or higher based on subjective test and analysis [31]. Therefore, we have considered the SNR of 18 dB as standard required threshold for reliable performance.

## 4 Proposed Scheme

In this paper, we mainly focused on the selection of an optimum power level for the secondary transmitter using power control module. To initiate information exchange, we have proposed the selection of a reliable carrier first using RSSI detection and comparison with a predefined system threshold. The primary reason for implementing this technique is to minimize interference with primary users. At the same time, to resolve hidden terminal problem, twin-scan concept at both ends with same carrier has been proposed. Receiver can also determine the RSSI from a supervisory tone sent from the given transmitter.

### 4.1 Receiver Initiated Protocol

In Underlay Cognitive Scenario, we have introduced a new method, where a secondary transmitter will communicate with the corresponding secondary receiver only after ensuring that the channel is reliable. The channel is selected using suitable handshaking protocol.

The transmitter makes a request to the receiver to switch to the desired channel frequency with help of the Request to Carrier Switch (RCS) command. After successful reception of the RCS command, the supervisory tone is used by the receiver to determine SNR on switched carrier frequency. The strength information of received signal is transmitted to the desired transmitter using Receiver Strength Information (RSI) command frame (Fig. 5). Now, the transmitter selects a power, 3 dB below the RF power

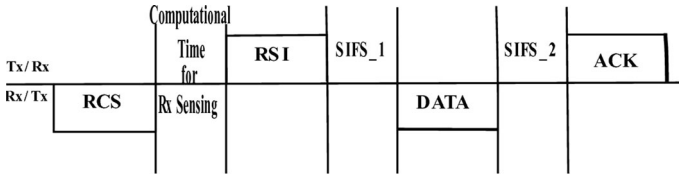


**Fig. 5** Proposed data communication methodology

corresponding to the receiver signal strength information. Basic transmission rate ( $R_{control}$ ) has been assigned for control frames ( $O_{cf}$ ). The total time required for reliable carrier selection and transmission of control command to the proper destination can be calculated as

$$\tau_{CI} = \tau_{comp} + \frac{O_{cf}}{R_{control}} \quad (21)$$

$\tau_{comp}$ , is the minimum receiver computational time for scanning and releasing the control frame with required information. In the worst case scenario, system computation time ( $\tau_{comp}$ ) calculation depends on PLL locking time (20 ms) [32], RSSI generation lag from IF processor IC SA 636 (10 ms) [33] and the program execution time. For our proposed system, 16 MHz clock has been considered. In general, information is conveyed when there is change in values of the signal. In our proposed scheme, sender ( $Tx$ ) starts sending data packets on flexibly defined RF power whenever it receives RSI command from the desired receiver (Fig. 6).

Total data transmission time from  $Tx$ - $Rx$  can be calculated as

$$\tau_{TD} = \frac{s}{\delta} + T_p + T_t \quad (22)$$

In the above equation, first term represents time to send all the bits on the link, where  $s$  = control bits + data frame (M) and  $\delta$  stands for uniform data transmission rate. Now to evaluate the maximum rate at which data can be transmitted over a given channel, we have chosen the capacity for a specified outage probability ( $p_{out}$ ) (Fig. 7). The probability that outage may occur signifies that the system cannot successfully recover the transmitted information. When received signal SNR is below the minimum system threshold, then the  $P_{out}$  will be  $-P(\lambda_{SU} < \lambda^*)$ . Since, the instantaneous CSI (Channel State Information) is not present at the transmitter. The constant data rate is

$$C_{out} = B \log_2(1 + \lambda_{SU}) \quad (23)$$

Now, Effective data rate is given by

$$\delta = \frac{\eta}{100} \times C \quad (24)$$

where, transmission efficiency ( $\eta$ ) is evaluated as,  $\frac{Actual\ data}{Total\ no.\ of\ transmitted\ data} \times 100$ . The second and third term in Eq. (22) denote Propagation delay time ( $T_p$ ) and channel processing time ( $T_t$ ).

**Fig. 6** Structure of transmitted information

HEADER INFORMATION					User Data
Destination ID	Source ID	Message ID	Packet ID	Control ID	



### 4.2 Optimal Power Selection

As is known, optimal transmitter power selection is very crucial in underlay cognitive network to avoid interference with licensed users (Primary receivers). To overcome this possibility, we have introduced a flexible transmit power concept. In our approach, power level selection will depend on receiver SNR or RSSI information transmitted with RSI command. To transmit at optimum RF power level, the SU applies power control logic. Secondary transmitter will finally transmit at the pre-defined RF power level, as per the condition defined in Eq. (25).

$$P_{(s\_flx)n} \leq T_{x_p} - 3 \text{ dB} < P_{pk} \tag{25}$$

In the Eq. (25),  $P_{pk}$  represents the received signal strength at the receiver on the carrier selected by the transmitter. The data transmission starts at the level, which is 3 dB below the detected receiver strength information. If the corresponding secondary receiver is not able to recover the data due to weak signal strength, the receiver will respond with Step-Up Transmission Power (SUTP) command signal. The RF power will increase in steps of 0.5 dB and the maximum limit is  $P_{pk}$ . Therefore,  $T_{x_p} = Kn$ , where  $K = 0.5 \text{ dB}$  and  $n$  is positive integer ( $1 \leq n < 16$ ) which represents the allowable power levels defined in Table 1. The SUTP command sequence is described in Fig. 9. The total frame consists of frame control bits, consisting of 2 byte information, followed by receiver address (RA), transmitter address (TA) and transmitter power level as shown in Fig. 8.

As soon as the secondary transmitter receives new power level information from respective secondary receiver, it switches to that RF power level and re-transmits the failed data sequence. This process will continue until the transmitted RF power level satisfies the receiver requirement.

Figure 9 shows the same data transmission sequence if the signal reception quality is poor at the receiver end. As per predefined algorithm, transmission power increase step by step towards peak transmission power till 'ACK' is received. If the received signal strength is still poor even with the peak transmitter power, then transmitter will again scan the available channels to choose another carrier frequency for reliable data communication.

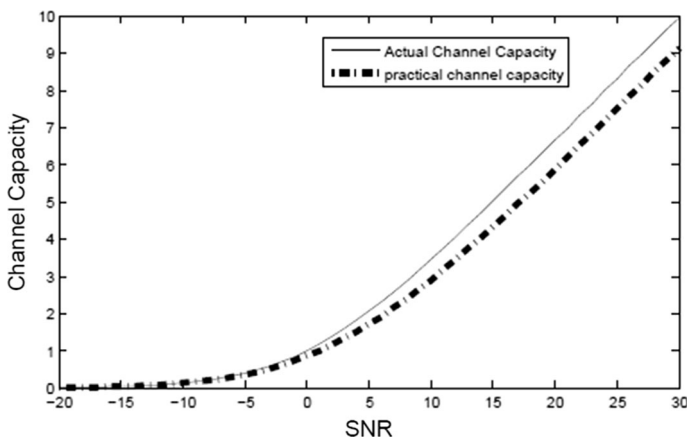
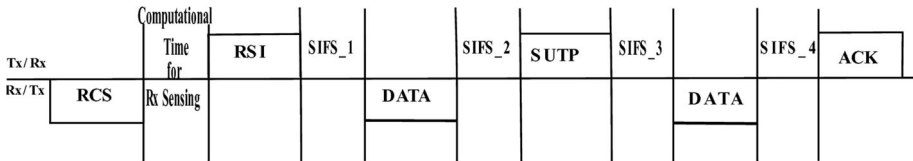
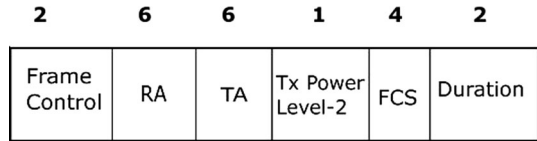


Fig. 7 Characteristics curve of channel capacity

**Table 1** Flexible power steps

Binary code	RF power level (mW)
0000	3.2
0001	4.0
0010	5.0
0011	6.3
0100	7.9
0101	10
0110	12.6
0111	15.8
1000	20
1001	25.1
1010	31.6
1011	39.8
1100	50.1
1101	63.1
1110	79.4
1111	100

**Fig. 8** Frame sequence of SUTP**Fig. 9** Data transmission sequence

The newly selected carrier frequency is also used by any other PU. The complete process will be repeated until data has been transmitted successfully.

### 4.3 Approximation of Error Rate

In underlay Cognitive Network, Secondary receiver receives signals on channels selected by Secondary transmitter. The secondary transmitter also selects the power level. The received power at SU Transmitter is

$$|h|^2 P_{(s\_flx)n}, \quad (26)$$

where  $|h|$  =  $a$  represents amplitude of PU signal and channel noise.

Therefore, effective SNR at the Secondary receiver is denoted by

$$SNR_e = \frac{P_{(s-f(x))n}|h|^2}{\sigma^2} = a^2 SNR. \tag{27}$$

Now the received signal strength (RSS) may be less than predefined system threshold due to high noise power (PU signal and channel noise). Then,

$$\begin{aligned} &RSS < \text{Noise power at receiver} \\ &a^2 P_{(s-f(x))n} < \sigma^2 \\ &a < \frac{1}{\sqrt{SNR}} \end{aligned} \tag{28}$$

The probability of error due to high noise factor is

$$p(e) = P_r \left( a < \frac{1}{\sqrt{SNR}} \right) = 1 - e^{-\frac{1}{3NR}}. \tag{29}$$

When the probability of error is very high then symbol error or bit error occurs at the secondary receiver end. Hence,

$$P_{BER} = P(n > \sqrt{P_{(s-f(x))n}}) = \int_{\frac{\sqrt{P}}{\sigma}}^{\infty} \frac{1}{\sqrt{2\pi}} e^{-\frac{t^2}{2}} dt = Q\left(\frac{\sqrt{P}}{\sigma}\right) = Q(\sqrt{SNR}).$$

Now for convenient approximation

$$\begin{aligned} Q(x) &\leq \frac{1}{2} e^{-\frac{1}{2}x^2} \\ Q(x) &\approx \frac{1}{2} e^{-\frac{1}{2}x^2} \\ Q(SNR) &\approx \frac{1}{2} e^{-\frac{1}{2}SNR^2} \end{aligned} \tag{30}$$

### 5 Hardware Implementation

In an underlay opportunistic cognitive radio network, the simultaneous existence of primary units (PUs) as well as multiple secondary units (SUs) has to be considered. The received signal strength quality at the SUs, expressed in terms of SNR and measureable by the RSSI voltage, has been used as a critical parameter for our scheme of operation. The basic objective of this type of network is to allow the SUs to operate without interfering with the PUs. Therefore, in our scheme, we first ensured that the transmitted RF power level of the SU is optimum so as not to cause damaging interference to the PUs. The SU will always know about the SNR of the signal received from any PU with the help of the RSSI voltage. In our scheme, to select the RF power level for the SU, RSSI is used as reference. The selection will always start at a level, which corresponds to 3 dB lower than the previously received SNR by SU from PU. It will increase in steps till the desired SNR value is reached. If this level of RF power fails to achieve the desired SNR level at corresponding SU, the carrier frequency is changed.

## 5.1 Power Control Module

In our scheme shown in Fig. 10, the decision for control of RF power level will be derived from the channel receiver performance indicator. Here, we have used SNR as an indicator. Any standard IF processor IC provides an output RSSI DC voltage, which is directly proportional to the SNR.

Therefore, in our circuit, we have digitized the received analog DC signal generated from the IF processor IC MC 13135 as RSSI with the help of ADC 0804. The ADC outputs are read by the controller 89C51. The controller is pre-loaded with a look-up table in which binary values corresponding to all possible RF power levels, to be considered, are stored. This consideration of RF power level is based on the RSSI values, received to attain the threshold value for SNR for reliable network operation.

In a typical power amplifier, for linearity, class-A or class-AB configuration is used. The usual objective is to control the biasing voltage of the power amplifier stage rather than controlling the driver stage. In our scheme, the RSSI voltage, after ADC conversion, is compared with the pre-programmed assumed binary values in the controller. If RSSI voltage is found to be lower than the desired threshold for a given network, the RF power decision (Table 1) is taken help of. This power table is programmed with a series of 4 bit binary pattern within 0000–1111. These values represent the different power levels. The binary pattern corresponding to the desired power is applied to IC UC1910 (voltage monitoring unit). The DC control voltage from this IC is used to control the DC-to-DC converter MAX8506. The output of 8506 finally controls the biasing voltage of RF power amplifier. Now, using our proposed command frame SUTP, secondary receiver instructs desired transmitter about requirement of enhanced power level with desired binary pattern. The RF power level from Table 1 is stored in transmitter controller. The entries in the RF power level column represent the levels required to attain different SNR value. As per command instruction, flexible transmitter power can be set for data transmission. This proposed scheme maintains optimum RF power level to minimize distortion due to interference with PUs.

### Proposed power allocation algorithm

1. Scan channel for  $Th_{(i)} = \lambda_h, 1 \leq i \leq \lambda_{pk}$
2. Compute  $Th_{(i)}$  [with the help of Eqs. (5) and (20)]
3. If yes, secondary Transmitter (Tx) generates RCS command [for secondary Receiver (Rx)]
4. Otherwise, repeat step (2) and (3)
5. Else, at Rx end, repeat step (1) and generate RSSI command
6. At Tx end, repeat step (2) and select RF power based on Eq. (25)
7. Secondary Tx starts transmission with selected power
8. Repeat step 2 at Secondary Rx
9. If none of the conditions are satisfied, then SUTP command is generated by secondary Rx
10. Secondary Tx increases power from Table 1 [as per Eq. (25)]
11. At step (8), if conditions are satisfied then ACK command is generated

Table 2 shows the mapping of binary codes with the receiver performance (in terms of SNR) on the channel, selected by the transmitter. As per current channel condition, the binary code will be sent to the secondary transmitter using proposed transmitter power step up command. The transmitter selects a power, 3 dB less than the power, corresponding to

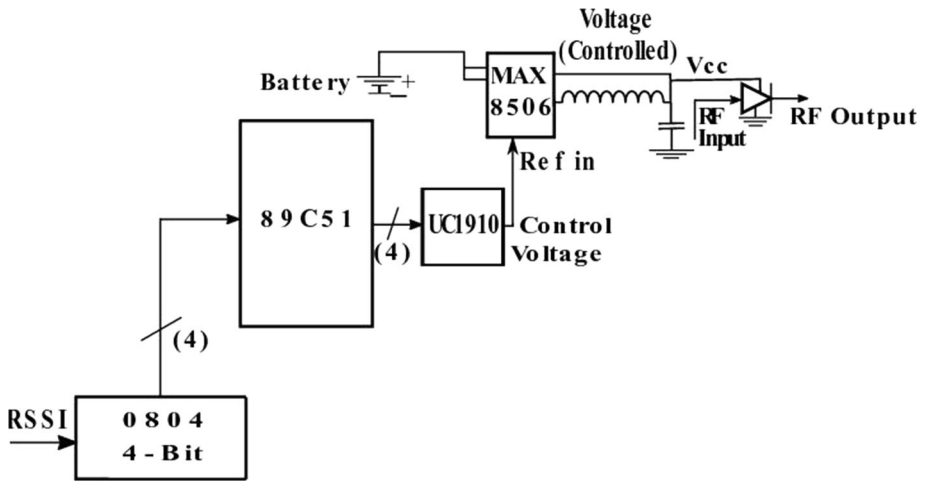


Fig. 10 Power control hardware module

Table 2 SNR corresponding to binary code

Binary code	SNR range (dB)
0000	5.051–5.9
0001	6.021–6.8
0010	6.9–7.8
0011	7.993–7.84
0100	7.9–8.974
0101	8.974–10
0110	10.1–11
0111	11.004–11.881
1000	11.987–12.9
1001	13.01–13.97
1010	13.979–14.994
1011	15–16
1100	16.01–16.994
1101	17–18
1110	18.1–19.3
1111	19.39–20

the received binary information. During this step by step increment process, if transmitter power reaches the maximum limit, set by interference constraint of primary user, the secondary transmitter opportunistically selects a new reliable carrier frequency. Now, to communicate with secondary receiver on the newly selected carrier frequency, the whole sequence will repeat.

## 5.2 Emulated Results

Here, we have set unlicensed channel spectrum (2.454 GHz) to perform data communication between primary and secondary node pairs simultaneously. We have varied primary transmitter power from 0.03 to 0.09 mW to observe secondary transmitter's transmit power adaptability by maintaining the minimum interference at primary units. Distance among nodes (Secondary  $T_x$ - $R_x$  and Primary  $T_x$ - $R_x$ ) has been kept at 5 m (Table 3).

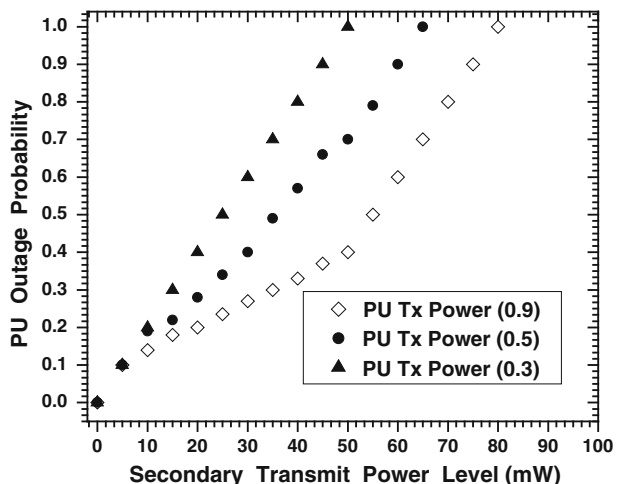
Figure 11 shows the almost linearly proportional variation of PU outage probability with secondary transmitted power level. Here, we have considered PU's transmission power as the parameter for each plot. Hence the outage probability will be more if the SU's transmit power level increases. Interference probability at the PU is inversely proportional with its own transmit power. We also have to consider the fact that higher value of PU's transmission power signifies that the separation between the PU and SU unit is more. Therefore outage probability decreases for higher PU transmit power.

Figure 12 shows, a linear increment of Cognitive users' channel capacity as the interference threshold limit of primary users' increase. However, simulated channel capacity is less than the actual channel capacity. It happens since in radio communication, we can expect presence of noise either from the link or from the circuits. It reduces SNR. It can be observed that higher is the value of secondary transmitter power, higher is the chances of

**Table 3** Various parameters

Emulating parameters	
Available channel frequency	2.4, 2432, 2.454, 2.481 GHz
Distance among nodes	5 m
Separation distance between primary and secondary units	10 m
$T_x$ - $R_x$ antenna height (secondary-primary unit)	0.1 m
Gain	1
Primary unit's $T_x$ power	0.03–0.09 mW

**Fig. 11** Probability of PU outage w.r.t secondary transmission power



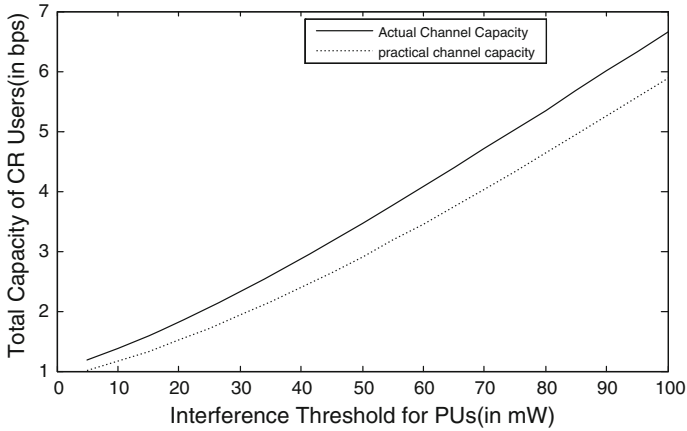
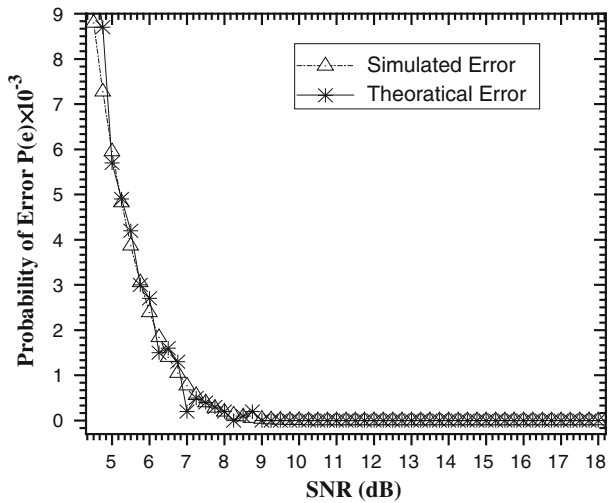


Fig. 12 Total capacity of the CR users versus the interference threshold

Fig. 13 Error probability versus SNR (dB)

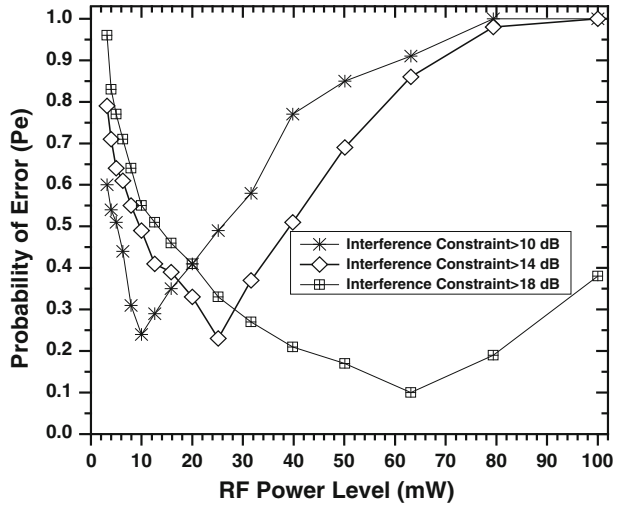


primary interference and it results in lower channel capacity of SUs. Therefore, channel capacity increases if we increase the interference threshold of PUs.

Probability of error  $P_e$  has been plotted against SNR shown in Fig. 13. It is logical that error probability ( $P_e$ ) will go down as SNR increases, since the reliability of detection improves with high SNR value. The above plot proves this concept. In fact, at values of SNR greater than 10 dB (approx),  $P_e$  reduces to almost zero. The simulated error differs slightly from the theoretically calculated plot because of presence of noise for a given channel.

In underlay cognitive radio network, SU transmit power level is to be chosen carefully to minimize outage probability of PU. Hence, in the above plot (Fig. 14), we have shown a relationship between error probability at primary receiver and RF power level of secondary transmitter. As can be seen,  $P_e$  will come down with increase in RF power level until it is less than or equal to the interference constraint at the primary receiver. After this, if RF

**Fig. 14** Error probability variation w.r.t power level for various Interference limit



power level is increased further, the outage probability of PU's will again increase. This phenomenon has been justified by the upward trend of above plots after predefined threshold limits.

## 6 Conclusion

In this paper, we have applied a flexible Transmitter power selection strategy to minimize the outage probability of primary users. Underlay cognitive network using opportunistic dual RSSI sensing based spectrum sharing method is proposed. This improves the overall performance of secondary users in terms of QoS and system throughput. As per channel SNR, transmit power is controlled by designed circuit. To evaluate channel SNR properly, optimum system threshold value has been assumed for both mathematical and graphical analysis. After the selection of reliable channel frequency, secondary transmitter initiates data communication at a given power level. This level is 3 dB below the level, required to achieve secondary receiver's RSSI level. A new receiver initiated incremental transmitter power command is used to support flexible power selection strategy. A step-by-step power adjustment concept has been implemented to maximize channel utilization and reliability for underlay cognitive network. During this process, transmitter power may reach the interference limit of PU. In such cases, without waiting for completion of primary communication, SU opportunistically switches to another licensed channel for secondary transmission. It not only improves the system throughput and QoS but also overcomes interference possibility with PUs. As per theoretical analysis, our emulated result shows almost similar error probability variation with SNR at the secondary receiver end. Graphical variation of error probability with respect to power level has been shown for various interference limits of PUs. Flexible selection of transmit power level, as per channel state information, has minimized the error rate. Hence, flexible transmit power selection with opportunistic spectrum sharing is the best possible method to achieve optimum performance in underlay cognitive radio network.



## References

1. Mitola, J. (2000). *Cognitive radio—an integrated agent architecture for software defined radio*. PhD Dissertation, KTH, Stockholm, Sweden.
2. Zhao, Q., & Sadler, B. M. (2007). A survey of dynamic spectrum access. *IEEE Signal Processing Magazine*, 24(3), 79–89.
3. Le, L. B., & Hossain, E. (2008). Resource allocation for spectrum underlay in cognitive radio networks. *IEEE Transactions on Wireless Communications*, 7(12), 5306–5315.
4. Kang, X., Liang, Y. C., Garg, H. K., & Zhang, L. (2009). Sensing-based spectrum sharing in cognitive radio networks. *IEEE Transactions on Vehicular Technology*, 58(8), 4649–4654.
5. Badawy, A., & Khattab, T. (2013, October). A hybrid spectrum sensing technique with multiple antenna based on GLRT. In *Wireless and Mobile Computing, Networking and Communications (WiMob), 2013 IEEE 9th International Conference on* (pp. 736–742). Lyon, France: IEEE. doi:10.1109/WiMOB.2013.6673438.
6. Yongjun, X., & Xiaohui, Z. (2013). Optimal power allocation for multiuser underlay cognitive radio networks under QoS and interference temperature constraints. *China Communications*, 10(10), 91–100.
7. Liu, Z., Wang, P., Xia, Y., Yang, H., & Guan, X. (2016). Chance-constraint optimization of power control in cognitive radio networks. *Peer-to-Peer Networking and Applications*, 9(1), 245–253.
8. Yao, H., Zhou, S., Liu, H., & Zhang, L. (2009, June). Optimal power allocation in joint spectrum underlay and overlay cognitive radio networks. In *Cognitive Radio Oriented Wireless Networks and Communications, 2009 (CROWNCOM'09) 4th International Conference on* (pp. 1–5) Germany: IEEE, Courtyard Hannover Maschsee. doi:10.1109/CROWNCOM.2009.5189342.
9. Wang, Y., Ren, P., Du, Q., & Sun, L. (2015). Optimal power allocation for underlay-based cognitive radio networks with primary user's statistical delay QoS provisioning. *IEEE Transactions on Wireless Communications*, 14(12), 6896–6910.
10. Gu, J., & Jeon, W. S. (2013). Optimal power allocation in an “off” spectrum sensing interval for cognitive radio. *IEEE Communications Letters*, 17(10), 1908–1911.
11. Benaya, A. M., Shokair, M., El-Rabaie, E. S., & Elkordy, M. F. (2015). Optimal power allocation for sensing-based spectrum sharing in MIMO cognitive relay networks. *Wireless Personal Communications*, 82(4), 2695–2707.
12. Chen, Y., Lei, Q., & Yuan, X. (2014). Resource allocation based on dynamic hybrid overlay/underlay for heterogeneous services of cognitive radio networks. *Wireless Personal Communications*, 79(3), 1647–1664.
13. Oh, J., & Choi, W. (2010, September). A hybrid cognitive radio system: A combination of underlay and overlay approaches. In *Vehicular Technology Conference Fall (VTC 2010-Fall), 2010 IEEE 72nd* (pp. 1–5). Ottawa, Ontario, Canada: IEEE. doi: 10.1109/VETECS.2010.5594302.
14. Qiu, T., Xu, W., Song, T., He, Z., & Tian, B. (2011, May). Energy-efficient transmission for hybrid spectrum sharing in cognitive radio networks. In *Vehicular Technology Conference (VTC Spring), 2011 IEEE 73rd* (pp. 1–5). Budapest, Hungary: IEEE. doi: 10.1109/VETECS.2011.5956224.
15. Lan, P., Sun, F., Chen, L., Xue, P., & Hou, J. (2013). Power allocation and relay selection for cognitive relay networks with primary QoS constraint. *IEEE Wireless Communications Letters*, 2(6), 583–586.
16. Lee, C. H., & Haenggi, M. (2012). Interference and outage in Poisson cognitive networks. *IEEE Transactions on Wireless Communications*, 11(4), 1392–1401.
17. Xing, Y., Mathur, C. N., Haleem, M. A., Chandramouli, R., & Subbalakshmi, K. P. (2007). Dynamic spectrum access with QoS and interference temperature constraints. *IEEE Transactions on Mobile Computing*, 6(4), 423–433.
18. Kang, X., Zhang, R., Liang, Y. C., & Garg, H. K. (2011). Optimal power allocation strategies for fading cognitive radio channels with primary user outage constraint. *IEEE Journal on Selected Areas in Communications*, 29(2), 374–383.
19. Bepari, D., & Mitra, D. (2014, February). GA based optimal power allocation for underlay cognitive radio networks. In *Electronics and Communication Systems (ICECS), 2014 International Conference on* (pp. 1–6). Coimbatore, India: IEEE. doi:10.1109/ECS.2014.6892554.
20. Rosas, A. A., Shokair, M., & El-dolil, S. A. (2015). Proposed optimization technique for maximization of throughput under using different multicarrier systems in cognitive radio networks. In *The Proceedings of Second International Conference on Electronics Engineering, Clean Energy and Green Computing (EECEGC)* (pp. 25–33). Konya, Turkey: Mevlana University, ISBN: 978-1-941968-12-3©2015 SDIWC.
21. Hou, L., Yeung, K. H., & Wong, K. Y. (2015). SEER: Spectrum-and energy-efficient routing protocol for cognitive radio ad hoc networks. *Wireless Networks*, 21(7), 2357–2368.

22. Lan, P., Chen, L., Zhang, G., & Sun, F. (2015). Optimal resource allocation for cognitive radio networks with primary user outage constraint. *EURASIP Journal on Wireless Communications and Networking*, 2015(1), 239.
23. Kang, X., Liang, Y. C., Nallanathan, A., Garg, H. K., & Zhang, R. (2009). Optimal power allocation for fading channels in cognitive radio networks: Ergodic capacity and outage capacity. *IEEE Transactions on Wireless Communications*, 8(2), 940–950.
24. Bala, I., Bhamrah, M. S., & Singh, G. (2015). Capacity in fading environment based on soft sensing information under spectrum sharing constraints. *Wireless Networks*, 23(2), 1–13.
25. Ozcan, G., & Gursoy, M. C. (2015). Optimal power control for underlay cognitive radio systems with arbitrary input distributions. *IEEE Transactions on Wireless Communications*, 14(8), 4219–4233.
26. Quan, Z., Cui, S., & Sayed, A. H. (2008). Optimal linear cooperation for spectrum sensing in cognitive radio networks. *IEEE Journal of Selected Topics in Signal Processing*, 2(1), 28–40.
27. Liu, X., Jia, M., & Tan, X. (2013). Threshold optimization of cooperative spectrum sensing in cognitive radio networks. *Radio Science*, 48(1), 23–32.
28. Zhao, Y., Li, S., Zhao, N., & Wu, Z. (2010). A novel energy detection algorithm for spectrum sensing in cognitive radio. *Information Technology Journal*, 9(8), 1659–1664.
29. Atapattu, S., Tellambura, C., & Jiang, H. (2011, June). Spectrum sensing via energy detector in low SNR. In *Communications (ICC), 2011 IEEE International Conference on* (pp. 1–5). Japan: IEEE, Kyoto International Conference Centre. doi: [10.1109/icc.2011.5963316](https://doi.org/10.1109/icc.2011.5963316).
30. Zhang, W., Mallik, R. K., & Letaief, K. B. (2009). Optimization of cooperative spectrum sensing with energy detection in cognitive radio networks. *IEEE Transactions on Wireless Communications*, 8(12), 5761–5766.
31. Lee, W. C. (2010). *Mobile communications design fundamentals* (Vol. 25). Hoboken: Wiley.
32. Semiconductor Components Industries, LLC. (2003). 3.3V/5V Programmable PLL Synthesized Clock Generator, NBC12429 (2003–Rev. 2) NBC12429/D, 1–2.
33. Philips Semiconductors, SA636. (1997). Low voltage high performance mixer FM IF system with high speed RSSI, IC17 Data Handbook, Nov 07.



**Prof. Sabyasachi Chatterjee** is presently working as an Assistant Professor in Electronics and Communication Engineering department at Heritage Institute of Technology, Kolkata. He obtained his B.E. degree from Visvesvaraya Technological University (VTU) and M.Tech. degree on communication from WBUT. Currently he is pursuing his Ph.D. degree from Jadavpur University. He joined academia in 2012. He has to his credit nearly 11 papers including 5 journal papers and one book chapter. His research interest at the moment is centered on Cognitive Radio Technology, Mobile Communication and Wireless Local Area Network.

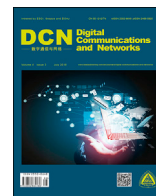


**Prof. (Dr.) Prabir Banerjee** is presently the head of Electronics and Communication Engineering department at Heritage Institute of Technology, Kolkata. He obtained his B.E., M.E. and Ph.D. (in engineering) from Jadavpur University. Prof. Banerjee started his career in Philips Telecommunication in the R and D department. He joined academia in 2003. Prof. Banerjee handled a number of trend-setting projects like synthesized VHF mobiles and repeater stations, POCSAG pagers, ATE for radios, HF networks while in Philips. He has to his credit nearly 30 papers including 8 journal papers and one book chapter. He has also executed IIPC activity successfully with AICTE granted fund. His research interest at the moment is centered on Cognitive Radio Technology and Ad Hoc wireless networks.



**Prof. (Dr.) Mita Nasipuri** is presently the Professor of Jadavpur University in Computer Science and Engineering department. She obtained his B.E., M.E. and Ph.D. (in engineering) from Jadavpur University. She joined academia in 1990. So far Prof. Nasipuri guided 12 scholars to get doctorate degree. Her research interest is centered on Image Processing, Pattern Recognition, Soft Computing, Artificial Intelligence and Bioinformatics.





# A new protocol for concurrently allocating licensed spectrum to underlay cognitive users

Sabyasachi Chatterjee<sup>a,\*</sup>, Prabir Banerjee<sup>a</sup>, Mita Nasipuri<sup>b</sup>

<sup>a</sup> Department of Electronics and Communication Engineering, Heritage Institute of Technology, Kolkata, India

<sup>b</sup> Department of Computer Science Engineering, Jadavpur university, Kolkata, India

## ARTICLE INFO

### Keywords:

Exponential back-off time  
Interference temperature limit  
Medium-access control protocol  
Received signal strength indicator  
Underlay cognitive user

## ABSTRACT

Cognitive radio technology makes efficient use of the valuable radio frequency spectrum in a non-interfering manner to solve the problem of spectrum scarcity. This paper aims to design a scheme for the concurrent use of licensed frequencies by Underlay Cognitive Users (UCUs). We develop a new receiver-initiated Medium Access Control (MAC) protocol to facilitate the selections of alternative reliable carrier frequencies. A circuit is designed to establish reliable carrier selections based on the Received Signal Strength Indicator (RSSI) at the receiving end. Based on both packet-level simulations and various performance parameters, a comparison is carried out among conventional techniques, including the Multiple Access with Collision Avoidance (MACA) and MACA by invitation (MACA-BI) techniques, and our scheme. The simulated results demonstrate that when conventional techniques are used, the system overhead time increases from 0.5 s on the first attempt to 16.5 s on the sixth attempt. In the proposed scheme under the same failure condition, overhead time varies from 0.5 s to 2 s. This improvement is due to the complete elimination of the exponential waiting time that occurs during failed transmissions. An average efficiency of 60% is achieved with our scheme while only 43% and 34% average efficiencies are achieved with the MACA and MACA-BI techniques, respectively. The throughput performance of our scheme on the fourth attempt is 7 Mbps, whereas for the MACA and MACA-BI protocols, it is 1.9 Mbps and 2.2 Mbps respectively.

## 1. Introduction

A Cognitive Radio (CR) has the ability to select a new operating channels dynamically whenever its current channel condition is poor [1]. The Dynamic Spectrum Access (DSA) technique allows Cognitive Secondary Users (CSUs) to use either a licensed spectrum band or the Primary Users' band. The latter is possible only doing so does not cause excessive interference with the owner of that band. According to the DSA policy, CR Networks (CRNs) can be categorized into three main paradigms: inter-wave, overlay, and underlay [2]. In the inter-wave approach, cognitive users can scan, or sense, the environment for either spectrum holes or white spaces that have been left vacant by Non Cognitive Users (NCUs) [3]. In the overlay approach, there is active cooperation between the Primary Users (PUs) and the Secondary Users (SUs). Thus, this approach enhances and assists the licensed users' transmissions to eliminate interference from the cognitive receiver by sharing both signal codebooks information and message sequences [4]. In the underlay approach, Secondary Cognitive Users (SCUs) use the

licensed spectrum at the same time as Primary Users (PUs) by keeping interference levels below the tolerance limit [5]. Hybrid schemes that use combinations of all of these paradigms [6] have great potential to improve the efficiency of spectrum sharing.

In Underlay Cognitive Networks (UCNs), it is very important to measure the Received Signal Strength (RSS) in terms of the Signal-to-Noise Ratio (SNR) due to the likelihood of interference [7]. To achieve higher spectrum utilizations in CRNs, Zheng et al. [8] proposed an optimal Bayesian-detector based spectrum sensing method. Ansari et al. [9] reported on a decentralized cognitive Medium-Access Control (MAC) protocol, CogMAC, based on a multi-channel preamble reservation scheme. Xing et al. [10] used a geometric programming technique to maintain a minimal Signal to Noise Ratio (SNR) for the required Quality of Service (QoS). Kim et al. developed a QoS-based joint-admission control and rate/power allocation framework [11] for DSA. Lan et al. [12] maintained the QoS required for the PU transmission by allocating an optimal power and relay selection strategy. Kim et al. [13] introduced an analytical model that was used by the SUs for the Call Admission

\* Corresponding author.

E-mail addresses: [sabyasachi.chatterjee@heritageit.edu](mailto:sabyasachi.chatterjee@heritageit.edu) (S. Chatterjee), [prabir.banerjee@heritageit.edu](mailto:prabir.banerjee@heritageit.edu) (P. Banerjee), [mnasipuri@cse.jdvu.ac.in](mailto:mnasipuri@cse.jdvu.ac.in) (M. Nasipuri).

<https://doi.org/10.1016/j.dcan.2017.04.004>

Received 2 June 2016; Received in revised form 3 March 2017; Accepted 14 April 2017

Available online 15 April 2017

2352-8648/© 2018 Chongqing University of Posts and Telecommunications. Production and hosting by Elsevier B.V. on behalf of KeAi. This is an open access article

under the CC BY-NC-ND license (<http://creativecommons.org/licenses/by-nc-nd/4.0/>).

Control (CAC) of voice traffic. A novel capacity-aware spectrum allocation model was developed in [14], and a wideband multi-channel spectrum sensing algorithm based on an energy detection and optimal resource allocation scheme was developed in [15] for efficient spectrum utilization in CRNs. Mathematical models based on graph theory were developed for spectrum sharing/access among SUs [16] and to solve the channel allocation problem in [17,18]. To guarantee high PU throughput transmissions and better SU utilization of channels, a Full-Duplex Spectrum Sensing (FD-SS) scheme was developed in [19]. The advent of MAC protocol identification methods using vector machine support [20] and a novel LU-MAC protocol for Cognitive Wi-Fi (CWF) networks [21] helped to increase the spectrum availability in both the licensed and unlicensed bands. In this paper, we propose a new approach for the concurrent sharing of any licensed portions of the spectrum by both types of users (PUs and SUs) without causing any degradation in the receiver's performance. In a wireless communication system, there is a probability of interference from other transmitters. In the MACA protocol, exponential back-off delays reduce data collisions but increase the waiting time. The receiver-initiated MACA-By Invitation (MACA-BI) protocol improves on MACA. However, MACA-BI also suffers from a back-off waiting time if there is a hidden terminal present, since the option to change channels does not exist at the receiver end. We also develop a new receiver-initiated MAC protocol to eliminate the back-off waiting time. The following are the main contributions of this paper to the field of CRN development:

1. The introduction of handshake technique for establishing a communication link before the exchange of actual information has been considered. A new receiver-initiated MAC protocol is proposed with respect to conventional protocols (including MACA and MACA-BI).
2. The transmission delay increases exponentially with the number of failed attempts in standard handshaking protocols due to the occurrence of multiple collisions. The proposed protocol eliminates exponential waiting time with a novel spectrum-sensing dynamic allocation scheme.
3. A circuit is designed based on the RSS Indicator(RSSI) detection technique to select a suitable channel for the UCUS with the least amount of noise.
4. Under even dense traffic conditions, an efficient system performance is achieved with both high throughput levels and a low system overhead time.

The remainder of this paper is organized as follows. Section 2 explains the relationship between the system temperature and both the interference and the noise. It also explains the relationship of the SNR and the RSSI. Section 3 presents the underlay CR communication system performance using well-known conventional protocols, including MACA and MACA-BI. The proposed receiver-initiated handshaking protocol is presented in Section 4. Section 5 highlights the design of the circuit for performing a spectrum sensing operation for reliable channel allocation to the UCUs. Section 6 describes the results and shows that the proposed method, achieves excellent throughput efficiency while meeting the optimum system performance. Section 7 concludes the paper.

## 2. Interference temperature model

Interference generally limits the useable range or effectiveness of communication signals and affects the efficiency of spectrum uses. To mitigate this growing problem, an interference temperature model was introduced by the Federal Communication Commission (FCC) of the United States to quantify and manage interference [22,23]. Underlay CRNs can measure and model the interference environment and adjust their transmission characteristics such that the interference encountered by their PUs is not above the regulatory limits while operating on the same channel frequency. To design an interference free UCN, a listen-before-talk mechanism is implemented based on the received

signal noise level measurement. The concept of interference temperature is identical to that of noise temperature. It is a measure of both the power and bandwidth (BW) occupied by either the noise or the interfering signal [23], given as

$$T_I(f_c, B) = \frac{P_I(f_c, B)}{KB} \quad (1)$$

where the average interference power  $P_I(f_c, B)$  and absolute temperature  $T_I(f_c, B)$  are present in the center of the receiver channel frequency with a certain bandwidth.  $B$ . Boltzmann's constant  $K$  defines the relationship between the temperature on an absolute scale and the kinetic energy. This energy causes interference, and Eq. (1) shows the relationship mathematically. The RSSI of the received signal has a linear relationship with the SNR. Hence, it can be used to determine the amount of energy necessary for a given transmission. Due to the interrelationships among interference, temperature, and bandwidth, the RSSI measurement is a powerful tool for CU channel selection. This is illustrated by

$$RSSI \propto \frac{P_r}{(P_{Ni} + P_{NI})} = \frac{P_r}{P_N} \quad (2)$$

where  $P_{Ni}$  and  $P_{NI}$  represent the internal and link noise, respectively. The 3-dB bandwidth of the receiver is considered while measuring the signal power of the received signal. Noise power is the summation of internal noise power and external factors, such as link noise and atmospheric noise. The noise voltage resulting from the presence of these factors both raises the system temperature and leads to a poor SNR value. Hence, we analyzed the temperature interference model in terms of RSSI.

## 3. Underlay communication paradigm

In an underlay communication scenario, both the primary and secondary transmissions may take place on a common channel [24]. In general, an MAC layer protocol [20,25] with a sensing capability is necessary to perform a fair allocation of resources among secondary users while avoiding collisions with primary users. Handshaking is a well-known procedure for initiating normal communication. It essentially creates a physical link between two parties [26]. There are three basic cycles present in the conventional MACA protocol proposed by Karn [27]. With the MACA technique, UCU initiates communication by sending a test signal from the sender to the receiver on the sender's selected channel.

The signal  $R(t)$  (Fig. 1) sniffed by the CR's secondary receiver is modelled as additive zero-mean Gaussian noise with a variance of  $\sigma_n^2$  in the time domain. The received radio signal is filtered by a band-pass filter in order to both limit the noise and select the bandwidth of interest. To detect simultaneous channel occupancy by licensed users and PUs, the received signal strength is compared with the locally set threshold. Here we employ a statistical approach and define two binary hypotheses,  $H_0$  and  $H_1$  related to the RSS [28], given as

$H_0$  :  $R(t) = S(t) + P(t) + U(t)$ , when the licensed user signal is present and  $H_1$  :  $R(t) = S(t) + U(t)$ , when the signal is absent.

When a PU is active in the interfering region of the SCR, the resulting receiver SNR can be represented as [28],  $R(t) = \frac{S(t)}{U(t)+P(t)}$  :  $H_0 < \lambda$ .

When a PU is not active in the interfering BW of the SCR, the resulting

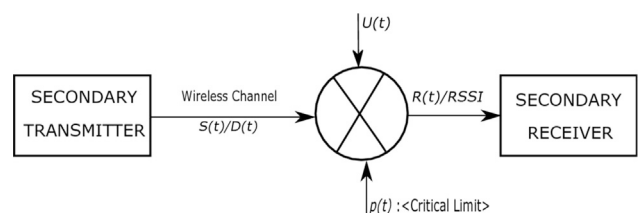


Fig. 1. Underlay communication system.

receiver SNR can be represented as [28],  $R(t) = \frac{S(t)}{U(t)} : H_1 > \lambda$ .

Here,  $\lambda$  represents the predefined system threshold for an acceptable SNR. Noise  $U(t)$  is independently and identically distributed over the channel. In general, the probability of events between these two hypotheses occurs depending on the test static. In the case of hypothesis  $H_0$ , the transmitter waiting time increases exponentially with the number of failed attempts. Now, due to the occurrence of the event  $H_1$ , the receiver transmits a Clear To Send (CTS) command to the sender to initiate the transmission. After decoding the CTS command successfully, the sender begins the transmission of data. The successful completion of data reception is indicated by the receiver with an acknowledge ACK command (Figs. 2 and 3).

In order to both minimize the system overhead and reduce the transmission delay, the MACA-BI protocol was proposed by Fabrizio Talucci [30]. This protocol uses the request to send RTS command, but if the transmitter and the receiver are separated by a large distance, then there is a high probability of errors occurring in the data reception. The correctness of the received data is assessed by considering another two binary hypotheses  $H_{00}$  and  $H_{11}$  (Figs. 4 and 5). Here,  $H_{00}$  signifies the error signal reception when RSS is below the predefined system threshold. On the other hand,  $H_{11}$  represents successful reception of the data on the first attempt due to a sufficiently high signal strength without strong noise. When a PU operates on the common carrier frequency selected by the secondary transmitter, a direct collision may occur between nodes due to the presence of either hidden nodes or spurious carrier frequencies. In such situations, the received SNR can be below the threshold limit because the RSSI is linearly proportional to the SNR. Therefore, we can write the RSSI as [28],  $RSSI \propto \frac{D(t)}{U(t)+P(t)} : H_{00} < \lambda$ .

When a PU is not active on the same channel, the data is received with both a high RSSI and a high SNR and can be represented by [28],  $RSSI \propto \frac{D(t)}{U(t)} : H_{11} > \lambda$ .

In general, the probabilities of these two hypotheses occurring depend on the received data signal strength,  $D(t)$ . Hypothesis  $H_{00}$  occurs when the received data contains errors. If the receiver does not send an ACK command due to the reception of corrupted data, the transmitter sends the same data again after a predefined period (determined by the back-off time). The retransmission attempts continue until the transmitter receives the ACK command (sent by the receiver after successful data reception). Hypothesis  $H_{11}$  occurs after successful data reception on the first attempt. In this paper, we propose a new approach to reducing both overhead timing and concurrent spectrum allocation in the cases of failure.

#### 4. Basic scheme

In the proposed scheme, each secondary receiver performs both spectrum sensing and detection to choose a carrier with an acceptable SNR before communicating with any other user. Reliable carrier information is exchanged using the proposed handshaking technique. This provides positive control over the use of the shared medium in the UCN. The primary reasons for implementing this technique are to minimize collisions with hidden terminals and to reduce the interference with PUs. In our experiment, the secondary transceiver scans all of the channels available in the ISM band (i.e., 2.4 GHz, 2.424 GHz, 2.454 GHz, and 2.484 GHz) and selects the channel most suitable for data transmission. It then generates a carrier to receive the CTR message with the desired transmitter address. This protocol is initiated by the receiver. The

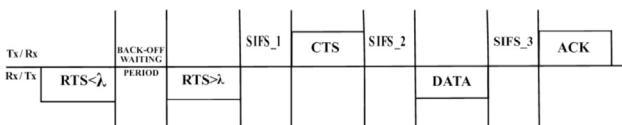


Fig. 2. Time sequence of hypothesis  $H_0$  [29].

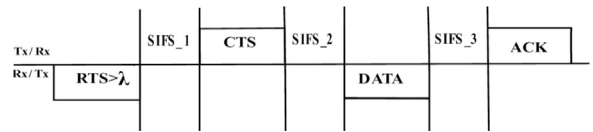


Fig. 3. Time sequence of hypothesis  $H_1$  [29].

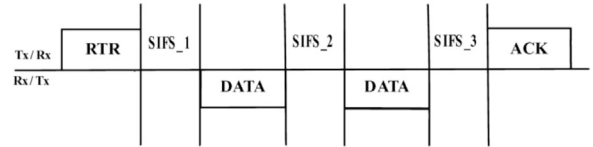


Fig. 4. Time sequence of hypothesis  $H_{00}$  [29].

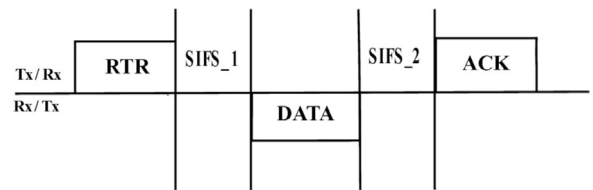


Fig. 5. Time sequence of hypothesis  $H_{11}$  [29].

message is a 21 byte long information frame that contains preamble bits (for synchronization), control bits (source-destination information), and checksum bits (Fig. 6).

The entire frame consists of frame control bits each consisting of 2 bytes of information followed by a 6-byte Receiver Address (RA) and six byte Transmitter Address (TA). The TA is followed by a 4-byte Frame Check Sequence (FCS). Here the Carrier Information (CI) of each byte carries suitable transmission frequency information to the neighboring SUs. Only the selected transceiver is acknowledged with data transmission. Fig. 7 shows a flow chart of the handshaking procedure for the receiver and the transmitter. Underlay communication takes place on the frequency shared between the PU and Cognitive Secondary User (CSU). However, failure is a distinct possibility because of the high level of interference from the PU, since the secondary receiver also operates on the same channel frequency. If this process fails, the receiver once again scans the available channels based on the RSSI signal. Now, without wasting time on retransmission attempts as in previous techniques, such as MACA and MACA-BI, the receiver will instantly communicate with the corresponding transmitter using the CTR command frame, which contains new carrier frequency information resulting in consistent communication.

#### 4.1. Optimum threshold selection

A novel receiver-initiated data transmission protocol is presented here. First, the operating carrier frequency is selected at the receiver based on a predefined SNR threshold. Therefore, the threshold determination at the receiver end is a crucial in terms of successful data transmission. The energy static, or decision static, of the received signal energy is given by [33]

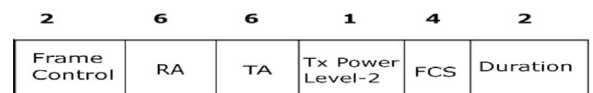


Fig. 6. Structure of CTR frame.

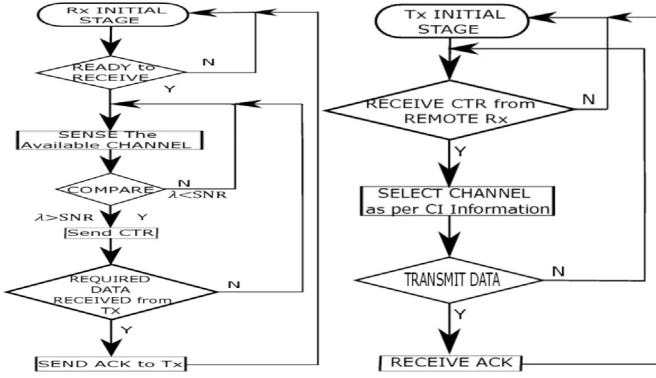


Fig. 7. Scheme of proposed communication system.

$$E_{si} = \frac{1}{N} \sum_{N=1}^N |r_i(t)|^2 dt \quad (3)$$

Comparing  $E_{si}$  with the pre-set threshold  $\lambda_i$  for the CR-enabled nodes, the presence or absence of a primary user signal can be determined by

$$\begin{aligned} H_0 &: E_{si} < \lambda_i \\ H_1 &: E_{si} \geq \lambda_i \end{aligned} \quad [33]$$

The SNR is defined as the ratio of the signal variance to the noise variance, given by [34]

$$\gamma = \frac{h_i^2 \sigma_s^2}{\sigma_n^2} \quad (4)$$

The energy received by the UCUs is utilized as a decision statistic [31] that follows both central and non-central chi-squared distributions (with a noncentrality parameter of 2), each with two  $\mu$  degrees of freedom, and is given by

$$E_{si} \approx \begin{cases} \chi_{2\mu}^2 \\ \chi_{2\mu(2\gamma)}^2 \end{cases} \quad (5)$$

When the number of samples of the received signal is large enough (i.e.,  $N \geq 100$ ), then the central limit theorem determines that the mean and variance of  $E_{si}$  under the hypothesis  $H_0$  are  $N\sigma_n^2$  and  $N\sigma_n^4$  respectively. Similarly, under the hypothesis  $H_1$ , the mean is  $N\sigma_n^2(1 + \gamma)$  and variance is  $N\sigma_n^4(1 + 2\gamma)$ . The  $Q(\cdot)$  function can be written as [32]  $Q(x) = \frac{1}{\sqrt{2\pi}} \int_x^\infty \exp\left(-\frac{t^2}{2}\right) dt$ .

Successful detection:  $H_1$  true, decide  $H_1$ : probability =  $p_{sd} =$

$$Q\left(\frac{\lambda_i - \mu H_1}{\sigma H_1}\right) \quad (6)$$

$$P_{sd} = Q\left(\left(\frac{\lambda}{N\sigma_n^2} - 1 - \gamma\right) \sqrt{\frac{N}{1 + 2\gamma}}\right)$$

False detection:  $H_0$  true, decide  $H_1$ : probability =  $P_{fd} = Q\left(\frac{\lambda_i - \mu H_0}{\sigma H_0}\right)$

$$P_{fd} = Q\left(\left(\frac{\lambda}{N\sigma_n^2} - 1\right) \sqrt{N}\right) \quad (7)$$

Miss Detection:  $H_1$  true, decide  $H_0$ : Probability =  $p_{md} = 1 - P_{sd}$  (8)

A pre-defined threshold  $\lambda_i$  that varies from 0 to  $\infty$  is a parameter that is commonly required for determining whether the PU signal is absent or present. Thus, the operating threshold selection is very important in the context of CRNs [34]. A false alarm is triggered when the SCUs falsely detect the presence of the PU signal within the interfering level. This misdetection occurs when the SCUs make an incorrect decision about the absence of PU signal interference on the same channel. A false alarm

condition arises when the radio receiver suffers from strong desensitization. Misdetection, on the other hand, may occur due to desensitization, and fading may occur due to interference. These two error probabilities reflect the spectrum utilization of the CR nodes and, therefore, the aim of threshold optimization is to decrease both the false alarm and the misdetection probabilities. The threshold is commonly set based on the false alarm probability. When  $\lambda_i$  increases (or decreases), both  $P_{fd}$  and  $P_{md}$  decrease (or increase). To achieve a high value,  $P_{sd}$ ,  $P_{fd}$  must be kept very low while  $P_{md}$  increases. Therefore, the optimal threshold selection can be viewed as the minimization of the total error rate, defined as [35]  $P_e \triangleq P_{fd} + P_{md}$ .

The error detection probability of  $CR_i$  can be written as [32]

$$P_{ei} = P(H_0)P_{fd} + P(H_1)P_{md}. \quad (9)$$

The conventional method maximizes the detection probability while minimizing the total error. The optimal threshold can be written as [33]

$$\lambda^* = \arg \min P_e(\lambda). \quad (10)$$

For an Additive White Gaussian Noise (AWGN) fading channel, the optimal threshold is given by [32]

$$\lambda^* = \arg \min \left( 1 + \frac{1}{2} \operatorname{Erfc}\left(\frac{\lambda - N\sigma_n^2}{\sqrt{2N}\sigma_n^2}\right) - \frac{1}{2} \operatorname{Erfc}\left(\frac{\lambda - N\sigma_n^2(1 + \gamma)}{\sqrt{2N(1 + \gamma)}\sigma_n^2}\right) \right) \quad (11)$$

Here,  $P_{fd} = \frac{1}{2} \operatorname{Erfc}\left(\frac{\lambda - N\sigma_n^2}{\sqrt{2N}\sigma_n^2}\right)$  and  $P_{sd} = \frac{1}{2} \operatorname{Erfc}\left(\frac{\lambda - N\sigma_n^2(1 + \gamma)}{\sqrt{2N(1 + \gamma)}\sigma_n^2}\right)$ , where  $\operatorname{Erfc}(\cdot)$  is the complimentary error function that is defined as [32]  $\operatorname{Erfc}(z) = \frac{2}{\sqrt{\pi}} \int_z^\infty e^{-t^2} dt$ , and the standard Q function is [32]  $Q(z) = \frac{1}{2} \operatorname{Erfc}\left(\frac{z}{\sqrt{2}}\right)$ . Therefore, the optimal threshold for any received signal with acceptable SNR value can be derived as [32].

$$\lambda^* = \frac{N\sigma_n^2}{2} \left( 1 + \sqrt{1 + 2\gamma \left( 1 + \frac{(1 + 2\gamma)\ln(1 + 2\gamma)}{N\gamma^2} \right)} \right) \quad (12)$$

When the RSS is very low, i.e.,  $\gamma \ll 1$ , then  $(1 + 2\gamma) \approx 1$ , the optimal threshold can be well approximated as [32], where

$$\lambda^* \approx \frac{N\sigma_n^2}{2} (1 + \sqrt{1 + 2\gamma}) \approx N\sigma_n^2 \quad (13)$$

In our work, we examine the factors that affect the channel performance and therefore result in SNR variation. We consider the AWGN fading channel performance to justify our work. Shadowing effects must be considered in modeling an accurate CR environment. If these are neglected, the path loss behavior becomes an unrealistic straight-line curve. To consider shadowing effects, a zero-mean Gaussian random variable with a positive or negative value and a standard deviation of  $\sigma$  can be utilized. This variable indicates that the optimal threshold of the received signal will have either a positive or a negative deviation in a real-time Radio Frequency (RF) propagation environment. In addition, to eliminate internal desensitization effects due to platform noise, we considered an internal noise factor  $\lambda_{int}$ , which acts as a correction factor in determining the local threshold value. Eq. (9) shows that the total error rate probability depends on both the false detection (positive deviation) and misdetection (negative deviation) probabilities. Therefore, the real-time optimal receiver threshold for the received SNR can be written as

$$\lambda_i^* \approx (N\sigma_n^2 \pm \sigma \cdot G + \lambda_{int}). \quad (14)$$

The main challenge is obtaining an optimum threshold that satisfies the system performance requirements. We can derive the desired SNR for an omni-directional antenna system analytically. For example, we can compare an underlay CR system with a conventional cellular system that reuses the same frequency. In a cellular system, the specified SNR is 18 dB or higher based on subjective tests and analysis [36]. Therefore,



consider an SNR of 18 dB the standard threshold for reliable performance.

#### 4.2. System throughput optimization

We first examine an example where, nodes ‘A’ and ‘B’ are 500 m apart and nodes ‘B’ and ‘C’ are 200 m apart. Assume that node ‘B’ initiates communication by generating a CTR command with a unique transmitter address A. Since nodes A and C receive carrier information simultaneously, only node A responds and starts sending data packets (Fig. 8).

The successful selection of the channel frequency leads to the initiation of the CTR transmission from the receiver end, which contains either preamble or header information as well as newly selected carrier information. In our scheme, the sender (Tx) starts sending data packets (Fig. 9) whenever it receives a CTR command from any receiver. Here, we assign a separate control channel frequency to exchange overhead control frames. A basic transmission rate  $R_{\text{control}}$  is assigned to control frame ( $O_{\text{cf}}$ ) that contains 21 bytes. The total time required for both reliable carrier selection and control & command transmission to the proper destination can be calculated as

$$\tau_{\text{Cl}} = \tau_{\text{comp}} + \frac{O_{\text{cf}}}{R_{\text{control}}} \quad (15)$$

where  $\tau_{\text{comp}}$ , is the minimum receiver computational time needed for scanning, comparing, and selecting a reliable channel frequency. In the worst case scenario, the system computation time  $\tau_{\text{comp}}$  calculation depends on the Phase-Locked Loop (PLL) locking time (20 ms) [38], the RSSI generation lag duration from the Intermediate Frequency (IF) processor Integrated Circuit (IC) SA 636 (10 ms) [39] and the program execution time. For the proposed system, a 16 MHz clock is implemented, resulting in a clock duration of 16  $\mu\text{s}$ . In general, information is conveyed by the changes in the signal values over time. When the CTR command is received by the control channel, the transmitter changes its data channel frequency according to the CI information sent from the receiver. Total data transmission time from Tx-Rx is calculated as

$$\tau_{\text{TD}} = \frac{S}{\delta} + T_p + T_t \quad (16)$$

In the equation above, the first term represents the time required to push all of the bits onto the link, where S is equal to the number of control bits added to the M data frame bits and  $\delta$  represents the uniform data transmission rate. To evaluate the maximum rate at which data can be transmitted over a given communication link or channel, we have applied Claude E. Shannon’s Equation [37] for channel capacity  $C =$

$\text{Blog}_2 \left( 1 + \frac{S}{N} \right)$ . Here, the channel capacity (C) or the maximum data rate, is related to both the channel BW and the SNR (18 dB for reliable data communication). The effective data rate is  $\delta = \frac{\eta}{100} \times C$  and the transmission efficiency ( $\eta$ ) is given by  $\frac{\text{Actual data}}{\text{Total no. of transmitted data}} \times 100$ . The second and third terms in Eq. (16) denote the propagation delay time ( $T_p$ ) and channel processing time ( $T_t$ ).

Based on the nature of CTR arrival probability, we propose two hypotheses:

- $H_1$  : Successful completion of data transmission on the first attempt.
- $H_0$  : Failure in data transmission on the first attempt.

Let S be the normalized system throughput, defined for one successful

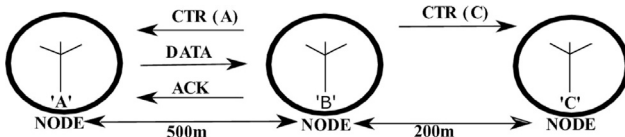


Fig. 8. Data transmission scheme using proposed protocol.

HEADER INFORMATION					User Data
Destination ID	Source ID	Message ID	Packet ID	Control ID	

Fig. 9. Structure of transmitted information.

cycle of data transmission as  $H_1$  (Fig. 10).

$$\tau_{\text{SD}} = \tau_{\text{TD}} + \tau_{\text{Cl}} + \tau_{\text{ACK}} + (2 \times \text{SIFS}) \dots \quad (17)$$

In Eq. (17), the total data transmission time ( $\tau_{\text{SD}}$ ) is calculated by considering all of the determining factors. The time required to send an ACK message from the receiver to the transmitter after the successful reception of data over the control channel is denoted by  $\tau_{\text{ACK}}$ .  $P_{\text{ct}}$  notes the probability of one cycle time completing a data transmission between two stations successfully, where each transmits with a probability of  $\gamma$ . Therefore,  $P_{\text{ct}} = 1 - (1 - \gamma)^n$ , where n represents number of parties simultaneously involved in data transmission over the same channel. The probability of successful transmission ( $P_{\text{st}}$ ) by at least one station on the first attempt is  $P_{\text{st}} = \frac{n\gamma(1-\gamma)^{n-1}}{P_{\text{ct}}} = 1$  (100% probability). Therefore, the system throughput for successful transmission on the first attempt can be calculated by

$$S = \frac{\text{Total no. of transmitted bits (overhead data + use full data)}}{\text{Total slot time}} \quad (18)$$

Under hypothesis  $H_0$ , transmission failure is caused by channel transmission error due to either the misdetection of PUs signals or the reception of the same Carrier Information (CI) from multiple sources. Let the transmission failure probability, or the error probability ( $P_e$ ), that occurs for misdetection or same CI reception be denoted by  $P_{\text{mis-f}}$  and  $P_{\text{Cl-f}}$ , respectively (Figs. 11 and 12).

From Eq. (9), the total error or failure probability can be written as  $P_{e-f} = P_{\text{mis-f}} + P_{\text{fd-f}}$ , where false detection is associated with a negligible amount of time required for receiver computation. Misdetection can lead to an incorrect carrier frequency selection at the receiver’s end, which causes unsuccessful data transmission on the first attempt. The minimum slot time requirement can be written as

$$\tau_{\text{mis-st}} = (2 \times \tau_{\text{TD}}) + (2 \times \tau_{\text{Cl}}) + \tau_{\text{ACK}} + (4 \times \text{SIFS}) \quad (19)$$

It may sometimes occur that two (secondary Rx-Tx) users belonging to two different geographical locations sense the same carrier frequency for transmission. Hence, if both of the receiver-initiated CTR commands containing common CI information are received by the same (secondary Tx-Rx) user, then both interference and data transmission blocking may occur. With the assistance of the collision detection technique, the (secondary Tx-Rx) user responds by broadcasting a repeat carrier to receive command. After receiving the repeat command, the initiating receiver again scans the local environment and selects the best possible available channel as the carrier. Data communication begins only after the reception of two different carriers’ channel information. The timing sequence for failed transmission is shown below.

It is clear that the exponential back-off time, or waiting time, has been eliminated by the selection of a carrier frequency without local noise. This simultaneously eliminates the possibility of multiple attempts, since

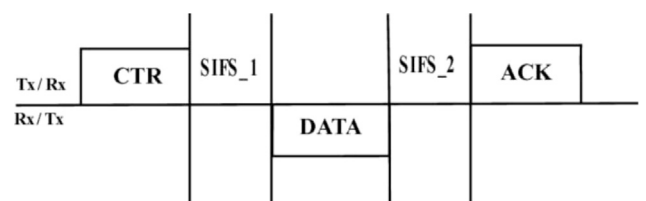


Fig. 10. Scheme of Data Transfer without failure.

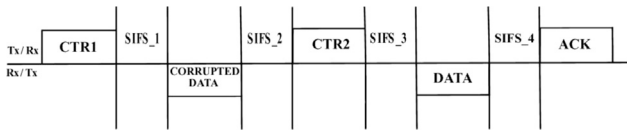


Fig. 11. Scheme of Data Transfer with  $p_{mis-f}$ .

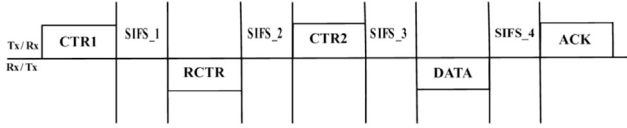


Fig. 12. Scheme of data transfer with  $p_{cl-f}$ .

the channel changes automatically. To allocate the carrier spectrum concurrently, we propose a hardware scheme that can perform the spectrum-sensing and detection tasks reliably.

### 4.3. Hardware scheme

The nature of radio communications places fundamental limitations on the reliability of wireless links. The paths between transmitters and receivers are extremely random because of various factors. Our scheme is based on a receiver-initiated protocol rather than a sender initiated protocol. This makes communication systems much more reliable by checking internal and external interference at the receiver constantly before the transmission. In our hardware scheme (Fig. 13), we focus on the SNR of the sensed radio signal at the receiver’s end. The SNR of the sensed signal is compared with the predefined system threshold for reliable data communication of 18 dB, and a decision is made about the present channel condition. If the SNR value for a particular sensed channel frequency is greater than the predefined threshold value, the channel frequency is selected for immediate data communication. Otherwise, the receiver continues to sense other channels to find an SNR greater than the threshold value.

To assess our spectrum-sensing scheme, we utilized the RF spectrum from 200-400 MHz. The total spectrum range is split up into  $n$  narrow bands described by the division ratio of the PLL IC, which is programmable, as described in the next paragraph. Using the Monte-Carlo optimization technique, one band of the  $n$  bands will be selected, and then the controller will lock the PLL at a frequency corresponding to  $n$ . The receiver performance in terms of the SNR, is checked directly with the RSSI value obtained from the first IF processor IC SA 636 [39]. If the SNR is higher than the threshold value for reliable network operation, the receiver will generate a CTR message to initiate the communication. If the SNR value falls short of the desired threshold for any value of  $n$ , the program will randomly select another  $n$ , and the same process will be undertaken. The CA 3160 operational amplifier has been used as a DC

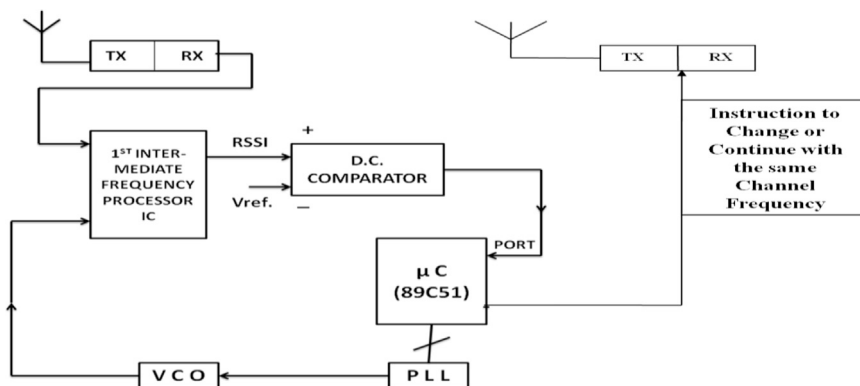


Fig. 13. Schematic block of proposed scheme.

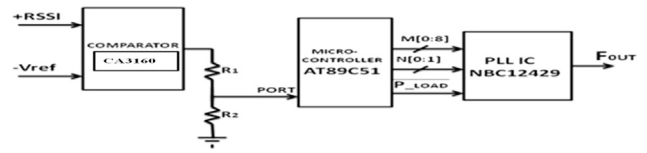


Fig. 14. Schematic diagram of emulation.

comparator to compare the sensed RSSI with the predefined reference voltage ( $V_{ref}$ ), which should be 0.8 V for the standard 18 dB threshold. The comparator output is connected to port P2.3 of the microcontroller, and the microcontroller’s output ports are connected with the M (8:0), N (1:0), and P\_LOAD inputs of the NBC12429 PLL IC [38]. First, M (8:0) and N (1:0) are set. Then, P\_LOAD is enabled by the microcontroller. When the comparator’s output is high, the microcontroller senses the condition, and there is no change in M(8:0) or N(1:0), which indicates that the corresponding frequency is locked by the PLL to within 20 ms [38]. However, for a low comparator output, the microcontroller’s input senses a negative condition. This causes the program to change both M (8:0) and N (1:0) in sequence, and the corresponding PLL  $F_{OUT}$  output changes in the range of 200-400 MHz. The change in frequency is measured by a frequency counter. A schematic diagram of this process is shown in Fig. 14.

### 4.4. Reliable channel selection

A voltage divider is used with a comparator so that the output of the voltage divider is no more than 5 V in order to provide compatibility with the microcontroller port. When the RSSI value corresponding to the sensed frequency is greater than  $V_{ref}$ , the output of the voltage divider  $V_{out}$  is 5 V and when the RSSI value corresponding to the sensed frequency is less than  $V_{ref}$ , the output of the voltage divider  $V_{out}$  is 0 V. Based on the basic state of the input voltage, the microcontroller makes a decision regarding the selection or rejection of the frequency locked by the PLL as the correct one to initiate the communication (Fig. 15). Thus, if the receiver encounters strong interference from any noise, either internal or external, it can change its operating frequency automatically according to its RSSI value. The RSSI voltage value represents the acceptable SNR value according to the data sheet of the IFIC [39].

NBC12429 is a general purpose PLL and can be programmed for a frequency between 25 and 400 MHz. The voltage-controlled oscillator within this PLL operates over a frequency range of 200-400 MHz. The PLL does not require any external components, as the loop filter of the PLL is fully integrated. The output frequency of the PLL can be represented theoretically [38] as

$$F_{OUT} = (F_{XTAL} \div 16) \times M \div N \quad (20)$$

where  $F_{OUT}$  is the output frequency of the PLL (Table 1),  $F_{XTAL}$  is the

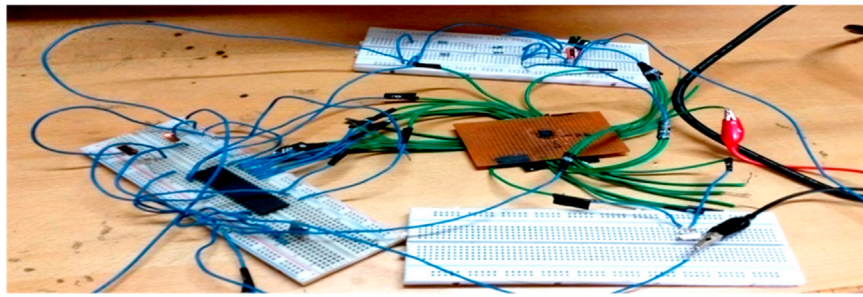


Fig. 15. Laboratory setup.

Table 1  
Hardware setup for channel frequency.

$V_{ref}$	RSSI	Microcontroller Port P2.3 connection	Channel Frequency ( $F_{out}$ )	Discussion
0.8	1.3	5 V DC Power Supply	242 MHz (random)	Select a receiver frequency using local sensing technique
0.8	0.5	Ground	314 MHz (random)	If received signal is below predefined threshold then Change is automatic
0.8	1.2	5 V DC Power Supply	Previously selected carrier frequency	Though received signal strength is greater than predefined system threshold and so operations Continue

crystal frequency,  $M$  is the loop divider modulus, and  $N$  is the output divider modulus. It is possible to select arbitrary values of  $M$  such that the PLL is unable to achieve loop lock. To avoid this,  $M$  is selected such that  $200 \leq M \leq 400$  for a 16 MHz input (crystal frequency) reference. The user can program the proper  $M$  and  $N$  values for a desired frequency using the above equations. Thus, if  $N [1:0] = 01$ . For  $N = 2$ ,  $F_{OUT} = M \div 2$  and  $M = 2 \times F_{OUT}$ . Therefore,  $M = 131 \times 2 = 262$ , so  $M [8:0] = 10000110$ . If  $M$  changes by 1,  $F_{out}$  changes by 2 MHz.

The proposed scheme eliminates the waiting time in case of failures due to collisions in the network. Fig. 16 shows a comparison of the time durations of the actual data and the overhead data. It is clear that the channel occupancy time has been minimized by the elimination of the exponential back off time. This indicates that the total data transmission time does not increase significantly because of the overhead increase caused by channel switching.

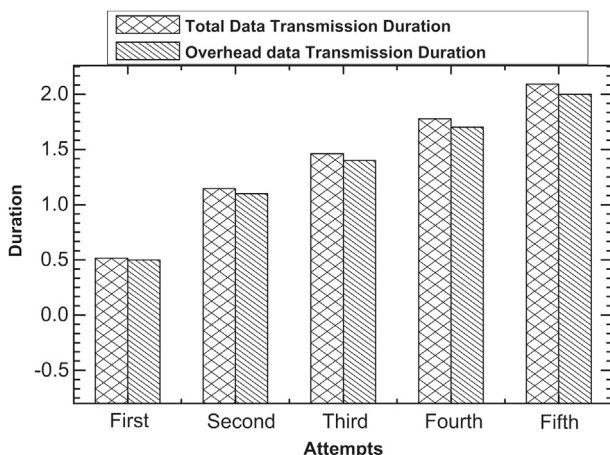


Fig. 16. Time durations of both actual transmitted and overhead data.

#### 4.5. Comparison among conventional methods

Handshake mechanisms are used to detect data lost due to collisions during data transfer. These mechanisms also add to system overhead in terms of delay. Under dense traffic conditions, multiple collisions usually occur, which can increase the transmission-delay exponentially. As a result, repeated data transmissions increase, causing the degradation of both throughput and system efficiency. To minimize the waiting time caused by multiple retransmission attempts, we propose a receiver-initiated protocol that begins with a spectrum-sensing technique. Simulation results show that our scheme can reduce the exponential back-off waiting time remarkably.

For CRNs, specific MAC protocols have yet to be designed. We analyze a couple of reliable MAC protocols, MACA and MACA-BI. Like protocols initiated by the sender, MACA suffers greatly, as the sender has no way of locating transmissions from hidden terminals located near the receiver. Therefore, data loss is frequent, leading to ‘back-off’. The results in the losses of both precious battery power and time. MACA-BI improves on this situation by avoiding the RTS command in initiating the packet transmission. Therefore, in terms of data completion time, MACA-BI requires less compared to the MACA protocol. Nevertheless, it is vulnerable to hidden terminal transmissions causing the back-off problem. To perform our simulation, we set the transmitter power to 0.01 mW. The gains of the transmitter/receiver antennas and the heights of the antennae are set to 1 and 0.1 m respectively. The distance between the secondary transmitter and receiver remains constant at 500 m along with a fixed data packet size of 1 Mbps and a slot duration of 10 ms.

In our scheme, we consider a dynamic pool of channels (in the ISM band for trial purposes) to be shared by the units of the CRN. In this network, both the primary and secondary units belong to a common network and operate on the same channel frequency of 2.454 GHz. The results are plotted along with the number of attempts against various parameters, including overhead time, throughput, and system efficiency. The proposed scheme switches its channel frequency among the four channels of the ISM band (provided in the experimental set-up) (Table 2).

In Fig. 17, typical variations of overhead time with numbers of attempts are plotted using MATLAB. The overhead time increases with the number of failed attempts, as is expected. The link establishment time for successful data transmission is equivalent to the system overhead time. The overhead time increases exponentially when either the MACA or the

Table 2  
Simulated frequencies of proposed scheme over multiple attempts.

Proposed Scheme	
Attempts	Channel frequency(GHz)
First	2.454
Second	2.4
Third	2.484
Fourth	2.424
Fifth	2.454
Sixth	2.4

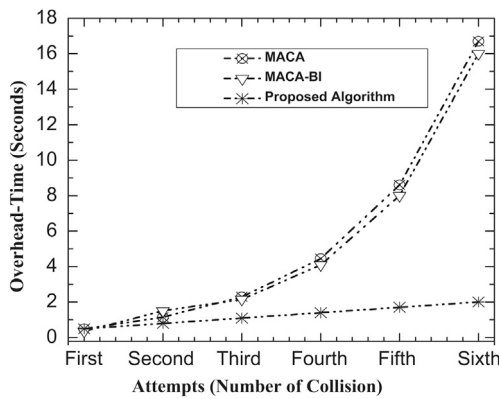


Fig. 17. Overhead data duration.

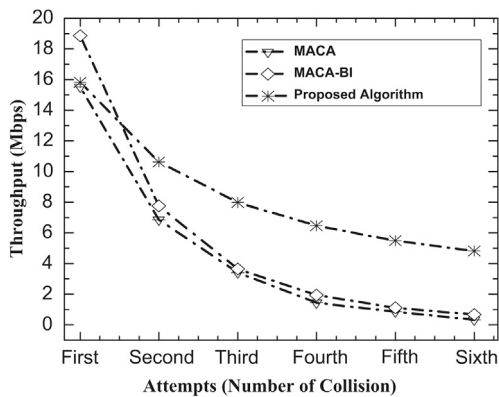


Fig. 18. Throughput Performance.

MACA-BI protocol is applied. MACA-BI provides a slightly better performance than the MACA protocol does. A very low overhead time is required for this proposed scheme, and this value remains nearly constant.

We compute the throughput (S) of the protocols under consideration for multiple collisions by keeping the maximum transmission range within about 500 m and fixing the packet length at 1Mbps. The (Fig. 18) maximum throughput efficiency is achieved when the proposed algorithm is implemented. The MACA and MACA-BI protocols are supposed to minimize the number of collisions that occur in communication systems. However, they are not suitable for dense and urban cognitive network scenarios. MACA-BI provides the highest throughput on the first attempt (successful transmission) of any protocol. However, after a collision occurs, the throughput falls sharply. Even in cases of multiple failures under dense traffic conditions, nearly constant high throughput is achieved by the proposed protocol.

The performance of a data communication system can be measured by two factors, the throughput and the bit error rate. A system has to satisfy both criteria in order to achieve efficiency and reliability. In this paper, we evaluate the system efficiency under multiple failures and compare the results of the proposed protocol with those of two standard ones. Fig. 19 indicates that the proposed scheme performs better than some of the well-known existing wireless MAC protocols do.

## 5. Conclusion

Our paper offers a new approach to the avoidance of the difficult hidden-terminal problem in CRNs. Underlay cognitive communication takes place on the shared carrier frequencies of PUs. During communication, interference with PUs and collisions with hidden terminals both affect the performance at the receiver's end. In our scheme, the receiver

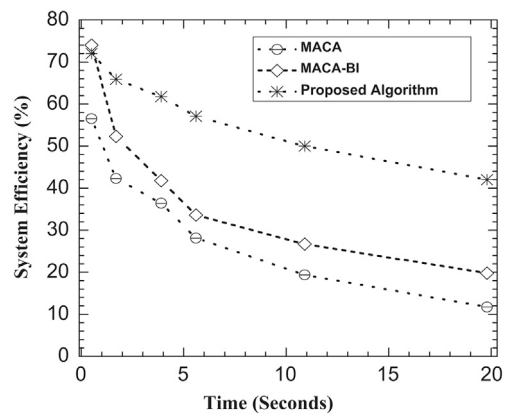


Fig. 19. System efficiency vs. user utility.

begins communications on its locally sensed least-noisy carrier frequency. The data transmission completes within two cycles in the case of successful first attempt transmission. Since exponential back-off, or waiting period, is not a factor for the new proposed protocol, the system overhead time is much lower than it is when other conventional techniques, such as MACA or MACA-BI, are used. Simulation results are used to compare the system's throughput and efficiency in the case of multiple failures occurring due to collisions. Both nearly constant throughput and consistent system efficiency are obtained by implementing the proposed scheme. If a collision occurs, the corresponding cognitive receiver responds instantly with a new channel frequency that has an SNR above the acceptable threshold value. Spectrum detection is carried out in the receivers with an RSSI sensor circuit. Concurrent spectrum allocation is possible for the UCUs under this scheme. The results demonstrate greater reliability and efficiency.

## References

- [1] Qing Zhao, Brian M. Sadler, A survey of dynamic spectrum access, *IEEE Signal Process. Mag.* 24 (3) (2007) 79–89.
- [2] A. Goldsmith, S.A. Jafar, I. Maric, S. Srinivasa, Breaking spectrum gridlock with cognitive radios: an information theoretic perspective, *Proc. IEEE* 97 (5) (2009) 894–914.
- [3] H. Li, H. Dai, C. Li, Collaborative quickest spectrum sensing via random broadcast in cognitive radio systems, *IEEE Trans. Wirel. Commun.* 9 (7) (2010) 2338–2348.
- [4] M.G. Khoshkholgh, K. Navaie, H. Yanikomeroglu, Optimal design of the spectrum sensing parameters in the overlay spectrum sharing, *IEEE Trans. Mob. Comput.* 13 (9) (2014) 2071–2085.
- [5] N.H. Mahmood, F. Yilmaz, M. Alouini, G.E. Oien, Cognitive interference modeling with applications in power and admission control, in: *IEEE International Symposium on Dynamic Spectrum Access Networks (DYSpan)*, IEEE (October 2012), pp. 434–439. doi: <https://doi.org/10.1109/DYSpan.2012.6478167>.
- [6] Z. Wu, B. Natarajan, Interference tolerant agile cognitive radio: Maximize channel capacity of cognitive radio, in: *Proceedings of 4th IEEE Consumer Communications and Networking Conference (CCNC-2007)* (January 2007), pp. 1027–1031, doi: <https://doi.org/10.1109/CCNC.2007.207>.
- [7] C.H. Lee, M. Haenggi, Interference and outage in Poisson cognitive networks, *IEEE Trans. Wirel. Commun.* 11 (4) (2012) 1392–1401.
- [8] S. Zheng, P.Y. Kam, Y.C. Liang, Y. Zeng, Spectrum sensing for digital primary signals in cognitive radio: a Bayesian approach for maximizing spectrum utilization, *IEEE Trans. Wirel. Commun.* 12 (4) (2013) 1774–1782.
- [9] J. Ansari, X. Zhang, P. Mähönen, A decentralized MAC protocol for opportunistic spectrum access in cognitive wireless networks, *Comput. Commun.* 36 (13) (2013) 1399–1410.
- [10] Y. Xing, C.N. Mathur, M.A. Haleem, R. Chandramouli, K.P. Subbalakshmi, Dynamic spectrum access with QoS and interference temperature constraints, *IEEE Trans. Mob. Comput.* 6 (4) (2007) 423–433.
- [11] D.I. Kim, L.B. Le, E. Hossain, Joint rate and power allocation for cognitive radios in dynamic spectrum access environment, *IEEE Trans. Wirel. Commun.* 7 (12) (2008).
- [12] P. Lan, F. Sun, L. Chen, P. Xue, J. Hou, Power allocation and relay selection for cognitive relay networks with primary qos constraint, *IEEE Wirel. Commun. Lett.* 2 (6) (2013) 583–586.
- [13] B. Kim, G.M. Lee, B.H. Roh, MAC protocol for quality-aware real-time voice delivery in cognitive radio-enabled WSNs, *Int. J. Distrib. Sens. Netw.* (2015).
- [14] M. Yousefvand, N. Ansari, S. Khorsandi, Maximizing network capacity of cognitive radio networks by capacity-aware spectrum allocation, *IEEE Trans. Wirel. Commun.* 14 (9) (2015) 5058–5067.

- [15] S. Dikmese, S. Srinivasan, M. Shaat, F. Bader, M. Renfors, Spectrum sensing and resource allocation for multicarrier cognitive radio systems under interference and power constraints, *EURASIP J. Adv. Signal Process.* 2014 (1) (2014) 68.
- [16] H. Zheng, C. Peng, Collaboration and fairness in opportunistic spectrum access, *IEEE International Conference on Communications (ICC2005)* (May 2005) (Vol. 5, pp. 3132–3136). doi:<https://doi.org/10.1109/ICC.2005.1494982>.
- [17] N. Nie, C. Comaniciu, Adaptive channel allocation spectrum etiquette for cognitive radio networks, *Mob. Netw. Appl.* 11 (6) (2006) 779–797.
- [18] O.B. Abdulghfoor, M. Ismail, R. Nordin, Application of game theory to underlay ad-hoc cognitive radio networks: An overview, *IEEE International Conference on Space Science and Communication (IconSpace)* (July 2013), pp. 296–301, doi:<https://doi.org/10.1109/IconSpace.2013.6599484>, 2013.
- [19] W. Cheng, X. Zhang, H. Zhang, Full-duplex spectrum-sensing and MAC-protocol for multichannel nontime-slotted cognitive radio networks, *IEEE J. Sel. Areas Commun.* 33 (5) (2015) 820–831.
- [20] S. Hu, Y.D. Yao, Z. Yang, MAC protocol identification using support vector machines for cognitive radio networks, *IEEE Wirel. Commun.* 21 (1) (2014) 52–60.
- [21] K. Karunambiga, M. Sundarambal, LU-MAC: licensed and unlicensed MAC protocol for cognitive WiFi network with jamming-resistant, *Procedia Comput. Sci.* 47 (2015) 424–433.
- [22] Federal Communications Commission, Notice of inquiry and notice of proposed rulemaking: in the matter of establishment of an interference temperature metric to quantify and manage interference and to expand available unlicensed operation in certain fixed. Mobile and Satellite Frequency Bands, *ET Docket*, (03-237) (2003).
- [23] P.J. Kolodzy, Interference temperature: a metric for dynamic spectrum utilization, *Int. J. Netw. Manag.* 16 (2) (2006) 103–113.
- [24] A.J. Goldsmith, L.J. Greenstein, N.B. Mandayam, H.V. Poor, *Principles of Cognitive Radio*, Cambridge University Press, 2012.
- [25] F. Xia, A. Rahim, *MAC Protocols for Cyber-Physical Systems* (ISBN: 978-3-662-46360-4), Springer Berlin Heidelberg, 2015.
- [26] R. Yadav, S. Varma, N. Malaviya, A survey of MAC protocols for wireless sensor networks, *UbiCC J.* 4 (3) (2009) 827–833.
- [27] P. Karn, MACA-a new channel access method for packet radio, In *ARRL/CRRL Amateur radio*, Vol. 140, in: *Proceedings of the 9th Computer Networking Conference* (September 1990), pp. 134–140.
- [28] K. Sithamparanathan, A. Giorgetti, *Cognitive Radio Techniques: Spectrum Sensing, Interference Mitigation, and Localization*, Artech House, 2012.
- [29] Chai K. Toh, *Ad Hoc Mobile Wireless Networks: Protocols and Systems*, Pearson Education, New Jersey, 2001.
- [30] F. Talucci, M. Gerla, MACA-BI (MACA by invitation). A wireless MAC protocol for high speed ad hoc networking, in: *Proceedings of the 6th International Conference on Universal Personal Communications Record, IEEE* (October 1997), (Vol. 2, pp. 913–917) doi: 10.1109/ICUPC.1997.627296, 1997.
- [31] Yaqin Zhao, Shuying Li, Nan Zhao, Zhilu Wu, **A novel energy detection algorithm for spectrum sensing in cognitive radio**, *Inf. Technol. J.* 9 (8) (2010) 1659–1664.
- [32] S. Atapattu, C. Tellambura, H. Jiang, Spectrum sensing via energy detector in low SNR, in: *proceedings of the IEEE International Conference on Communications (ICC)*, (June 2011), pp. 1–5. <https://doi.org/10.1109/icc.2011.5963316>.
- [33] Z. Quan, S. Cui, A.H. Sayed, Optimal linear cooperation for spectrum sensing in cognitive radio networks, *IEEE J. Sel. Top. Signal Process.* 2 (1) (2008) 28–40.
- [34] X. Liu, M. Jia, X. Tan, Threshold optimization of cooperative spectrum sensing in cognitive radio networks, *Radio Sci.* 48 (2013) 23–32, <https://doi.org/10.1029/2012RS005009>.
- [35] W. Zhang, R.K. Mallik, K.B. Letaief, Optimization of cooperative spectrum sensing with energy detection in cognitive radio networks, *IEEE Trans. Wirel. Commun.* 8 (12) (2009) 5761–5766.
- [36] W.C. Lee, *Mobile Communications Design Fundamentals*, 25, John Wiley & Sons, 2010.
- [37] D.J. Costello, G.D. Forney, Channel coding: The road to channel capacity, *Proc. IEEE* 95(6) (2007), 1150–1177.
- [38] NBC12429, Semiconductor Components Industries, LLC, Rev.2, NBC12429/D (January 2003), pp. 1–20.
- [39] SA636, NXP B.V. (5 December 2012), pp. 1–31.